MODELING BIODEGRADATION OF CHLORINATED GROUNDWATER CONTAMINANTS UNDER IRON-REDUCING CONDITIONS OF A CONSTRUCTED WETLAND: A SYSTEM DYNAMICS APPROACH

THESIS

Max E. Johnson, First Lieutenant, USAF

AFIT/GEE/ENV/01M-04

DEPARTMENT OF THE AIR FORCE
AIR UNIVERSITY

AIR FORCE INSTITUTE OF TECHNOLOGY

Wright-Patterson Air Force Base, Ohio

The views expressed in this thesis are those of the author and do not reflect the official policy or position of the United States Air Force, Department of Defense, or the U. S. Government.

AFIT/GEE/ENV/01M-04

MODELING BIODEGRADATION OF CHLORINATED GROUNDWATER CONTAMINANTS UNDER IRON-REDUCING CONDITIONS OF A CONSTRUCTED WETLAND: A SYSTEM DYNAMICS APPROACH

THESIS

Presented to the Faculty

Department of Systems and Engineering Management

Graduate School of Engineering and Management

Air Force Institute of Technology

Air University

Air Education and Training Command

In Partial Fulfillment of the Requirements for the

Degree of Master of Science in Engineering and Environmental Management

Max E. Johnson, B.S.

First Lieutenant, USAF

March 2001

AFIT/GEE/ENV/01M-04

MODELING BIODEGRADATION OF CHLORINATED GROUNDWATER CONTAMINANTS UNDER IRON-REDUCING CONDITIONS OF A CONSTRUCTED WETLAND: A SYSTEM DYNAMICS APPROACH

Max E. Johnson, B.S.
First Lieutenant, USAF

Approved:

Michael L. Shelley (Chairman)	2 Mar 01 date
Charles A. Bleckmann (Member)	1 Mar 01 date
Abinash Agrawal (Member)	March 1, 2001 date

Acknowledgments

First, and foremost, I give praise to my God. Without Him, none of this would have been possible. Praise be to GOD!!

I would like to express my gratitude to my advisory committee members, Dr. Charles Bleckmann and Dr. Abinash Agrawal, for their guidance, knowledge, and support throughout the course of this thesis effort. Your contributions and expertise kept my study on track and were greatly appreciated.

I am greatly indebted to my advisor and advisory committee chairman, Dr. Michael Shelley. Your patience, understanding, encouragement, and confidence helped me through every step of this effort. My accomplishments would not have been possible without your support.

I would like to thank my wife for her unconditional love and support. Her supportive hugs and words of encouragement helped me through all the good and "not-so-good" times. My thanks also goes out to my friends and family whose prayers and support were greatly appreciated.

Max E. Johnson

Table of Contents

Page

List of Figures

Figure Page

List of Tables

Abstract

The purpose of this study is to determine and explore the fundamental processes associated with biodegradation of chlorinated ethenes in iron-reducing conditions of a constructed wetland and to evaluate the impacts of changing conditions (both natural and engineer-controlled) on the system. The modeler uses a system dynamics approach to construct a model that represents behavior in the iron-reducing environment. The model incorporates hematite, a form of oxidized iron (Fe^{3+}), as the electron acceptor in microbial biodegradation in the system.

Vinyl chloride, *cis*-dichloroethene, and *trans*-dichloroethene are known to anaerobically degrade to carbon dioxide in the presence of oxidized iron. Other biodegrading processes, including those associated with hydrogen and natural organic materials, compete with the contaminant degrading processes for the oxidized iron. These processes are all incorporated into the model.

Model simulations show that the organic material parameters have a greater influence on hematite depletion compared with parameters of the modeled contaminants. By increasing the amount of hematite in the soil, the time period that biodegrading processes exist in the constructed wetlands increases proportionally. Also, by increasing flow rate through the constructed wetland, a higher amount of contaminant is degraded. With the increases flow rate, however, a greater amount of contaminants flow through the iron-reducing environment unreacted.

MODELING BIODEGRADATION OF CHLORINATED GROUNDWATER CONTAMINANTS UNDER IRON-REDUCING CONDITIONS OF A CONSTRUCTED WETLAND: A SYSTEM DYNAMICS APPROACH

I. Introduction

Background

Groundwater and soil surveys taken beneath United States Air Force bases in the late 1970's revealed significant plumes of potentially carcinogenic contaminants. Further investigations exposed similar contaminant plumes beneath numerous other United States Department of Defense (DOD) installations. In fact, the Environmental Protection Agency (EPA) reported that in 1993, approximately 7,300 sites at over 1,800 locations held by DOD contain soil contaminants (National Research Council, 1994:27) associated with chlorinated solvents. Cleanup of these sites requires strict standards to be met; thus, the process is complicated and costly. One estimate by the Office of Management and Budget states that future remediation efforts at sites owned by the Departments of Defense, Energy, Interior, and Agriculture will cost between $234 and $389 billion. This estimate incorporates remediation activities for the next seventy-five years (National Research Council, 1997:18). Incorporating all contaminated sites in the United States (estimated between 300,000 and 400,000), the estimated costs grow to between $300 billion to $1 trillion in the upcoming decades (National Research Council, 1997:18).

Even with the enormous estimated cleanup costs over future decades, the industrial sector continues to use chlorinated solvents. Global use of perchloroethene (PCE), trichloroethene (TCE), and 1,1,1-trichloroethane (1,1,1-TCA) in 1994 totaled an

estimated 900,000 metric tons. Because of widespread use, chlorinated solvents often appear as groundwater contaminants. Whether escaping through leaky underground storage tanks, being disposed carelessly, or being spilled accidentally, nine of the twenty top chemicals at major contamination sites (Superfund sites) are categorized as chlorinated solvents (National Research Council, 1997:113).

This thesis effort focuses specifically on two common groundwater contaminants: dichloroethene (DCE), and vinyl chloride (VC). Though not considered carcinogenic, DCE at high concentrations causes damage to the liver, kidneys, and central nervous system (Masters, 1997:184). Additionally, DCE is normally difficult to volatilize. VC, listed as a probable human carcinogen, is persistent and is slightly soluble in water.

One objective of this thesis is to model and evaluate the biodegradation of the aforementioned chlorinated contaminants introduced into a multi-layered constructed wetland. For years, constructed wetlands have intercepted surface runoff and provided protection to delicate ecosystems. Today, scientists propose that these constructed wetlands provide a long-term, cost-effective alternative for biodegradation of chlorinated contaminants. The model in this study demonstrates the concept of using a constructed wetland for bioremediation. Specifically, the constructed wetland modeled in this study uses a layered sediment configuration. This system design includes various soils, with different degrading characteristics, layered on one another. The contaminated groundwater is pumped beneath the constructed wetland and flows vertically through the system's layers. As the groundwater progresses through each layer of the constructed

wetland system, various microorganisms, at different stages of the degradation process, intercept the contaminants and use them as sources of food.

Bioremediation using constructed wetlands, as proposed, is a favorable alternative when compared to existing groundwater treatment technologies. The bioremediation process relies on microorganisms existing in the subsoil. These organisms transform the chlorinated contaminants into less toxic compounds. The reactions occur at various depths in the subsurface depending on the oxygen content (aerobic vs. anaerobic). Occasionally, the microorganisms need additional nutrients, enzymes, and substrates, which are not available in the soil or groundwater. These materials, in some circumstances, can be added to the subsurface environment for optimal degradation. Additionally, chemical reactions, both natural and induced, support the degradation of the contaminants. Unlike other contaminant removal technologies that require additional disposal procedures, biological and chemical degradation can completely destroy organic contaminants, degrading them to non-toxic compounds such as carbon dioxide. Additionally, because the microorganisms are naturally occurring and reproduce as required, maintenance costs are minimal for the system.

Another category of groundwater remediation, in comparison, involves solidification, stabilization, and containment. Methods that incorporate this technology are intended to decrease solubility, volatility, and/or permeability of the contaminants. Examples of these technologies include soil mixing (using augers to mix stabilizing agents with existing soil), passive-reactive barriers (using permeable barriers with reactive properties to intercept contaminant plumes), and permanent wall structures

(using slurry walls, sheet pile walls, or grout walls to contain the contaminants) (National Research Council, 1997:90). Unlike bioremediation efforts, these methods do not destroy the contaminants; instead, they stabilize the chemical for further removal processes. Therefore, costs associated with maintenance and disposal tend to be greater than bioremediation. Another category of groundwater remediation uses technology to separate, mobilize and physically extract contaminant plumes from the soil. Once detached from soil particles using heat, chemicals, vacuums, or electrical current, the contaminants are pumped to the surface for further disposal processes. Again, these technologies do not destroy the contaminants; they simply separate the chemicals for disposal. Maintenance and high quality labor costs, as well as disposal costs of the contaminants, make these technologies more costly than bioremediation methods.

As described, all systems performing groundwater remediation processes require energy to operate. This energy, however, comes from various sources. Bioremediation systems, for example, use energy from natural sources such as sun, wind, rain, and biomass (Kadlec and Knight, 1996:3). Only small amounts of energy are required to initially pump the groundwater into the constructed wetland. Also, once constructed, only limited personnel are required to operate the system. Other systems, such as traditional pump-and-treat, for example, require large amounts of energy and personnel to operate groundwater pumps and associated equipment (Masters, 1997:249). When comparing groundwater degradation processes, long-term operating costs favor bioremediation over other technologies.

For the purpose of this study, a portion of a three-layered wetland system will be modeled. The United States Air Force has funded and constructed a wetland system located at Wright-Patterson Air Force Base, OH. This constructed wetland is a research endeavor focusing on chlorinated contaminant degradation. The model created in this study represents a portion of the microbial activity in the actual wetland system. In the constructed wetland, a geomembrane liner surrounds the constructed wetland to create an impermeable boundary and keeps the contaminated groundwater in the system. Just above the liner and below the lowest layer of constructed wetland, pipes, embedded in approximately twelve inches of gravel, allow the contaminated groundwater to be pumped below the system. As the contaminated water enters the system, it accumulates in the gravel before flowing vertically and evenly throughout the layered constructed wetland. The first layer the contaminated groundwater encounters is the methanogenic zone. This zone, approximately eighteen inches in depth, has conditions that allow anaerobic microbial activity to initiate degradation of the contaminants. As the water continues its vertical flow through the system, it reaches the next constructed layer of the system. This layer, referred to as the iron zone, contains increased levels of oxidized iron (modeled as hematite, Fe_2O_3) used in the degradation process. The iron zone of this constructed wetland is a unique layer placed in the constructed wetland for research purposes. This iron zone will be evaluated to determine if it benefits the degradation process. Microorganisms in the iron zone use oxygenated iron (Fe^{3+}) as an electron acceptor. Using the electron acceptors through chemical reactions, microbes in the iron layer degrade the contaminants into carbon dioxide and capture energy for biological

activities. Ideally, the iron content in this layer should amount to approximately one percent of the iron layer's soil composition by mass. In the constructed wetland of concern, however, the iron content value varies below one percent. The depth of the iron zone is approximately eighteen inches, and the soil condition is considered anaerobic, allowing microbes to perform degradation processes on the contaminants flowing through the system. As the water exits the iron zone, it reaches the third and final layer of the system. This layer, called the aerobic zone, contains roots from a variety of plant species on the surface of the constructed wetland. The roots supply this zone with oxygen, which, in turn, dominates the final stages of the degradation process in the constructed wetland system. The aerobic zone is approximately eighteen inches in depth and borders the surface of the constructed wetland. At the surface, various plant species supply nutrients and oxygen for microbial degradation in the aerobic zone. In the aerobic zone, oxygen dominates chemical reactions and microbial processes. As the groundwater exits the constructed wetland system and flows at the surface, the degradation processes of the constructed wetland are complete. At this point, the water is released back into the existing groundwater aquifer or transferred to a wastewater treatment plant for further disposal.

The purpose of this study is to model, examine, and understand the biodegradation activities occurring in the iron zone of a multi-layered constructed wetland. The degradation activities in the iron zone are only a portion of the overall degradation processes occurring in the constructed wetland. Other natural chemical reactions occur in the iron zone; however, this study focuses on the degradation processes of DCE and VC.

This thesis effort uses a system dynamics approach to produce a model of behavior in the iron zone of a constructed wetland. The system dynamics approach allows development of an understanding of a system by conceptualizing and portraying the dynamic relationships between internal parts of the system mechanistically. The method should produce long term internal behavior of the system for investigation. Once a system dynamics model is produced and validated, sensitivity analysis can be performed to determine particular mechanisms causing specific behavior patterns in the system. With numerous interrelated processes, ecological systems tend to be ideal for system dynamics models.

Previous work by Captain Colby D. Hoefar from the Air Force Institute of Technology gives a system dynamics model of an entire constructed wetland. This thesis effort identifies a specific portion of the constructed wetland (the iron zone) and demonstrates the chemical and biological processes thereof.

Problem Statement

At multiple locations across the United States and around the world, the United States Air Force has contaminated plumes in the subsurface, which must be contained or remediated. These plumes are the result of spills and careless disposal of chlorinated contaminants such as PCE, TCE, DCE, and VC. Existing technologies for remediation of these chlorinated plumes are extremely expensive. New technologies, such as constructed wetland bioremediation, however, are not fully understood for optimum degradation performance. This thesis serves as a portion of the overall understanding of degradation in a constructed wetland. The model produced by this effort provides

information about behavior patterns, specifically in the iron zone, and allows designers to optimize parameters in a constructed wetland for maximum degradation.

Research Questions

1. Which parameters significantly impact degradation processes and interrelationships in a system dynamics model of the iron zone of a constructed wetland?
2. Which parameters in the system dynamics model are able to be engineer-controlled and what impact on the degradation processes occur when these engineer-controlled parameters are changed?
3. Which parameters in the system dynamics model require further experimentation for increased confidence in the model?

Scope/ Limitations

This thesis focuses on the conditions in the iron zone of a layered constructed wetland. Parameters that influence degradation in this zone include concentration of contaminants and availability of electron acceptors. Initially, the iron zone is rich with Fe^{3+}, an electron acceptor in the degradation process. Over time, however, the oxidized iron is depleted through degradation processes and other naturally occurring activities in the soil. The model representing the iron zone is based on typical soil conditions. For example, soil porosity and organic content are unique from location to location. Parameters for this model will represent conditions for the actual constructed wetland funded by the United States Air Force at Wright-Patterson Air Force Base, Ohio.

II. Literature Review

Engineered bioremediation focuses on microbial activity degrading harmful groundwater contaminants into non-toxic compounds that can be released into the environment without significant impact. Many present-day groundwater remediation processes require high costs and maintenance. The simple pump-and-treat process, for example, requires pumps to extract contaminated water from the subsurface. The groundwater is then treated at an aboveground treatment facility before being released back into the soil or directed to a wastewater facility for further disposal (Masters, 1998:238). Costs associated with the pump-and-treat procedure, as well as personnel required for maintenance of associated equipment, make this technique costly and demanding. Also, site-specific soil conditions and factors tend to vary pump-and-treat costs depending on the treatment location. One calculated cost for perchloroethene (PCE) removal from groundwater using simple pump-and-treat techniques was $2.21 per 1000 liters treated. This value, as reported, incorporated capital, operation, and maintenance costs (total system cost) for the simple pump-and-treat method (Quinton et al, 1997:14). A different source estimated the cost for the pump-and-treat method (using EPA cost estimates) to be $14.74 per 1000 liters treated. As before, this estimate includes total system costs (Masters, 1996:249). These estimated values do not appear to be significant until the volume of groundwater treated is considered. The first estimate treated approximately 4.4 billion liters with a total cost of 9.8 million dollars (Quinton et al, 1997:14), and the second estimate treated 190 million liters of groundwater with a total cost of over 2.8 million dollars (Masters, 1996:249). Due to the high costs associated

with other forms of remediation, scientists are now investigating the benefits of microbial degradation. Within the past two decades, studies focusing on microbial activity have demonstrated that certain types of bacteria living in aerobic and anaerobic conditions can obtain carbon sources and energy for life-supporting activities from chlorinated compounds (Lee et al, 1998:428). These chlorinated compounds are found as groundwater contaminants in aquifers worldwide. The naturally occurring microorganisms provide contaminant destruction energy with no direct costs, which significantly reduces overall costs of the system compared to other methods of remediation. Therefore, in recent years, scientists have proposed using constructed wetlands to provide an adequate environment for degradation of harmful groundwater contaminants (Masters, 1996:582). Complex processes involving microorganisms found naturally in the soil degrade the harmful contaminants. By-products of one degradation process in the constructed wetland act as a food and energy source for another process in the system. Working in sequence, microorganisms degrade harmful contaminants into non-toxic compounds such as carbon dioxide (CO_2) and water.

Constructed Wetlands

Constructed wetlands are man-made environments that have the ability to provide conditions necessary for microbial degradation. Complex systems evolve as the constructed wetlands mature and adapt to the environmental conditions. In general, constructed wetlands can be categorized into surface flow or subsurface flow wetlands.

For surface flow constructed wetlands, water in the system tends to remain on the ground surface, creating a shallow flowing water layer for the system. This water layer

provides essential nutrients for the emergent wetland vegetation in the constructed wetland (Kadlec and Knight, 1996:562). General components of a surface flow constructed wetland include a water supply system, acreage, vegetation, and a discharge device. Many options are available for the water supply system. Groundwater pumps or wells, for example, supply a constructed wetland with water adjacent or near the wetland site. Another viable option is a system of pipes and appropriate pumps that allow contaminated groundwater to be transferred from distant sites. The pipes and appropriate pumps allow the constructed wetland to be built in strategic locations to minimize disturbance of other environments and maximize productivity of the system. Requirements for surface flow constructed wetland acreage depend specifically on the function of the wetland. Size, shape, and water holding capacity for the constructed wetland are directly associated with microbial reaction kinetics required to achieve appropriate contaminant levels for regulatory discharge or disposal specifications. Vegetation associated with the constructed wetland allows nutrient cycling and oxygen exchanges in the system. The roots of the plants also provide ideal protection and nutrient supply to microbial populations involved in the degradation processes. Naturally, the vegetation must be able to survive conditions and contaminants associated with the constructed wetland function. Other characteristics associated with plant selection include contaminant uptake and storage abilities, costs to produce and maintain biomass, and additional benefits to surrounding ecosystems. The final component to surface flow constructed wetlands, the discharge device, collects water from the surface of the constructed wetland. The collected water is then tested and appropriately pumped

back into the constructed wetland, pumped to another functional constructed wetland, released into the environment (in streams, rivers, or lakes), or disposed in water sewage systems for further processing.

Another type of constructed wetland uses horizontal and vertical flows of contaminated groundwater (Kadlec and Knight, 1996:562). These constructed wetlands, known as subsurface flow constructed wetlands, contain degrading microorganisms similar to surface flow constructed wetland described previously. The microorganisms exist naturally throughout the soil and attach to soil particles and roots of the vegetation. Subsurface flow constructed wetlands generally do not have extended periods with water standing at the surface of the wetland. Constant groundwater flow through the constructed wetland, however, maintains a saturated soil environment to a depth just below the surface. To operate effectively, subsurface flow constructed wetlands must maintain continual groundwater flow through the system. Though the flow is minimal, it transfers contaminants and by-products of the degrading reactions through the system. Components for the subsurface flow constructed wetland include an input device, the wetland basin, microbial-enriched soil, vegetation, and an output device. Similar to the surface flow constructed wetland, the input device supplies the contaminated groundwater beneath the system. The soil used in the constructed wetland system naturally contains appropriate microorganisms unless soil conditions do not favor growth or existence of the appropriate organisms. Vegetation chosen for the constructed wetland follows the same criteria as the surface flow constructed wetland. Finally, as with the surface flow system, the output device catches the groundwater exiting the system. Unlike the surface flow

constructed wetland, however, these devices collect the exiting water at a depth of 0.3 to 0.6 meters below the surface of the wetland (Kadlec and Knight, 1996:563).

Current Air Force Project

At the time of this thesis effort, the United States Air Force in conjunction with Wright State University has funded and constructed two research cells representing subsurface constructed wetlands. These operational constructed wetland cells are research endeavors that allow scientists to observe and study behaviors in the systems. Located on Wright-Patterson Air Force Base in Dayton, Ohio, each of the cells measures approximately one hundred forty feet by sixty feet by six feet. Both cells have geomembrane liners that create an impermeable layer between the constructed wetland environment and surrounding subsurface soil. A system of pipes and electric pumps move groundwater, contaminated with PCE, from a nearby underground plume to an area beneath the cells. As the groundwater is pumped into the system, it is forced to flow vertically through the constructed wetland cells. Microbial activity and chemical reactions in the constructed wetland soils degrade contaminants and produce various by-products. Some of the by-products formed in the process are as toxic, or more toxic, than the original contaminant (PCE). Vinyl chloride (VC), for example, is produced as a by-product of the microbial degradation of PCE. As VC flows through the constructed wetland, however, other microbial activity and chemical reactions in the soil continue the degradation of VC to non-toxic compounds such as CO_2. To accomplish the continual degradation of contaminants, the constructed wetland cells are designed with multiple functional layers. These layers, having various soil characteristics, create optimal soil

conditions for contaminant degradation. One of the constructed wetland cells in the United States Air Force project, in particular, is designed with a three-layered configuration. The deepest layer, known as the methanogenic zone, is directly above the supply piping system. This zone contains organic-rich soil that favors methanogenic conditions. Having high organic matter concentration and no significant supply of oxygen, anaerobic microorganisms known as dechlorinators feed on the contaminants, initiating the degradation of PCE. By-products of this degradation include (but are not limited to) trichloroethene (TCE), various isomers of dichloroethene (DCE), vinyl chloride (VC), methane (CH_4), carbon dioxide (CO_2), and water (H_2O). The vertical flow of the constructed wetland forces these by-products (and non-reacted PCE) to the next layer of the system. This layer, an experimental layer unique to this constructed wetland, is known as the iron zone. This anaerobic layer contains soils with increased amounts of oxidized iron (Fe^{3+}), which act as electron acceptors with microbial activity to continue the degradation of several by-products from the methanogenic layer. The most significant degradation expected in the iron zone is performed on the isomers of DCE and VC. Theoretically, TCE may also degrade under iron zone conditions, but minimal evidence exists supporting this degradation. The constructed wetland flow moves contaminants out of the iron zone and into the third and final layer of the constructed wetland cell. This layer borders the ground surface and contains roots of the wetland vegetation. Therefore, oxygen is available to microorganisms through direct transfer from the atmosphere and through root exchange (from the vegetation) into the soil. This layer is referred to as the aerobic zone and provides the last microbial degradation processes on the contaminants

and by-products in the constructed wetland system. At the surface of the constructed wetland cell, a water collection device provides an outflow from the system. The existing design for outflow of both cells in the United States Air Force project transports the remediated water to the local community's sanitary sewer system for further disposal.

Iron Zone of a Constructed Wetland

The iron zone contains oxidized iron (Fe^{3+}) that serves as an electron acceptor in microbial degradation of the chlorinated contaminants DCE and VC. Expert opinions vary regarding the amount of iron content required for soil to be considered iron-rich. Most of the experts agree, however, that a soil with an iron content of at least one-percent of the soil composition by mass is iron-rich. In many soils (as in the iron zone of the United States Air Force project), however, the iron content values vary below one-percent of the soil composition.

Oxygen is not available in the iron zone, creating a strictly anaerobic environment in the soil. The microorganisms existing in the iron zone, categorized as anaerobes, thrive in anaerobic conditions. In fact, most microorganisms living in the anaerobic conditions cannot tolerate the presence of oxygen. The anaerobes survive by gaining energy through natural reduction processes.

The reduction of Fe^{3+} in the iron zone of the constructed wetland is not limited to chlorinated contaminant degradation. In fact, many other microbial processes and chemical reactions also utilize Fe^{3+} reduction in their functions. Therefore, competition for the Fe^{3+} resource exists in the iron zone. Although many processes compete for the Fe^{3+}, this thesis effort focuses on three significant reactions known to exist in the iron

zone environment. The first reaction, as mentioned previously, involves the mineralization of chlorinated contaminants such as DCE and VC. Published results of experimental data show the significant mineralization of these contaminants under Fe^{3+} reducing conditions (Bradley and Chapelle, 1997:2694). A second reaction competing for Fe^{3+} in the iron zone is hydrogen (H_2). When hydrogen is introduced as the electron donor and Fe^{3+} is available as an electron acceptor, microorganisms gain required energy for growth through the Fe^{3+} reduction process (Lovley et al, 1989:700). Organic compounds also significantly compete for Fe^{3+} in the iron zone. These compounds transfer through the constructed wetland with the flowing groundwater. Thus, when they enter the iron zone, they compete for the available Fe^{3+}. Microorganisms, naturally existing in the iron zone soil, use Fe^{3+} as an electron acceptor to oxidize the organic compounds (Lovley, 1991:264).

Iron Reduction

The reduction of Fe^{3+} to Fe^{2+} has been proven as a degradation pathway for DCE and VC under anaerobic conditions (Bradley and Chapelle, 1997:2692). This pathway follows an oxidation/reduction process; anaerobic microorganisms oxidize groundwater contaminants while reducing available Fe^{3+} (Lovley, 1991:263).

In one study, the addition of Fe^{3+} to an anaerobic aquifer microcosm caused significant mineralization of VC to CO_2 within eighty-four hours. This mineralization (15 to 34% of the VC) was significantly higher than the VC mineralization (2.8 to 4.6%) of the unchanged (without Fe^{3+} addition) control microcosms. The author attributed the mineralization observed in the experiments to microbial activity because no observable,

significant mineralization was reported in the microcosms that were sterilized (Bradley and Chapelle, 1996:2085). The following year, the same authors published results of an experiment demonstrating the mineralization of DCE under Fe^{3+} reduction conditions. Similar to the VC experiments, the sterilized controls produced no significant mineralization of the chlorinated material. Therefore, the authors attributed the mineralization to biological activity and Fe^{3+} reduction (Bradley and Chapelle, 1997:2794).

In contaminated anaerobic groundwater environments, Fe^{3+} is the most abundant potential electron acceptor for organic matter decomposition (Lovley, 1991:268). Consequently, while iron remains in oxidized (Fe^{3+}) form, no significant levels of organic matter exist in the iron zone of the constructed wetland cell.

Under conditions where iron reduction is favored, other processes, specifically sulfate reduction and methane production, are inhibited. When iron was introduced into a sulfate-reducing environment, the sulfate reduction was inhibited up to ninety percent (Lovley and Phillips, 1987:2637). A similar experiment performed by the same authors demonstrated the reduction of methane production upon the addition of a Fe^{3+} source. The declining methane production corresponded to the increase of Fe^{3+} reduction (Lovley and Phillips, 1986:685). The results reported by Lovley and Phillips directly associate the inhibition of sulfate reduction and methane production to substrate limitation.
The following figures display the behavior of sulfate reduction and methane production.

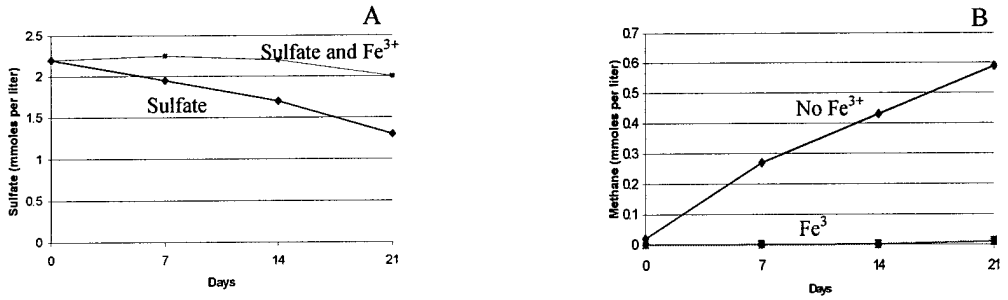

Figure 1. Effect of Fe^{3+} on Sulfate Reduction (A) and Methane Production (B) (Adapted from Lovley and Phillips, 1987)

The concept of iron concentration toxicity added to the system was rejected when additional substrate (namely hydrogen) was added to the system and sulfate reduction and methane production resumed (Lovley and Phillips, 1987:2638).

Microbial Kinetics

One kinetic modeling technique generally used to represent biological degradation is the Michaelis-Menten model for non-elementary reactions. In many instances throughout nature, microorganisms require the use of an enzyme to use available food sources. The enzyme is not consumed in the process, and the following stoichiometry results:

$$E + S \rightarrow E + P \qquad (1)$$

E = Enzyme required by microorganism

S = Substrate or food source

P = Product of food consumption

The purpose of the enzyme is to lower the activation energy for the reaction or facilitate other reactions. As the reaction proceeds, an intermediate enzyme-substrate complex (ES) follows this general behavior:

$$E + S \underset{k_2}{\overset{k_1}{\Leftrightarrow}} ES \overset{k_3}{\rightarrow} E + P \quad (2)$$

A mathematical derivation of this behavior can be written:

$$\frac{d[S]}{dt} = \frac{-k_1 k_2 [S][E]_0}{k_1[S] + k_m} \quad (3)$$

The variable k_m is defined in this equation as:

$$k_m = \frac{k_2 + k_3}{k_1} \quad (4)$$

Equation (3) is a specific variation of the Michaelis-Menten equation (Clark, 1996:447). This equation incorporates specific substrate and enzyme parameters as well as associated coefficient values (k_1, k_2, k_3) for the represented system.

In more general terms, the Michaelis-Menten equation can be written:

$$V = \frac{V_{\max} C}{k_m + C} \quad (5)$$

V = a characteristic of the system (normally changing over time)

V_{max} = the maximum value (maximum exiting velocity for this case) in the system

C = the concentration of materials directly affecting the changing velocity (or represented characteristic)

k_m = a constant determined by specific behavior of the system (normally generated empirically for the system being evaluated)

The Michaelis-Menten equation has several unique mathematical characteristics. Equation (5) will be used to explain the mathematical characteristics. First, when the concentration value used in equation (5) is very small, C (in the denominator of the equation) becomes insignificant and the expression becomes:

$$V = \frac{V_{\max} C}{k_m} \qquad (6)$$

Therefore, when low concentration values are associated with Michaelis-Menten kinetics, equation (6) creates a first-order rate expression. When the concentration values are very high, a different expression results. The k_m value in the denominator becomes insignificant and the concentration values in the equation cancel. Thus, a zero-order rate expression forms:

$$V = V_{\max} \qquad (7)$$

The following curve represents the relationship between V and C in equation (5).

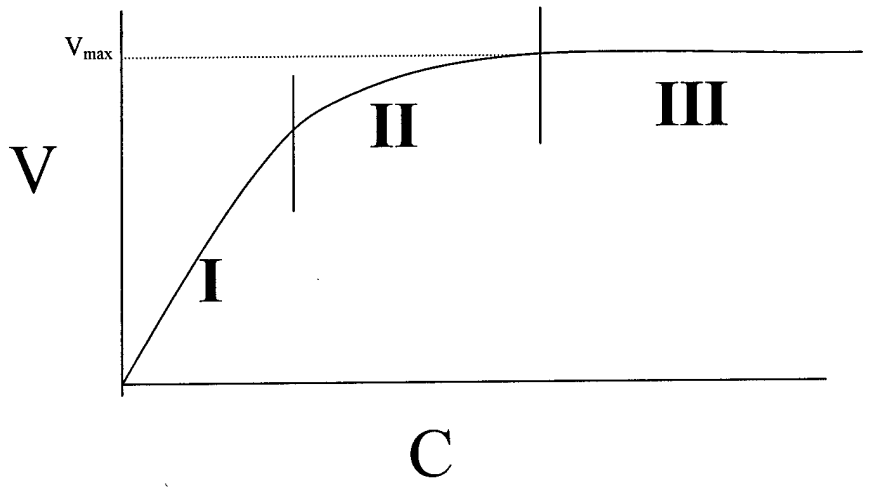

Figure 2. Michaelis-Menten Behavior Curve

In region I, the concentration is small creating a first-order rate curve, as previously described. Region III represents high concentrations, creating a zero-order rate curve. Intermediate concentrations, region II, cannot be represented with simple mathematical expressions like the other regions. Thus, values for this region must be found by referring to the Michaelis-Menten equation presented in equation (5).

Understanding the kinetics of chlorinated contaminant mineralization is vital in modeling the behavior associated with a constructed wetland. Bradley and Chapelle (1997) demonstrate that VC mineralization under Fe^{3+} reducing conditions follows Michaelis-Menten kinetics. The kinetics associated with DCE mineralization, however, follow first order behavior. The percentage rates of DCE mineralization did not vary significantly with changes in the concentration values under Fe^{3+} reducing conditions.

Therefore, the authors conclude that DCE mineralization under Fe^{3+} reducing conditions follows first-order kinetics (Bradley and Chapelle, 1997:2695).

Wetland Modeling

Constructing accurate models of wetland environments (whether natural or man-made) is difficult and complicated. Countless parameters must be considered and incorporated into these models. Each wetland environment has unique and dynamic characteristics; therefore, modelers are challenged to evaluate each parameter appropriately. In general terms, models can be grouped according to basic characteristics of the wetland environments they represent. Trends and basic properties may be identical between the wetlands in these groups. Specific model structure and rate constants, however, tend to be site specific and must be evaluated for each model.

The hydrochemical complexities of wetlands are perhaps the most important and complex physical features that control the function of the system (Mitsch et al, 1988:218). Chemical and microbial activities are dependent and closely related to the hydrology of the system. Accurate field measurements and good laboratory practices are essential for accurate model application. A general understanding of the chemical and microbial activity in the wetland system allows the modeler to evaluate the system and study internal behavior and relationships in the wetland system.

Soil conditions throughout the wetland environment are continually changing. Chemical, hydrologic, and organic changes, for example, keep the wetland environment ever changing. As contaminants move through the system and microorganisms act upon them, reactions occur, creating by-products that continually change the soil conditions.

The constant change throughout the wetland environment creates difficulty in modeling the system.

In addition to conditions within the wetland system, exchanges occur between adjacent ecosystem environments. These exchanges keep the wetland environments chemically balanced and must be represented in the modeling system. Without incorporating the exchanges between ecosystems, the accuracy of the model declines significantly.

Wetland Definitions

To accurately represent parameters in any portion of a constructed wetland, general characteristics of the system's behavior must be defined and understood. The following definitions help in understanding the background of wetland behavior.

Hydraulic Loading Rate: the rainfall equivalent of the flow rate for the constructed wetland system. The value represented is not necessarily the physical distribution of water at the wetland surface as the rainfall reference may suggest. Instead, the hydraulic loading rate is generally referred to as the contaminated groundwater flow into the system. A general equation for the hydraulic loading rate (q) is:

$$q = \frac{Q}{A} \quad (8)$$

Q = contaminated groundwater flow, volume/time, m^3/d

A = wetland area (accepting the groundwater flow), area, m^2

Note: q has units of length/time, m/d

A vertical flow constructed wetland system has continuous inlet flow so the hydraulic loading rate represents the time average linear flow rate (Kadlec and Knight, 1996:84).

Mean Water Depth: the average depth of water throughout the entire wetland.

The general equation for the mean water depth (h') is:

$$h' = \int_0^L \int_0^W h(x,y)\,dy\,dx \qquad (9)$$

L = wetland length, length, m

W = wetland width, length, m

h = water depth at coordinates (x,y), length, m

x = longitudinal distance, length, m

y = transverse distance, length, m

Note: h' typically has units of meters or centimeters

Wetland Water Volume: the volume for a subsurface flow wetland, dependent on the porosity of the system. This value is often difficult to determine due to the various physical characteristics of the soils in the system. Most constructed wetlands consisting of clean gravel or sand have a porosity range of 0.3 to 0.45 (Kadlec and Knight, 1996:85). Matter in the soil, such as decayed organic matter or minerals associated with treatment, however, tend to influence this porosity value. Although minimal, lateral flow through the system also affects the calculation of this parameter.

A general equation for the wetland water volume (V) is:

$$V = \int_0^L \int_0^W \int_0^h \varepsilon(x, y, z)dxdydz = \varepsilon V_{T'} = \varepsilon A h' \quad (10)$$

L = length of constructed wetland, length, m

W = width of constructed wetland, length, m

h = water depth, length, m

ε = water volume fraction in water column (porosity), unitless, m^3/m^3

V_T = total water volume between water and ground surface, volume, m^3

Nominal Detention Time: the time that the contaminated groundwater is in the constructed wetland. The general equation for nominal detention time (t) is:

$$t = \frac{V}{Q} = \frac{\varepsilon A h'}{Q} \quad (11)$$

Note: units for t are: time, d

For calculation purposes, the flow is generally defined as average flow (inlet flow plus outlet flow divided by 2). When variations in the total flow exist throughout the system, however, integration must be performed for an accurate flow value. For most constructed wetland systems, nominal detention times are not consistent with actual detention times. The actual detention times are usually smaller due to spatial variations in the flow conditions. Nominal times also assume that the entire volume of water is involved with the flow. Kadlec and Knight (1996) report an example of the variation in nominal and actual detention times. In the Boggy Gut treatment wetland, the nominal detention time

was estimated at nineteen days; however measurements of actual detention times yielded a time of only two days. Again, the difference in these times was associated with large areas of wetland soils not directly associated with the flow path (Kadlec and Knight, 1996:85).

Actual Velocity: flow velocity observed through the system. The general equation for the actual velocity (υ) is:

$$\upsilon = \frac{Q}{(\varepsilon A)_c} \qquad (12)$$

υ = velocity of the groundwater through the constructed wetland, velocity, m/d

$(\varepsilon A)_c$ = open area perpendicular to flow, area, m^2

Superficial velocity: calculated velocity through system disregarding porosity parameter. The general equation for the superficial velocity (u) is:

$$u = \frac{Q}{A_c} \qquad (13)$$

u = superficial velocity through system, velocity, m/d

A_c = area perpendicular to flow, area, m^2

Therefore, it is clear that the relationship between superficial and actual velocities is the porosity term:

$$u = \varepsilon \upsilon \qquad (14)$$

Hydroperiod: a general wetland term relating to the number of days per year a wetland environment has surface water present. If a wetland site were dry ten percent of the year, for example, the hydroperiod for the wetland would be 328 days. Continuous source treatment wetlands (such as the Air Force project constructed wetland) typically have hydroperiods of 365 days. The hydroperiod exists throughout the year due to continual pumping through the wetland system.

Water Mass Balance: the change in water volume through inputs and outputs of the system over a period of time. The water budget is extremely dynamic for a constructed wetland system. Gains to the system include influent, precipitation, runoff, and snowmelt. Depending on the system design, another possible input to the water balance is infiltration. Losses to the constructed wetland system include the effluent, evapotranspiration, bank loss and (again, depending on design) infiltration to groundwater. A general equation that incorporates the gains and losses is:

$$\frac{dV}{dt} = Q_i - Q_o + Q_c - Q_b - Q_{gw} + Q_{sm} + PA_w + ETA_w \quad (15)$$

Q_i = influent rate, volume/time, m^3/d

Q_o = effluent rate, volume/time, m^3/d

Q_c = catchment runoff rate, volume/time, m^3/d

Q_b = bank loss rate, volume/time, m^3/d

Q_{gw} = infiltration to groundwater, volume/time, m^3/d

Q_{sm} = snowmelt rate, volume/time, m^3/d

P = precipitation rate, unit/time, m/d

A_w = wetland top surface area, area, m^2

ET = evapotranspiration rate, unit/time, m/d

The influent and effluent rates are controllable in a constructed wetland and depend on treatment requirements and design. The evapotranspiration and precipitation rates are not generally controllable. Values for these parameters can be estimated with climate, historical data, and surrounding environments. The bank loss rate and infiltration can be controlled in a constructed wetland with an impermeable membrane or dense clay layer surrounding the wetland soil. Certain design parameters such as berms and borders also limit the runoff rates. As with precipitation, the snowmelt factor depends on the geographic location of the constructed wetland site. Evaluating the water budget for a constructed wetland is important for numerous reasons. With too much water loss in the system, contaminant concentrations increase and exit the system. Additionally, too much water can dilute or overload the system, affecting behavior of the microorganisms performing the treatment degradations (Kadlec and Knight, 1996:88).

Hydrogen Association in Fe^{3+} Zone

Naturally occurring hydrogen (H_2) in a constructed wetland system plays a significant role in the reduction of Fe^{3+}. For many years, scientists have claimed that the reduction of Fe^{3+} to Fe^{2+} (in association with H_2) provides for the growth of microorganisms (Balashova and Zavarzin, 1980:635). Balashova and Zavarzin (1980) performed an experiment using hydrogen bacteria in the presence of H_2. They wanted to evaluate the difference in microbial biomass with and without the availability of Fe^{3+}. In

the experiments, a yeast extract was required for growth of the microorganisms. Under strict anaerobic conditions, the experiment yielded the following data after 10 days:

Table 1. Experimental Data Collected from Microbial Growth in the Presence of H_2 and Yeast Extract (Adapted from Balashova and Zavarzin, 1980)

	Cells/ml	Fe(3+) mg/l	Fe(2+) mg/l
Sterile oxygen (no microorganisms)	0	120	0
Medium without iron source	3,000	0	0
Complete medium	4,000,000	0	112

Clearly, the anaerobic growth on the yeast extract is significantly less (approximately 10^3 times less) without Fe^{3+} available. Balashova and Zavarzin concluded that the iron reduction supplies the organism with added energy for growth. Other work on hydrogen bacteria identified a microorganism that grew with H_2 acting as the electron donor and Fe^{3+} acting as the electron acceptor (Lovley et al, 1989:700). Unlike previous experiments, however, the yeast extract (referenced in Balashova and Zavarzin's 1980 experiment) was not required for the microbial growth. The microorganisms, identified as *Alteromonas putrefaciens*, oxidized H_2 as Fe^{3+} was reduced to Fe^{2+}. The metabolism directly relates to cell growth, as there was no cell growth in the experimental H_2 atmosphere samples without Fe^{3+}. Results of the experiments are shown in Table 2

and Figure 3 below:

Table 2. Fe^{3+} Reduction by *A. putrefaciens* ATCC 8071 with Hydrogen as Potential Electron Donor (Adapted from Lovley et al, 1989)

Electron donor(s)	Fe(2+) produced *a*	Hydrogen consumed *a*	Fe(2+)/H2
None	0.3	0	n/a
Hydrogen *b*	150	78	1.9

a Micromoles of Fe^{3+} produced or H_2 consumed during 20-hour incubation period

b Initial H_2 partial pressure ca. 11 Pa

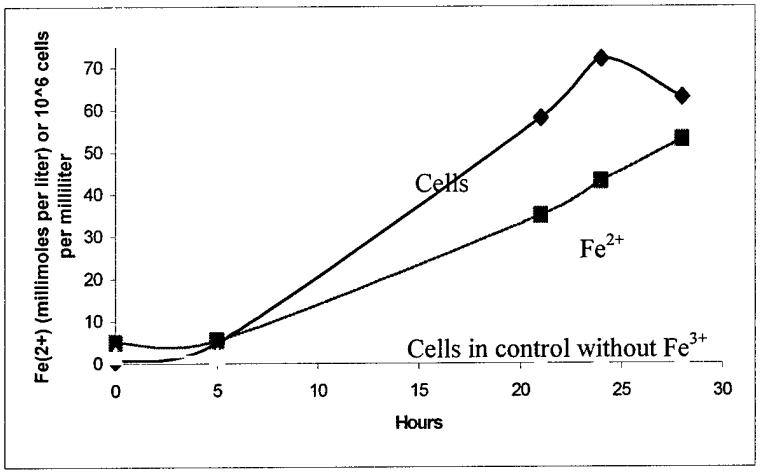

Figure 3. Growth of *A. putrefaciens* ATCC 8071 with H_2 as the Electron Donor and Fe^{3+} as the Electron Acceptor (Adapted from Lovley et al, 1989)

From the experimental results, approximately two moles of H_2 were consumed for each mole of Fe^{3+} reduced. This ratio corresponds to the findings of Balashova and Zavarzin (1980). The following reaction results:

$$H_2 + 2Fe^{3+} \rightarrow 2H^+ + 2Fe^{2+} \quad (16)$$

Lovley et al. (1989) concluded that *A. putrefaciens* obtained energy from the oxidation of H_2 coupled with the reduction of Fe^{3+} (Lovley et al., 1989:704). This conclusion matches

previous work by others (Balashova and Zavarzin (1980), for example). The microorganisms in Lovley's experiments, however, did not require a yeast extract associated with the hydrogen for growth (Lovley et al, 1989:704).

Further work by Lovley et al. identified *Pelobacter carbinolicus* as another microorganism that grows in a medium with H_2 as an electron donor and Fe^{3+} reduced to Fe^{2+} (Lovley et al, 1995:2134). The experimental data supports reaction (16) above.

Organic compounds influencing reduction of Fe^{3+}

Numerous organic compounds form as products from organic matter decomposition in the initial degrading processes of a constructed wetland. Organic compounds also exist naturally throughout the wetland soil. Regardless of origin, these organic compounds transfer through the soil with the moving groundwater. Therefore, organic compounds are introduced to Fe^{3+} available in the soil. This interaction creates the potential for significant release of nutrients from mineralization processes with Fe^{3+} as the electron acceptor (Lovley and Phillips, 1986:683). Kamura et al (1963) demonstrated that added acetate (in an environment containing Fe^{3+}) was directly associated with carbon dioxide production and Fe^{2+} accumulation. In the experiment (as in nature), the acetate, acting as the electron donor, enables the Fe^{3+} reduction to Fe^{2+}. This result, duplicated and supported by Lovley in 1986, suggests that Fe^{3+} has potential to be a significant source for organic decomposition in anaerobic conditions (Lovley and Phillips, 1986:687). Further study identified GS-15 as a microorganism that couples organic matter oxidation (specifically acetate in these studies) with Fe^{3+} reduction to provide for growth under anaerobic conditions (Lovley et al, 1987:253).

The following three figures (Figure 4, 5, and 6) illustrate Lovley's findings involving acetate metabolism and GS-15 growth in association with Fe^{3+} reduction:

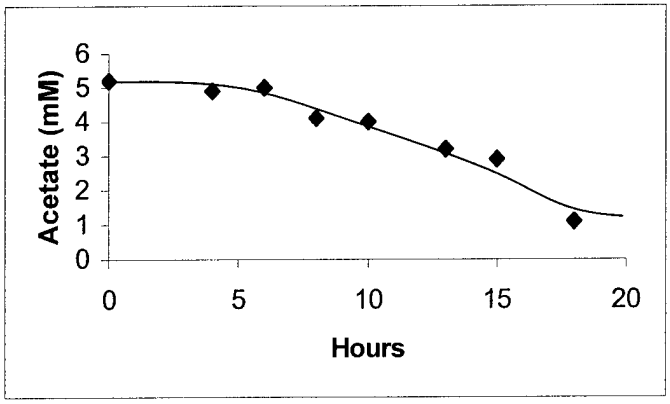

Figure 4. Concentration of Acetate Over Time in Fe^{3+}-citrate Medium Inoculated with GS-15 Microorganisms (Adapted from Lovley and Phillips, 1988)

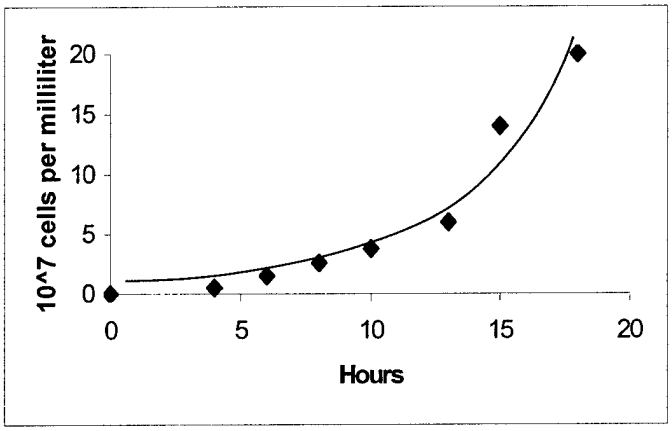

Figure 5. Concentration of GS-15 Cell Numbers Over Time in Fe^{3+}-citrate Medium (Adapted from Lovley and Phillips, 1988)

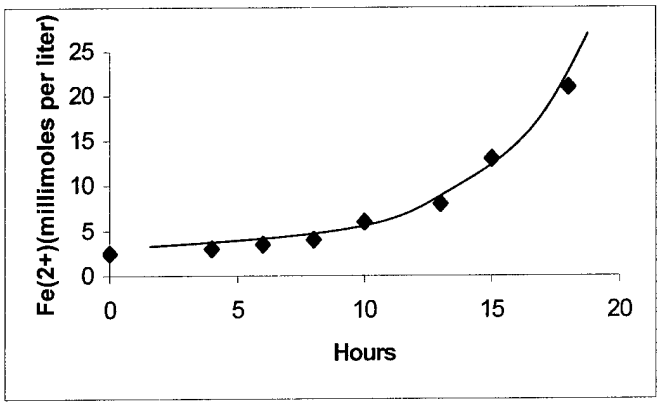

Figure 6. Concentration of Fe^{2+} Over Time in a Fe^{3+}-citrate Medium Inoculated with GS-15 Microorganisms (Adapted from Lovley and Phillips, 1988)

The acetate consumption for the above experiment indicates that acetate was the sole electron donor for the Fe^{3+} reduction (Lovley and Phillips, 1988:1476). The stoichiometry for the acetate consumption and Fe^{2+} accumulation includes one mole of acetate oxidized to two moles of carbon dioxide and eight moles of Fe^{3+} to eight moles of Fe^{2+}. A general expression for the acetate metabolism is:

$$CH_3COO^- + 8Fe^{3+} + 3H_2O \rightarrow 8Fe^{2+} + HCO_3^- + CO_2 + 8H^+ \quad (17)$$

The products of this expression show carbon dioxide in two forms. The HCO_3^- (bicarbonate) term represents the carbon dioxide dissolved in water. The CO_2 term represents the carbon dioxide formed in the reaction that is not dissolved in water. As illustrated, both forms of carbon dioxide are produced in this reaction; formation of the various forms is dependent on the pH of the system. The actual reaction in nature is more complicated than this simple expression. Various forms of iron sources and cell synthesis create complexity in this expression (Lovley and Phillips, 1988:1476).

Additional experiments show that microorganisms can also oxidize formate with the reduction of Fe^{3+} (Lovley et al, 1989:702). Similar to acetate metabolism, the microorganisms, identified as *A. putrefaciens*, obtain energy for growth by oxidizing the formate and reducing Fe^{3+} (Lovley et al, 1989:703).

The following figures illustrate results from the formate metabolism experiments:

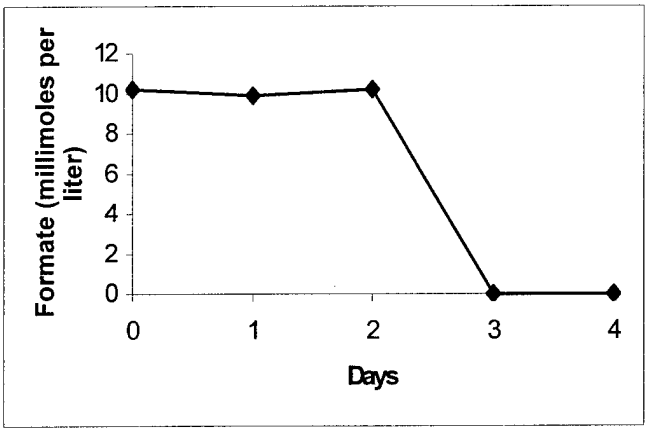

Figure 7. Concentration of Formate Over Time with Fe^{3+} Reduction by *A. putrefaciens* (Adapted from Lovley et al, 1989)

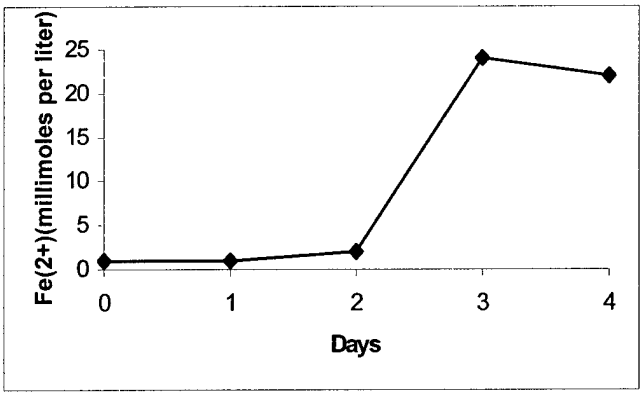

Figure 8. Fe^{2+} Accumulation Over Time with *A. putrefaciens* Microorganism Growth (Adapted from Lovley et al, 1989)

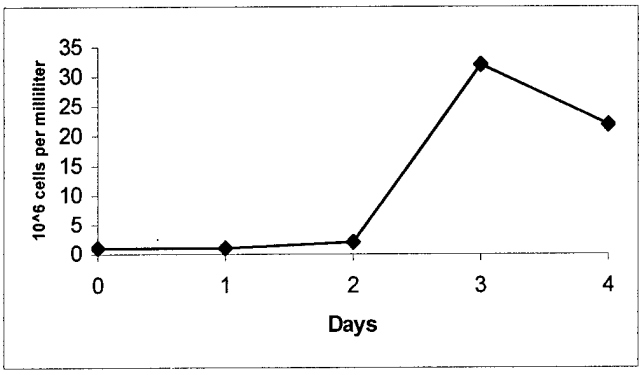

Figure 9. Growth of *A. putrefaciens* with Formate as Electron Donor and Fe^{3+}-citrate as Electron Acceptor (Adapted from Lovley et al, 1989)

The stoichiometry for the formate consumption includes one mole of formate oxidized to one mole of carbon dioxide and two moles of Fe^{3+} reducing to two moles of Fe^{2+}. A general expression for this formate oxidation is:

$$HCOO^- + H_2O + 2Fe^{3+} \rightarrow HCO_3^- + 2H^+ + 2Fe^{2+} \quad \textbf{(18)}$$

Similar to the acetate expression, the carbon dioxide formed in this reaction is in the bicarbonate (HCO_3^-) form. The carbon dioxide formed is dissolved in water.

III. Methodology

Constructed wetlands are biologically complex systems with countless interactions and relationships among internal parameters. One method to evaluate internal behavior and relationships in the constructed wetland is system dynamics. Using a mechanistic model of the constructed wetland, system dynamics incorporates internal feedback loops, time-sensitive behavior, and conditional changes associated with the complexity of the system.

System dynamics simulates basic internal behavior patterns; it focuses on the fundamental relationships and processes involved in the constructed wetland. System dynamics differs from other empirically based modeling techniques that tend to overlook the underlying processes (Moorehead et al, 1996:138). Through simulation, system dynamics allows the study of internal relationships, system boundaries, and behavior of individual parameters in the system.

The system dynamics approach is divided into four separate phases. The first, called conceptualization, familiarizes the modeler with the general problem area and develops organizations concepts. Formulation, the second phase of system dynamics, involves building a model and selecting parameter values in the system. The third phase is testing; in this phase, behavior and structure configuration of the mechanistic model is evaluated. The final phase, called implementation, demonstrates the practical use of the model in managing the system. Because the system dynamics process is iterative in nature, portions of the model may require multiple reformulation steps and, in turn,

require the modeler to repeat the previously described phases to provide a mechanistic representation of the processes under consideration.

Conceptualization

The model presented in this thesis effort is a detailed section of another mechanistic model produced by Captain Colby Hoefar of the Air Force Institute of Technology in 2000. The structural framework of Hoefar's model (and ultimately this thesis effort) is presented as a cross-sectional area of the constructed wetland. The constructed wetland cell modeled in this thesis effort has three distinctive soil layers where individual and sequential bioremediation processes degrade the contaminants.

This thesis effort specifically models the middle zone in the constructed wetland system. This zone, called the iron zone, is a research endeavor and is a unique layer introduced into this constructed wetland cell. The literature provides limited information about the oxidized iron depletion in contaminant degradation processes. Three contaminants known to degrade through a mineralization process with oxidized iron as an electron acceptor are VC, *cis*-DCE, and *trans*-DCE. These contaminants are daughter products from degradation processes in the methanogenic zone. These three contaminants will be modeled and evaluated in this thesis effort. Other contaminants in the constructed wetland system (non-reacted PCE and TCE, for example) flow through the iron zone and will not be considered in this thesis effort. In addition to the described contaminants, organic matter also reacts with the oxidized iron in the iron zone. This organic matter flows into the iron zone with the groundwater flow from the methanogenic zone. The organic material flowing into the iron zone exists in many forms. Modeling

every form of organic material in the iron zone is unrealistic for this thesis effort. Therefore, five organic acids and two types of alcohol have been chosen to represent the organic material in the iron zone. The organic acids modeled will be acetic acid, formic acid, propionic acid, butyric acid, and lactic acid. The two forms of alcohol modeled will be ethanol and methanol. Although other organic material may also react with the oxidized iron, the modeler and committee of this thesis believe that the reactions of these seven organics are significant and represent the majority of the organic material activity in the iron zone. Another component modeled in this thesis effort is hydrogen. Through the oxidized iron depletion processes occurring in the iron zone, hydrogen (H_2) and the hydrogen ion (H^+) are produced. These forms of hydrogen then continue the degradation of oxidized iron or flow out of the iron zone with groundwater flow.

Figure 10 is a conceptual illustration of the oxidized iron depletion in the iron zone in the context of the entire constructed wetland system. The arrows in the figure represent where the chemicals initiate (tail of arrow) and flow (head of arrow). Arrows going across a zone (PCE, TCE, CH_4, CO_2, and H^+ crossing the iron zone, for example) show that these chemicals do not degrade and move directly through the zone.

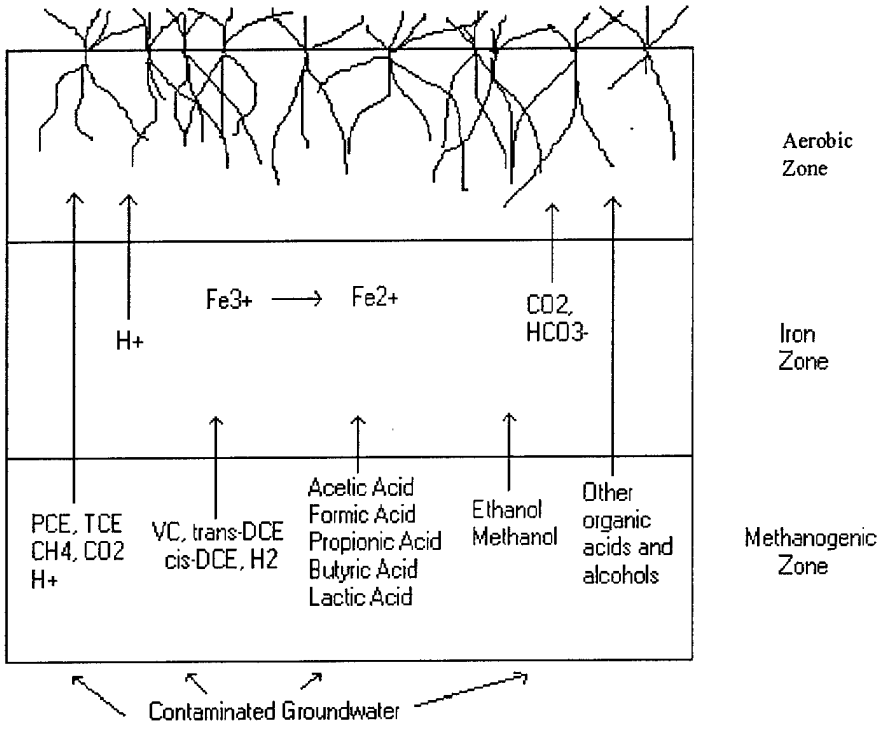

Figure 10. Cross-sectional Illustration of Degrading Materials in Constructed Wetlands

Formulation

In preparation for producing a model of the iron zone, an appropriate software package must be chosen. For this thesis effort, STELLA 6.0 Research, provided by High Performance Systems is chosen. The software uses stocks (accumulations in the model) and flows (rates of movement) to model the system. Model development requires knowledge of degrading processes occurring in the iron zone. In general, the model produced in this thesis effort has been produced using a mass balance approach; educated assumptions for reaction rates and other parameters will be used when not available in the literature.

To model microbial activity in the iron zone, reactions for oxidized iron depletion, contaminant degradation, hydrogen reduction, and organic reduction are necessary.

Representing every possible reaction occurring in the iron zone is unrealistic due to the countless microbial interactions and dynamic behavior of microorganisms in the system. Additionally, limited information in the literature about oxidized iron depletion makes representing the reaction in the iron zone a difficult task. Therefore, for the purpose of modeling in this thesis effort, the modeler has proposed the following ten reactions. These reactions, formed using the contaminants, hydrogen, and organic materials listed previously in this chapter, represent the dominant degradation activity in the iron zone. Note that the form of oxidized iron throughout the reactions is hematite (Fe_2O_3). Also, the reduced form of iron in the reactions is $Fe(OH)_2$. Although numerous other forms of oxidized and reduced iron are available in nature, these forms of iron have been chosen to simplify the modeling process. The first reaction involves VC:

$$C_2H_3Cl + Fe_2O_3 + 5H_2O \rightarrow 2CO_2 + 2Fe(OH)_2 + 9H^+ + Cl^-$$

The next reaction represents both isomers of dichloroethene (*cis*-DCE and *trans*-DCE):

$$C_2Cl_2H_2 + Fe_2O_3 + 5H_2O \rightarrow 2CO_2 + 2Fe(OH)_2 + 8H^+ + 2Cl^-$$

Hydrogen is represented in the model with the following reaction:

$$2H_2 + Fe_2O_3 + H_2O \rightarrow 2Fe(OH)_2 + 2H^+$$

The next five reactions represent the reaction for the organic acids modeled:

Acetic Acid:

$$CH_3COOH + Fe_2O_3 + 5H_2O \rightarrow 2HCO_3^- + 2Fe(OH)_2 + 8H^+$$

Formic Acid:

$$HCOOH + Fe_2O_3 + 2H_2O \rightarrow HCO_3^- + 2Fe(OH)_2 + H^+$$

Propionic Acid:

$$C_2H_5COOH + Fe_2O_3 + 3H_2O \rightarrow CH_3COOH + 2Fe(OH)_2 + CO_2 + H_2$$

Butyric Acid:

$$C_3H_7COOH + Fe_2O_3 + 5H_2O \rightarrow CH_3COOH + 2Fe(OH)_2 + 2CO_2 + 5H_2$$

Lactic Acid:

$$2C_3H_5O_3H + Fe_2O_3 + H_2O \rightarrow C_2H_5COOH + CH_3COOH + 2Fe(OH)_2 + CO_2$$

The last two reactions represent the two forms of alcohol modeled:

Ethanol:

$$C_2H_5OH + Fe_2O_3 + 4H_2O \rightarrow 2CO_2 + 2Fe(OH)_2 + 10H^+$$

Methanol:

$$CH_3OH + Fe_2O_3 + 2H_2O \rightarrow CO_2 + 2Fe(OH)_2 + 4H^+$$

In natural soils, levels of biomass (given acceptable soil conditions) generally exist at relatively constant levels. For the purpose of this thesis effort, the biomass existing in the iron zone is assumed to support the modeled reactions. Biomass growth and death rates will not be considered in this model. With the increased organic and contaminant concentrations entering the iron zone, this simple assumption may not be

appropriate for modeling the activity in the iron zone. Future study and model modification is required to determine the impact of this assumption on the system.

In order to maintain simplicity in the model and for the reader, the iron zone model (found in Appendix A) has been separated into numerous sectors. The first sector (Fe^{3+} reduction to Fe^{2+}) represents the degradation of oxidized iron (hematite) to reduced iron ($Fe(OH)_2$). The reduction is represented by the "Reduction Contribution" flow and contains input from other sectors in the model. Note the conversion factor reducing hematite (Fe_2O_3) to $Fe(OH)_2$.

The "Contaminant Degradation" sector incorporates the three chlorinated contaminants modeled in the system. Through the use of arrays, each contaminant (VC, *cis*-DCE, and *trans*-DCE) is separately represented in the model. The contaminant stock represents the accumulation of each contaminant in the system. A single inflow feeds the "Contaminant" stock. The degradation of the contaminants is represented by the "Mineralization" flow out of the "Contaminant" stock. Built into the model is a Michaelis-Menten equation, which incorporates a K_m value for the oxidized iron in the system. Note that the "Mineralization" flow is arrayed; the following equation represents the VC (one of the three contaminants modeled) portion of the model:

$$Mineralization_{VC} = \frac{(V_{\max(VC)})(C_{VC})(C_{hematite})}{(K_{m(VC)} + C_{VC})(K_{m(hematite)} + C_{hematite})} \quad \textbf{(19)}$$

Appropriate conversion factors will be built into the model to account for the molar equivalent mass for each reactant and product in the reaction in order to maintain mass balance in the model (VC to CO_2, for example). Bulk groundwater flow transports any

hydrogen ion and chloride ion (produced in the contaminant degradation) out of the iron zone in accordance with its concentration in the water.

The next sector is the "Hydrogen" sector. A "Hydrogen in Fe Zn" stock accounts for the accumulation of hydrogen in the iron zone. This stock is fed by the inflow of hydrogen from the methanogenic zone as well as flows from the "Propionic Acid" and "Butyric Acid" sectors. As with the contaminants, a Michaelis-Menten equation (incorporating the oxidized iron's K_m) represents the reduction of hydrogen in the system:

$$reduction(H_2) = \frac{(V_{\max(H_2)})(C_{H_2})(C_{hematite})}{(K_{m(H_2)} + C_{H_2})(K_{m(hematite)} + C_{hematite})} \qquad (20)$$

The bulk groundwater flow transports hydrogen not used in the iron zone degradation to the aerobic zone; the system's flow moves the hydrogen in accordance with its concentration in the water. Again, appropriate conversion factors maintain mass balance in the model.

With noted exceptions, the seven organic materials' model structures are similar. Each sector contains a stock, which accounts for the accumulation of the organic material in the system. Each stock in the organic sectors is fed by the methanogenic zone. Additionally, several stocks have multiple inputs; acetic acid, for example, is fed by the "Propionic Acid," "Butyric Acid," and "Lactic Acid" sectors. The reduction of the organic materials in the model is represented by a Michaelis-Menten equation (incorporating the oxidized iron's K_m):

$$reduction(organic) = \frac{(V_{\max(organic)})(C_{organic})(C_{hematite})}{(K_{m(organic)} + C_{organic})(K_{m(hematite)} + C_{hematite})} \qquad (21)$$

Materials (such as bicarbonate, carbon dioxide, hydrogen, and hydrogen ion) produced in individual reactions will be modeled by flows exiting the appropriate sectors. The reaction involving acetic acid, for example, produces hydrogen ion. Therefore, a flow exists between the "Acetic Acid" and "Hydrogen Ion" sectors. In each organic sector, a bulk water flow moves any non-reacted organic material out of the iron zone in accordance with its concentration in the water. Appropriate conversion factors, built into the model, account for the molar equivalent mass for each reactant and product in the reactions.

The "CO_2" sector has the "CO_2 in Fe Zn" stock that is fed by numerous flows. First, CO_2 inflow from the methanogenic zone enters the stock. Additionally, the stock is fed by the "Contaminant Degradation" (all three contaminants modeled), "Propionic Acid," "Butyric Acid," "Lactic Acid," "Ethanol," and "Methanol" sectors. The CO_2 entering and produced in the iron zone flows to the aerobic zone with the groundwater flow of the constructed wetland.

The "Bicarbonate" sector contains the "Bicarbonate in Fe Zn" stock that is fed by the inflow from the methanogenic zone as well as the "Acetic Acid" and "Formic Acid" sectors. Similar to carbon dioxide in the "CO_2" sector, bicarbonate entering and formed in the iron zone flows to the aerobic zone with the groundwater flow of the system.

The "Hydrogen Ion" sector is centered around the "Hydrogen ion in Fe Zn" stock that is fed by the inflow from the methanogenic zone as well as the "Contaminant Degradation" (all three contaminants modeled), "Hydrogen," "Acetic Acid," "Formic Acid," "Ethanol," and "Methanol" sectors. Groundwater flow moves any hydrogen ion

out of the iron zone (and into the aerobic zone) in accordance with its concentration in the water.

The final sector in the model is the "Parameters for Model" sector. In this sector, parameters for the model are defined. Also, conversion factors accounting for the molecular differences for the reduction of iron in the "Fe^{3+} reduction to Fe^{2+}" sector are in this sector.

Testing

Testing the Model Dynamics. Before using the model for simulations of natural activity, two model runs will be performed to verify that the basic mechanisms and internal parameter relationships produce appropriate behavior. Values (original values for the model) will be inserted into the model, and the first model run will be performed. Then, the organic material inflows will be set to zero. With no other materials competing for the hematite in the system, the contaminant degradation should remain constant throughout the second run. This behavior will be evaluated. If observed behavior is not appropriate, the model will be evaluated to determine whether the internal relationships are correctly represented. Expected behavior does not necessarily prove that the model is correct. It simply builds confidence in this portion of testing.

Structure-verification Test. This test relates the structure of the model to that of the actual system it represents. Throughout model construction, the modeler will evaluate each stock, flow, and converter put into the model. Then, after completion of the model, experts knowledgeable about the actual system will review the model structure. The model's structure must not contradict the structural integrity of the actual system.

Additionally, the model structure will be compared with previous models of constructed wetlands (notably Hoefar's model).

Extreme-conditions Test. This test determines if the model behaves appropriately given extreme conditions. Three model runs will be performed to test the model. Parameter values, including groundwater flow, concentration of contaminants, concentration of organics, and concentration of hydrogen, will be changed to represent extreme high and low values. For the first model run, parameters will be set to original values. This run will allow the modeler to compare the extreme runs to a run under normal parameter values. The second run will incorporate extremely high parameter values, and the third run will incorporate extremely low parameter values. The extreme values will be chosen by the modeler and reported with the output results in Chapter Four. Model output for runs two and three will be observed for unsuspected behavior and model failure.

Implementation

Testing procedures, as described, do not prove model correctness in relation to the actual system. As more tests are performed and "passed," however, the modeler builds confidence in the model and the system dynamics approach. Once this confidence is gained, the model can be utilized to explore various parameter combinations and determine optimal contaminant destruction. Further, sensitivity analysis on parameters in the model can be used to determine the areas of the model which have the most impact to the system. From the results of the sensitivity analysis, model users can optimize

treatment conditions for the constructed wetland cell as well as establish research priorities based on parameters found to be important in contaminant treatment.

Once the iron zone portion of the constructed wetland is produced and tested, simulations will be run to evaluate the behavior and contaminant treatment ability of the constructed wetland system. The first two sets of simulations (described below) perform sensitivity analyses on uncertain parameters in the model. By observing the results of these analyses, conclusions can be drawn about the importance for additional sampling and work to determine actual tested values for the questionable parameters. The other four sets of simulations involve changing engineered-controlled parameters of the model and observing the resulting behavior.

In several of the following simulation sets, the modeler chooses to evaluate the behavior of the ten simulations. The ten simulations allow the modeler to represent a wide range of parameter values and parameter value combinations in the system. By limiting the simulations to ten, however, results can be easily interpreted. Future studies on this model may include expanding these numbers of simulations and combinations in the system. Additionally, the combinations chosen in the following simulation sets have no direct association to literature or experimental sampling. The modeler attempts to provide a wide range of parameters and combine various parameter values for the materials modeled. Additionally, values chosen in model simulations incorporate expert opinions. For example, in the majority of the simulations, the modeler chooses higher concentration values for acetic and formic acid compared to the other organics, hydrogen, and contaminants. Though these values and combinations are not directly associated with

literature or experimental work (at the time of this thesis effort), expert opinions lead the modeler to the parameter selections. Again, future studies may expand these combinations or use parameter values associated with future samples taken from the actual constructed wetland.

The first set of simulations involves V_{max} parameters in the system. A total of sixty-seven simulations will be performed in this set. The V_{max} parameter plays a vital role in the Michaelis-Menten kinetics of contaminant, hydrogen, and organic reactions. Results of laboratory experiments providing values for V_{max} parameters are limited in the literature. Therefore, it is necessary to evaluate the importance (by studying the impact) of these numbers for each material modeled in the system. Values assigned to each material modeled come from the limited experiments in the literature (Bradley and Chapelle (1997) for example), previous models (Hoefar's model), and educated approximations (for materials not found in literature or previous models). These values assigned will be referred to as original values for the model. For each contaminant, organic, and hydrogen, five values (a total of fifty-five values) will be chosen incorporating a range for each material. The original value for each material falls approximately in the middle of these ranges. Values chosen for each material will be order of magnitudes below and above the original values. The values chosen for each material is reported in Chapter Four. The modeler expects the actual V_{max} value for each material to be in the simulated range. Fifty-five simulations will be run using values chosen for each material modeled. While individual parameters are changed for each simulation, the other parameters in the model will remain constant (as original values).

Next, ten simulations will be run representing intermediate V_{max} values for the system. The intermediate values (for each material) used in the simulations will be in the same range used for the first fifty-five simulations of this set. As described earlier in this chapter, these ten simulations incorporate possible combinations of V_{max} values. Instead of changing individual material parameters per simulation, however, all material parameters will be changed for each of the ten simulations. Parameter values used in these simulations will be reported in Chapter Four. Finally, two simulations will be run representing extreme values for V_{max} parameters. For the first simulation, all material V_{max} parameters will be set to the lowest values used in the respective ranges. Then, all material V_{max} parameters will be set to the highest values used in the respective ranges (values used will be reported in Chapter Four).

The second set of simulations modifies the K_m parameters in the system. A total of seventy-seven simulations will be performed in this set. Similar to the V_{max} parameter, K_m values are important in the Michaelis-Menten equations in the model, but limited experiments (found in the literature) place values on these parameters. In addition to the materials simulated in the first set, hematite also has a K_m value, which must be evaluated. Values assigned to each material (referred to as original values) come from limited experiments in the literature (Bradley and Chapelle (1997) for example), previous models (Hoefar's model), and educated approximations (for materials not found in literature or previous models). For each contaminant, organic, and hydrogen, five values (a total of fifty-five values) will be chosen incorporating a range for each material. Also, ten values will be chosen for hematite. Note the additional values to be simulated for

hematite. These additional values (and ultimately simulations) will be performed because hematite's K_m value exists in all Michaelis-Menten equations in the model. The original value for each material (contaminants, hydrogen, organics, and hematite) falls approximately in the middle of the respective ranges; values chosen for each material will be orders of magnitude below and above the original values and can be found in Chapter Four. Sixty-five simulations (five for each contaminant, hydrogen and organic and ten for hematite) will be run using values chosen for each material modeled. While individual parameters will be changed for each simulation, the other parameters in the model will remain constant (as original values). Next, ten simulations will be run representing intermediate K_m values for the system. The intermediate values (for each material) used in the simulations will be in the same range used in earlier simulations in this set. These ten simulations incorporate possible combinations of K_m values. Instead of changing individual material parameters per simulation, however, all material parameters will be changed for each of the ten simulations. Parameter values used in these simulations will be reported in Chapter Four. Finally, two simulations will be run representing extreme values for K_m parameters. For the first simulation, all material K_m parameters will be set to the lowest values used in the respective ranges. Then, all material K_m parameters will be set to the highest values used in the respective ranges (values used will be reported in Chapter Four).

The third set of simulations involves the "Fe3 Hematite" stock parameter. A total of fifteen simulations will be performed in this set. In the field, engineers can not evaluate the exact amount of hematite in the soil. Therefore, these simulations vary the

amount of hematite with all of the other parameters held constant (as original values). Hematite depletion behavior can be evaluated with these simulations. The smallest value simulated is approximately one ten-thousandth of a percent (0.0001 %) of the soil (by mass), and the highest value is approximately one percent (1 %) of the soil (by mass). Other simulations (between these extreme values) will also be simulated.

The fourth set of simulations involves the groundwater flow parameter. Recall that the model assumes continuous groundwater flow through the constructed wetland system. A total of twenty-five simulations will be performed in this set. For the United States Air Force project, the desired retention time for groundwater flow through the entire constructed wetland is approximately five to twenty-five days. This retention time relates to groundwater flow through the wetland of 15.71 gallons/minute to 3.14 gallons/minute, respectively. Realistically, however, the groundwater retention time could vary between one day and twenty-five days or longer (groundwater flow 78.55 gallons/minute to 3.14 gallons/minute). Flow rates associated with retention times lower than one day are not desired and may negatively affect the design of the constructed wetland. Channeling, for example, may occur (at high flow rates) throughout the wetland and compromise the evenly distributed flow (assumed throughout the constructed wetland). Also, flow rates associated with retention times higher than twenty-five days are not desired. When retention times reach high levels (above twenty-five days, for example), the total volume flow through the constructed wetland may become less than that required to capture the contaminated groundwater plume. As a result, actions would need to be taken to contain the contaminated groundwater until the constructed wetland

could treat it. For this thesis effort, flow rates will be simulated starting at one-day retention time (groundwater through the entire constructed wetland system) and increased in increments to twenty-five days retention time. Values used in these simulations will be reported in Chapter Four.

The fifth and sixth sets of simulations involve the inflow concentration parameters for each material in the system. The fifth set contains thirty-two simulations while the sixth set contains forty-seven. Naturally, the contaminants, hydrogen, and organics flow into the iron zone at various concentrations. Without sampling the groundwater entering the iron zone of an operational constructed wetland (not available at the time of this thesis effort), exact values for the concentrations are not available. Therefore, educated approximations for each material's inflow concentrations will be made and entered into the model. Concentration values of identical materials in similar soils will be taken into consideration when approximating these values. Once entered into the model, the approximations will be known as original values. The fifth set of simulations accounts for the contaminants and hydrogen. For each contaminant and hydrogen, five values (a total of twenty simulations) will be chosen incorporating a range for each material. Similarly, in the sixth set of simulations, five values are chosen for each organic (totaling thirty-five simulations). Values chosen for each material are orders of magnitude below and above the original values. For these first simulations (first twenty in fifth set and thirty-five in sixth set) individual parameters are changed for each simulation while the other parameters in the model remain constant (as original values). The next ten simulations for each set will be run representing intermediate inflow concentration

values. The values (for each material) used in these simulations are in the range used in previous simulations (just described). The ten simulations for the fifth set will represent possible combinations of contaminant. Likewise, the ten simulations in the sixth set will represent possible organic combinations (contaminant and hydrogen constant at original values) in the system. Values used in these simulations will incorporate combinations from the entire ranges for each material. Parameter values used in these simulations will be reported in Chapter Four. The final two simulations (for each simulation set) represent extreme values for the inflow concentration parameters. In the fifth set, the contaminant and hydrogen values will be simultaneously minimized (in relation to respective ranges) for one simulation and simultaneously maximized for another simulation. For the sixth set, similar simulations will be run for all the organic materials.

IV. Results and Discussion

The results of testing and model simulations are reported in this chapter to build confidence in the iron zone model of a constructed wetland. Model simulations representing behavior in the iron zone (described in Chapter 3) will be discussed to provide understanding of the dynamic processes in the constructed wetland system. This model, combined with studies of the other layers in the constructed wetland, provide understanding for a viable, cost-effective alternative for groundwater remediation. This chapter will also serve to answer the research questions found in Chapter One.

After constructing the iron zone model (found in Appendix A), certain tests build confidence in the model's structure. The first test evaluates the model's dynamics. To perform this test, the modeler runs two simulations with the model. For the first run, the modeler uses original parameter values for all materials in the model. Then, for the second simulation, the modeler sets inflow values of the organic material in the system to zero. Figure 11 compares the VC degradation output curves for the two simulations. VC is one of three contaminants evaluated in the model; therefore, comparing differences in the output curves for the VC degradation in the model is justified.

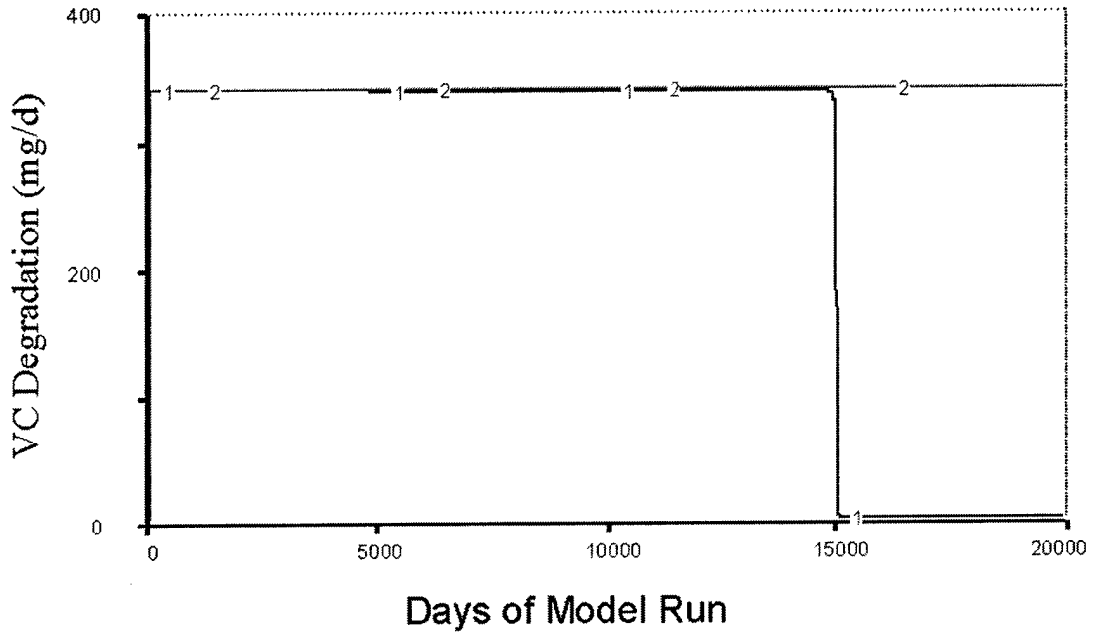

Figure 11. Comparison of VC Degradation with and without Organic Inflow Influence. Curve 1 shows VC degradation in the model simulation with all of the organic material influences. Curve 2 shows the VC degradation in the system when the inflows of all organic material are set to zero.

As the first simulation begins, VC enters the iron zone with groundwater flow. The output curve (curve 1, Figure 11) shows that VC degradation quickly reaches a steady state level. This level is determined by the reaction rate equation built into the model. The VC degradation remains at this steady state level using hematite as the electron acceptor in the degradation process. Due to the contaminant and organic influence in the simulations, the hematite in the iron zone is exhausted at approximately 15,000 days. At this point, the VC degradation drastically declines as seen in the model output. Without the hematite acting as an electron acceptor, significant VC degradation in the model simulation ceases. The second simulation (curve 2, Figure 11) also shows VC

degradation reaching a steady state quickly. Instead of dropping like the first simulation, however, the VC degradation remains constant for the remainder of the simulation. Without organic influence, the hematite in the system is not exhausted (over the evaluated period), and the VC degradation continues at its steady state level throughout the simulation. Although output graphs are not shown, similar behavior occurs for the other contaminants (*cis*-DCE and *trans*-DCE) in the test. Therefore, the modeler gains confidence in the model through this testing procedure.

The next test, described in Chapter Three, is the structure-verification test. This test is on going through the construction of the model. As the modeler builds each sector of the model, personal knowledge of the system is constructed into the model. On more than one occasion, questions arise about parameter representation in the model. Reaction rate equations, for example, need accurate representation for each material in the model. Experienced modelers and individuals knowledgeable about the system provide guidance on model construction. Upon completion of construction, the modeler and other committee members evaluate the model for structural flaws. Also, the modeler compares the model to Hoefar's previously constructed wetland model. No major problems are detected during these evaluations, and the modeler continues to gain confidence in the model.

Next, the modeler performs the extreme-conditions test on the model. This test evaluates model behavior when extreme parameter values are put into the model. The modeler uses the hematite depletion output graph to evaluate model behavior in this test. Figure 12 illustrates model output for three simulations performed in this test;

additionally, the accompanying table provides parameter values used for each simulation in the test.

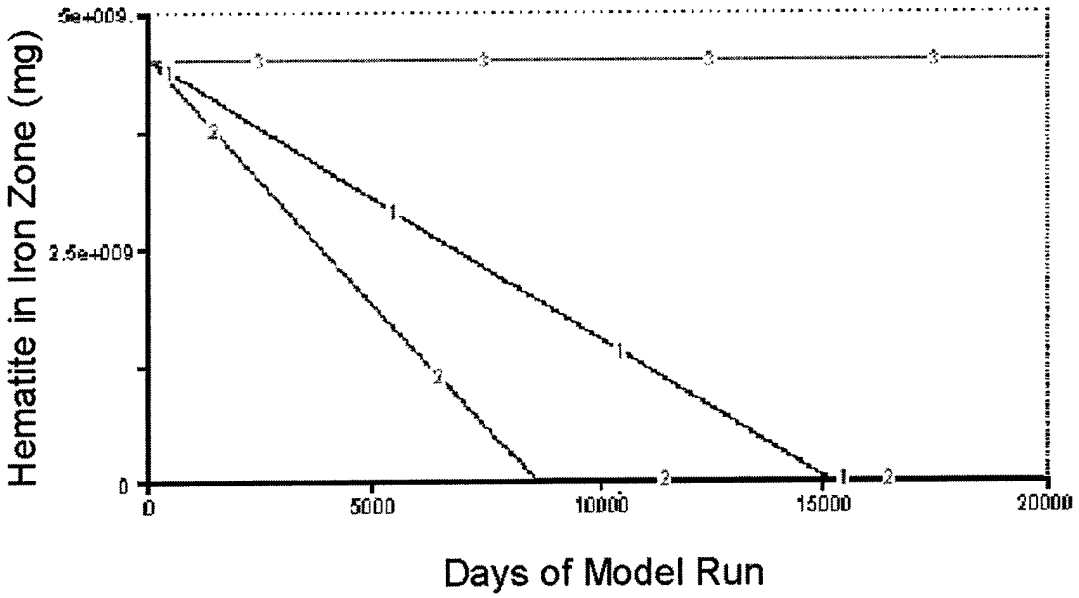

Figure 12. Comparison of Hematite Degradation with Original and Extreme Conditions for Flow Rate and Inflow Concentrations. Curve 1 shows hematite depletion in the system with original parameter values for each input variable. Curve 2 incorporates extremely high values into the model. Curve 3 shows hematite depletion output for extremely low parameter values.

Table 3. Values Used for Extreme-conditions Test. Units are displayed next to each input variable. Simulation 1 incorporates original values for model. Simulation 2 uses extremely high values for each input variable. Simulation 3 incorporates extreme low variables into the model for each given input variable.

Input Variable	Simulation		
	1	2	3
Flow rate (m^3/d)	10.5	1000	1.00E-06
VC inflow conc (mg/d)	0.01	1000	1.00E-11
cis-DCE inflow conc (mg/d)	0.015	1000	1.00E-11
trans-DCE inflow conc (mg/d)	0.005	1000	1.00E-11
Ethanol inflow conc (mg/d)	1	1000	1.00E-11
Methanol inflow conc (mg/d)	0.5	1000	1.00E-11
Lactic Acid inflow conc (mg/d)	0.75	1000	1.00E-11
Propionic Acid inflow conc (mg/d)	1	1000	1.00E-11
Formic Acid inflow conc (mg/d)	5	1000	1.00E-11
Butyric Acid inflow conc (mg/d)	0.75	1000	1.00E-11
Acetic Acid inflow conc (mg/d)	10	1000	1.00E-11
Hydrogen inflow conc (mg/d)	4.00E-07	1000	1.00E-11

Clearly, the model does not crash when extreme values are entered for parameters. In fact, the output curves in Figure 12 illustrate expected behavior for the model under extreme conditions. Curve 2, illustrating the depletion of hematite with extremely high parameter values in the model, decreases much more quickly than curve 1 (original parameter values). Naturally, with higher concentrations of reacting materials in the iron zone, the hematite depletes quicker. When parameters are set to extreme low values (represented by curve 3), the amount of hematite in the iron zone does not appear to decrease. Because of the small concentrations of reacting materials, only a minute amount of hematite depletes. The output graph (Figure 12) is scaled so curve 3 shows no decline through the model run.

The testing simulations previously performed on the model do not prove that the model is "correct." However, these tests allow the modeler to gain confidence in the model and the system dynamics approach. Therefore, after completing the testing simulations, the modeler gains confidence to implement the model for the purpose of this thesis effort. As described in Chapter Three, the modeler implements the model through numerous sets of simulations.

For the first implementing set of simulations, V_{max} parameters throughout the system are changed and evaluated. Details of the individual simulations are found in Chapter Three. The modeler categorizes the model output (hematite depletion) as changing minimally, moderately, or significantly when influenced by changing V_{max} parameters. Recall that depletion of hematite is influenced by all contaminants, hydrogen, and organics as the model is run. Therefore, as these materials are introduced into the iron zone, the hematite depletes continually through the model simulations. This set of simulations evaluates the changes in hematite depletion as different V_{max} parameters are changed.

Figure 13 shows an example of minimal hematite depletion variation when VC (one of the contaminants modeled in the system) V_{max} is changed.

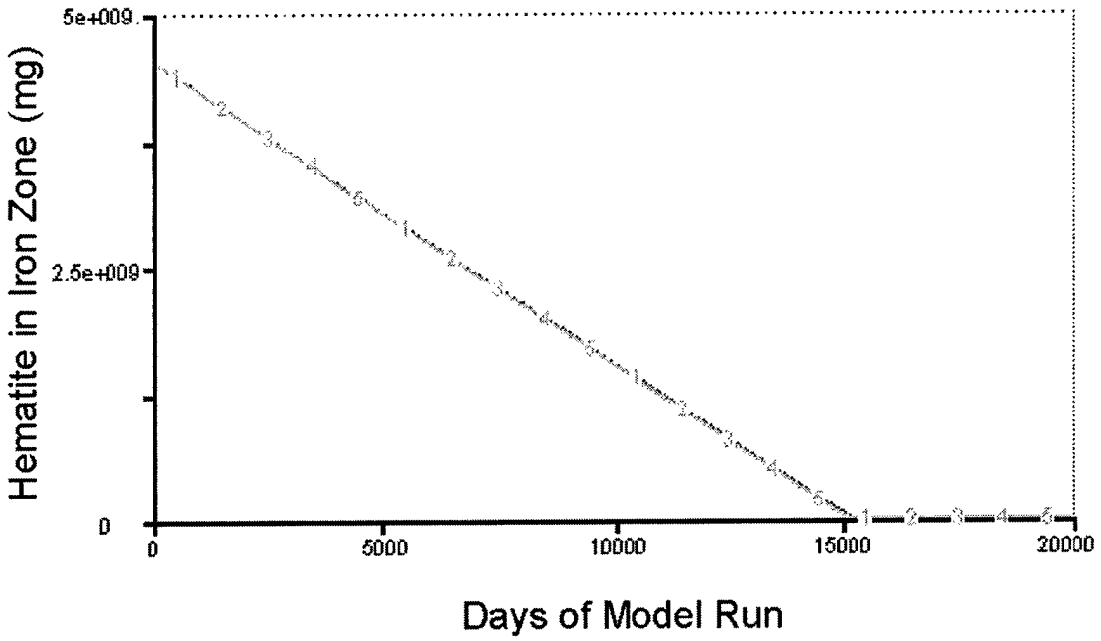

Figure 13. Hematite Depletion with Changing VC V_{max}. The 5 simulations incorporate increasing VC V_{max} parameter values.

VC V_{max} values used in the five simulations shown are found in Appendix C. Comparing the five simulations, the hematite depletion varies minimally (scale of graph makes depletion curves appear to be identical) with the values of VC V_{max} set at different orders of magnitude. Because the concentrations of contaminants (VC in this example) are less than other materials in the system (i.e., the organics), the impact of VC V_{max} variations on the depletion of hematite in the system is minimal.

Next, the V_{max} parameter simulations for butyric acid show an example of a moderate influence of hematite depletion.

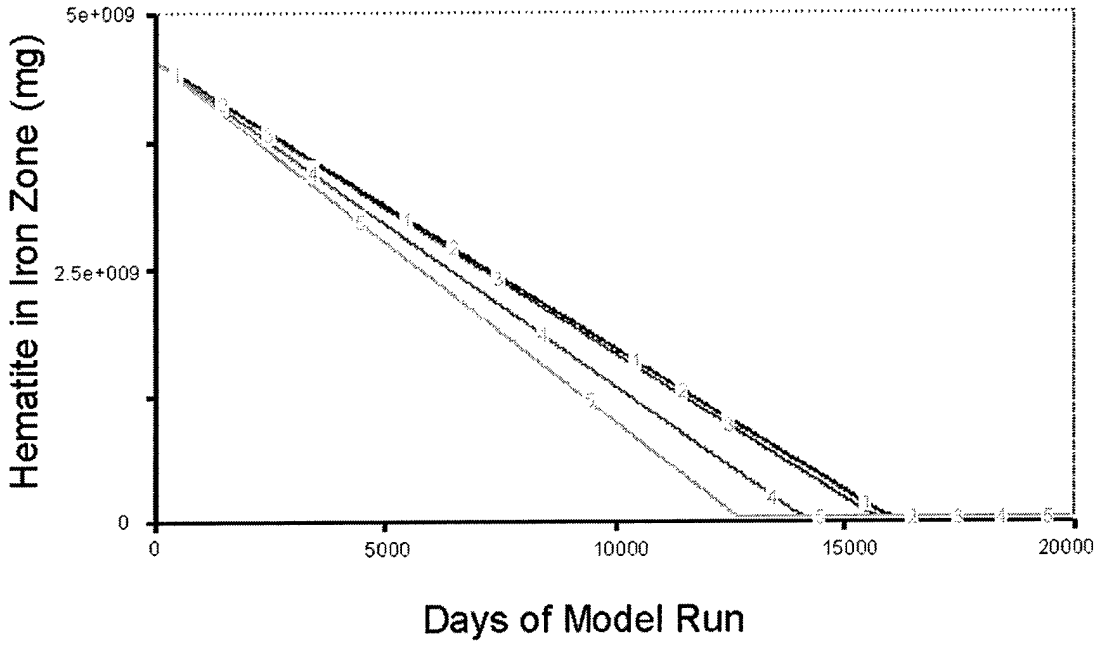

Figure 14. Hematite Depletion with Changing Butyric Acid V_{max}. The 5 simulations incorporate increasing Butyric Acid V_{max} parameter values.

Unlike the VC V_{max} example, these simulations show a moderate change in the hematite depletion curves when different values of butyric acid V_{max} (found in Appendix C) are set in the model. When only the butyric acid V_{max} parameter is changed, the hematite in the iron zone appears to be exhausted (to a value approaching zero) between a range of approximately 12,500 days and 16,000 days.

The acetic acid V_{max} parameter simulations show an example of a significant influence on hematite depletion.

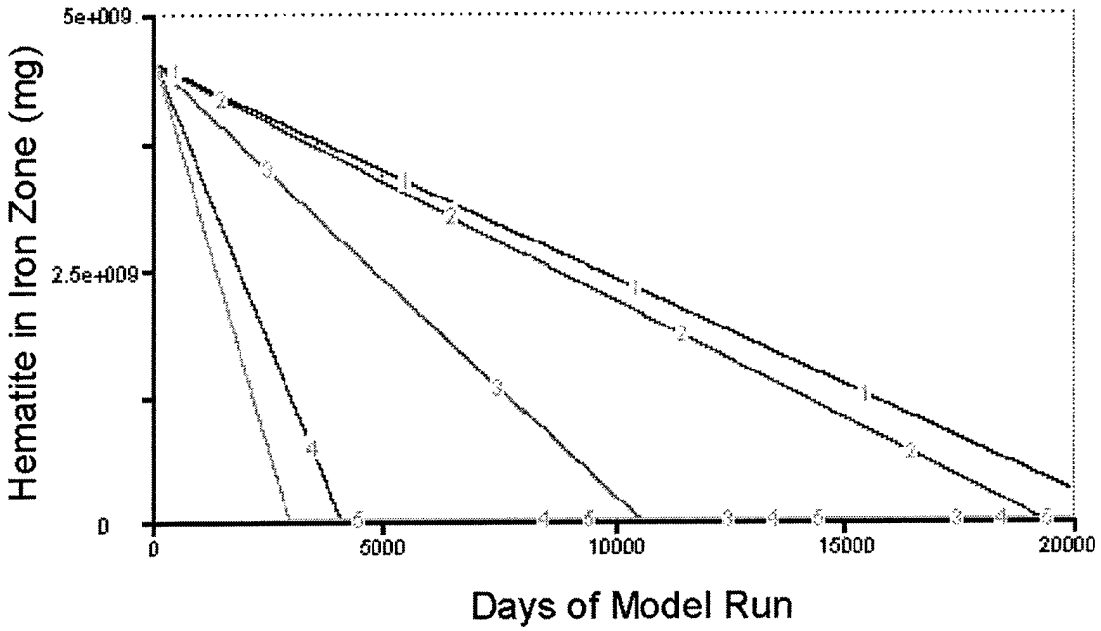

Figure 15. Hematite Depletion with Changing Acetic Acid V_{max}. The 5 simulations incorporate increasing Acetic Acid V_{max} parameter values.

As the values of acetic acid V_{max} (found in Appendix C) are changed in the five simulations, significant changes result in the hematite depletion. Therefore, the acetic acid V_{max} parameter appears to have a large influence on hematite depletion. When only the acetic acid V_{max} parameter (as set in the simulations) is changed, hematite appears to be exhausted between a range of 3000 days and over 20,000 days. This range illustrates the significant influence that the acetic acid parameter has on the model.

The following table categorizes the influence that V_{max} parameters (of each material modeled in the system) have on the constructed wetland system. Note that the examples shown above (Figures 13 through 15) are included in Table 4.

Table 4: Influence of Vmax and Approximate Range of Hematite Degradation for Each Material in System

Material	Influence of Vmax parameter in simulations	Approximate Range of Hematite Depletion (days)	
		low	High
VC	minimal	15100	15100
cis-DCE	minimal	15100	15100
trans-DCE	minimal	15100	15100
H2	moderate	13000	15100
Acetic Acid	significant	3000	20000+
Formic Acid	significant	4000	20000+
Propionic Acid	moderate	12000	16500
Butyric Acid	moderate	13000	16000
Lactic Acid	moderate	14000	15500
Ethanol	moderate	11000	17000
Methanol	moderate	11000	17000

For each simulation in this set, output graphs of contaminant degradation are found in Appendix C. The following figure gives an example of VC degradation behavior when changes in H_2 V_{max} are simulated.

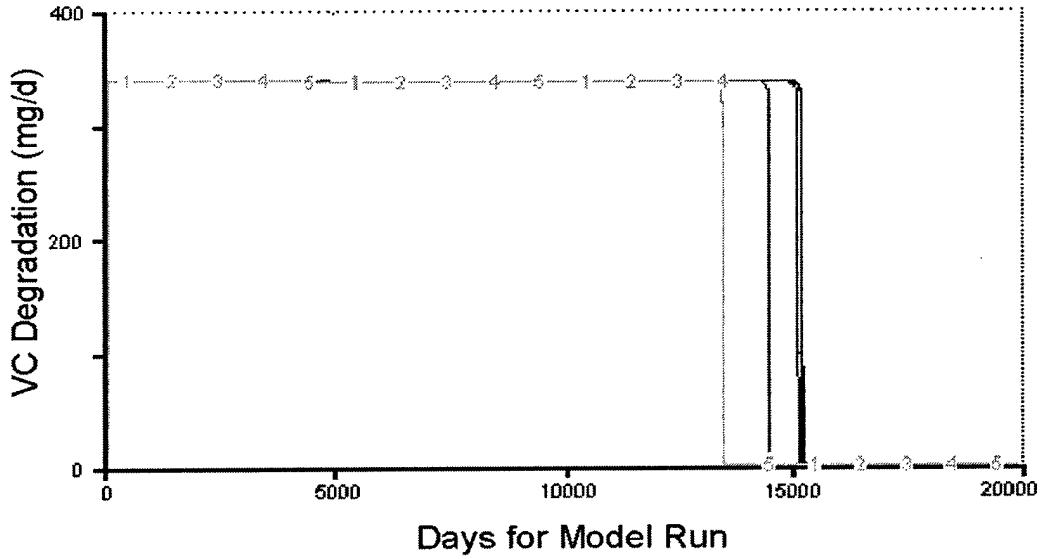

Figure 16: VC Degradation with Changing H_2 V_{max}. The 5 simulations incorporate increasing hydrogen V_{max} parameters in the model.

Figure 16 shows that, as the model runs, the VC degradation quickly reaches a steady state value of approximately 340 mg/d. As the model continues, the hematite in the iron zone is eventually exhausted (time to deplete hematite is specific to each simulation). As a result, the VC degradation drastically falls to a level near zero milligrams per day. In this example (Figure 16), the VC degradation drops significantly between approximately 13,000 and 15,100 days.

Similar behavior for *cis*-DCE and *trans*-DCE is observed for each model simulation in graphs found in Appendix C. As model simulations run, the observed levels of degradation (comparable to 340 mg/d for VC in this example) are approximately 500 mg/d and 165 mg/d, respectively. The different values observed for contaminant degradation result from different parameter values (i.e., V_{max}, inflow concentrations, and K_m) put into the Michaelis-Menten reaction equations (described in Chapter 2) for each individual contaminant.

In three specific cases, contaminant degradation output curves do not reach identical steady state levels for simulated V_{max} values. The first of these cases appears in the VC degradation output graph when VC V_{max} changes are simulated. The following output graph shows the different levels of VC degradation resulting from simulated changes in VC V_{max} (provided in accompanying table).

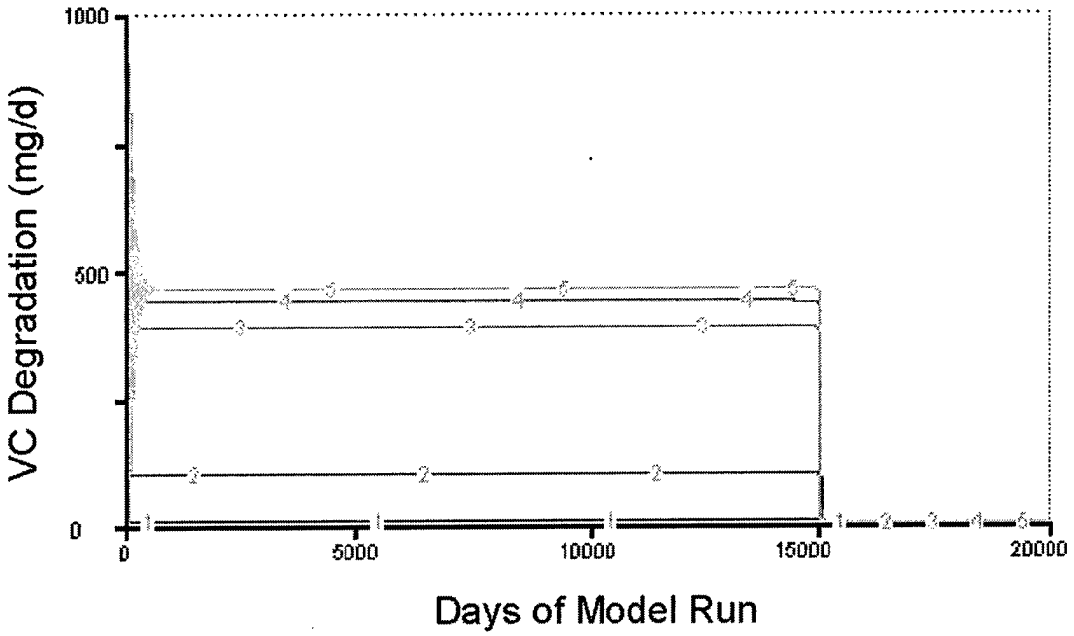

Figure 17. VC Degradation Changing VC V_{max}. The 5 simulations incorporate increasing VC V_{max} parameter values as shown in Table 5.

TABLE 5: Values Used for Changing VC V_{max} Simulations. Units for VC V_{max} are mg/d.

Input Variable	Simulation				
	1	2	3	4	5
VC Vmax (mg/d)	10	1000	10000	15000	19200

Clearly, the changing V_{max} parameters influence the level of VC degradation. Note that as the VC V_{max} increases, the degradation of VC in the system also increases. This behavior results from the influence of the V_{max} parameter in the Michaelis-Menten reaction rate equation. However, because each contaminant has individual reaction rate equations, the

changing VC V_{max} parameter does not directly influence the reaction rate (and, ultimately, the steady state degradation level) for *cis*-DCE and *trans*-DCE. Therefore, in this example, the output graph and accompanying value table show that the *cis*-DCE and *trans*-DCE degradation rates are sensitive to their respective V_{max} parameters, not the changing VC V_{max} parameter. The other two cases of varying levels of degradation in response to changing V_{max} parameters are *cis*-DCE degradation rate when *cis*-DCE V_{max} changes and *trans*-DCE degradation rate when *trans*-DCE changes. Output graphs for these simulations are in Appendix C.

The next simulations (still in the first set of simulations) combine various V_{max} values for the contaminants, hydrogen, and organics. Though the modeler performed ten simulations with various combinations, Figure 18 provides only five of the ten combination runs. By eliminating five of the combination simulations (for Figure 18), no significant data or behavior is lost, the output graph is easier to read, and the output curves are labeled according to the simulation.

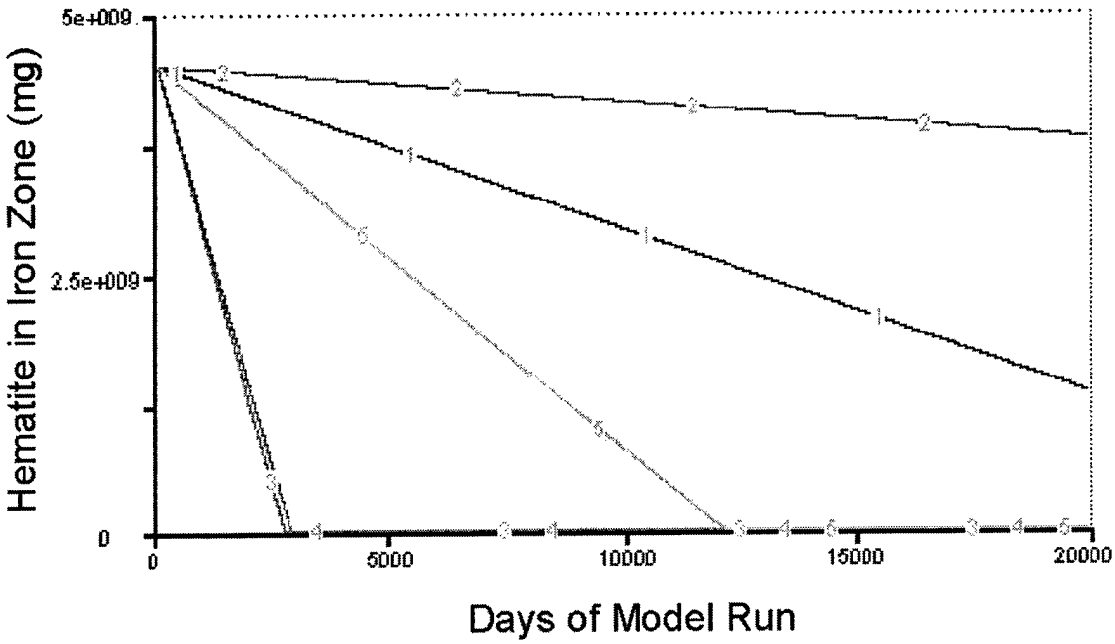

Figure 18. Hematite Depletion with Combination V_{max} Values. The V_{max} parameter values used for each simulation are defined in Table 6 below. These simulations incorporate various combinations of V_{max} parameters in the system.

Table 6. Values Used in Combination Simulations, Set 1. Units for each V_{max} value are mg/d

Input Variable	Simulation				
	1	2	3	4	5
VC Vmax (mg/d)	4000	12000	10000	3000	1000
cis-DCE Vmax (mg/d)	5000	15000	12000	10000	16000
trans-DCE Vmax (mg/d)	5000	20000	12000	5000	20000
H2 Vmax (mg/d)	10000	7000	150000	1000	800000
Acetic Acid Vmax (mg/d)	25000	5000	700000	400000	50000
Formic Acid Vmax (mg/d)	25000	5000	90000	300000	40000
Propionic Acid Vmax (mg/d)	15000	3000	150000	200000	50000
Butyric Acid Vmax (mg/d)	12500	4000	300000	80000	70000
Lactic Acid Vmax (mg/d)	11000	3000	50000	90000	30000
Ethanol Vmax (mg/d)	10000	2000	100000	75000	20000
Methanol Vmax (mg/d)	10000	2000	20000	75000	20000

In Figure 18, the hematite depletes at various rates according to the parameter values used for each simulation. The first simulation tends to decrease all the V_{max} parameters in the model. As a result, the hematite depletion rate decreases rather significantly. In the second simulation, the contaminant V_{max} values are elevated and the organic V_{max} values are decreased. The resulting hematite depletion output curve (curve 2) shows that the organic material has a greater influence on the depletion of hematite compared to the contaminant materials. Simulations three and four also support this claim. When the organic V_{max} values are increased, the hematite depletion rate (slope of the output curve)

significantly increases. Figure 19 shows the output graph for VC behavior associated with the five combination simulations of Figure 18 and Table 6.

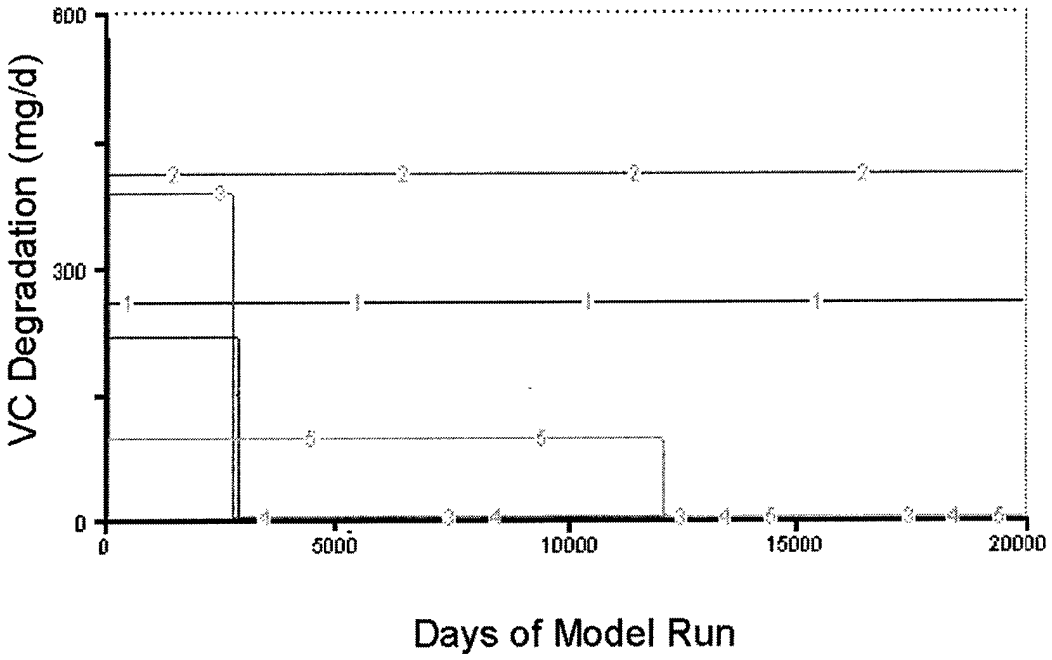

Figure 19. VC Degradation with Combination V_{max} Values. The V_{max} parameter values used for each simulation are defined in Table 6. These simulations incorporate various combinations of V_{max} parameters in the system.

The output graph shows that the degradation of VC is dependent on the parameters of the simulations. According to Figure 19, the VC degradation quickly reaches its steady state value (dependent on the reaction rate parameter values) and remains at that value until the hematite in the system is exhausted. Similar results are found in the *cis*-DCE and *trans*-DCE behavior output graphs in Appendix C. Also, for further reference, the complete set of ten combination simulations and accompanying value tables are found in Appendix C.

The final two simulations in the first set of simulations represent extreme minimum and maximum V_{max} values for the materials in the system. With all V_{max} parameters set at a minimum (described in Chapter 3), the hematite in the system shows no sign of depletion. The small V_{max} parameters, components of the Michaelis-Menten degradation equations for each material, limit the degradation of contaminants, hydrogen, and the organics; ultimately, this also limits the amount of hematite depletion in the simulation. The output graphs associated with the extreme minimum V_{max} values are in Appendix C. At the other extreme, maximum V_{max} values appear to deplete the hematite rapidly. Within 2000 days, the hematite in the system is exhausted. This behavior shows that large V_{max} parameters influence the system with large degradation rates and hematite depletion. The output graphs for contaminant degradation show larger amounts of contaminants degrading while the hematite is available. Again, the higher degradation rates result from the extreme maximum V_{max} parameters in the Michaelis-Menten equations for each contaminant in the system. Output graphs and accompanying tables showing the extreme V_{max} parameters are in Appendix C.

The second set of simulations (as described in Chapter 3) changes and evaluates the K_m values throughout the model. Recall that the K_m values for each material in the system represent a component in the denominator of the Michaelis-Menten equation. Refer to Chapter Two for further explanation of the Michaelis-Menten equation. Similar to the V_{max} influence in the first set of simulations, the modeler categorizes the model output (hematite depletion) as changing minimally, moderately, or significantly when individual K_m values in the system are changed. Figures 13, 14, and 15 give examples of

minimal, moderate, and significant V_{max} influence, respectively. These examples represent similar relationships for categorizing the influence of changing K_m parameters. A complete set of model output representing the influence of changing K_m values for each material in the system is in Appendix C. The following table (comparable to Table 4 in the first set of simulations) categorizes the influence that K_m parameters have on the system. An additional parameter also exists in this set of simulations. The hematite in the system has a K_m value that is represented in every Michaelis-Menten equation in the model. Thus, the influence of hematite's K_m value is also categorized at the bottom of the following table.

Table 7. Influence of K_m and Approximate Range of Hematite Degradation for Each Material in System.

Material	Influence of Km parameter in simulations	Approximate Range of Hematite Depletion (days)	
		low	high
VC	minimal	15100	15100
cis-DCE	minimal	15100	15100
trans-DCE	minimal	15100	15100
H2	moderate	13000	15100
Acetic Acid	significant	14000	20000+
Formic Acid	significant	13000	20000+
Propionic Acid	moderate	13000	16000
Butyric Acid	moderate	13000	16000
Lactic Acid	moderate	14000	15100
Ethanol	moderate	12000	17000
Methanol	moderate	11500	16500
Hematite	significant	15000	20000++

The next simulation (still in the second set of simulations) combines various K_m values for contaminants, hydrogen and organics. As in the first set of simulations, only

five of the ten actual simulations performed are shown in the following output graph and table.

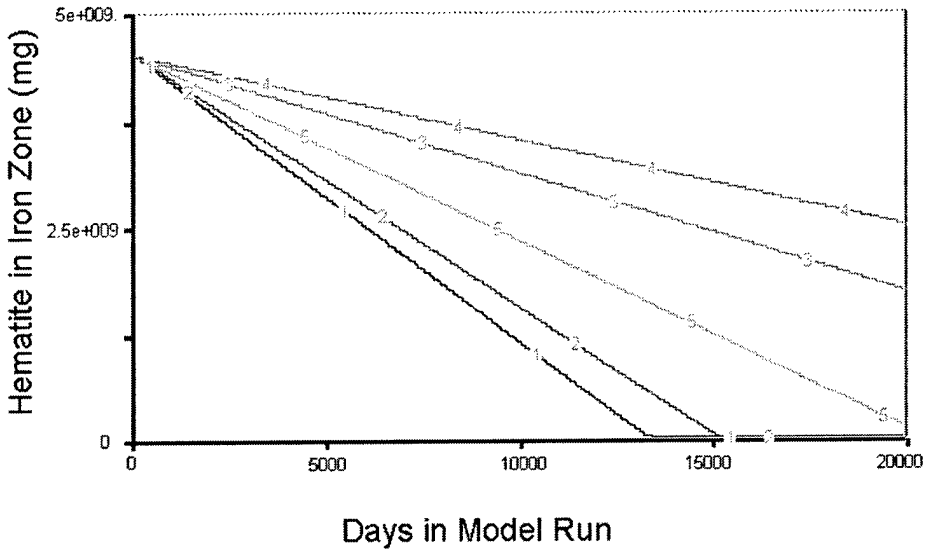

Figure 20. Hematite Depletion with Combination K_m Values. The K_m parameter values used for each simulation are defined in Table 8 below. These simulations incorporate various combinations of K_m parameters in the system.

Table 8. Values Used in Combination Simulations, Set 2. Units for each Km variable are mg/L.

Input Variable	Simulation				
	1	2	3	4	5
VC Km (mg/L)	2	0.5	0.05	1000	0.5
cis-DCE Km (mg/L)	5	1	0.1	1200	1
trans-DCE Km (mg/L)	5	1	0.1	1200	1
H2 Km (mg/L)	10	0.1	100	0.5	0.1
Acetic Acid Km (mg/L)	5	0.5	2000	25	10000
Formic Acid Km (mg/L)	5	0.25	100	100	7500
Propionic Acid Km (mg/L)	1	10	0.5	0.75	100
Butyric Acid Km (mg/L)	1	5	20	1000	0.01
Lactic Acid Km (mg/L)	1	10	5	50	0.75
Ethanol Km (mg/L)	0.5	10	2	5	10000
Methanol Km (mg/L)	0.5	5	1	25	2000
Hematite Km (mg/L)	5	0.1	7.5	20	0.01

As shown in the output curves of Figure 20, the contamination K_m values influence hematite depletion in the system. As a component in the Michaelis-Menten reaction rate equations for each material in the model, varying K_m values tend to deplete the hematite slower than simulations with lower K_m values. This observation matches the expected behavior of Michaelis-Menten reaction rate equations. With higher K_m values placed into the Michaelis-Menten equation (all other parameters held constant), a smaller degradation rate results. This degradation rate ultimately affects the influence of the material on the system. The combination simulations also provide information about material influence in the model. In the first simulation, for example, contaminant K_m values are all increased; additionally, certain organic material Km values in the simulation are decreased. The resulting output curve shows an increased hematite depletion rate. Therefore, the influence associated with the changing organic K_m values outweighs the influence of the changing contaminant K_m values. The following output graph (Figure 21) gives the VC behavior associated with the five combinations used in Figure 20 and Table 8.

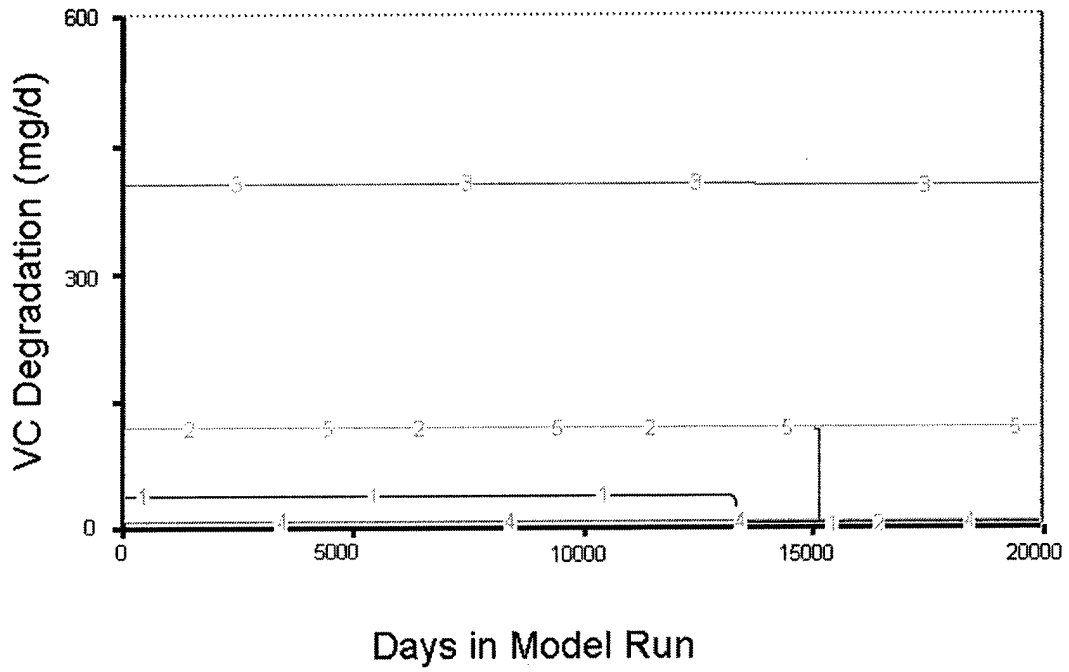

Figure 21. VC Degradation with Combination K_m Values. The K_m parameter values used for each simulation are defined in Table 8. These simulations incorporate various combinations of K_m parameters in the system.

The output curves for each combination simulation show that the levels of VC degradation are dependent on the changing VC K_m values. In the third simulation, for example, a low VC K_m value (compared with other VC K_m values simulated) is used. The resulting output curve shows a higher steady state level than the other simulations. Additionally, in the fourth simulation, a high VC K_m value is simulated, and a low steady state level of VC degradation results. Therefore, these simulations demonstrate that the K_m component of the Michaelis-Menten reaction rate equation influences degradation rates of associated materials. Output graphs, showing similar results for *cis*-DCE and *trans*-DCE behavior, are in Appendix C. Instead of only five simulations, however,

Appendix C output graphs illustrate all ten simulations that were run. A complete list of values used and the output graphs for all ten simulations are also in Appendix C.

The final two simulations in the second set represent extreme K_m values for the materials in the system. These simulations are similar to the extreme value simulations in the first set; however, K_m values replace the V_{max} values. The results of the K_m extreme value simulations appear to be opposite of the V_{max} extreme simulations. With all K_m values set to minimum values, the hematite depletes rapidly. When all K_m values are set to maximum values, the hematite shows no sign of depletion throughout the simulation. These results show the influence that the K_m parameters have on the system. Because of the structure of the Michaelis-Menten equation, the resultant of the equation is not directly proportional to the K_m parameters. Instead, the K_m parameter is added to the material's concentration (the material specific to the equation) to make the denominator of the equation. Therefore, because the output curves are sensitive to changes in the K_m parameters, the concentrations used in the equations are small and do not overpower the K_m parameters. The output curves for hematite depletion and contaminant degradation under the extreme K_m parameter values are in Appendix C.

The third set of simulations changes the amount of hematite available in the iron zone and evaluates behavior of the system. In Chapter Three, the procedure reports that fifteen simulations were performed. Appendix C contains the output graph for all fifteen simulations and the values used for the simulations. The following output graph, however, shows only five of the fifteen simulations performed. By only using five

simulations, the output graph shows a simplified version of the behavior and labels the model simulation runs.

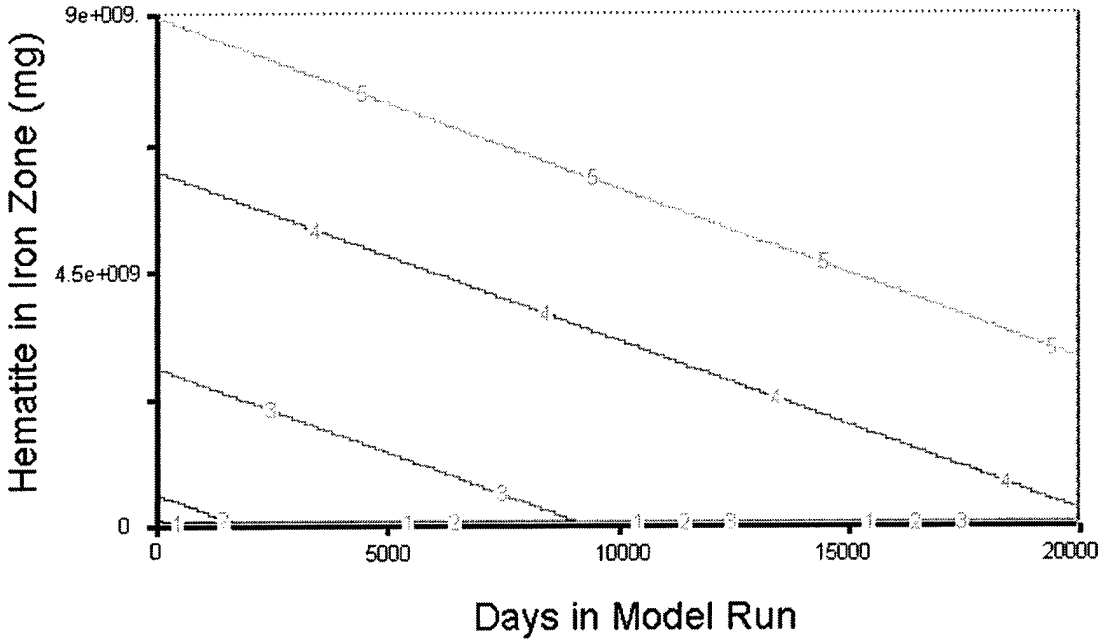

Figure 22. Hematite Depletion with Changing Hematite Values. The output curves represent the hematite depletion behavior in the system when increasing hematite values are

Table 9. Values Used in Changing Hematite Simulations. Units of hematite are mg.

Input Variable	Simulation				
	1	2	3	4	5
Fe3 Hematite (mg)	891975	4.50E+08	2.70E+09	6.20E+09	8.90E+09

Figure 22 shows that the amount of hematite available in the soil directly influences the period of time hematite remains in the system. Naturally, the more hematite in the

system, the longer period it is available in the model. Figure 23 illustrates VC behavior for the five simulations performed in this set and reported in Figure 22 (and Table 9).

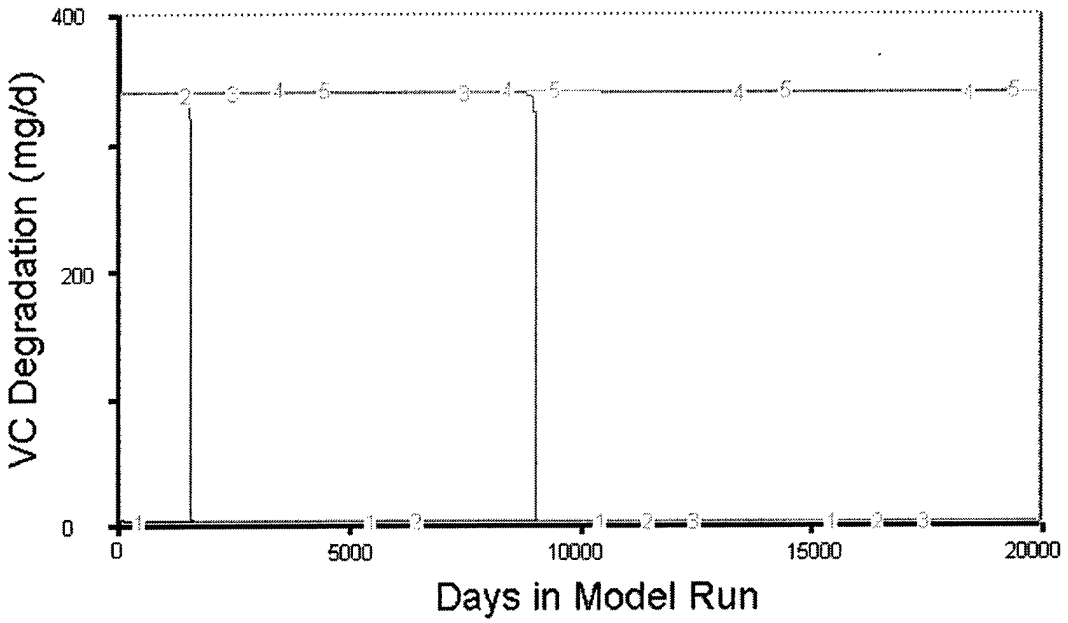

Figure 23. VC Degradation with Changing Hematite Values. The hematite parameter values used for each simulation are defined in Table 9. These simulations show the VC degradation behavior with increasing hematite values.

The degradation of VC in Figure 23 behaves much like simulations performed in the first and second set of simulations. The degradation quickly reaches steady state (determined by the Michaelis-Menten rate equation and original parameter values for the model) and remains constant until the hematite in the system is exhausted. Note that the degradation for each simulation drastically decreases when the hematite in the model is exhausted. The drop in VC degradation for each simulation in Figure 23 directly relates to the respective point in Figure 22 when the hematite is depleted from the system. Similar observations were made for the behavior for *cis*-DCE and *trans*-DCE. Output graphs for

contaminant degradation behavior are in Appendix C. The graphs in Appendix C, however, incorporate all fifteen simulations performed instead of only the five shown in Figures 22 and 23.

The next set of simulations changes the flow rate through the constructed wetland and evaluates the behavior in the iron zone. Twenty-five simulations were performed using the model with various flow rates. The description of the simulated runs in Chapter Three depicts how the groundwater flow values used in the simulations were calculated. An output graph and values table incorporating all twenty-five simulations is found in Appendix C. To report and discuss the results of this simulation set, however, five of the twenty-five simulation output curves are shown in the following figure.

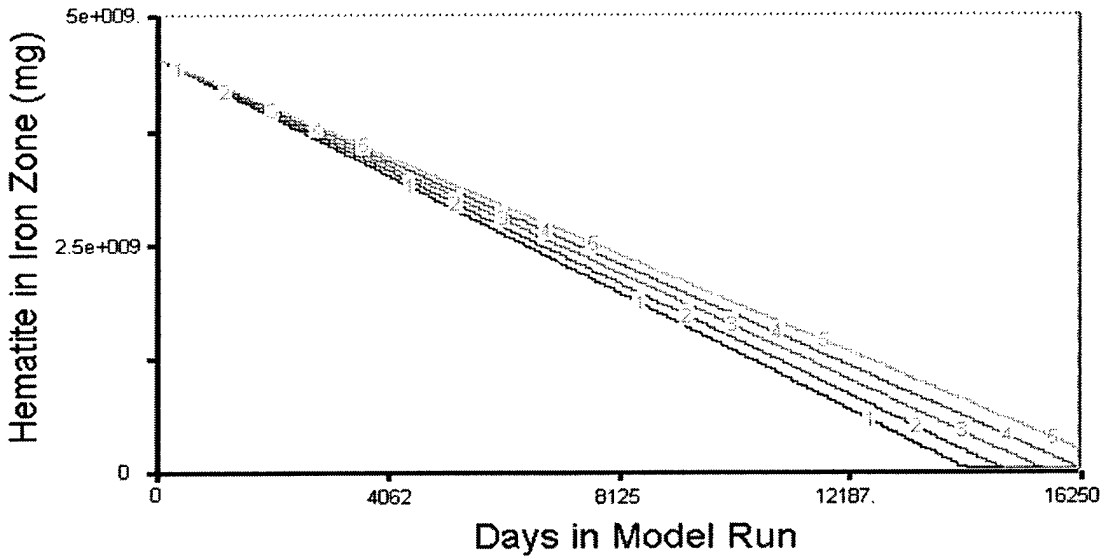

Figure 24. Hematite Depletion with Changing Groundwater Flow. The output curves represent the hematite depletion behavior in the system when increasing flow rate values are put into the model.

Table 10. Values Used in Changing Flow Rate Simulations. Units of the flow rate parameters are gal/min. These flow rates incorporate the groundwater flow through the system into these simulations.

Input Variable	Simulation				
	1	2	3	4	5
Flow rate (gal/min)	78.5	13.10	6.55	4.36	3.14

The output curves in Figure 24 show that the rate of hematite depletion increases as the flow rate through the system increases. In the model, contaminant, hydrogen, and organic degradation reactions are assumed to be instantaneous. Therefore, higher flow rates do not influence the effectiveness of the degradation processes. As long as hematite is available to act as an electron acceptor, the contaminant degradation is only limited by Michaelis-Menten equations (specific for each contaminant). The simulation output curve for the first simulation (seen in Figure 24) shows the greatest hematite depletion rate. The groundwater flow in this simulation has the greatest value of all simulations. As the groundwater flow simulation values are decreased (as in simulations 2 through 5), the rate of hematite depletion appears to also decrease proportionally. Therefore, with a decreased rate of hematite depletion, the hematite remains available in the system for a longer period of time. For the simulations performed, the range of time from the beginning of model simulation to the point where hematite is exhausted is approximately 13,000 days to 17,000 days. Though only an estimate, this range identifies the influence of groundwater flow on hematite depletion. Compared to other parameters of the system, the changing groundwater flow has a moderate influence on the depletion of hematite in

the iron zone. Figure 25 shows the output graph for VC behavior associated with the five simulations in Figure 24.

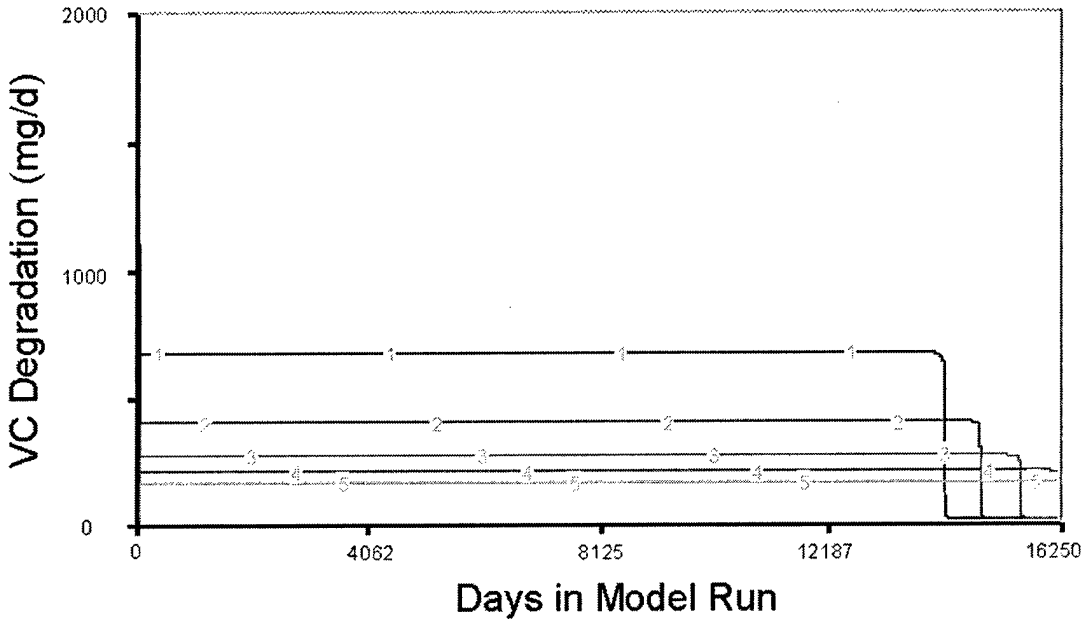

Figure 25. VC Degradation with Changing Flow Rate Simulations. The flow rate parameter values used for each simulation are defined in Table 10. These simulations show the VC degradation behavior with increasing flow rate values.

The VC degradation curves quickly reach the steady state level for the system. This level is directly influenced by the flow rate through the system. As the output graph shows, the level of VC degraded increases (in separate simulations) as the flow rate through the wetland increases. After reaching its steady state value, the level of degradation for each simulation remains constant until the hematite in the system is exhausted. At this point, the degradation rate drastically decreases to a level near zero milligrams per day. Note that the drastic decrease takes place earlier in the model simulations for higher flow rates. This observation supports the claim that the hematite depletes more rapidly in the system

when higher flow rates are simulated. Appendix C contains output graphs for *cis*-DCE and *trans*-DCE. Behavior of these contaminants is similar to VC degradation in Figure 25. However, in Appendix C, the output graphs include all twenty-five simulations associated with the simulation set.

The fifth set of simulations changes inflow concentration values for the contaminants and hydrogen. With all other parameters held constant, model behavior (hematite depletion and contaminant degradation) is evaluated. By simulating changes in individual contaminant inflow concentrations by orders of magnitude, the influence on the degradation of hematite in the system appears minimal. Output graphs for these simulations are in Appendix C. The following figure illustrates VC degradation behavior when *cis*-DCE inflow concentration changes are simulated.

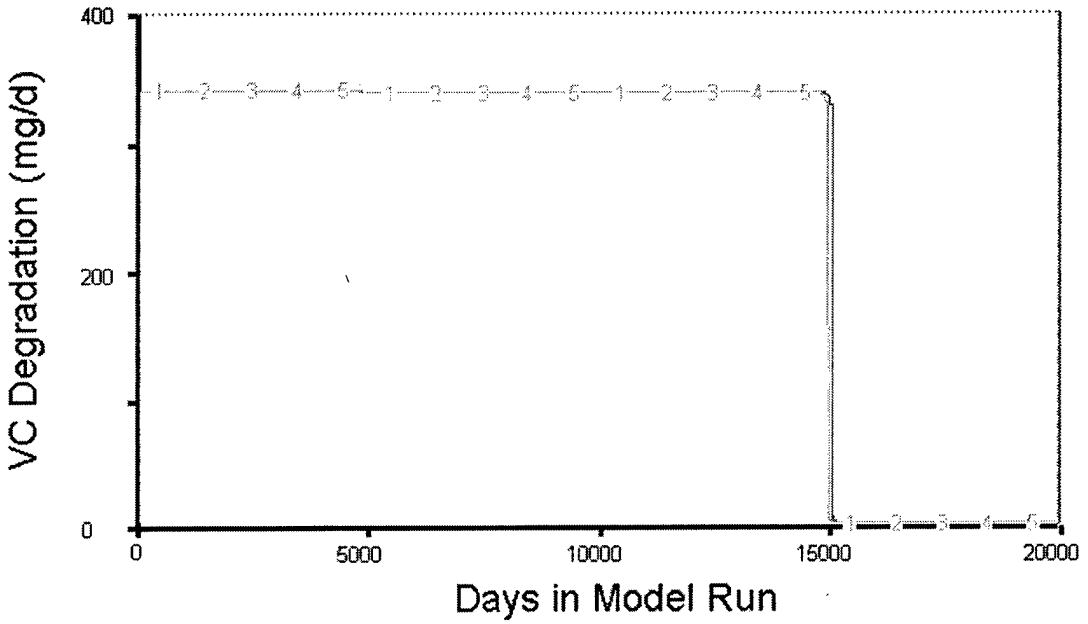

Figure 26. VC Degradation with Changing *cis*-DCE Inflow Concentrations. The *cis*-DCE inflow concentration value is increased for each of the 5 simulations. These output curves show the VC degradation behavior associated with the increasing *cis*-DCE inflow values.

The VC degradation quickly reaches a steady state level and remains at this level until the hematite in the system is exhausted. At that point, the level of contaminant degradation falls dramatically to a level near zero milligrams per day. Similar behavior for *cis*-DCE and *trans*-DCE are found in Appendix C.

Also, in the fifth simulation set, various hydrogen inflow concentrations were simulated. As with the contaminants, the influence of hydrogen on hematite depletion and contaminant degradation is minimal. Output graphs of the hydrogen simulations are in Appendix C.

In addition to individual changes to contaminant inflow concentrations, simulations with combination parameter values were performed. Values used for each combination simulation are available in Appendix C. The simulation output graphs using

combination inflow concentration values show that the contaminant inflow concentration values have minimal influence on the hematite depletion. The output graphs that support these observations are in Appendix C. Additionally, minimum and maximum values for each contaminant inflow concentration were entered into the model. As with the combination simulations, the minimum and maximum values show minimal influence on hematite depletion of the system (refer to Appendix C for output graph).

In the final set of model simulations, the inflow concentration values for organic materials in the system are changed and evaluated. These values are significantly higher than the contaminant inflow concentration values. Therefore, parameter changes for the organic materials tend to influence more hematite depletion activity in the model. To provide results of the simulations in this set, the modeler categorizes the influence each organic material's inflow concentration has on the depletion of the hematite. A similar categorization was performed for the V_{max} parameters in the first set of simulations. Refer to Figures 13, 14, and 15 (in this chapter) for examples of minimal, moderate, and significant influences on hematite depletion, respectively. Though these figures represent the influence of different parameters, the magnitude of influence can be incorporated to this set of simulations. For each organic material, five simulations were performed changing inflow concentration values. Output graphs and value tables for each simulation are found in Appendix C. The influence of each organic material on hematite depletion was evaluated by the changed rate of hematite depletion for each simulation. As the rate of hematite depletion changed for each simulation, the period of time to the depletion of hematite in the system also changed. By evaluating these changes, an

approximate range of hematite depletion can be determined for each organic material in the system. The following table identifies each organic material and its influence on the depletion of hematite in the system. The approximate range of hematite depletion for each material is also provided in the table.

Table 11. Influence of Organic Inflow Concentrations and Approximate Range of Hematite Depletion for Each Organic Material

Material	Influence of inflow concentration parameter in simulations	Approximate Range of Hematite Depletion (days)	
		low	High
Acetic Acid	significant	14000	20000+
Formic Acid	significant	13000	20000+
Propionic Acid	moderate	13000	16000
Butyric Acid	moderate	13000	16000
Lactic Acid	moderate	14000	15500
Ethanol	significant	12000	18000
Methanol	significant	10500	16000

Contaminant degradation steady state values did not change when the organic inflow concentrations were changed. The only changes observed in the contaminant degradation output graphs were the time periods when the degradation drastically dropped. These time periods are associated with the depletion of hematite. In each contaminant degradation output graph found in Appendix C, the degradation level dropped at the point where the hematite in the system is exhausted.

Similar to previous simulation sets, ten simulations were performed using combinations of the organic inflow concentrations. Chapter Three explains the setup of these simulations. The following output graph shows five of the ten simulations performed.

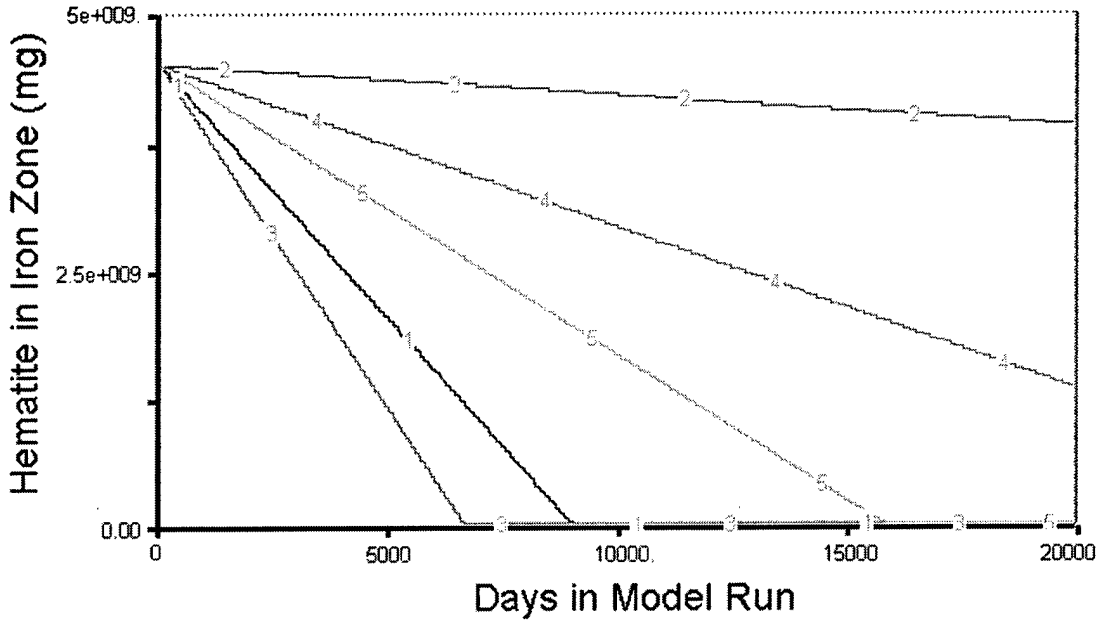

Figure 27. Hematite Depletion with Combination Organic Inflow Concentrations. The organic inflow concentration parameter values used for each simulation are defined in Table 12 below. These simulations incorporate various combinations of organic inflow concentrations in the system.

Table 12. Values Used in Combination Simulations, Set 6. Units of the inflow concentration parameters are mg/d.

Input Variable	Simulation				
	1	2	3	4	5
Lactic Acid Inflow Conc (mg/d)	5	0.05	40.00	0.50	0.01
Propionic Acid Inflow Conc (mg/d)	5	0.05	80	0.5	0.5
Formic Acid Inflow Conc (mg/d)	40	0.1	80	1	25
Butyric Acid Inflow Conc (mg/d)	5	0.05	70	0.5	1
Acetic Acid Inflow Conc (mg/d)	50	0.5	75	5	30
Ethanol Inflow Conc (mg/d)	2	0.01	50	0.1	0.1
Methanol Inflow Conc (mg/d)	2	0.01	10	0.1	0.25

The combination simulations show different depletion rates for hematite in the system. Compared to other parameters in the model, the organic inflow concentration values influence the depletion of hematite significantly. When lower values are simulated, the reaction rate for hematite tends to decrease resulting in a longer period that hematite is available. As with previous simulations, the contaminant degradation behavior is only influenced when the hematite is exhausted. In each combination simulation, the contaminant degradation output curves quickly reach steady state values and remain constant until the hematite in the system is exhausted. Output graphs showing this observation are in Appendix C.

The final simulations performed set all organic material inflow concentrations at minimum and maximum values. The following figure shows the results of these simulations.

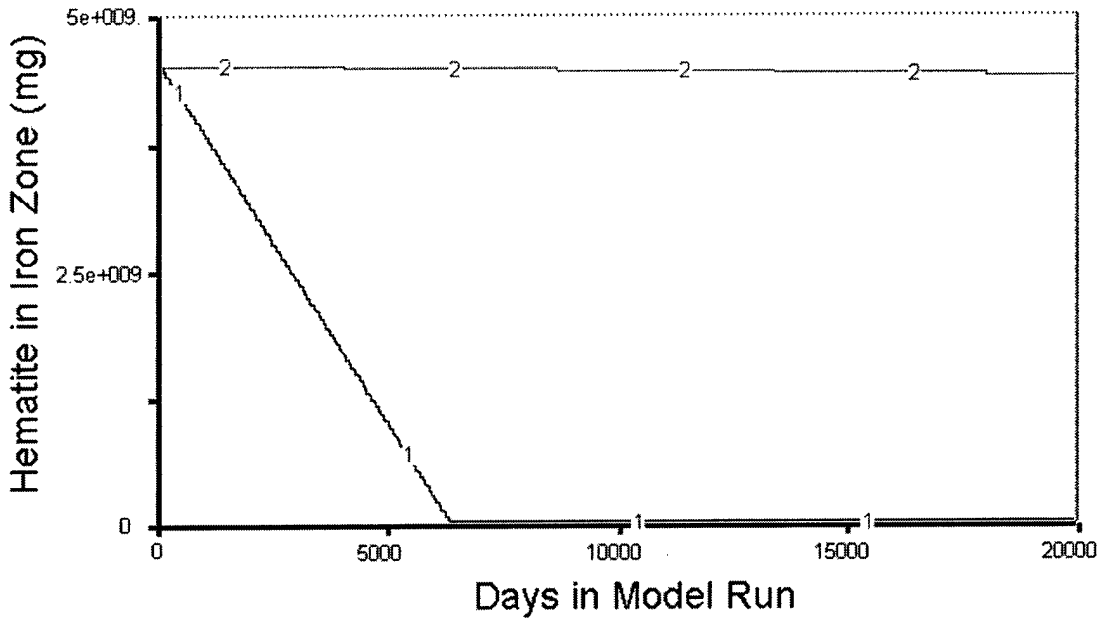

Figure 28. Hematite Depletion with Minimum and Maximum Organic Inflow Concentration Values. The organic inflow concentration parameter values used for each simulation are defined in Table 13 below. These simulations incorporate maximum and minimum organic inflow concentrations for the system.

Table 13. Values Used in Maximum and Minimum Organic Inflow Concentration Simulations. Units of the inflow concentration parameters are mg/d.

Input Variable	Simulation	
	1	2
Lactic Acid Inflow Conc (mg/d)	100	0.1
Propionic Acid Inflow Conc (mg/d)	100	0.1
Formic Acid Inflow Conc (mg/d)	100	0.1
Butyric Acid Inflow Conc (mg/d)	100	0.1
Acetic Acid Inflow Conc (mg/d)	100	0.1
Ethanol Inflow Conc (mg/d)	100	0.1
Methanol Inflow Conc (mg/d)	100	0.1

Definitions for parameters in the table (Inflow con 1, for example) are in Appendix B. Clearly, the organic inflow concentration values significantly influence the depletion of hematite in the system. With the concentration values set at maximum levels, the hematite is depleted rapidly (in approximately 7000 days). When set to minimum values, the hematite depletes minimally.

V. Conclusions and Recommendations for Further Studies

The purpose of this thesis effort was to model, examine, and understand biodegradation activity occurring in the iron zone of a multi-layered constructed wetland. A system dynamics approach was taken to accomplish the thesis effort. Compared to other modeling approaches that focus on analytical techniques, the system dynamics approach studied the dynamic relationships between internal components of the system mechanistically.

Conclusions

Hematite, the form of oxidized iron modeled in this thesis effort, acts as the electron acceptor for contaminant degradation and other organic reactions in the iron zone. Output graphs of model simulations show that the hematite depletion in the iron zone results from influences by the materials flowing through the constructed wetland. The organic material reactions (i.e., organic acids and alcohol) influence the hematite depletion more than the contaminant degradation processes. In fact, the majority of hematite depletion results from organic influence. Simulating changes in the organic material reaction rates equations impacted the hematite depletion rate significantly. Similar simulations changing contaminant reaction rate components resulted in minimal changes to the hematite depletion rate. Therefore, the organic material reactions have greater influence on hematite depletion compared with contaminant degradation in the model.

Chapter Four labels each material modeled as having minimal, moderate, or significant influence on hematite depletion. Providing sample data for these materials

(especially those labeled moderate or significant) will build additional confidence in the model output for further implementation.

One engineer-controlled parameter identified in the model is the amount of hematite in the iron zone. Increasing the amount of hematite in the system allows for contaminant and organic degradation to continue over a longer period of time. The degradation processes in the iron zone continue until the available hematite is exhausted.

Another engineer-controlled parameter is the flow rate through the system. Because reactions in the iron zone are considered instantaneous in the model, higher flow rates result in higher physical amounts of contaminants and organics degraded. The efficiency of these reactions, however, is not increased with higher flow rates. The level of degradation for the contaminants and organics result from individual Michaelis-Menten reaction rate equations. Additionally, over similar time periods, simulations with higher flow rates through the wetland require more groundwater than the simulations with lower flow rates. Therefore, factors such as groundwater supply or containment of chlorinated plumes need to be considered when setting the flow rate through the system.

Model Limitations

Through all of the model simulations, hematite acts as an electron acceptor for degradation processes in the iron zone. The values chosen to represent the amount of hematite in the system were based on the percentage of iron (approximated) in the soil. The model simulates the depletion of all available hematite in the system; therefore, it does not account for any hematite that may not be available (due to physical properties or other unique conditions of the soil) for biodegrading activities. Literature addresses the

proposed issue of bioavailability of oxidized iron (i.e., hematite). For this thesis effort, however, these issues are not incorporated into the model.

Secondly, biomass growth and death rates are not included in the model. Instead, the model incorporates an assumption that biomass levels through the simulation accommodate maximum reaction rate equation levels for each material in the system. When the simulations begin, model output shows an immediate increase for contaminant degradation to its steady state level. With accountability for biomass growth, however, the degradation rates would be limited in the initial parts of the simulations by the growth of the biomass in the system.

Lastly, many parameters used in the model simulations had no sample data and limited literature support. One of the limited literature sources that provided appropriate parameter values for the model in this thesis effort was Bradley and Chapelle (1997). The authors reported a value for VC V_{max} under Fe III-reducing laboratory conditions. Assuming the value does not change significantly when subjected to the natural environment, the modeler incorporated the value from Bradley and Chapelle (1997) into the model. For parameters not addressed in the literature, the modeler simulated wide ranges of values to evaluate changing behavior of the model.

Recommendations for Further Study

The model constructed in this thesis effort could benefit by adding a biomass sector into the model. This sector represents behavior of the biomass in the system including applicable growth and death rates. The existing model does not account for biomass levels in the system; it simply assumes that ample biomass exists throughout the

system to support degradation activity as defined by individual Michaelis-Menten reaction equations for each material. Further study can incorporate biomass kinetics and their limit on contaminant degradation during growth of the biomass (initial part of the simulations).

A second recommendation is to sample the wetland constructed in the United States Air Force project. The sampling data will provide better approximations for material concentrations in the model. For the existing model, material concentration values were formed from limited literature sources and general knowledge about each material. Therefore, by using the sampling data from the operating constructed wetland, confidence in the model is gained. Additionally, by sampling the actual constructed wetland, confidence in the chemical composition of the iron zone is gained. Any material (i.e., organic acids or forms of alcohol) discovered in significant concentrations can be evaluated for incorporation into the model.

Further development of V_{max} and K_m parameters will also benefit the model. Currently, limited data supports the values used for these parameters in the model. Additional lab work focusing on the specific materials modeled under the soil conditions in the constructed wetland will provide better approximations for these parameters and build confidence in the model.

Representing every reaction in the complex, dynamic iron zone is unrealistic. Therefore, the reactions in this thesis effort represent the significant degrading processes of the system. Numerous other reactions, not represented in the model, may influence the hematite depletion or contaminant degradation in the iron zone. Further study can

evaluate the impact of reactions in the iron zone that are not represented in the model. If appropriate, the additional study can expand the model's system boundary to incorporate the impact of additional reactions.

A final recommendation is to incorporate the existing model with other models representing the entire constructed wetland. Recall that this thesis effort studied one layer of a three-layered system. By combining the models from other research efforts with this thesis effort, an increased understanding of the wetland results. The combined model then can serve as a tool for evaluating future remediation efforts by using constructed wetlands.

Final Assessment of the Thesis Effort

Bioremediation within the iron zone of a constructed wetland involves extremely complex processes. The reactions and relationships that drive the bioremediation are dynamic. Therefore, an ideal approach to studying the behavior in the iron zone is using a system dynamics model. The system dynamics paradigm yields insight into the behavior and interrelationships of the overall system. By constructing the model and running simulations, the modeler begins to understand the complexity of the interactions and interdependencies that encompass the system.

The system dynamics approach focuses on the behavior and relationships of all parameters in the system. Therefore, this approach is favored over other modeling techniques that evaluate only one influential parameter in the system. After building confidence in the system dynamics model, specific parameters can be optimized to maximize bioremediation benefits of the constructed wetland.

Appendix A – Model in Sectors

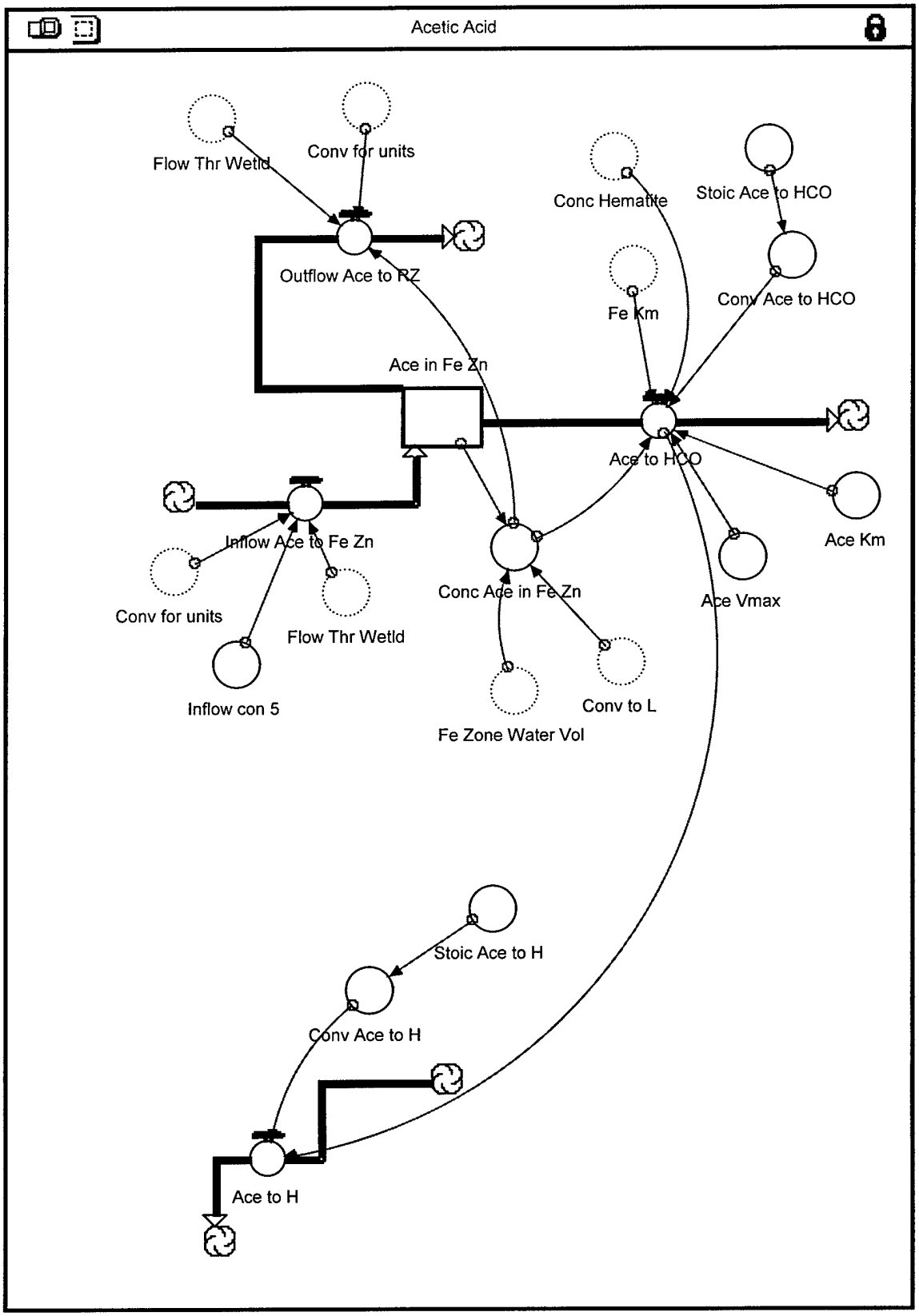

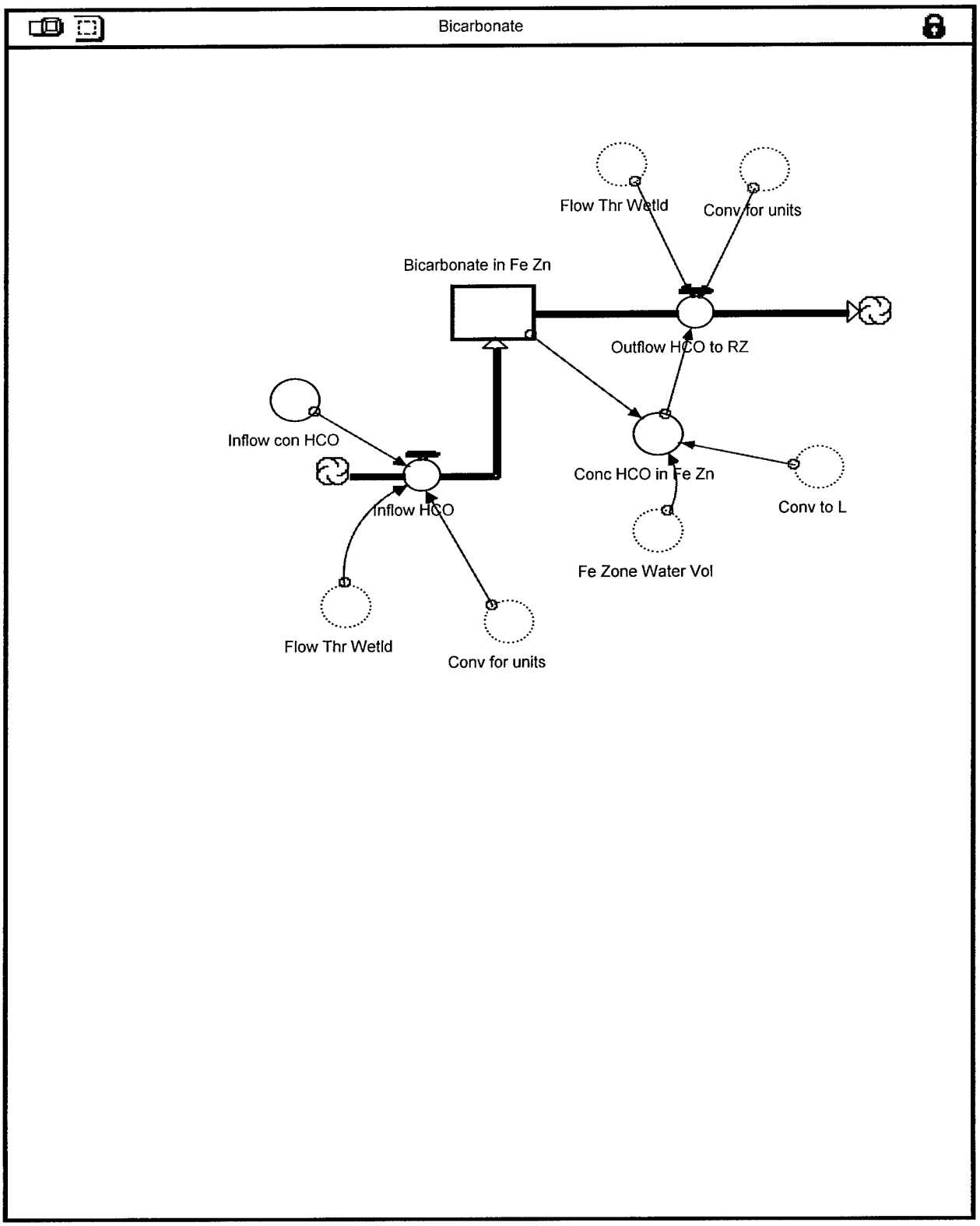
Bicarbonate
Flow Thr Wetld
Conv for units
Bicarbonate in Fe Zn
Outflow HCO to RZ
Inflow con HCO
Conc HCO in Fe Zn
Conv to L
Inflow HCO
Fe Zone Water Vol
Flow Thr Wetld
Conv for units

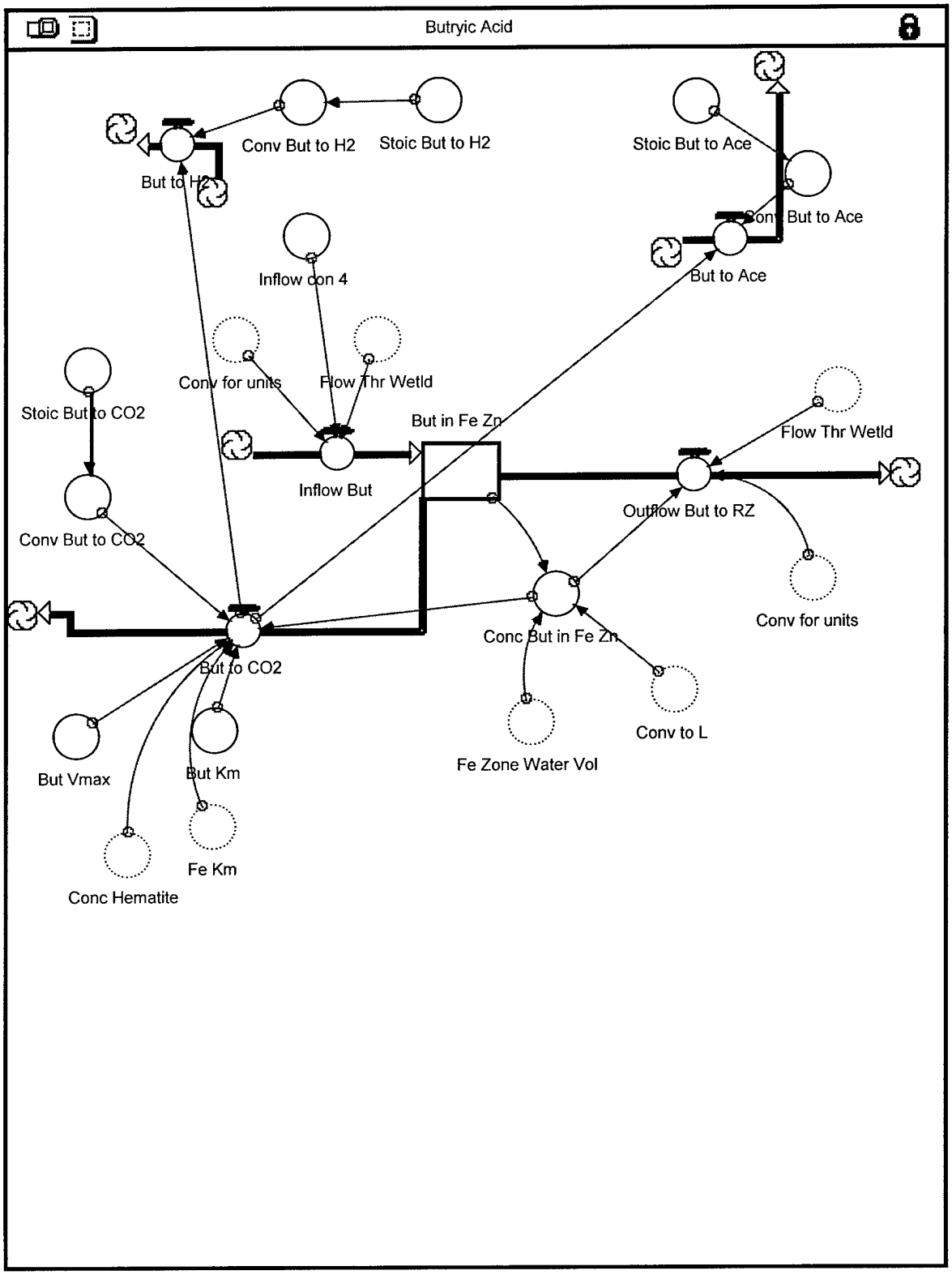
Butryic Acid
Conv But to H2
Stoic But to H2
But to H2
Stoic But to Ace
Conv But to Ace
But to Ace
Inflow con 4
Conv for units
Flow Thr Wetld
Stoic But to CO2
But in Fe Zn
Flow Thr Wetld
Inflow But
Outflow But to RZ
Conv But to CO2
Conv for units
Conc But in Fe Zn
But to CO2
Conv to L
Fe Zone Water Vol
But Vmax
But Km
Fe Km
Conc Hematite

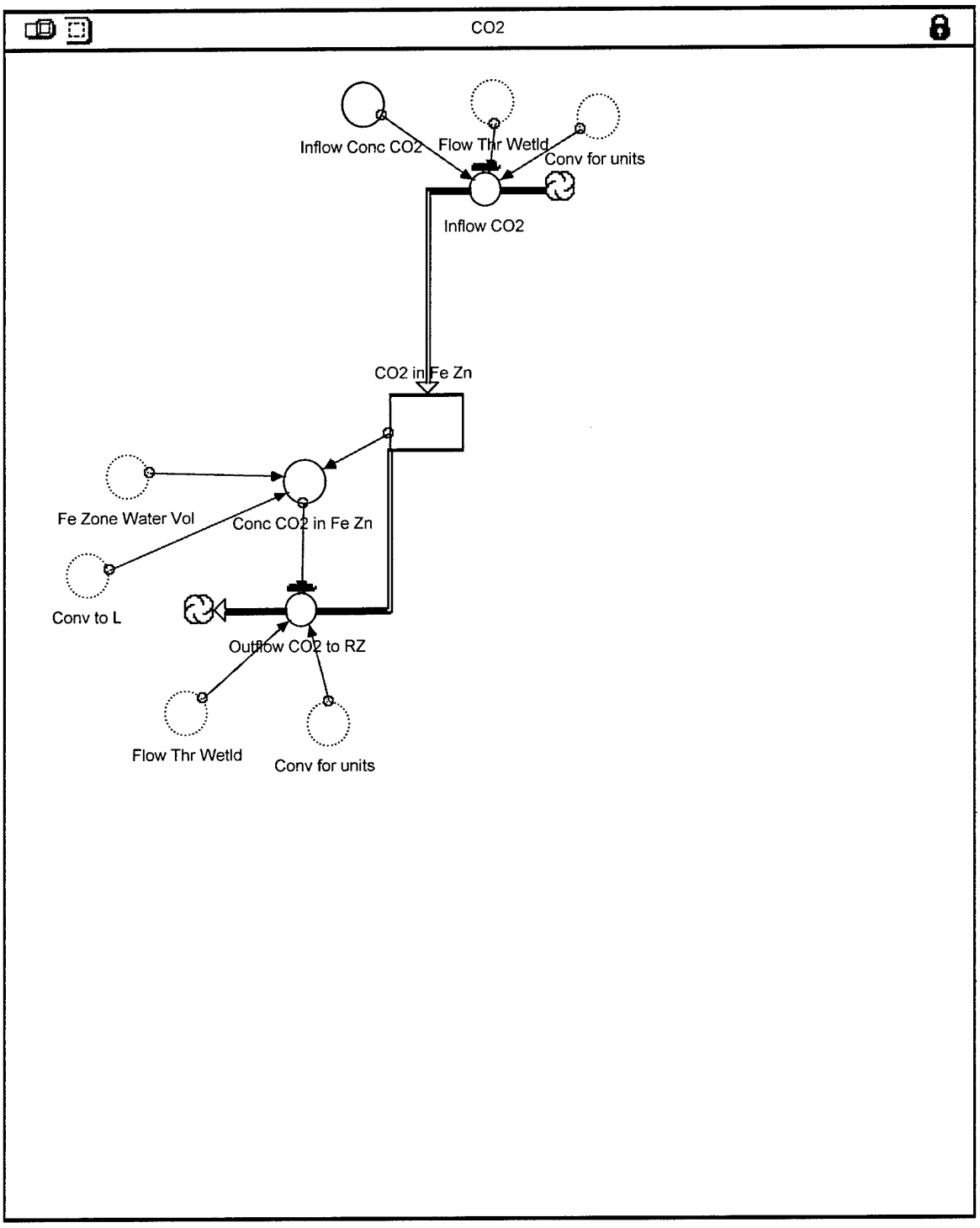
CO2
Inflow Conc CO2
Flow Thr Wetld
Conv for units
Inflow CO2
CO2 in Fe Zn
Fe Zone Water Vol
Conc CO2 in Fe Zn
Conv to L
Outflow CO2 to RZ
Flow Thr Wetld
Conv for units

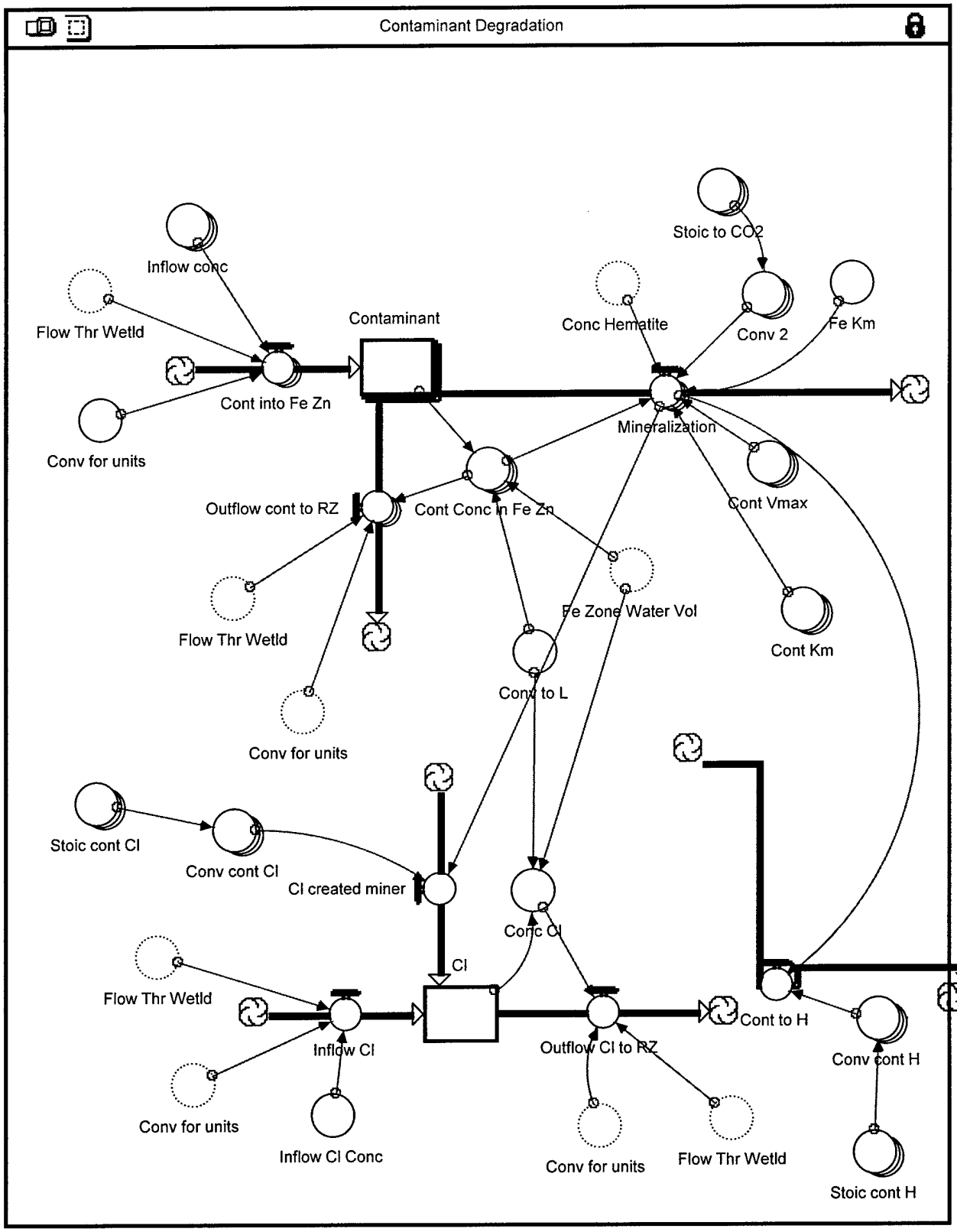
Contaminant Degradation
Inflow conc
Flow Thr Wetld
Contaminant
Cont into Fe Zn
Conv for units
Stoic to CO2
Conc Hematite
Conv 2
Fe Km
Mineralization
Cont Vmax
Outflow cont to RZ
Cont Conc in Fe Zn
Flow Thr Wetld
Fe Zone Water Vol
Cont Km
Cont to L
Conv for units
Stoic cont Cl
Conv cont Cl
Cl created miner
Conc Cl
Cl
Flow Thr Wetld
Inflow Cl
Outflow Cl to RZ
Cont to H
Conv cont H
Conv for units
Inflow Cl Conc
Conv for units
Flow Thr Wetld
Stoic cont H

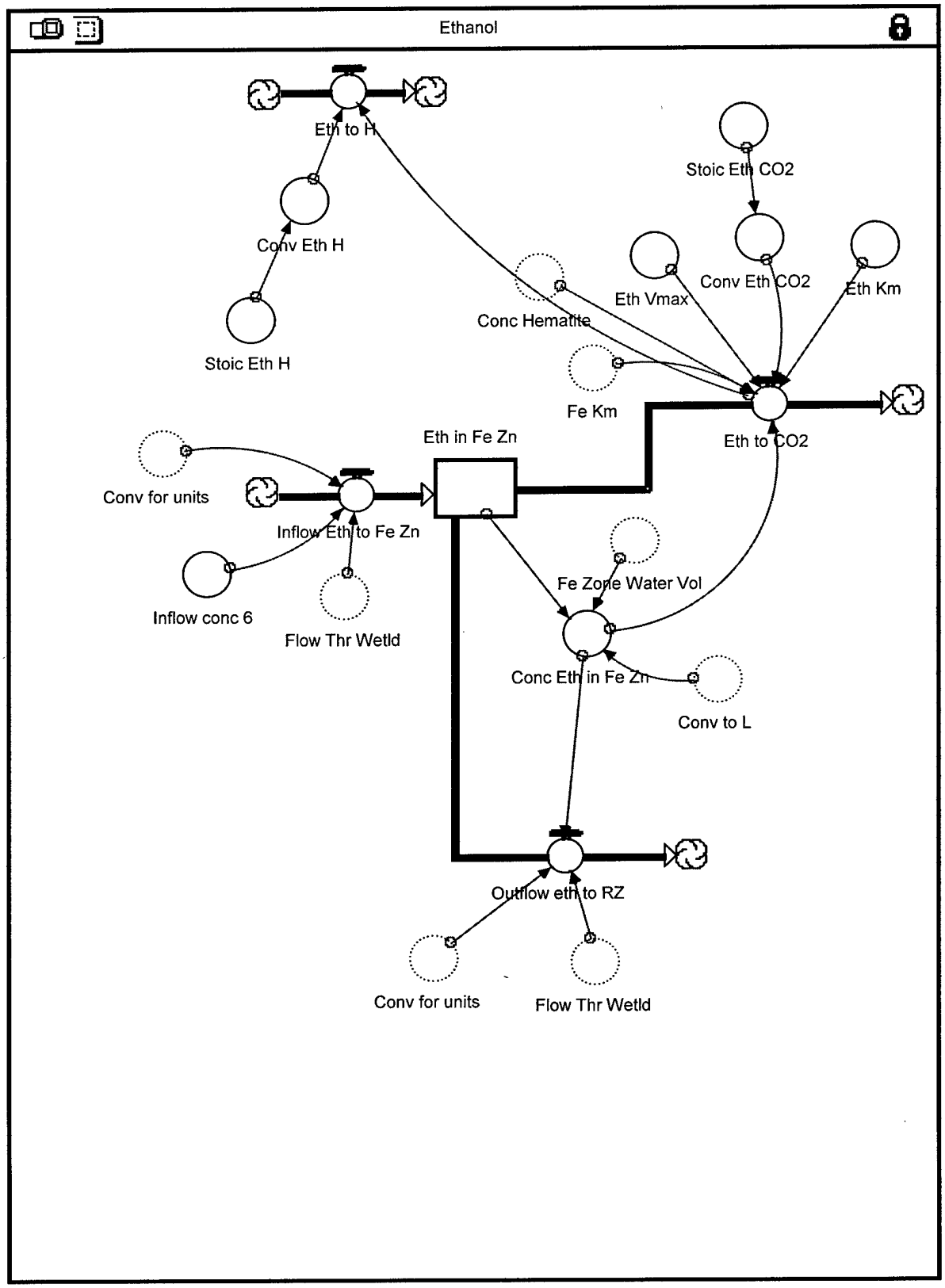
Ethanol
Eth to H
Conv Eth H
Stoic Eth H
Stoic Eth CO2
Conv Eth CO2
Eth Km
Eth Vmax
Conc Hematite
Fe Km
Eth to CO2
Eth in Fe Zn
Conv for units
Inflow Eth to Fe Zn
Inflow conc 6
Flow Thr Wetld
Fe Zone Water Vol
Conc Eth in Fe Zn
Conv to L
Outflow eth to RZ
Conv for units
Flow Thr Wetld

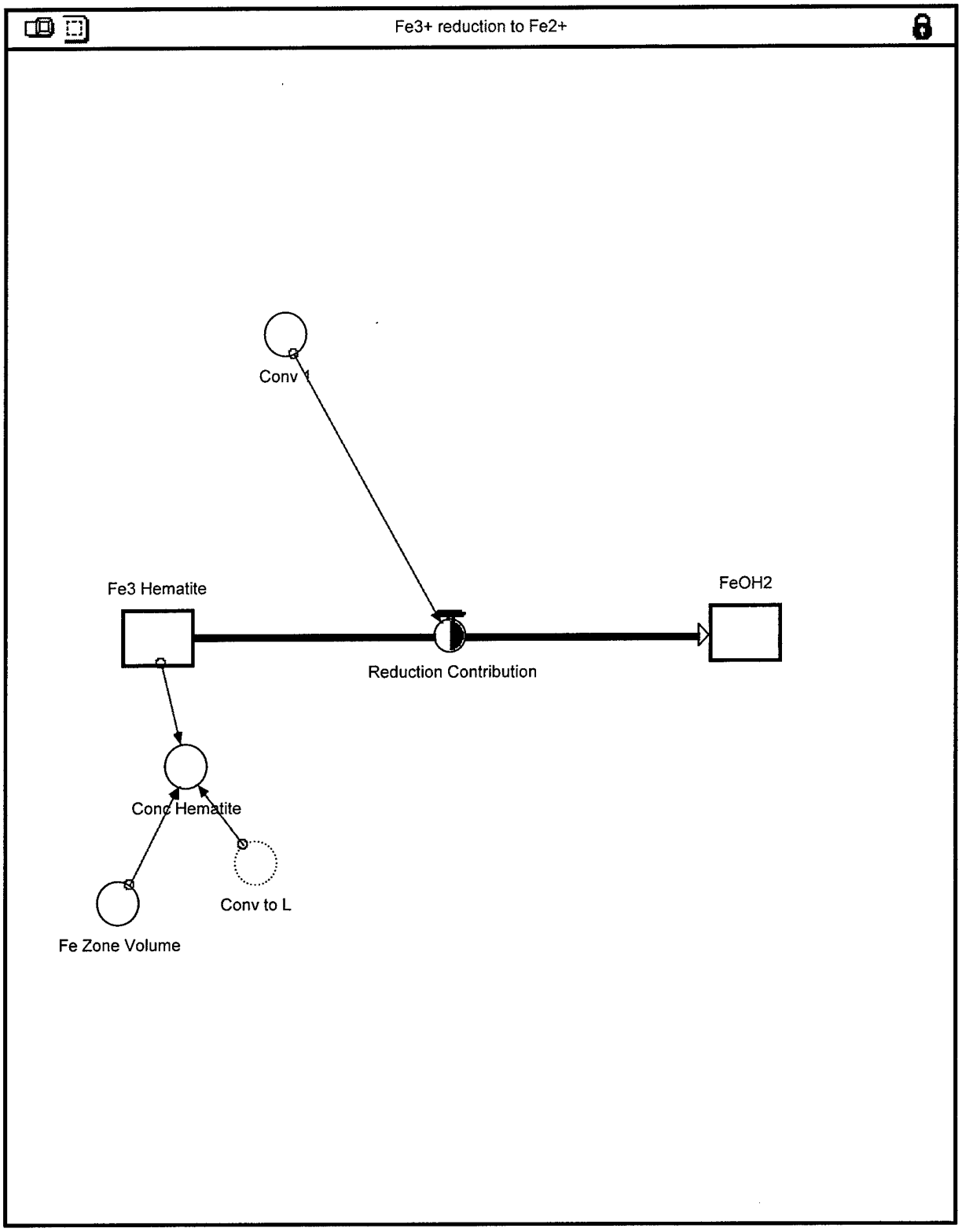
Fe3+ reduction to Fe2+
Conv 1
Fe3 Hematite
FeOH2
Reduction Contribution
Conc Hematite
Conv to L
Fe Zone Volume

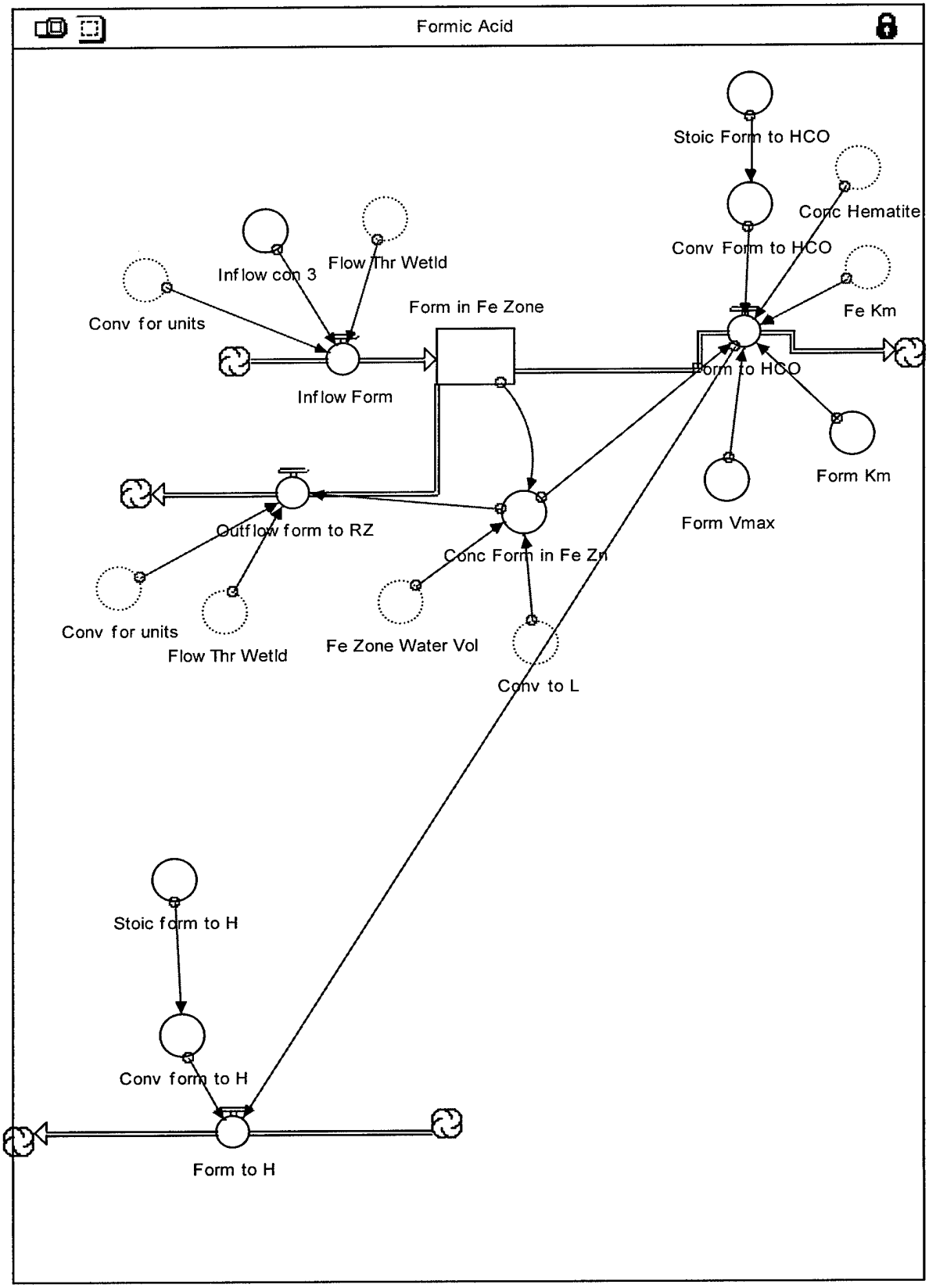
Formic Acid
Stoic Form to HCO
Conc Hematite
Conv Form to HCO
Fe Km
Inflow con 3
Flow Thr Wetld
Conv for units
Form in Fe Zone
Inflow Form
Form to HCO
Form Km
Form Vmax
Outflow form to RZ
Conc Form in Fe Zn
Conv for units
Flow Thr Wetld
Fe Zone Water Vol
Conv to L
Stoic form to H
Conv form to H
Form to H

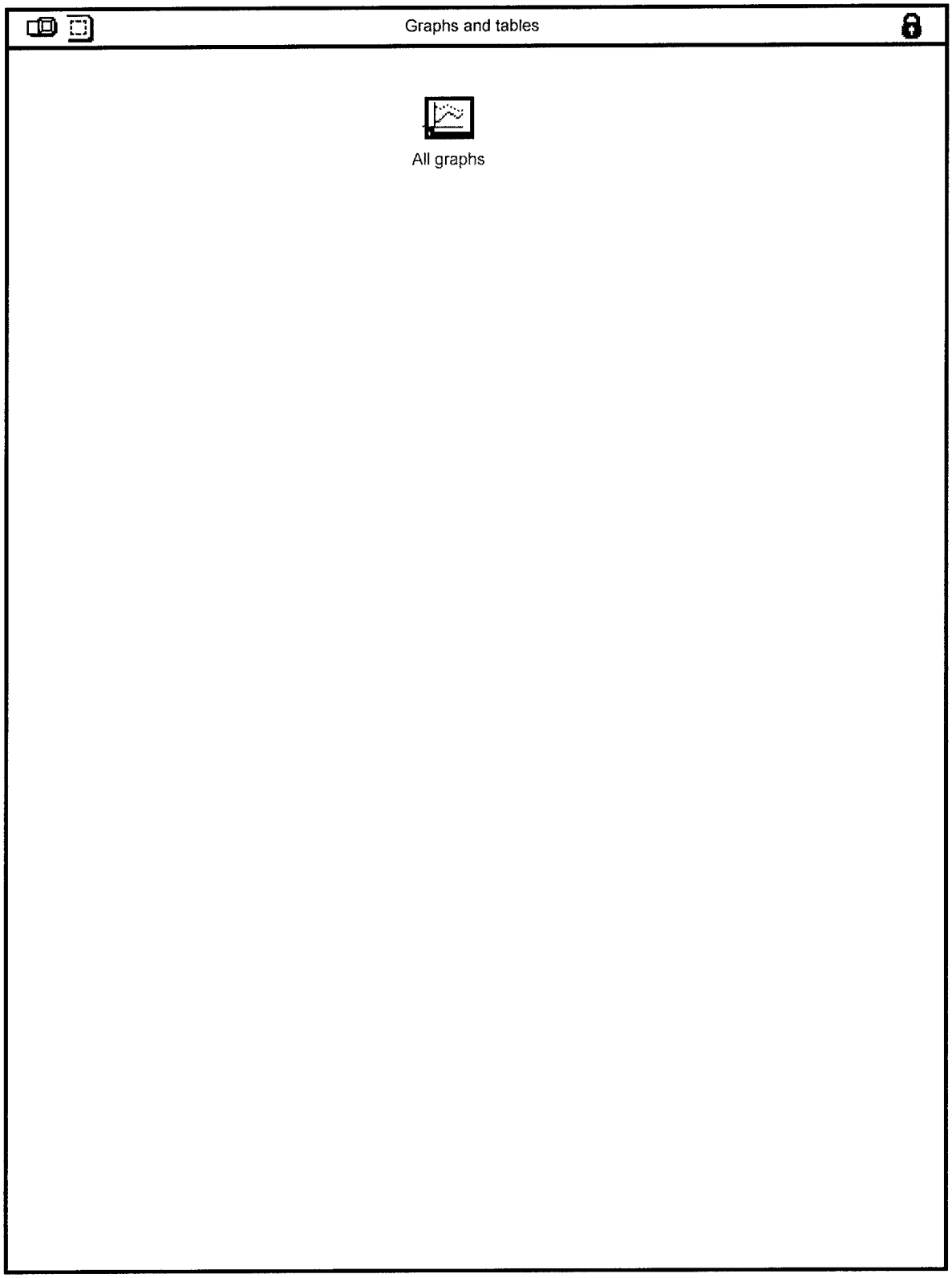
Graphs and tables
All graphs

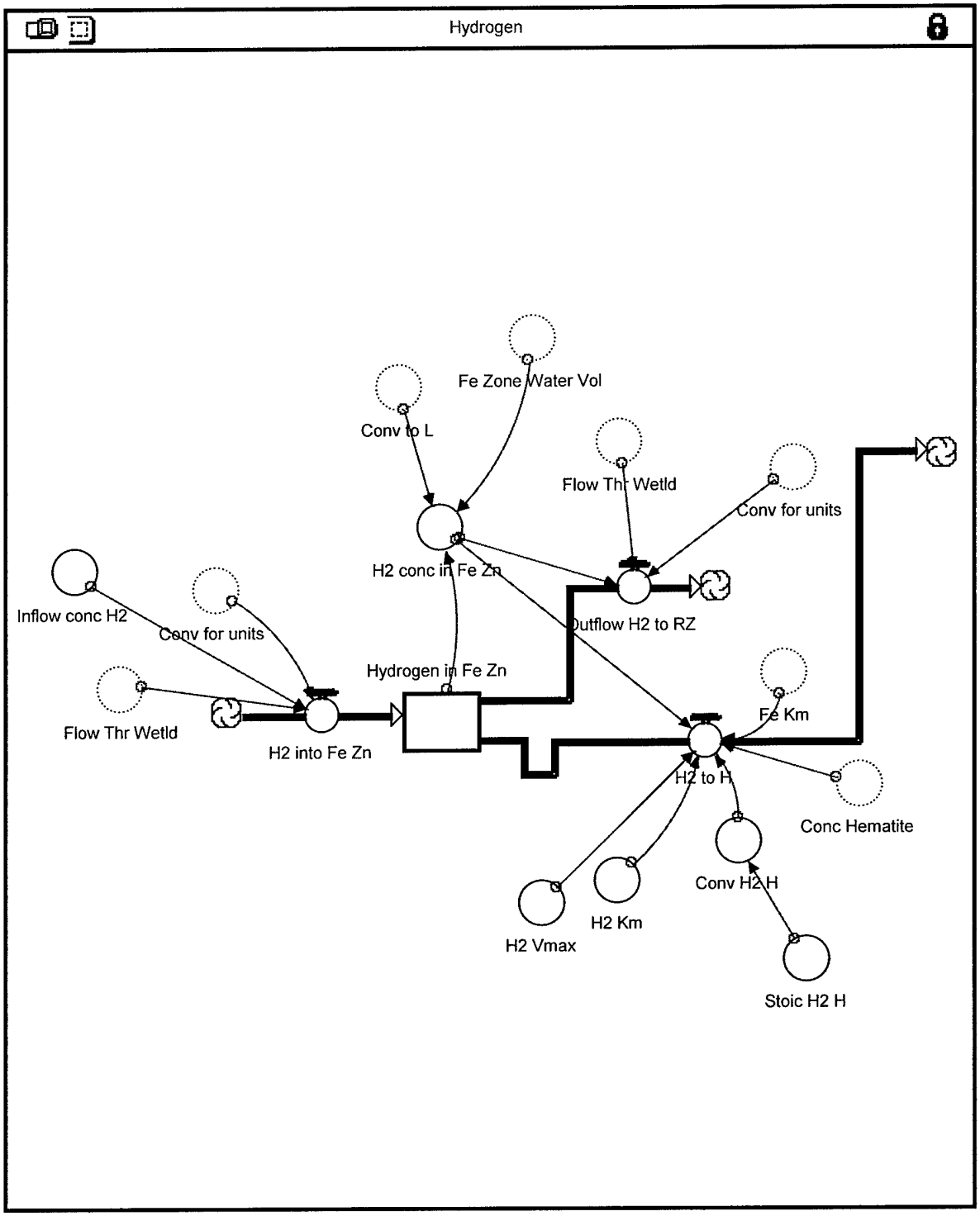
Hydrogen
Fe Zone Water Vol
Conv to L
Flow Thr Wetld
Conv for units
H2 conc in Fe Zn
Inflow conc H2
Conv for units
Outflow H2 to RZ
Hydrogen in Fe Zn
Fe Km
Flow Thr Wetld
H2 into Fe Zn
H2 to H
Conc Hematite
Conv H2 H
H2 Km
H2 Vmax
Stoic H2 H

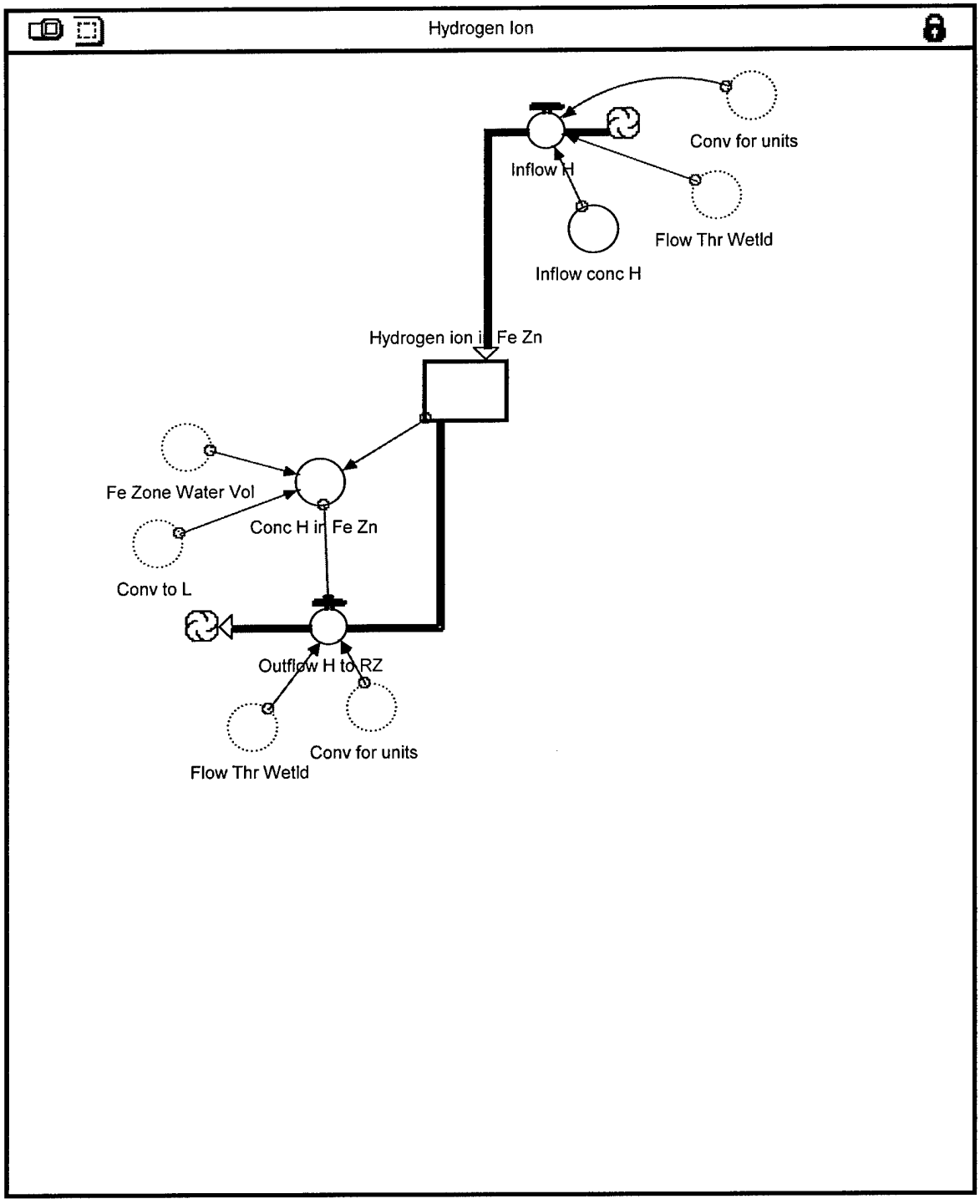
Hydrogen Ion
Conv for units
Inflow H
Flow Thr Wetld
Inflow conc H
Hydrogen ion in Fe Zn
Fe Zone Water Vol
Conc H in Fe Zn
Conv to L
Outflow H to RZ
Conv for units
Flow Thr Wetld

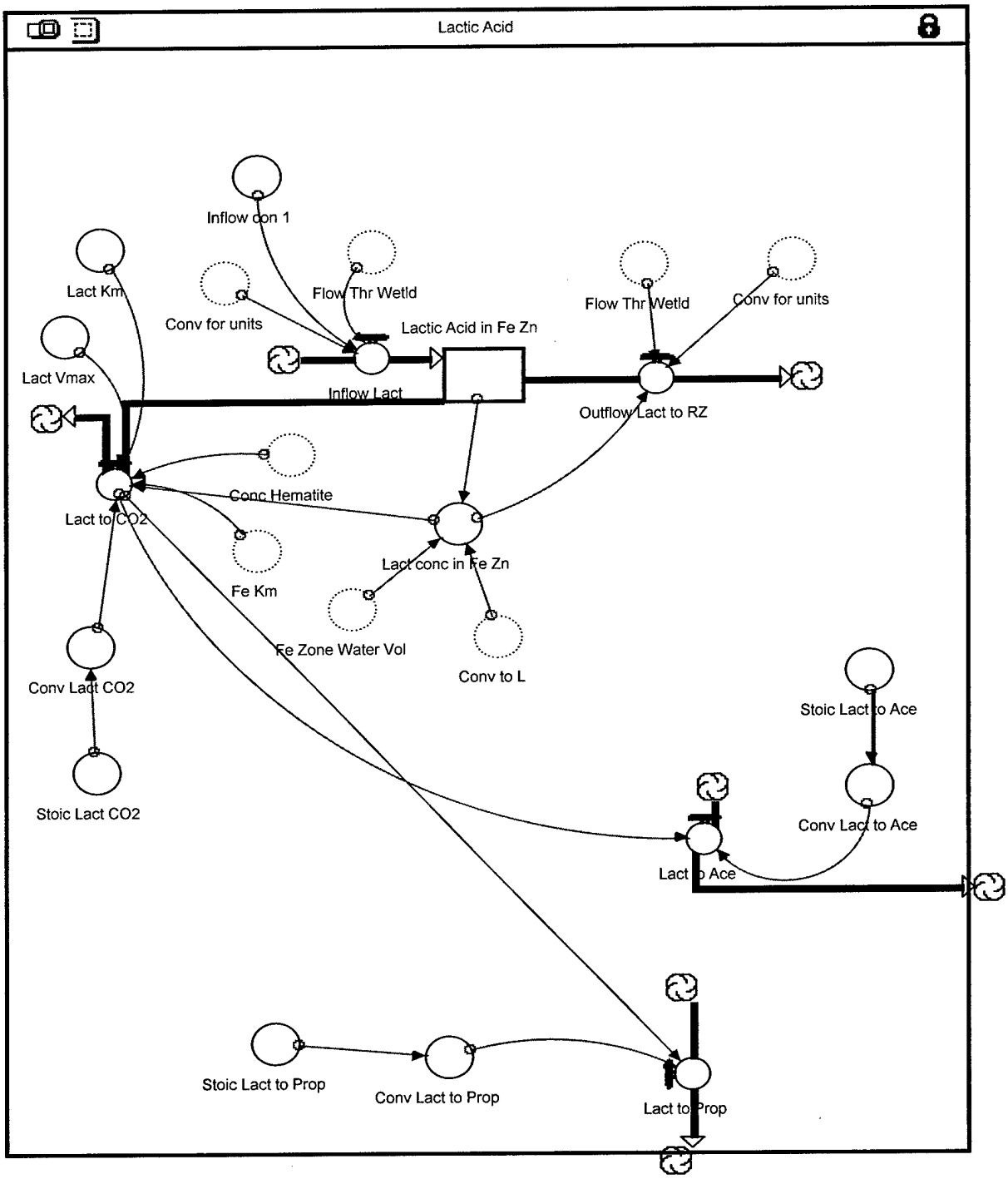
Lactic Acid
Inflow con 1
Lact Km
Flow Thr Wetld
Conv for units
Lactic Acid in Fe Zn
Flow Thr Wetld
Conv for units
Lact Vmax
Inflow Lact
Outflow Lact to RZ
Conc Hematite
Lact to CO2
Lact conc in Fe Zn
Fe Km
Fe Zone Water Vol
Conv to L
Conv Lact CO2
Stoic Lact to Ace
Stoic Lact CO2
Conv Lact to Ace
Lact to Ace
Stoic Lact to Prop
Conv Lact to Prop
Lact to Prop

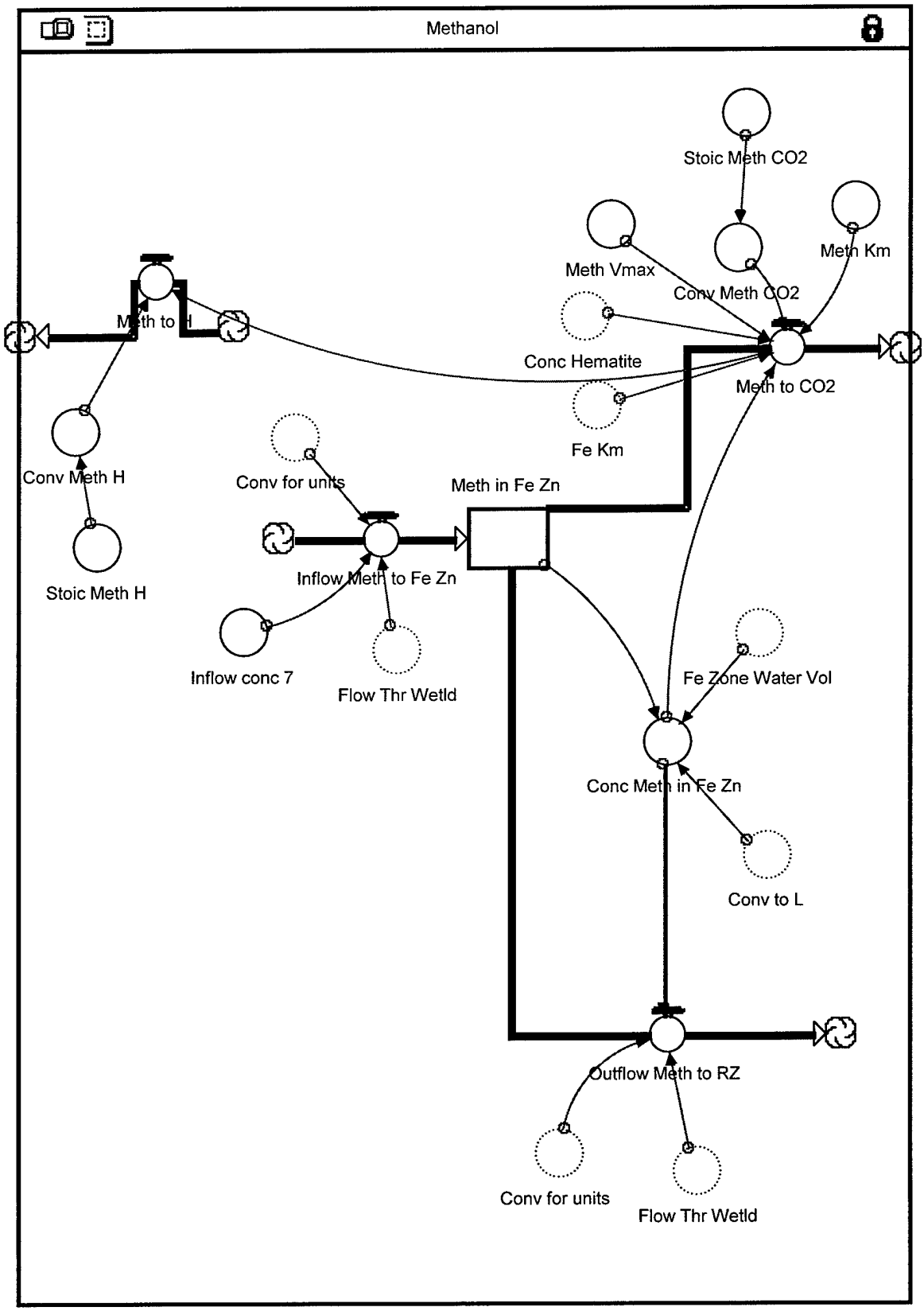
Methanol
Stoic Meth CO2
Meth Vmax
Meth Km
Conv Meth CO2
Meth to H
Conc Hematite
Meth to CO2
Fe Km
Conv Meth H
Conv for units
Meth in Fe Zn
Inflow Meth to Fe Zn
Stoic Meth H
Inflow conc 7
Flow Thr Wetld
Fe Zone Water Vol
Conc Meth in Fe Zn
Conv to L
Outflow Meth to RZ
Conv for units
Flow Thr Wetld

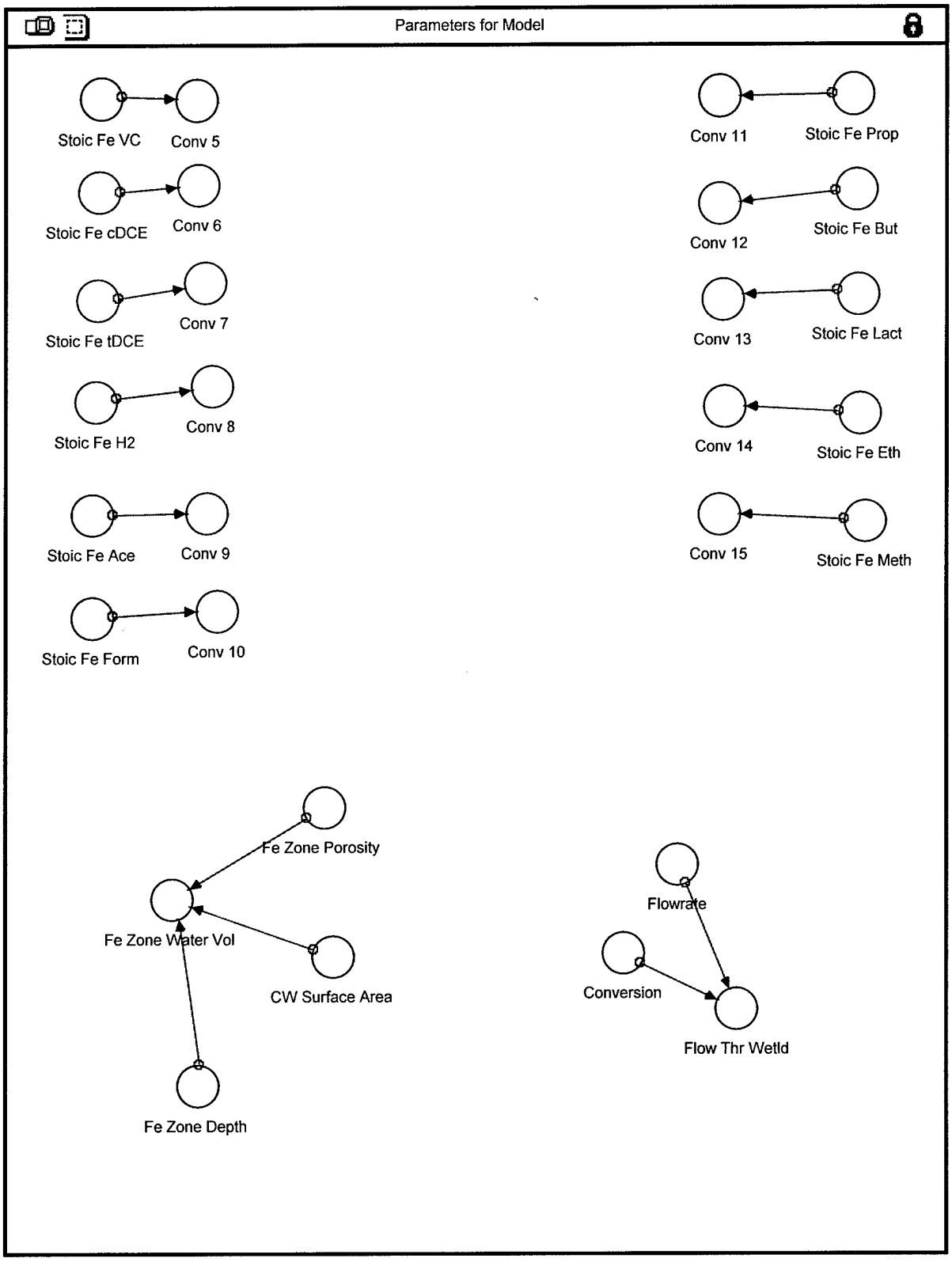
Parameters for Model
Stoic Fe VC
Conv 5
Stoic Fe cDCE
Conv 6
Stoic Fe tDCE
Conv 7
Stoic Fe H2
Conv 8
Stoic Fe Ace
Conv 9
Stoic Fe Form
Conv 10
Conv 11
Stoic Fe Prop
Conv 12
Stoic Fe But
Conv 13
Stoic Fe Lact
Conv 14
Stoic Fe Eth
Conv 15
Stoic Fe Meth
Fe Zone Porosity
Fe Zone Water Vol
CW Surface Area
Fe Zone Depth
Flowrate
Conversion
Flow Thr Wetld

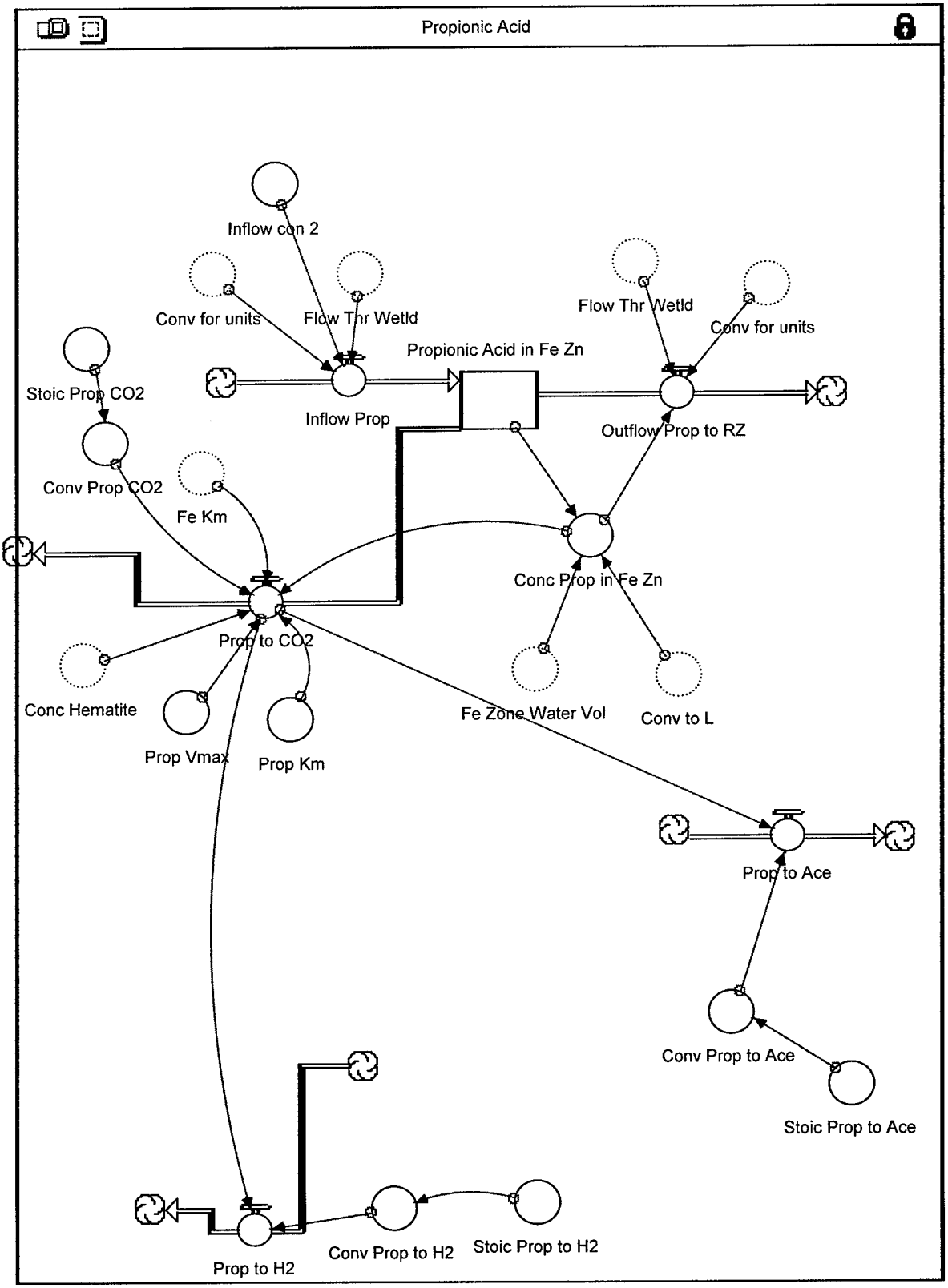
Propionic Acid
Inflow con 2
Conv for units
Flow Thr Wetld
Flow Thr Wetld
Conv for units
Propionic Acid in Fe Zn
Stoic Prop CO2
Inflow Prop
Outflow Prop to RZ
Conv Prop CO2
Fe Km
Conc Prop in Fe Zn
Prop to CO2
Conc Hematite
Fe Zone Water Vol
Conv to L
Prop Vmax
Prop Km
Prop to Ace
Conv Prop to Ace
Stoic Prop to Ace
Prop to H2
Conv Prop to H2
Stoic Prop to H2

Appendix B – STELLA Parameter Descriptions

Model Equations

Acetic Acid

Ace_in_Fe_Zn(t) = Ace_in_Fe_Zn(t - dt) + (Lact_to_Ace + Prop_to_Ace + But_to_Ace + Inflow_Ace_to_Fe_Zn - Ace_to_HCO - Outflow_Ace_to_RZ) * dt
INIT Ace_in_Fe_Zn = 0

INFLOWS:
Lact_to_Ace (IN SECTOR: Lactic Acid)
Prop_to_Ace (IN SECTOR: Propionic Acid)
But_to_Ace (IN SECTOR: Butryic Acid)
Inflow_Ace_to_Fe_Zn = Conv_for_units*Flow_Thr_Wetld*Inflow_con_5
OUTFLOWS:
Ace_to_HCO(o) = (Ace_Vmax*Conc_Ace_in_Fe_Zn*Conc_Hematite)/((Ace_Km+Conc_Ace_in_Fe_Zn)*(Conc_Hematite+Fe_Km))
Outflow_Ace_to_RZ = Conc_Ace_in_Fe_Zn*Conv_for_units*Flow_Thr_Wetld
Ace_to_H = Ace_to_HCO*Conv_Ace_to_H

INFLOW TO: Hydrogen_ion_in_Fe_Zn (IN SECTOR: Hydrogen Ion)
Ace_Km = 2
DOCUMENT: See ethanol Km

Ace_Vmax = 40000
DOCUMENT: See ethanol Vmax

Conc_Ace_in_Fe_Zn = (Ace_in_Fe_Zn/Fe_Zone_Water_Vol)*Conv_to_L
Conv_Ace_to_H = (8*1)/(Stoic_Ace_to_H*60)
Conv_Ace_to_HCO = (2*61)/(Stoic_Ace_to_HCO*60)
Inflow_con_5 = 10
Stoic_Ace_to_H = 1
Stoic_Ace_to_HCO = 1

Bicarbonate

Bicarbonate_in_Fe_Zn(t) = Bicarbonate_in_Fe_Zn(t - dt) + (Form_to_HCO + Ace_to_HCO + Inflow_HCO - Outflow_HCO_to_RZ) * dt
INIT Bicarbonate_in_Fe_Zn = 0

INFLOWS:
Form_to_HCO (IN SECTOR: Formic Acid)
Ace_to_HCO (IN SECTOR: Acetic Acid)
Inflow_HCO = Conv_for_units*Flow_Thr_Wetld*Inflow_con_HCO

OUTFLOWS:
Outflow_HCO_to_RZ = Conc_HCO_in_Fe_Zn*Conv_for_units*Flow_Thr_Wetld
Conc_HCO_in_Fe_Zn = (Bicarbonate_in_Fe_Zn/Fe_Zone_Water_Vol)*Conv_to_L
Inflow_con_HCO = 0.05

Butyric Acid

But_in_Fe_Zn(t) = But_in_Fe_Zn(t - dt) + (Inflow_But - But_to_CO2 - Outflow_But_to_RZ) * dt
INIT But_in_Fe_Zn = 0

INFLOWS:
Inflow_But = Conv_for_units*Flow_Thr_Wetld*Inflow_con_4

OUTFLOWS:
But_to_CO2(o) =
(But_Vmax*Conc_But_in_Fe_Zn*Conc_Hematite)/((But_Km+Conc_But_in_Fe_Zn)*(Fe_Km+Conc_Hematite))
Outflow_But_to_RZ = Conc_But_in_Fe_Zn*Conv_for_units*Flow_Thr_Wetld
But_to_Ace = But_to_CO2*Conv_But_to_Ace

INFLOW TO: Ace_in_Fe_Zn (IN SECTOR: Acetic Acid)
But_to_H2 = But_to_CO2*Conv_But_to_H2

INFLOW TO: Hydrogen_in_Fe_Zn (IN SECTOR: Hydrogen)
But_Km = 2
DOCUMENT: See ethanol Km

But_Vmax = 35000
DOCUMENT: See ethanol Vmax

Conc_But_in_Fe_Zn = (But_in_Fe_Zn/Fe_Zone_Water_Vol)*Conv_to_L
Conv_But_to_Ace = (1*60)/(Stoic_But_to_Ace*88)
Conv_But_to_CO2 = (2*44)/(Stoic_But_to_CO2*88)
Conv_But_to_H2 = (5*2)/(Stoic_But_to_H2*88)
Inflow_con_4 = .75
Stoic_But_to_Ace = 1
Stoic_But_to_CO2 = 1
Stoic_But_to_H2 = 1

CO2
CO2_in_Fe_Zn(t) = CO2_in_Fe_Zn(t - dt) + (Mineralization[Contaminants] + Mineralization[VC] + Mineralization[cDCE] + Mineralization[tDCE] + Inflow_CO2 + Eth_to_CO2 + Meth_to_CO2 + Lact_to_CO2 + Prop_to_CO2 + But_to_CO2 - Outflow_CO2_to_RZ) * dt
INIT CO2_in_Fe_Zn = 0

INFLOWS:
Mineralization[Contaminants] (IN SECTOR: Contaminant Degradation)
Inflow_CO2 = Conv_for_units*Flow_Thr_Wetld*Inflow_Conc_CO2
Eth_to_CO2 (IN SECTOR: Ethanol)
Meth_to_CO2 (IN SECTOR: Methanol)
Lact_to_CO2 (IN SECTOR: Lactic Acid)
Prop_to_CO2 (IN SECTOR: Propionic Acid)
But_to_CO2 (IN SECTOR: Butryic Acid)

OUTFLOWS:
Outflow_CO2_to_RZ = Conc_CO2_in_Fe_Zn*Conv_for_units*Flow_Thr_Wetld
Conc_CO2_in_Fe_Zn = (CO2_in_Fe_Zn/Fe_Zone_Water_Vol)*Conv_to_L
Inflow_Conc_CO2 = 0.05

Contaminant Degradation
Cl(t) = Cl(t - dt) + (Inflow_Cl + Cl_created_miner - Outflow_Cl_to_RZ) * dt
INIT Cl = 0

INFLOWS:
Inflow_Cl = Conv_for_units*Flow_Thr_Wetld*Inflow_Cl_Conc
Cl_created_miner =
Mineralization[VC]*Conv_cont_Cl[VC]+Mineralization[cDCE]*Conv_cont_Cl[cDCE]+Mineralization[tDCE]*Conv_cont_Cl[tDCE]

OUTFLOWS:
Outflow_Cl_to_RZ = Conc_Cl*Conv_for_units*Flow_Thr_Wetld
Contaminant[Contaminants](t) = Contaminant[Contaminants](t - dt) + (Cont_into_Fe_Zn[Contaminants] - Mineralization[Contaminants] - Outflow_cont_to_RZ[Contaminants]) * dt
INIT Contaminant[Contaminants] = 0
DOCUMENT: Initial value of contaminants in the Fe Zone is 0. Units are mg.

INFLOWS:
Cont_into_Fe_Zn[Contaminants] = Conv_for_units*Flow_Thr_Wetld*Inflow_conc[Contaminants]
DOCUMENT: Gives the amount of contaminant entering the Fe Zone. Units are mg/day

OUTFLOWS:
Mineralization[Contaminants](o) =
(Cont_Vmax[Contaminants]*Cont_Conc_in_Fe_Zn[Contaminants]*Conc_Hematite)/((Cont_Km[Contaminants]+Cont_Conc_in_Fe_Zn[Contaminants])*(Fe_Km+Conc_Hematite))
Outflow_cont_to_RZ[Contaminants] =
Cont_Conc_in_Fe_Zn[Contaminants]*Conv_for_units*Flow_Thr_Wetld
DOCUMENT: Allows for a pathway other than mineralization. This flow is the amount of contaminants that flow to the root zone.

Cont_to_H =
Mineralization[VC]*Conv_cont_H[VC]+Mineralization[cDCE]*Conv_cont_H[cDCE]+Mineralization[tDCE]*Conv_cont_H[tDCE]

INFLOW TO: Hydrogen_ion_in_Fe_Zn (IN SECTOR: Hydrogen Ion)
Conc_Cl = (Cl/Fe_Zone_Water_Vol)*Conv_to_L
Cont_Conc_in_Fe_Zn[Contaminants] = (Contaminant[Contaminants]/Fe_Zone_Water_Vol)*Conv_to_L
Cont_Km[VC] = 0.0806
DOCUMENT: Values found in Lovley 1997, units are mg/L.

Cont_Km[cDCE] = 0.096
DOCUMENT: See documentation for VC

Cont_Km[tDCE] = 0.096
DOCUMENT: See documentation for VC

Cont_Vmax[VC] = 7000
DOCUMENT: VC values found in Lovley 1997. Units are mg/d. Values for DCE isomers taken from Hoefar's model. The original value given by Lovley is multiplied by the amount of liters in the iron zone. This comes out to be 356.79 m^3*0.4(porosity)*1000L/m^3(conversion) = 142716.9 L

Cont_Vmax[cDCE] = 5000
DOCUMENT: See documentation for VC

Cont_Vmax[tDCE] = 5000
DOCUMENT: See documentation for VC

Conv_2[VC] = (2*44)/(Stoic_to_CO2[VC]*62)
DOCUMENT: Stoic of CO2*MW CO2/Stoic of VC*MW VC

Conv_2[cDCE] = (2*44)/(Stoic_to_CO2[cDCE]*96)
Conv_2[tDCE] = (2*44)/(Stoic_to_CO2[tDCE]*96)
Conv_cont_Cl[VC] = (1*35)/(Stoic_cont_Cl[VC]*62)
Conv_cont_Cl[cDCE] = (2*35)/(Stoic_cont_Cl[cDCE]*96)
Conv_cont_Cl[tDCE] = (2*35)/(Stoic_cont_Cl[tDCE]*96)
Conv_cont_H[VC] = (8*1)/(Stoic_cont_H[VC]*62)
Conv_cont_H[cDCE] = (8*1)/(Stoic_cont_H[cDCE]*96)
Conv_cont_H[tDCE] = (8*1)/(Stoic_cont_H[tDCE]*96)
Conv_for_units = 1000
DOCUMENT: Converts initial conc (mg/L) and groundwater flow (m^3/day) into mg/day

Conv_to_L = 0.001
DOCUMENT: 0.001m^3/L

Fe_Km = 2
Inflow_Cl_Conc = 0.00001
DOCUMENT: Units are mg/L. Value chosen as a very small concentration value entering the iron zone. This minute amount is a product of reductive dechlorination in the methanogenic zone.

Inflow_conc[VC] = 0.01
DOCUMENT: Value estimated from Hoefar's model with PCE value of 0.05 mg/l entering the constructed wetland system. Units are mg/L

Inflow_conc[cDCE] = 0.015
DOCUMENT: Value estimated from Hoefar's model with 0.05 mg/l PCE entering the constructed wetland. Units are mg/L

Inflow_conc[tDCE] = 0.005
DOCUMENT: Value estimated from Hoefar's model with 0.05 mg/L PCE entering constructed wetland. . . units are mg/l

Stoic_cont_Cl[VC] = 1
Stoic_cont_Cl[cDCE] = 1
Stoic_cont_Cl[tDCE] = 1
Stoic_cont_H[VC] = 1
Stoic_cont_H[cDCE] = 1
Stoic_cont_H[tDCE] = 1
Stoic_to_CO2[VC] = 1
Stoic_to_CO2[cDCE] = 1
Stoic_to_CO2[tDCE] = 1

Ethanol
Eth_in_Fe_Zn(t) = Eth_in_Fe_Zn(t - dt) + (Inflow_Eth_to_Fe_Zn - Outflow_eth_to_RZ - Eth_to_CO2) * dt
INIT Eth_in_Fe_Zn = 0

INFLOWS:
Inflow_Eth_to_Fe_Zn = Inflow_conc_6*Flow_Thr_Wetld*Conv_for_units

OUTFLOWS:
Outflow_eth_to_RZ = Conc_Eth_in_Fe_Zn*Conv_for_units*Flow_Thr_Wetld
Eth_to_CO2(o) =
(Eth_Vmax*Conc_Eth_in_Fe_Zn*Conc_Hematite)/((Conc_Eth_in_Fe_Zn+Eth_Km)*(Conc_Hematite+Fe_Km))
Eth_to_H = Eth_to_CO2*Conv_Eth_H

INFLOW TO: Hydrogen_ion_in_Fe_Zn (IN SECTOR: Hydrogen Ion)
Conc_Eth_in_Fe_Zn = (Eth_in_Fe_Zn/Fe_Zone_Water_Vol)*Conv_to_L
Conv_Eth_CO2 = (2*44)/(Stoic_Eth_CO2*46)
Conv_Eth_H = (10*1)/(Stoic_Eth_H*46)
Eth_Km = 2
DOCUMENT: Found using Fennel and Gossett values. Units are mg/L.

Eth_Vmax = 35000
DOCUMENT: Found by using value from Fennel and Gossett. Assumed value of biomass as slightly less than 1% of mass in Fe zone (2.5x10^10 mg). Then, for conversion, 24 h/day, 1 mol/ 10^6 umol, MW/1 mol, 1000 mg/g. Units are mg/d.

Inflow_conc_6 = 1
Stoic_Eth_CO2 = 1
Stoic_Eth_H = 1

Fe3+ reduction to Fe2+
Fe3_Hematite(t) = Fe3_Hematite(t - dt) + (- Reduction_Contribution) * dt
INIT Fe3_Hematite = 4500000000

DOCUMENT: This number found by taking volume of Fe Zone (356.79 m^3) and multiplying by 2.5 Mg/m^3 (a general value for density of soil -- recommended by Dr Shelley in second committee meeting). This value is then multiplied by .5% (0.005) in order to figure the approximate amount of hematite in the soil. The value given is in mg.

OUTFLOWS:
Reduction_Contribution(o) =
Mineralization[VC]*Conv_5+Mineralization[cDCE]*Conv_6+Mineralization[tDCE]*Conv_7+H2_to_H*Conv_8+Ace_to_HCO*Conv_9+Form_to_HCO*Conv_10+Prop_to_CO2*Conv_11+But_to_CO2*Conv_12+Lact_to_CO2*Conv_13+Eth_to_CO2*Conv_14+Meth_to_CO2*Conv_15
FeOH2(t) = FeOH2(t - dt) + (Reduction_Contribution) * dt
INIT FeOH2 = 1125000000

DOCUMENT: This value is the initial amount of Fe(OH)2 in the soil. It was found as 1/4 of the amount of hematite initially found in the soil. Units are mg.

INFLOWS:
Conv_1 = (2*90)/(1*160)
DOCUMENT: Unit conversion between hematite and Fe(OH)2. Units are unitless. Conversion is found by multiplying the number of moles of Fe(OH)2 by the molecular weight and dividing by the number of moles of hematite by the molecular weight. Because the number of moles is identical for all reactions in this thesis effort, the unit conversion can be used.

Conc_Hematite = (Fe3_Hematite/Fe_Zone_Volume)*Conv_to_L
Conv_1 = (2*90)/(1*160)
DOCUMENT: Unit conversion between hematite and Fe(OH)2. Units are unitless. Conversion is found by multiplying the number of moles of Fe(OH)2 by the molecular weight and dividing by the number of moles of hematite by the molecular weight. Because the number of moles is identical for all reactions in this thesis effort, the unit conversion can be used.

Fe_Zone_Volume = 356.7922506

Formic Acid
Form_in_Fe_Zone(t) = Form_in_Fe_Zone(t - dt) + (Inflow_Form - Form_to_HCO - Outflow_form_to_RZ) * dt
INIT Form_in_Fe_Zone = 0

INFLOWS:
Inflow_Form = Conv_for_units*Flow_Thr_Wetld*Inflow_con_3

OUTFLOWS
Form_to_HCO(o) =
(Form_Vmax*Conc_Form_in_Fe_Zn*Conc_Hematite)/((Form_Km+Conc_Form_in_Fe_Zn)*(Fe_Km+Conc_Hematite))
Outflow_form_to_RZ = Conc_Form_in_Fe_Zn*Conv_for_units*Flow_Thr_Wetld
Form_to_H = Form_to_HCO*Conv_form_to_H

INFLOW TO: Hydrogen_ion_in_Fe_Zn (IN SECTOR: Hydrogen Ion)
Conc_Form_in_Fe_Zn = (Form_in_Fe_Zone/Fe_Zone_Water_Vol)*Conv_to_L
Conv_form_to_H = (1*1)/(Stoic_form_to_H*46)
Conv_Form_to_HCO = (1*61)/(Stoic_Form_to_HCO*46)
Form_Km = 2
DOCUMENT: See ethanol Km

Form_Vmax = 40000
DOCUMENT: See ethanol Vmax

Inflow_con_3 = 5
Stoic_form_to_H = 1
Stoic_Form_to_HCO = 1

Hydrogen
Hydrogen_in_Fe_Zn(t) = Hydrogen_in_Fe_Zn(t - dt) + (H2_into_Fe_Zn + Prop_to_H2 + But_to_H2 - Outflow_H2_to_RZ - H2_to_H) * dt
INIT Hydrogen_in_Fe_Zn = 0.125

DOCUMENT: Initial value must be larger than zero in order for Fe reduction to take place. Assume that the concentration of H2 in the Fe Zone behaves in accordance with Lovley, 1994 paper.

INFLOWS:
H2_into_Fe_Zn = Conv_for_units*Flow_Thr_Wetld*Inflow_conc_H2
Prop_to_H2 (IN SECTOR: Propionic Acid)
But_to_H2 (IN SECTOR: Butryic Acid)

OUTFLOWS:
Outflow_H2_to_RZ = Conv_for_units*Flow_Thr_Wetld*H2_conc_in_Fe_Zn
H2_to_H =
((H2_Vmax*H2_conc_in_Fe_Zn*Conc_Hematite)/((H2_Km+H2_conc_in_Fe_Zn)*(Fe_Km+Conc_Hematite)))*Conv_H2_H
Conv_H2_H = (2*1)/(Stoic_H2_H*2)
H2_conc_in_Fe_Zn = (Hydrogen_in_Fe_Zn/Fe_Zone_Water_Vol)*Conv_to_L
H2_Km = 2
H2_Vmax = 15000
DOCUMENT: Value estimated from concentration value given in Lovley, 1994 of 0.2 nM and flow through wetland with appropriate conversions. Units are mg/d

Inflow_conc_H2 = 0.0000004
DOCUMENT: Units are mg/L. . .Values comes from Lovley 1994 H2 concentrations of .2 nM. Units are converted to mg/L using 2 g H2/mol H2 and 1000 mg/g

Stoic_H2_H = 2

Hydrogen Ion
Hydrogen_ion_in_Fe_Zn(t) = Hydrogen_ion_in_Fe_Zn(t - dt) + (Cont_to_H + Inflow_H + Eth_to_H + Meth_to_H + Form_to_H + Ace_to_H + H2_to_H - Outflow_H_to_RZ) * dt
INIT Hydrogen_ion_in_Fe_Zn = 0

INFLOWS:
Cont_to_H (IN SECTOR: Contaminant Degradation)
Inflow_H = Conv_for_units*Flow_Thr_Wetld*Inflow_conc_H
Eth_to_H (IN SECTOR: Ethanol)
Meth_to_H (IN SECTOR: Methanol)
Form_to_H (IN SECTOR: Formic Acid)
Ace_to_H (IN SECTOR: Acetic Acid)
H2_to_H (IN SECTOR: Hydrogen)

OUTFLOWS:
Outflow_H_to_RZ = Conc_H_in_Fe_Zn*Conv_for_units*Flow_Thr_Wetld
Conc_H_in_Fe_Zn = (Hydrogen_ion_in_Fe_Zn/Fe_Zone_Water_Vol)*Conv_to_L
Inflow_conc_H = 0.001

Lactic Acid
Lactic_Acid_in_Fe_Zn(t) = Lactic_Acid_in_Fe_Zn(t - dt) + (Inflow_Lact - Lact_to_CO2 - Outflow_Lact_to_RZ) * dt
INIT Lactic_Acid_in_Fe_Zn = 0

INFLOWS:
Inflow_Lact = Conv_for_units*Flow_Thr_Wetld*Inflow_con_1
Lact_to_CO2(o) =
(Lact_Vmax*Lact_conc_in_Fe_Zn*Conc_Hematite)/((Lact_Km+Lact_conc_in_Fe_Zn)*(Conc_Hematite+Fe_Km))

OUTFLOWS:
Outflow_Lact_to_RZ = Conv_for_units*Flow_Thr_Wetld*Lact_conc_in_Fe_Zn
Lact_to_Ace = Lact_to_CO2*Conv_Lact_to_Ace

INFLOW TO: Ace_in_Fe_Zn (IN SECTOR: Acetic Acid)
Lact_to_Prop = Lact_to_CO2*Conv_Lact_to_Prop

INFLOW TO: Propionic_Acid_in_Fe_Zn (IN SECTOR: Propionic Acid)
Conv_Lact_CO2 = (1*44)/(Stoic_Lact_CO2*90)
Conv_Lact_to_Ace = (1*60)/(Stoic_Lact_to_Ace*90)
Conv_Lact_to_Prop = (1*74)/(Stoic_Lact_to_Prop*90)
Inflow_con_1 = .75
Lact_conc_in_Fe_Zn = (Lactic_Acid_in_Fe_Zn/Fe_Zone_Water_Vol)*Conv_to_L
Lact_Km = 2
DOCUMENT: See ethanol Km

Lact_Vmax = 35000

Stoic_Lact_CO2 = 2
Stoic_Lact_to_Ace = 2
Stoic_Lact_to_Prop = 2

Methanol
Meth_in_Fe_Zn(t) = Meth_in_Fe_Zn(t - dt) + (Inflow_Meth_to_Fe_Zn - Outflow_Meth_to_RZ - Meth_to_CO2) * dt
INIT Meth_in_Fe_Zn = 0

INFLOWS:
Inflow_Meth_to_Fe_Zn = Conv_for_units*Flow_Thr_Wetld*Inflow_conc_7

OUTFLOWS:
Outflow_Meth_to_RZ = Conv_Meth_in_Fe_Zn*Conv_for_units*Flow_Thr_Wetld
Meth_to_CO2(o) = (Meth_Vmax*Conc_Meth_in_Fe_Zn*Conc_Hematite)/((Meth_Km+Conc_Meth_in_Fe_Zn)*(Fe_Km+Conc_Hematite))
Meth_to_H = Meth_to_CO2*Conv_Meth_H

INFLOW TO: Hydrogen_ion_in_Fe_Zn (IN SECTOR: Hydrogen Ion)
Conc_Meth_in_Fe_Zn = (Meth_in_Fe_Zn/Fe_Zone_Water_Vol)*Conv_to_L
Conv_Meth_CO2 = (1*44)/(Stoic_Meth_CO2*32)
Conv_Meth_H = (4*1)/(Stoic_Meth_H*32)
Inflow_conc_7 = .5
Meth_Km = 2
DOCUMENT: See ethanol Km

Meth_Vmax = 35000
DOCUMENT: See ethanol Vmax

Stoic_Meth_CO2 = 1
Stoic_Meth_H = 1

Parameters for Model

Conversion = 5.45
DOCUMENT: This conversion takes the given flow rate (in gal/min) and converts it into m^3/day. Conversion is as follows: 60 min/1 hr*24 hr/day*0.003785412m^3/gal.

Conv_10 = (1*160)/(Stoic_Fe_Form*46)
Conv_11 = (1*160)/(Stoic_Fe_Prop*74)
Conv_12 = (1*160)/(Stoic_Fe_But*88)
Conv_13 = (1*160)/(Stoic_Fe_Lact*90)
Conv_14 = (1*160)/(Stoic_Fe_Eth*46)
Conv_15 = (1*160)/(Stoic_Fe_Meth*32)
Conv_5 = (1*160)/(Stoic_Fe_VC*62)
Conv_6 = (1*160)/(Stoic_Fe_cDCE*96)
Conv_7 = (1*160)/(Stoic_Fe_tDCE*96)
Conv_8 = (1*160)/(Stoic_Fe_H2*2)
Conv_9 = (1*160)/(Stoic_Fe_Ace*60)
CW_Surface_Area = 780.3855
DOCUMENT: Area of constructed wetlands in meters squared

Fe_Zone_Depth = 0.4572
DOCUMENT: Iron Zone depth in meters

Fe_Zone_Porosity = 0.4
DOCUMENT: Taken from discussion in second committee meeting (range between 0.3 and 0.5).

Fe_Zone_Water_Vol = CW_Surface_Area*Fe_Zone_Depth*Fe_Zone_Porosity
DOCUMENT: Units are cubic meters

Flow rate = 10.5
Flow_Thr_Wetld = Flow rate*Conversion
DOCUMENT: Based on a 10.5 gallon per minute flow rate which gives a value for the retention time half way between what is desired (according to Dr Shelley) of 5 and 15 days. . .flow is m^3/day (by conversion factor).

Stoic_Fe_Ace = 1
Stoic_Fe_But = 1
Stoic_Fe_cDCE = 1
Stoic_Fe_Eth = 1
Stoic_Fe_Form = 1
Stoic_Fe_H2 = 2
Stoic_Fe_Lact = 2
Stoic_Fe_Meth = 1
Stoic_Fe_Prop = 1
Stoic_Fe_tDCE = 1
Stoic_Fe_VC = 1

Propionic Acid

Propionic_Acid_in_Fe_Zn(t) = Propionic_Acid_in_Fe_Zn(t - dt) + (Lact_to_Prop + Inflow_Prop - Prop_to_CO2 - Outflow_Prop_to_RZ) * dt
INIT Propionic_Acid_in_Fe_Zn = 0

INFLOWS:

Lact_to_Prop (IN SECTOR: Lactic Acid)

Inflow_Prop = Conv_for_units*Flow_Thr_Wetld*Inflow_con_2

OUTFLOWS:
Prop_to_CO2(o) =
(Prop_Vmax*Conc_Prop_in_Fe_Zn*Conc_Hematite)/((Prop_Km+Conc_Prop_in_Fe_Zn)*(Fe_Km+Conc_Hematite))
Outflow_Prop_to_RZ = Conc_Prop_in_Fe_Zn*Conv_for_units*Flow_Thr_Wetld
Prop_to_Ace = Prop_to_CO2*Conv_Prop_to_Ace

INFLOW TO: Ace_in_Fe_Zn (IN SECTOR: Acetic Acid)
Prop_to_H2 = Prop_to_CO2*Conv_Prop_to_H2

INFLOW TO: Hydrogen_in_Fe_Zn (IN SECTOR: Hydrogen)
Conc_Prop_in_Fe_Zn = (Propionic_Acid_in_Fe_Zn/Fe_Zone_Water_Vol)*Conv_to_L
Conv_Prop_CO2 = (1*44)/(Stoic_Prop_CO2*74)
Conv_Prop_to_Ace = (1*60)/(Stoic_Prop_to_Ace*74)
Conv_Prop_to_H2 = (1*2)/(Stoic_Prop_to_H2*74)
Inflow_con_2 = 1
Prop_Km = 2
DOCUMENT: See ethanol Km

Prop_Vmax = 35000
DOCUMENT: See ethanol Vmax

Stoic_Prop_CO2 = 1
Stoic_Prop_to_Ace = 1
Stoic_Prop_to_H2 = 1

Appendix C: Model Output Graphs for All Simulations

Key for this Appendix

Degradation of hematite in units of mg
Contaminant mineralization in units of mg/d
Vmax in units of mg/d
Km in units of mg/L
X axis on graphs are in units of days (as marked)
Inflow parameters in mg/day
Flow rate parameters in gal/min

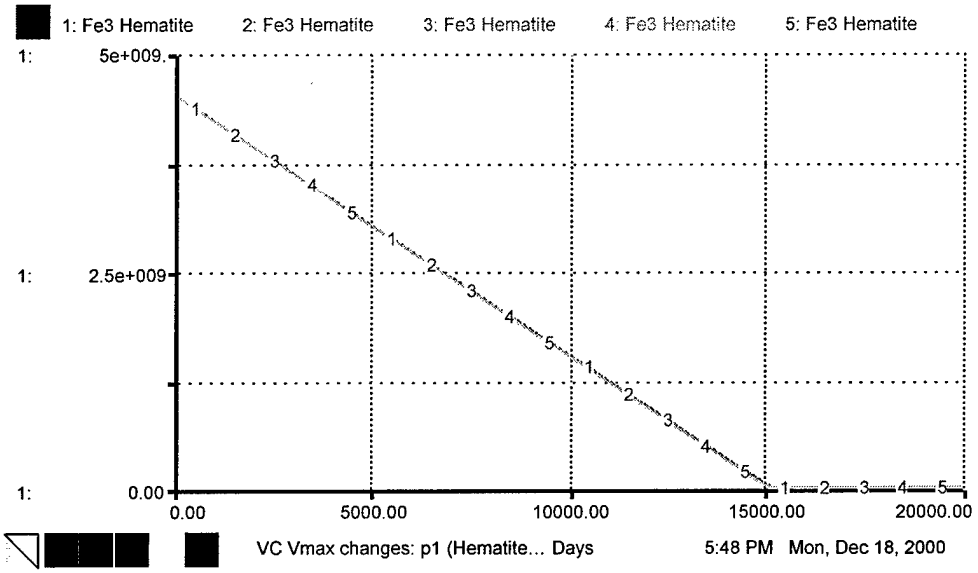

Hematite Behavior – Simulation Set 1, Changing VC Vmax

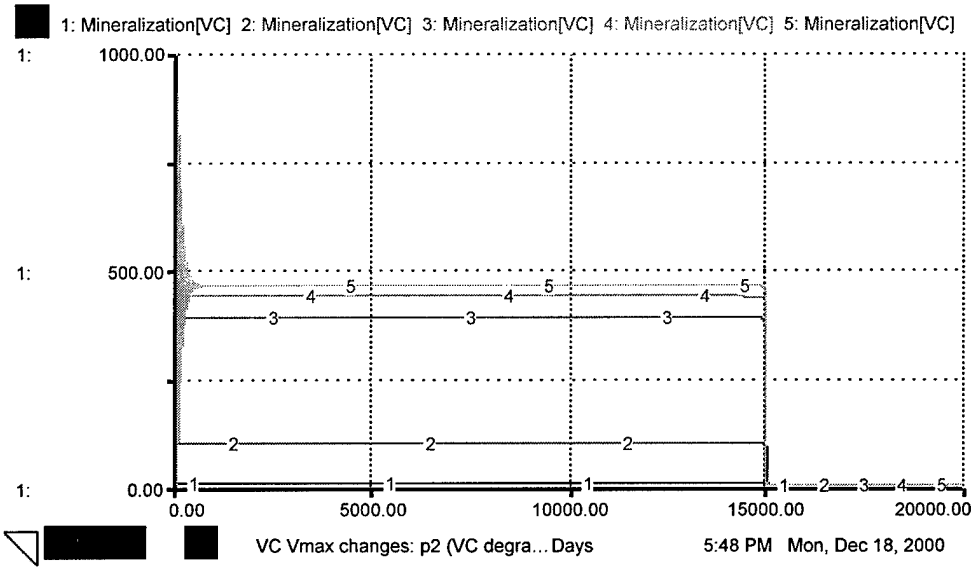

VC Behavior – Simulation Set 1, Changing VC Vmax

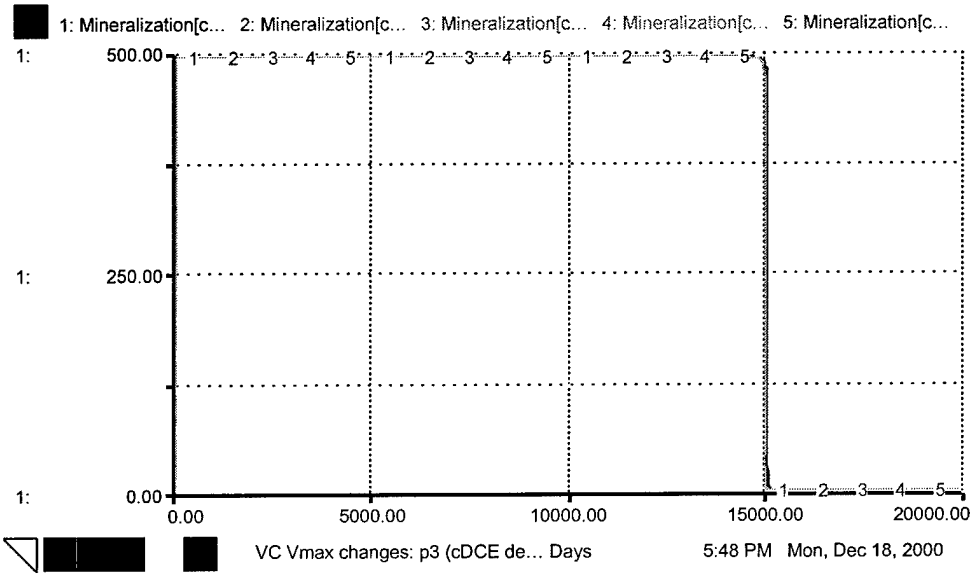

***cis*-DCE Behavior – Simulation Set 1, Changing VC Vmax**

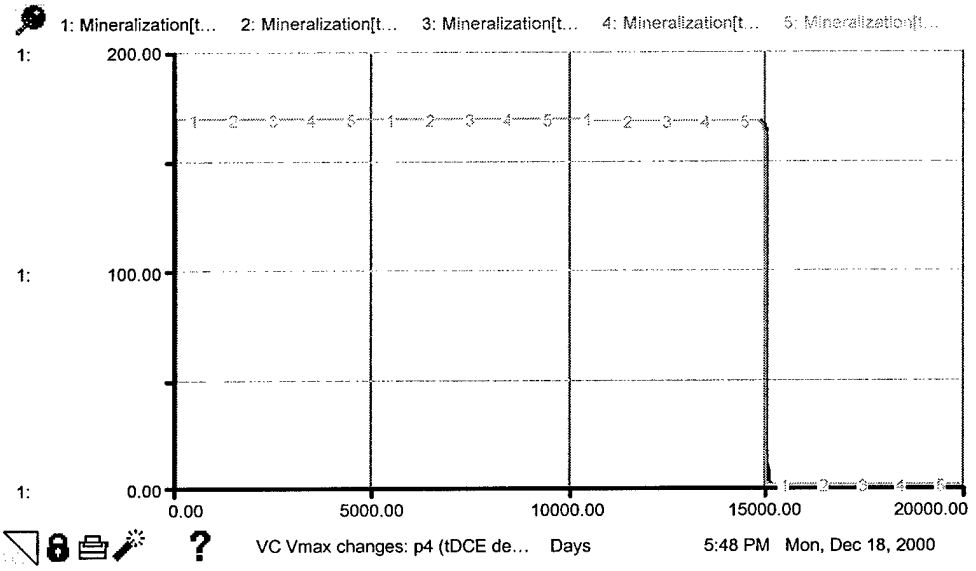

***trans*-DCE Behavior – Simulation Set 1, Changing VC Vmax**

Setup #1	Mon, Dec 18, 2000 5:40 PM
Input Variables	
Run #	Cont Vmax[VC]
1	10.0
2	1000
3	10000
4	15000
5	19200

Vmax Values used for Changing VC Simulations (Runs)

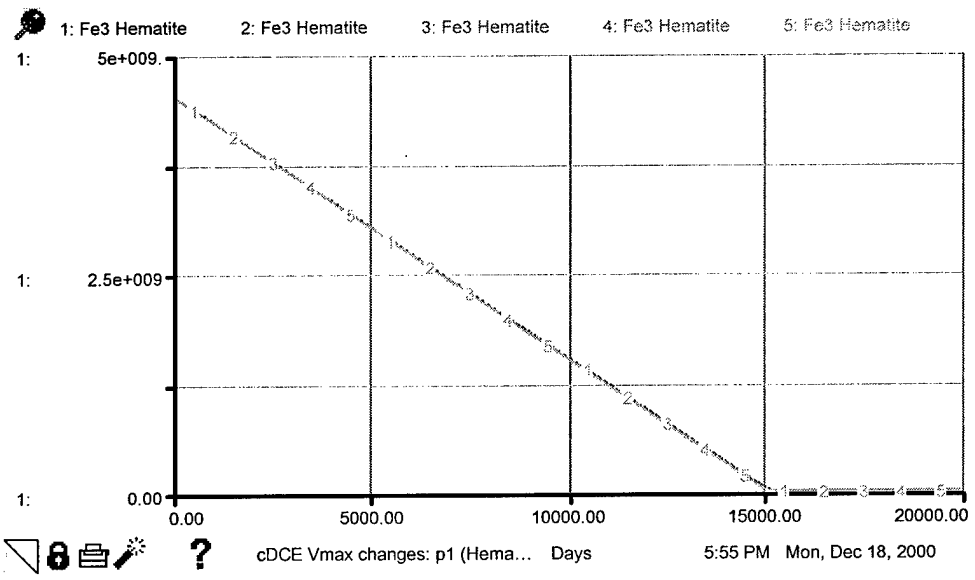

Hematite Behavior – Simulation Set 1, Changing *cis*-DCE Vmax

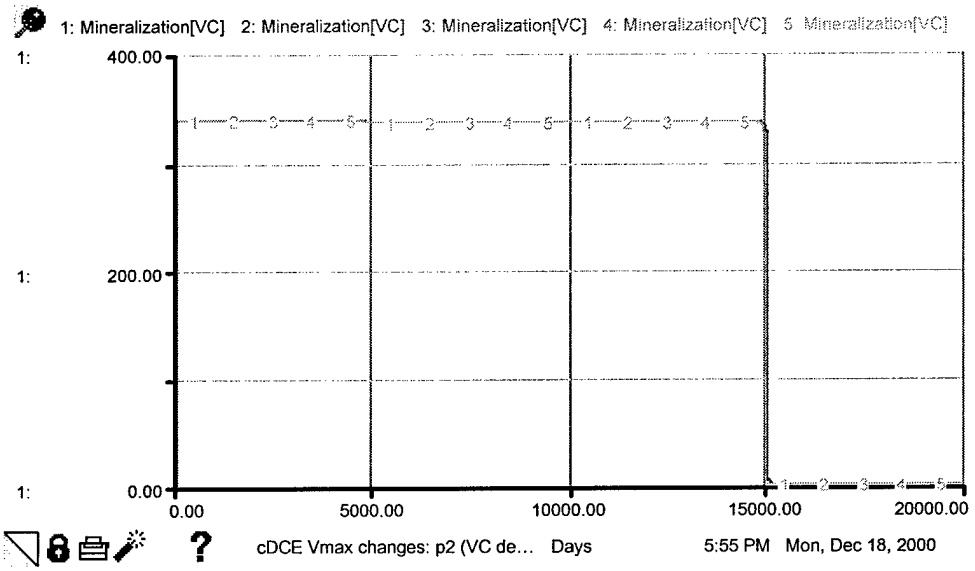

VC Behavior – Simulation Set 1, Changing *cis*-DCE Vmax

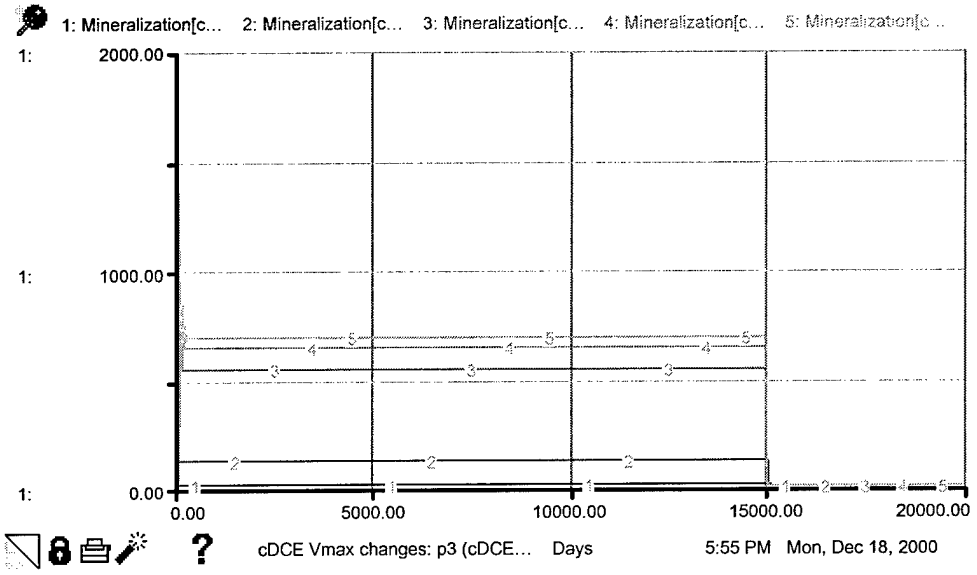

***cis*-DCE Behavior – Simulation Set 1, Changing *cis*-DCE Vmax**

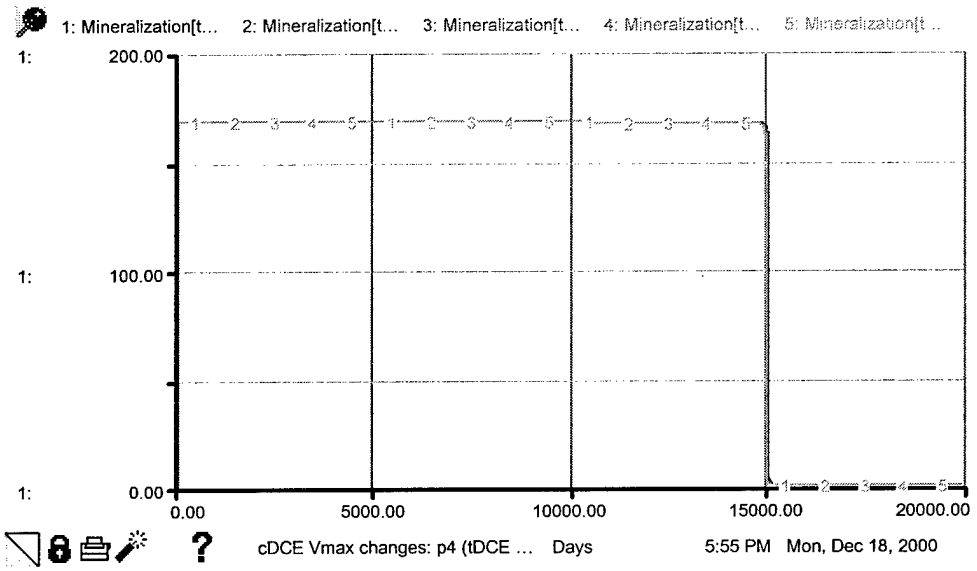

***trans*-DCE Behavior – Simulation Set 1, Changing *cis*-DCE Vmax**

Setup #2	Mon, Dec 18, 2000 5:51 PM
Input Variables	
Run #	Cont Vmax[cDCE]
1	10.0
2	1000
3	10000
4	17000
5	23000

Vmax Values used for Changing *cis*-DCE Simulations (Runs)

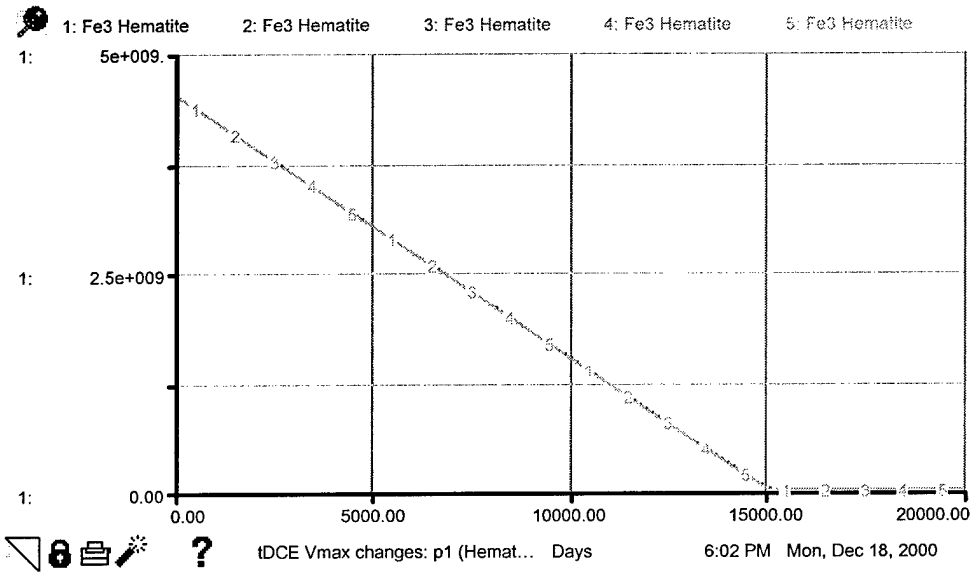

Hematite Behavior – Simulation Set 1, Changing *trans*-DCE Vmax

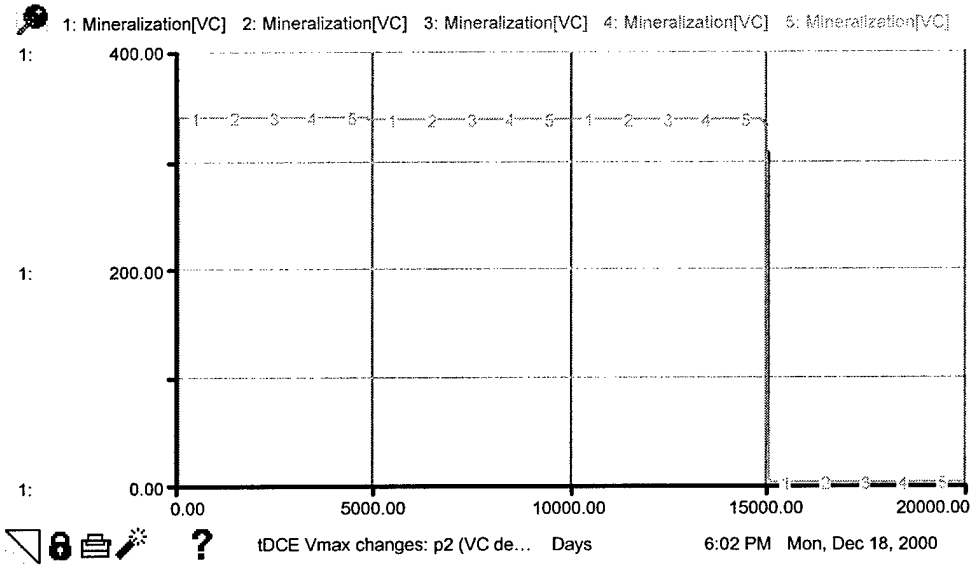

VC Behavior – Simulation Set 1, Changing *trans*-DCE Vmax

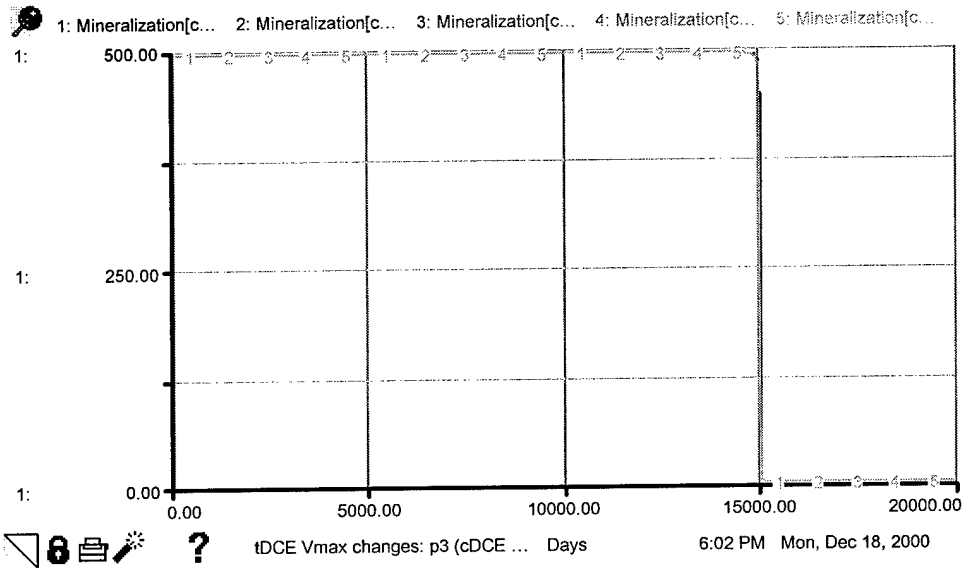

***cis*-DCE Behavior – Simulation Set 1, Changing *trans*-DCE Vmax**

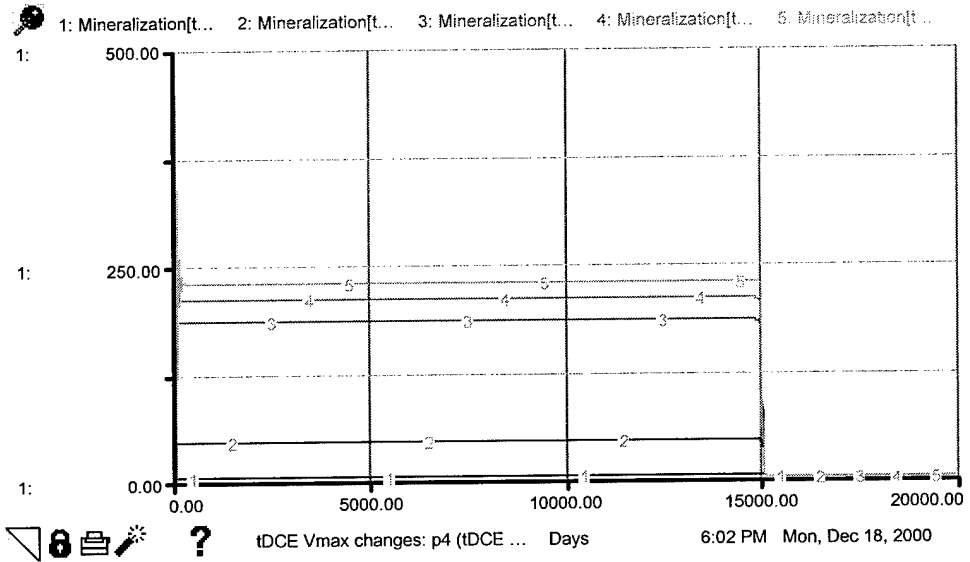

***trans*-DCE Behavior – Simulation Set 1, Changing *trans*-DCE Vmax**

Setup #3	Mon, Dec 18, 2000 5:58 PM
Input Variables	
Run #	Cont Vmax[tDCE]
1	10.0
2	1000
3	10000
4	15000
5	22000

Vmax Values used for Changing *trans*-DCE Simulations (Runs)

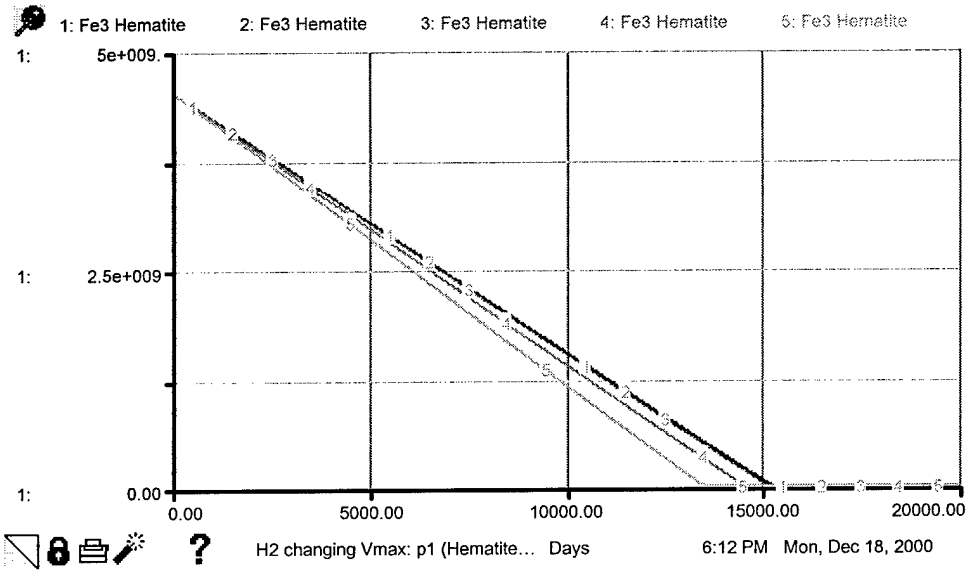

Hematite Behavior – Simulation Set 1, Changing H_2 Vmax

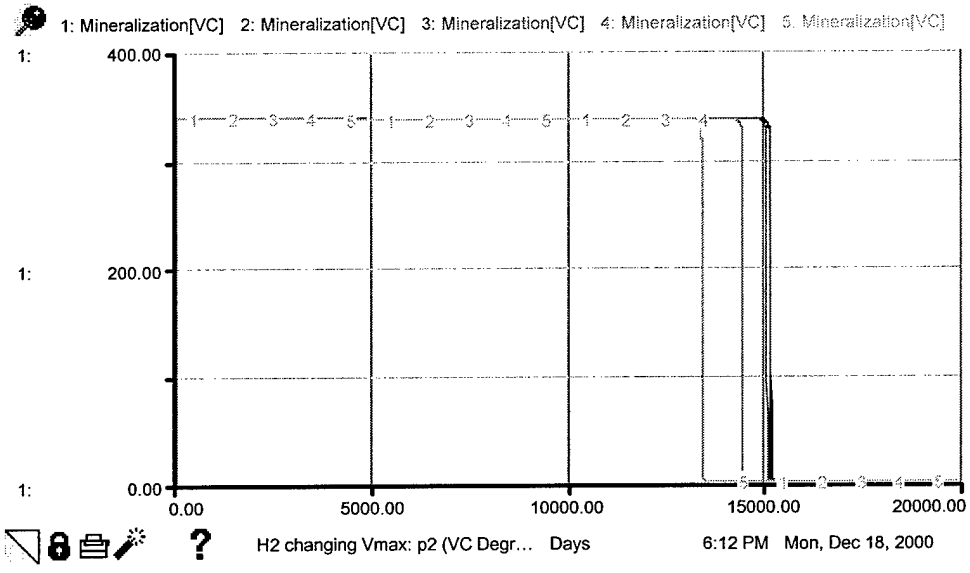

VC Behavior – Simulation Set 1, Changing H_2 Vmax

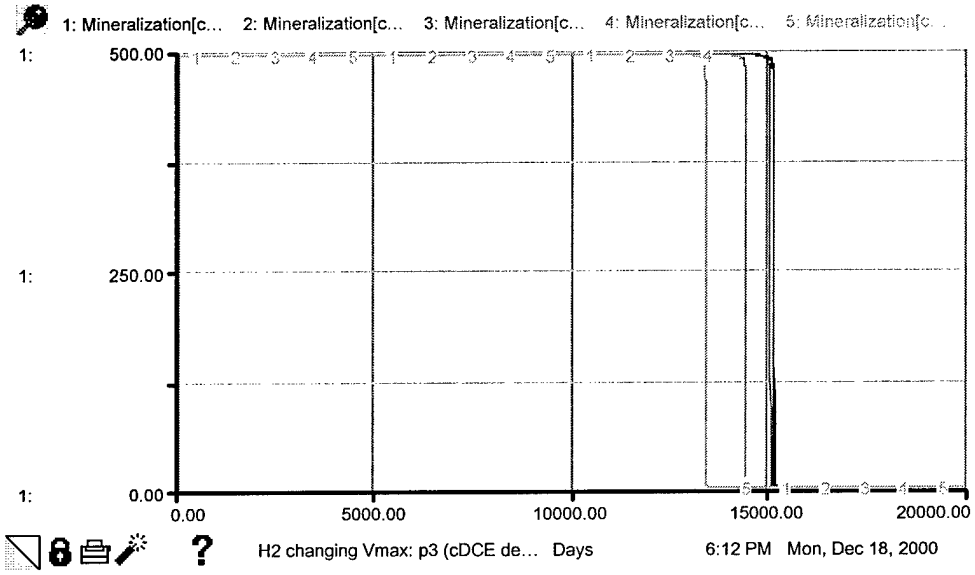

***cis*-DCE Behavior – Simulation Set 1, Changing H_2 Vmax**

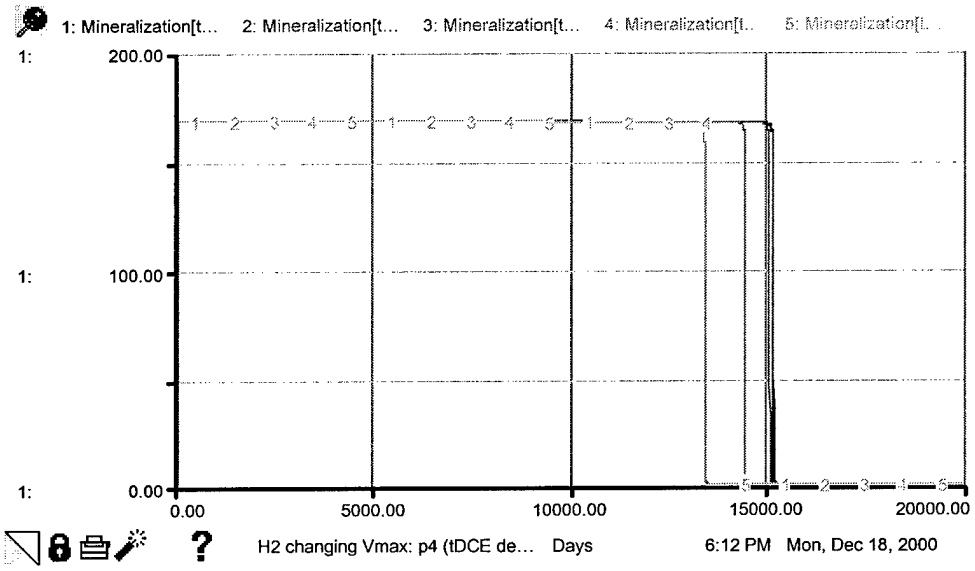

***trans*-DCE Behavior – Simulation Set 1, Changing H_2 Vmax**

Setup #4	Mon, Dec 18, 2000 6:08 PM
Input Variables	
Run #	H2 Vmax
1	10.0
2	1000
3	10000
4	100000
5	900000

Vmax Values used for Changing H_2 Simulations (Runs)

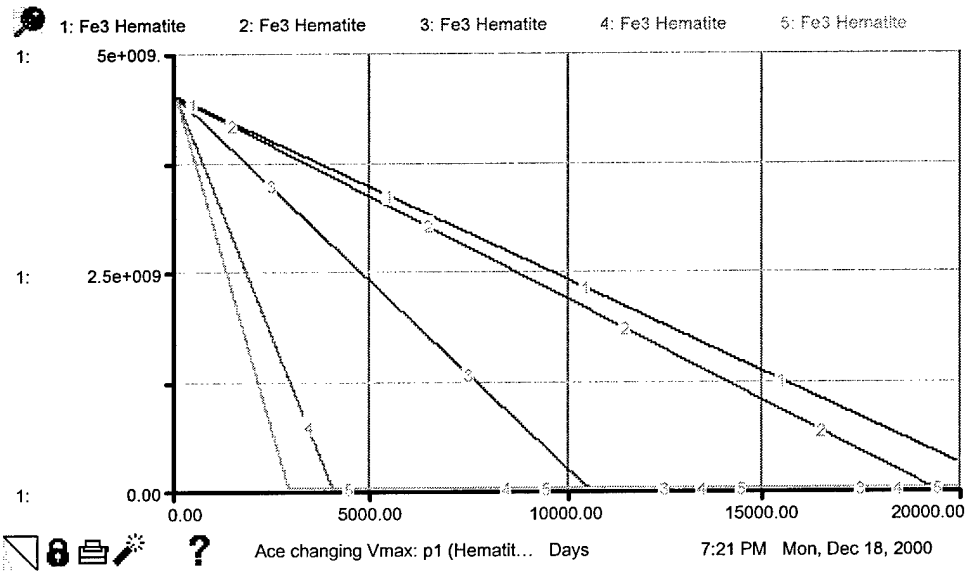

Hematite Behavior – Simulation Set 1, Changing Acetic Acid Vmax

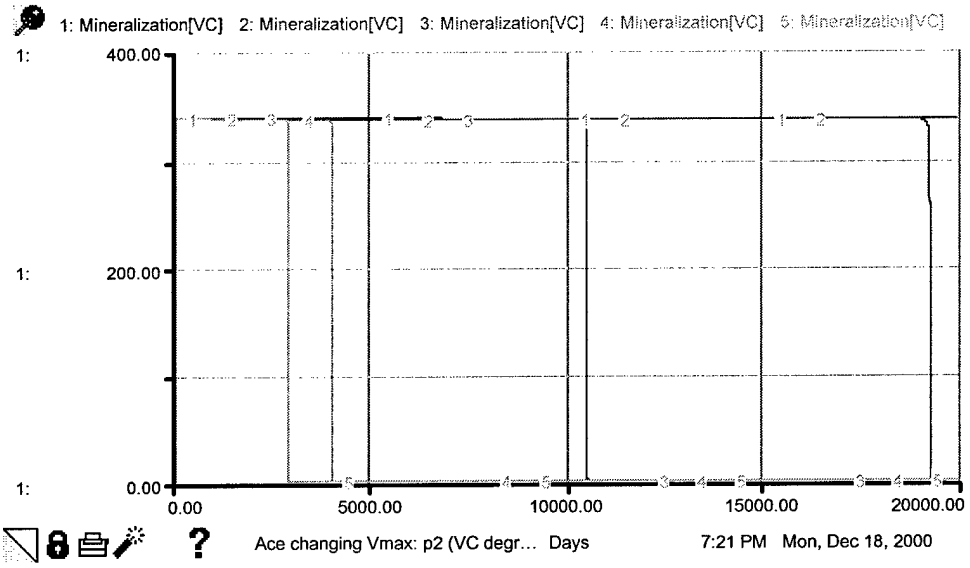

VC Behavior – Simulation Set 1, Changing Acetic Acid Vmax

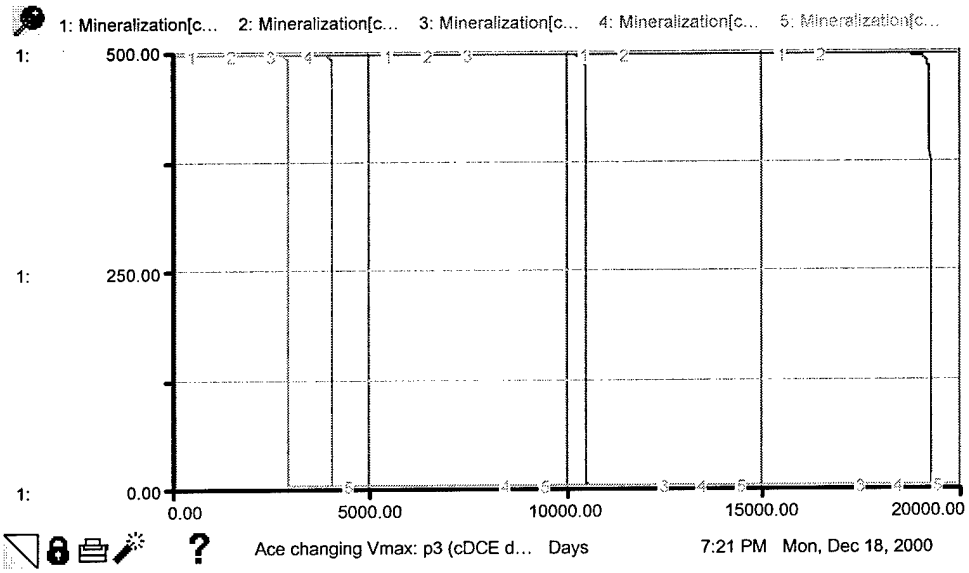

***cis*-DCE Behavior – Simulation Set 1, Changing Acetic Acid Vmax**

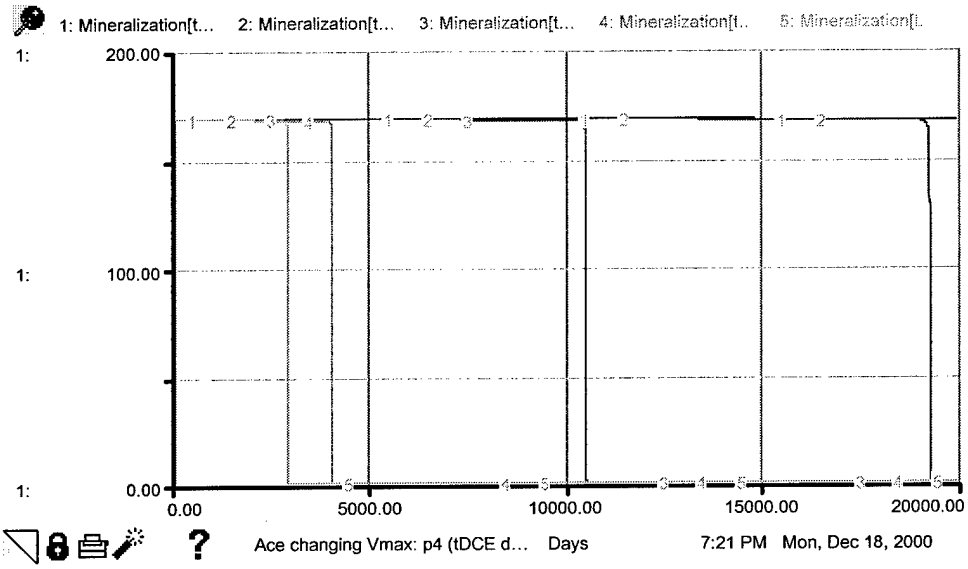

***trans*-DCE Behavior – Simulation Set 1, Changing Acetic Acid Vmax**

Setup #11	Mon, Dec 18, 2000 7:17 PM
Input Variables	
Run #	Ace Vmax
1	10.0
2	10000
3	100000
4	500000
5	1.2e+006

Vmax Values used for Changing Acetic Acid Simulations (Runs)

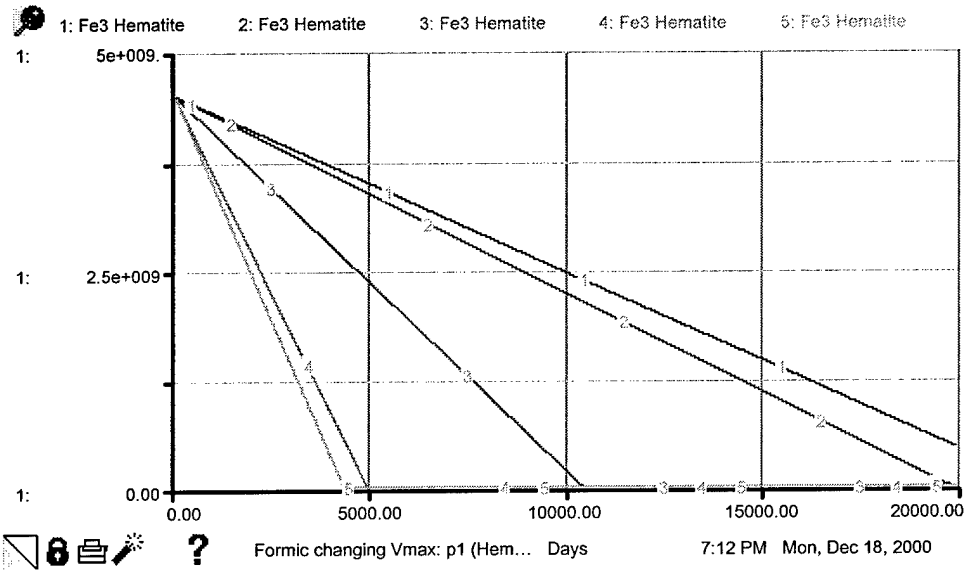

Hematite Behavior – Simulation Set 1, Changing Formic Acid Vmax

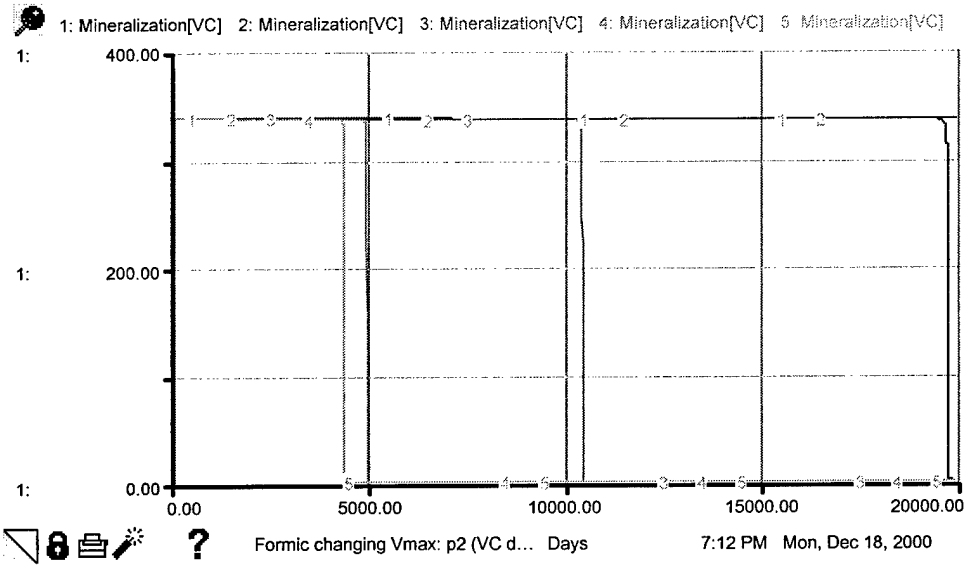

VC Behavior – Simulation Set 1, Changing Formic Acid Vmax

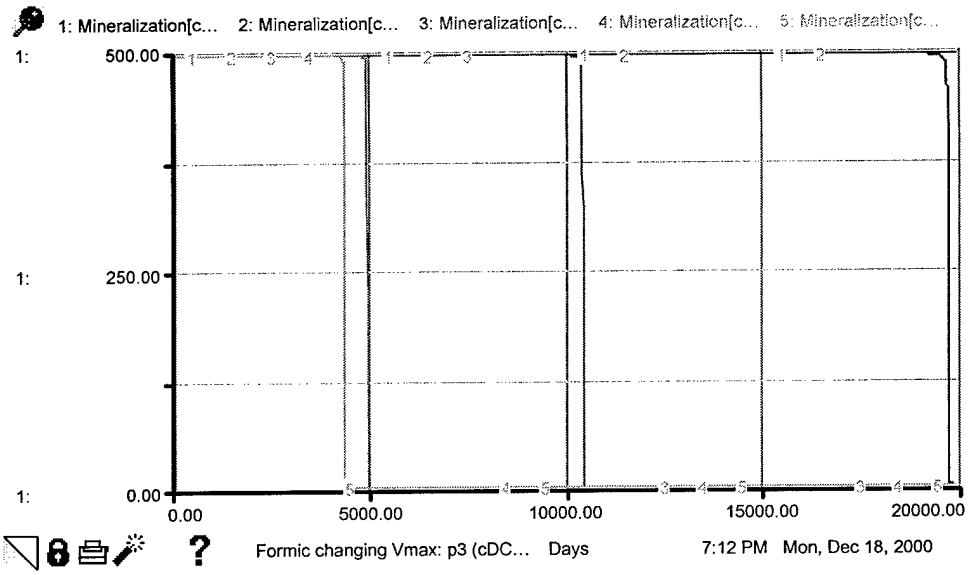

***cis*-DCE Behavior – Simulation Set 1, Changing Formic Acid Vmax**

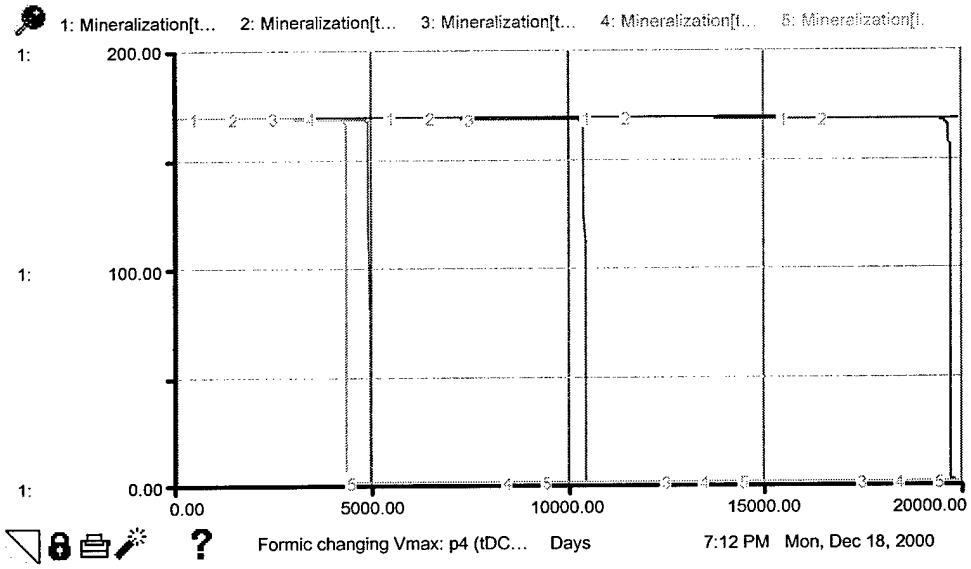

***trans*-DCE Behavior – Simulation Set 1, Changing Formic Acid Vmax**

Setup #10		Mon, Dec 18, 2000 7:08 PM
	Input Variables	
Run #	Form Vmax	
1	10.0	
2	10000	
3	100000	
4	500000	
5	870000	

Vmax Values used for Changing Formic Acid Simulations (Runs)

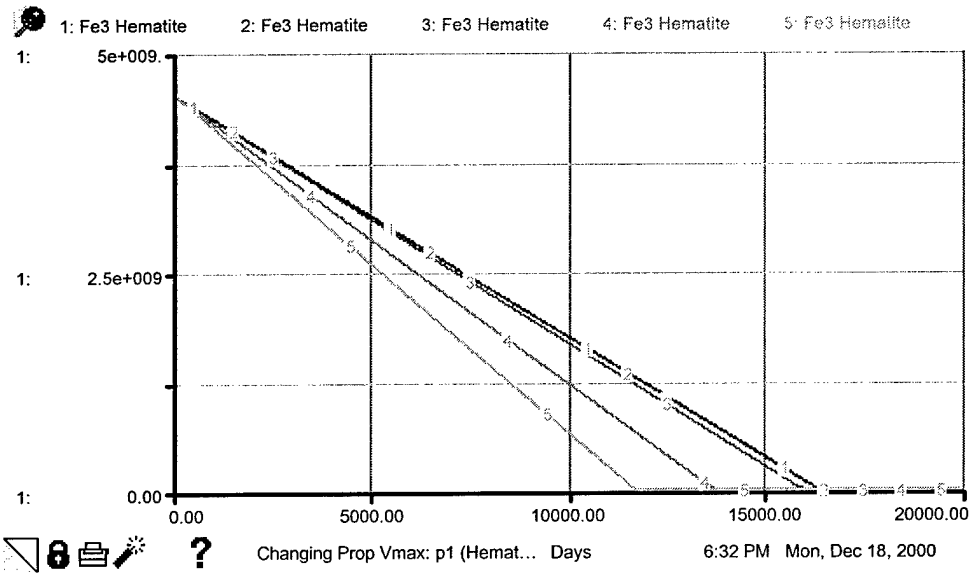

Hematite Behavior – Simulation Set 1, Changing Propionic Acid Vmax

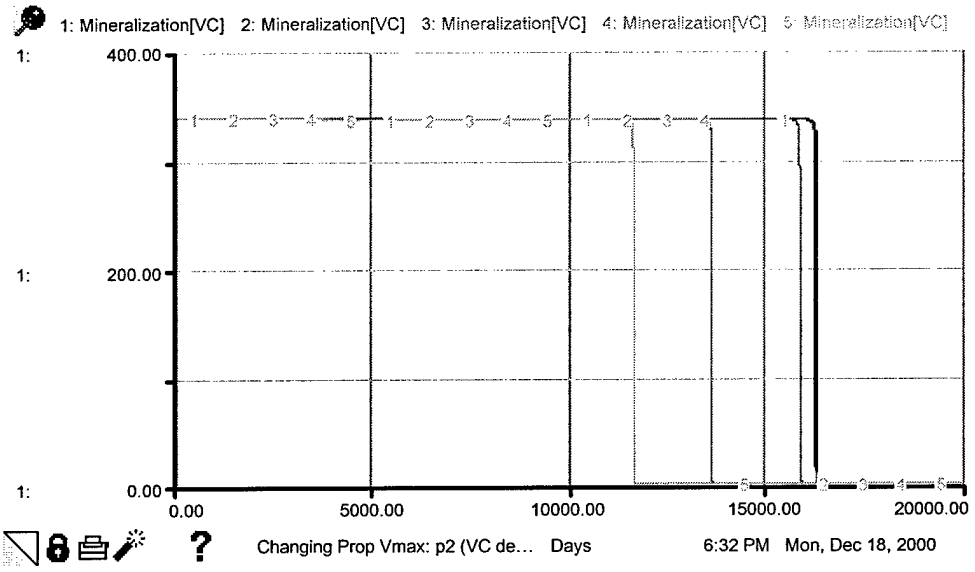

VC Behavior – Simulation Set 1, Changing Propionic Acid Vmax

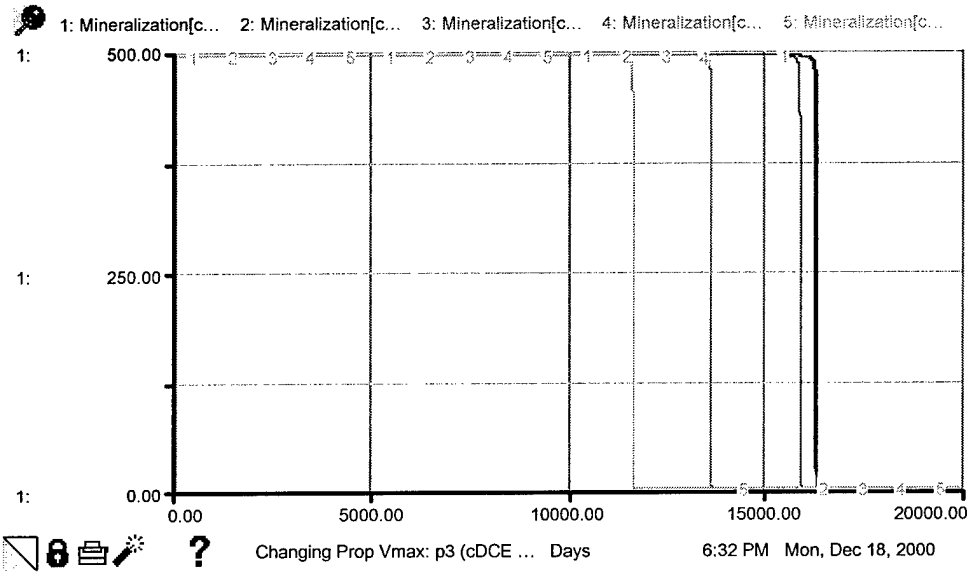

***cis*-DCE Behavior – Simulation Set 1, Changing Propionic Acid Vmax**

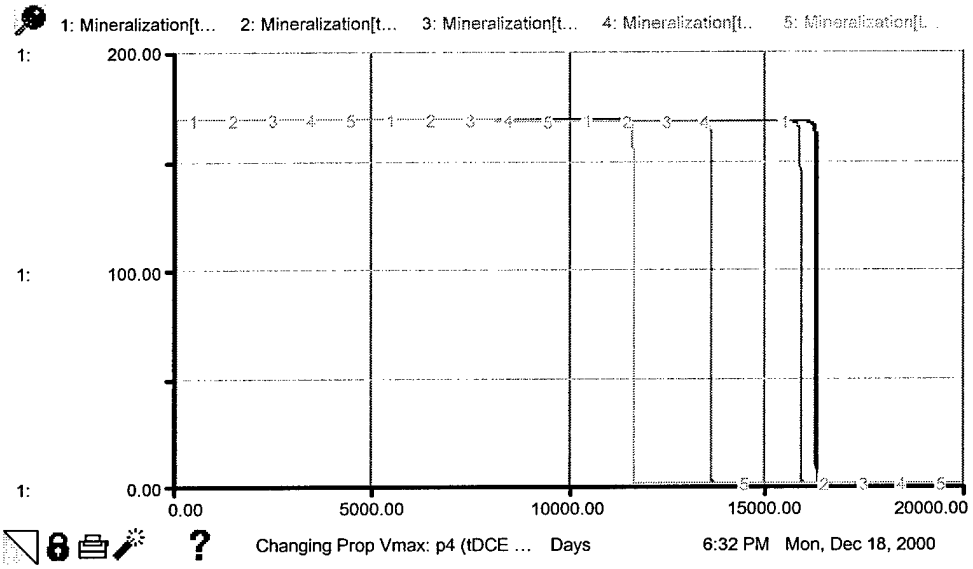

***trans*-DCE Behavior – Simulation Set 1, Changing Propionic Acid Vmax**

Setup #6	Mon, Dec 18, 2000 6:28 PM
Input Variables	
Run #	Prop Vmax
1	10.0
2	1000
3	10000
4	100000
5	550000

Vmax Values used for Changing Propionic Acid Simulations (Runs)

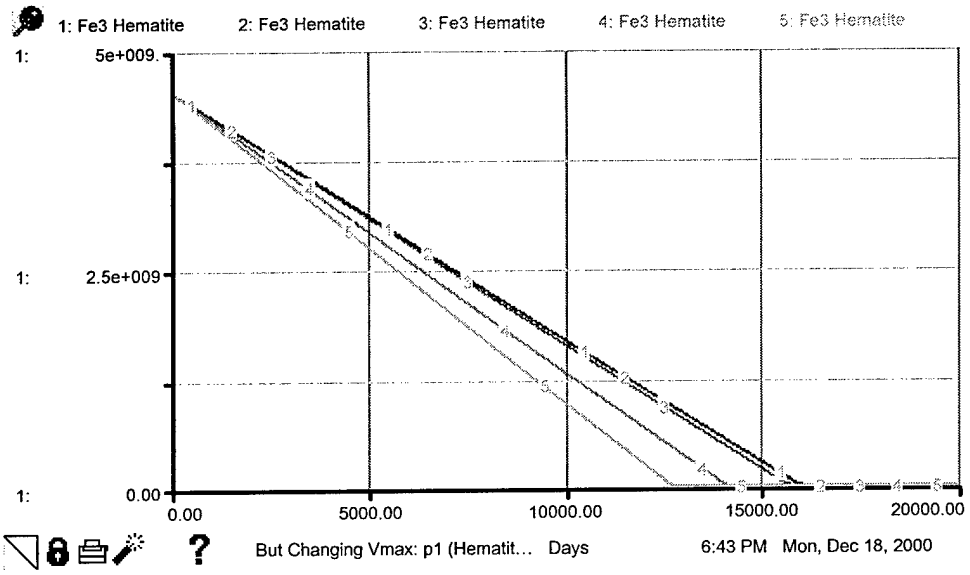

Hematite Behavior – Simulation Set 1, Changing Butryic Acid Vmax

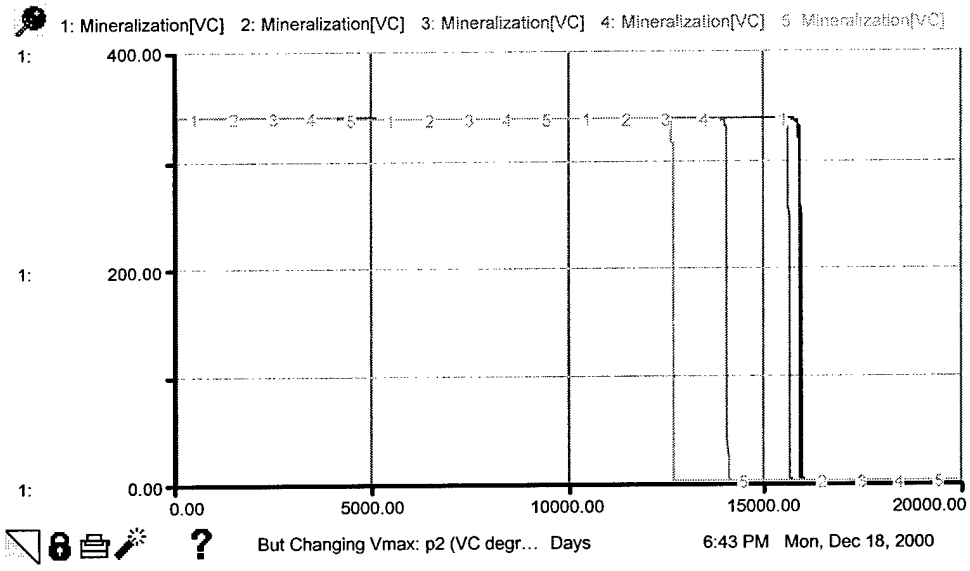

VC Behavior – Simulation Set 1, Changing Butryic Acid Vmax

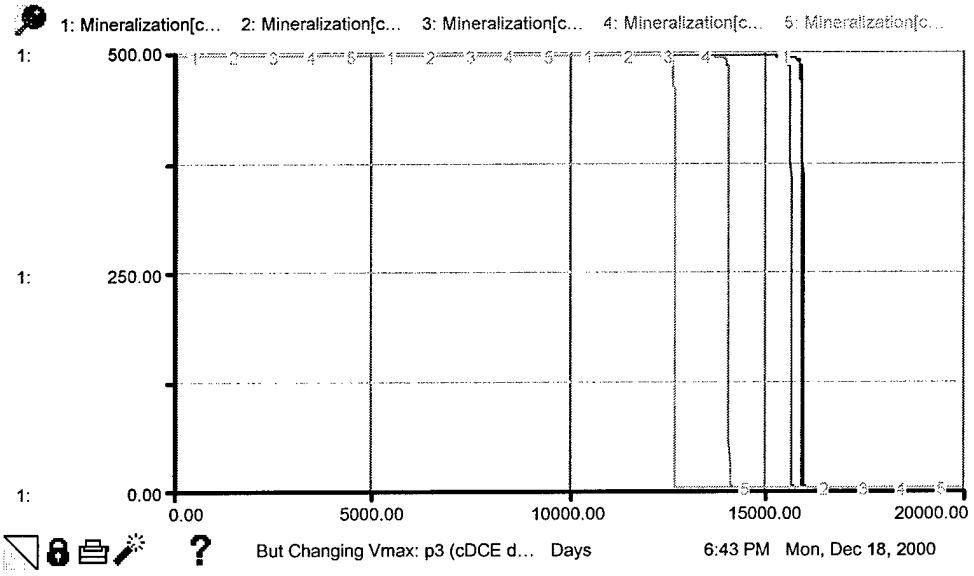

***cis*-DCE Behavior – Simulation Set 1, Changing Butryic Acid Vmax**

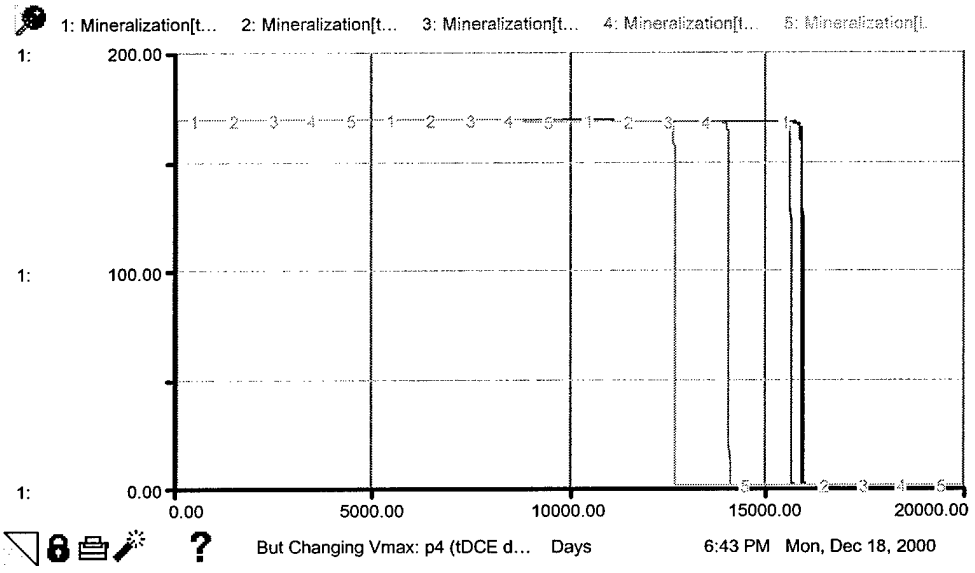

***trans*-DCE Behavior – Simulation Set 1, Changing Butryic Acid Vmax**

Setup #7	Mon, Dec 18, 2000 6:40 PM
Input Variables	
Run #	But Vmax
1	10.0
2	1000
3	10000
4	100000
5	520000

Vmax Values used for Changing Butryic Acid Simulations (Runs)

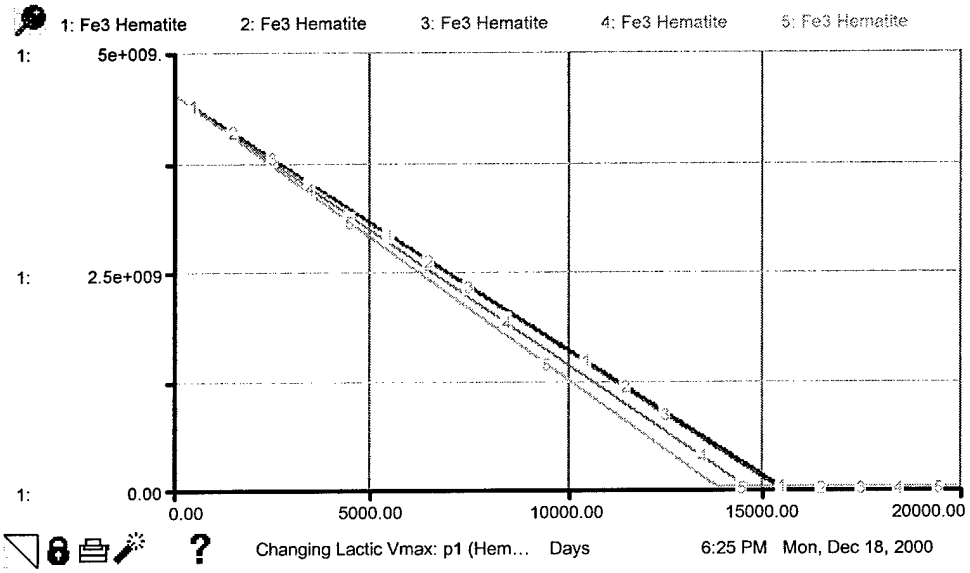

Hematite Behavior – Simulation Set 1, Changing Lactic Acid Vmax

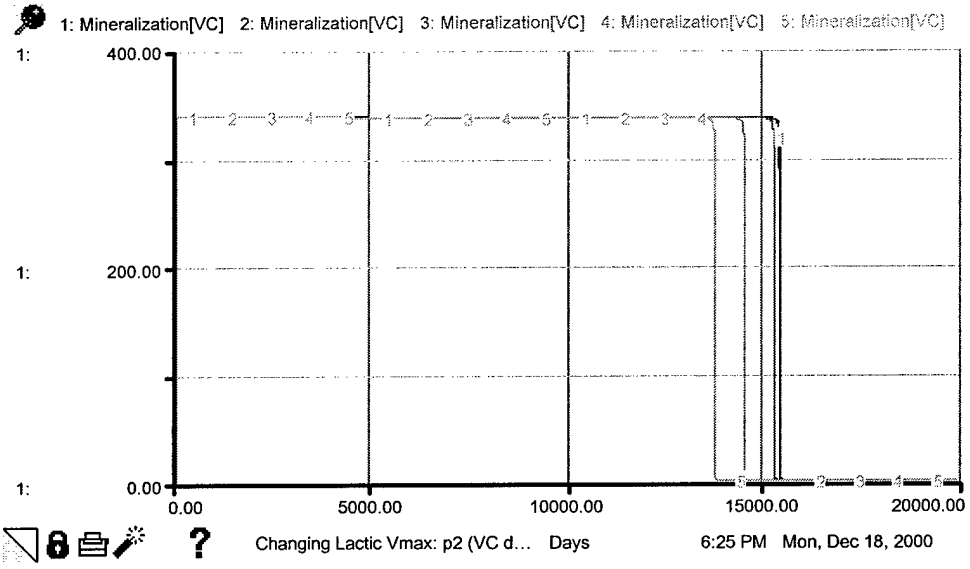

VC Behavior – Simulation Set 1, Changing Lactic Acid Vmax

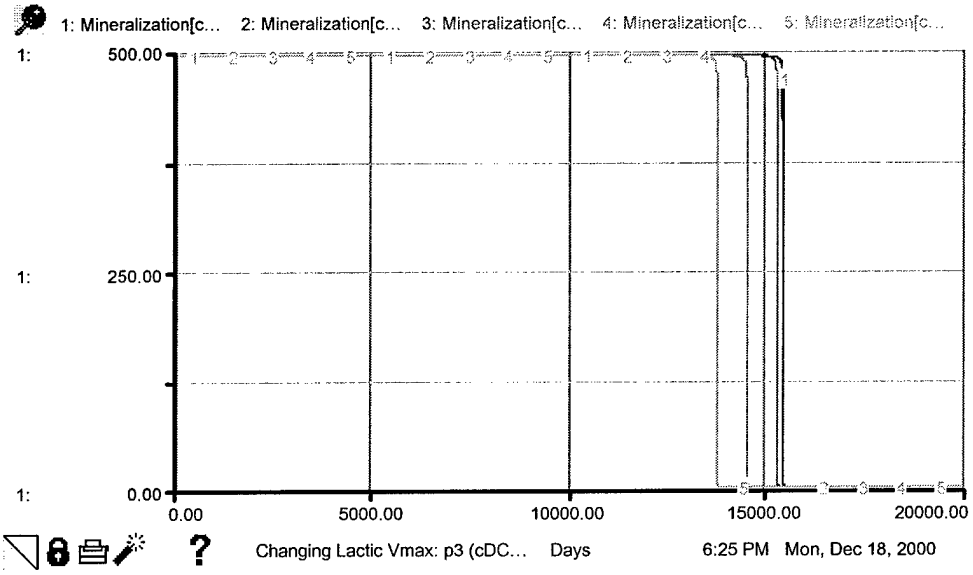

***cis*-DCE Behavior – Simulation Set 1, Changing Lactic Acid Vmax**

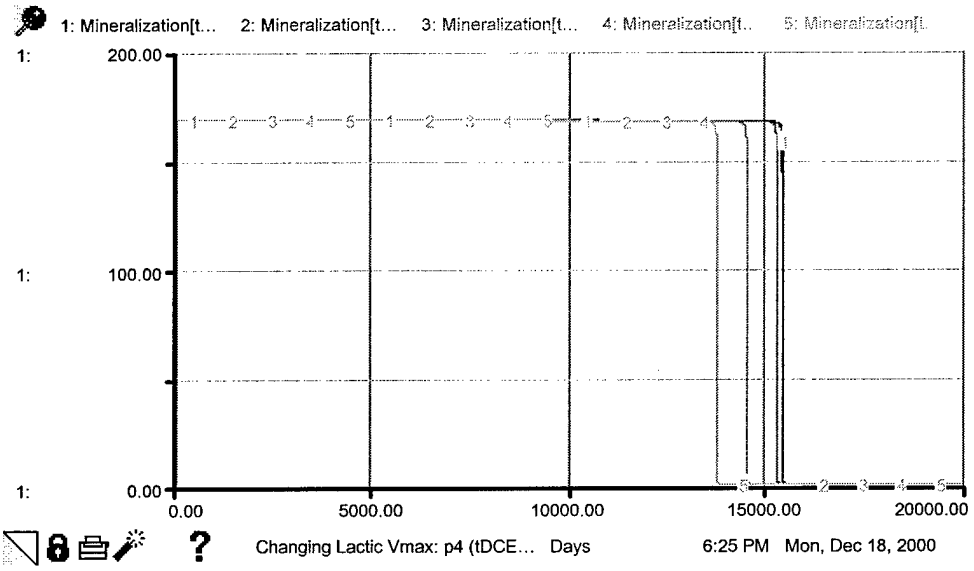

***trans*-DCE Behavior – Simulation Set 1, Changing Lactic Acid Vmax**

Setup #5	Mon, Dec 18, 2000 6:21 PM
Input Variables	
Run #	Lact Vmax
1	10.0
2	1000
3	10000
4	100000
5	520000

Vmax Values used for Changing Lactic Acid Simulations (Runs)

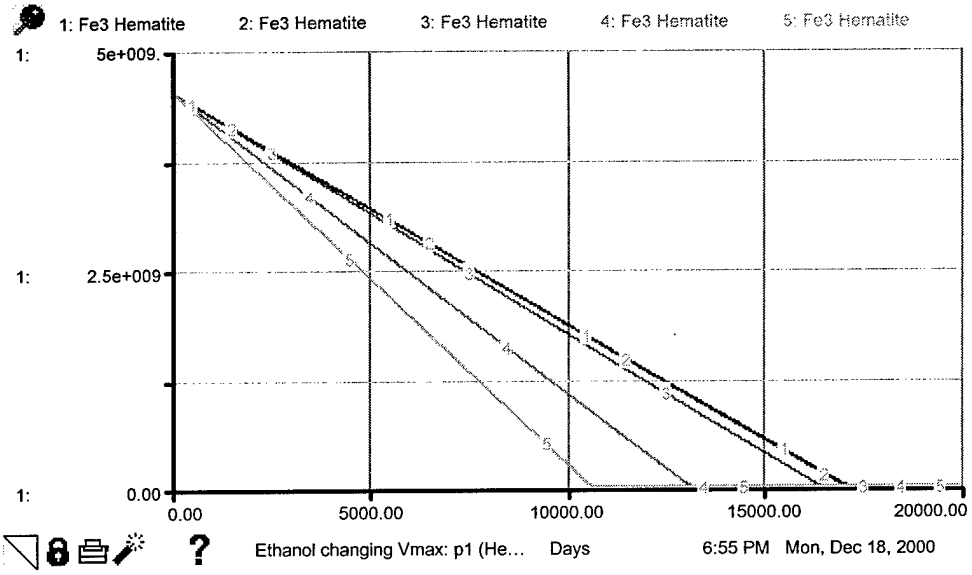

Hematite Behavior – Simulation Set 1, Changing Ethanol Vmax

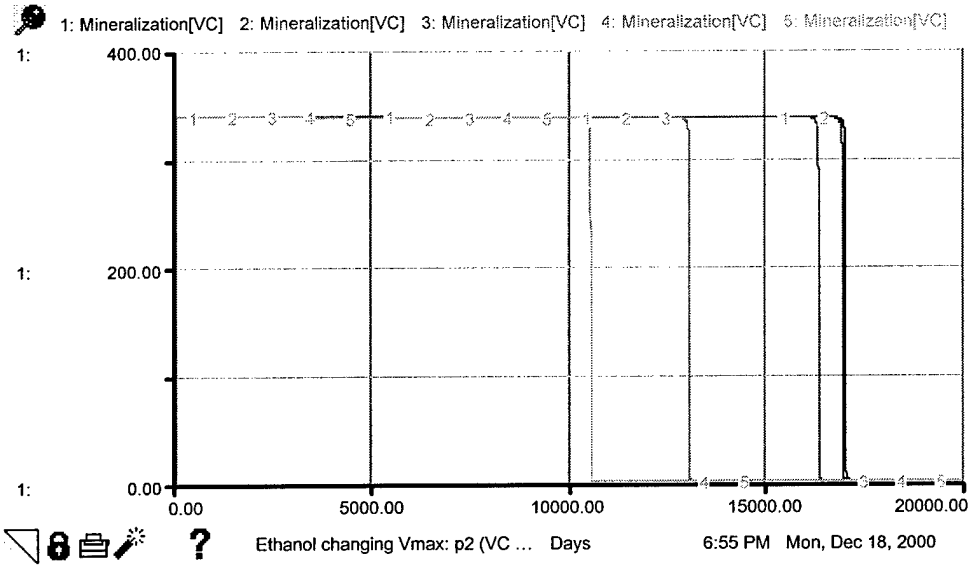

VC Behavior – Simulation Set 1, Changing Ethanol Vmax

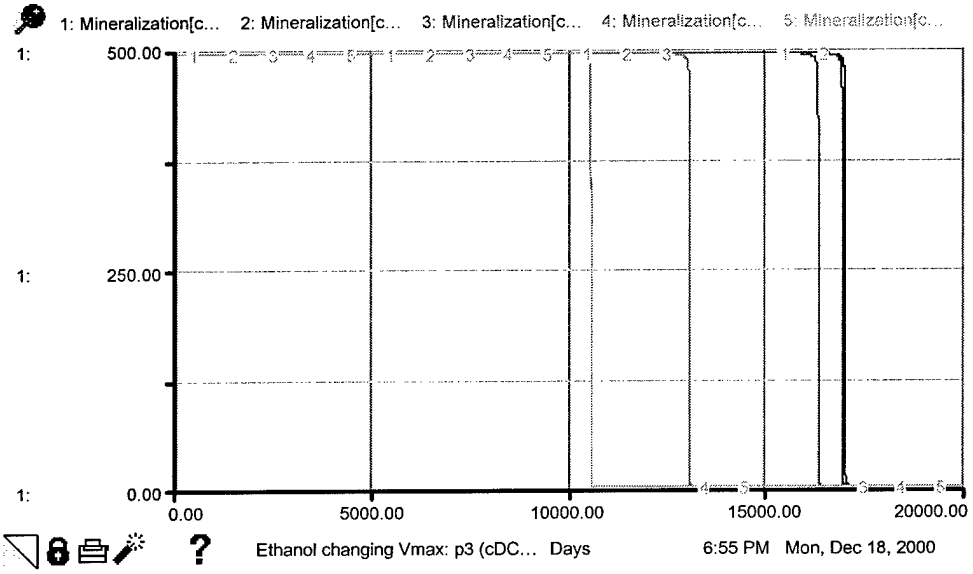

***cis*-DCE Behavior – Simulation Set 1, Changing Ethanol Vmax**

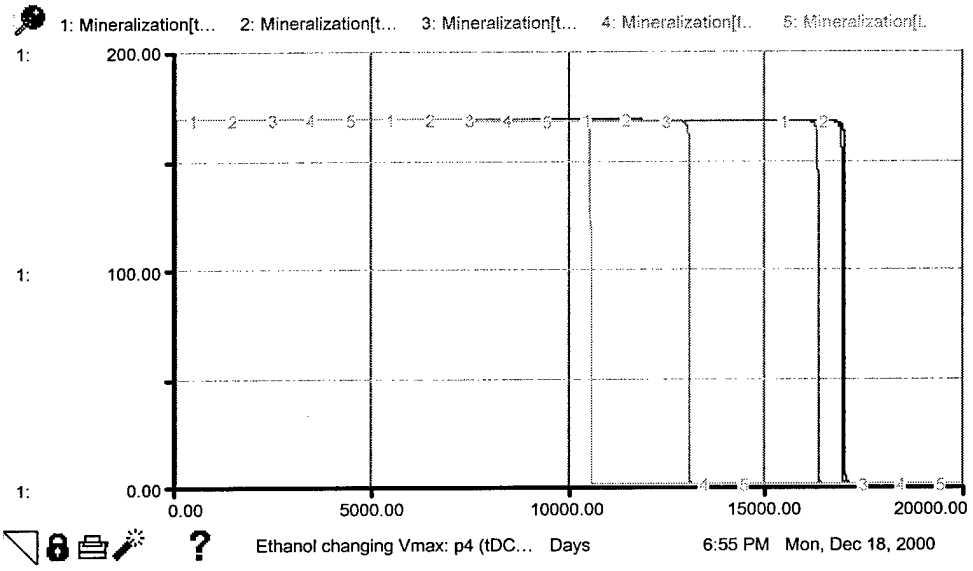

***trans*-DCE Behavior – Simulation Set 1, Changing Ethanol Vmax**

Setup #8 — Mon, Dec 18, 2000 6:51 PM

Input Variables

Run #	Eth Vmax
1	10.0
2	1000
3	10000
4	100000
5	540000

Vmax Values used for Changing Ethanol Simulations (Runs)

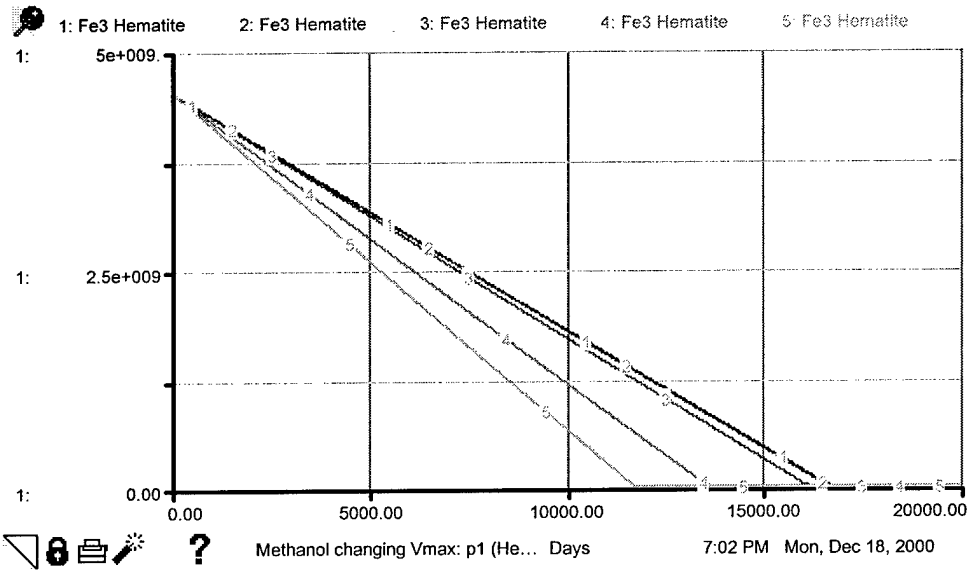

Hematite Behavior – Simulation Set 1, Changing Methanol Vmax

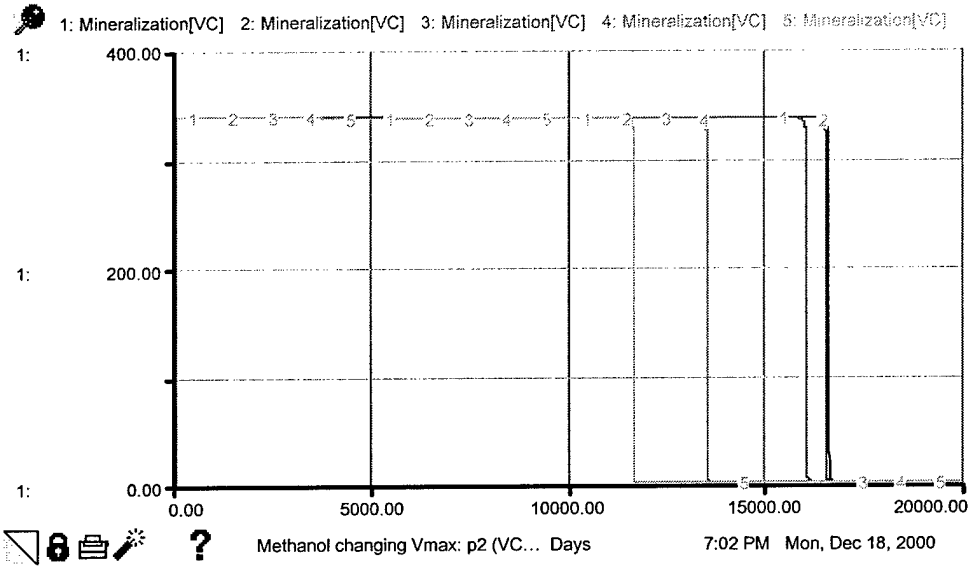

VC Behavior – Simulation Set 1, Changing Methanol Vmax

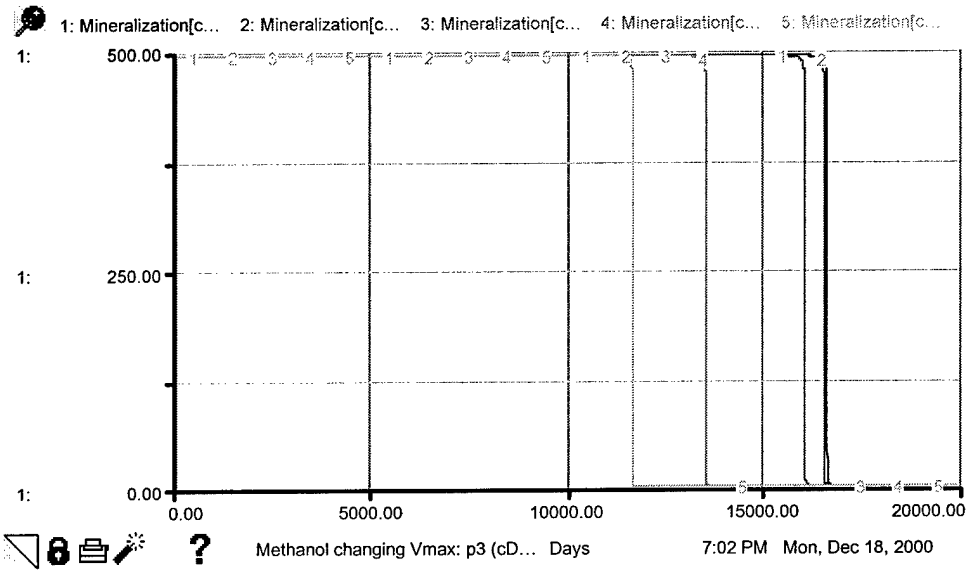

***cis*-DCE Behavior – Simulation Set 1, Changing Methanol Vmax**

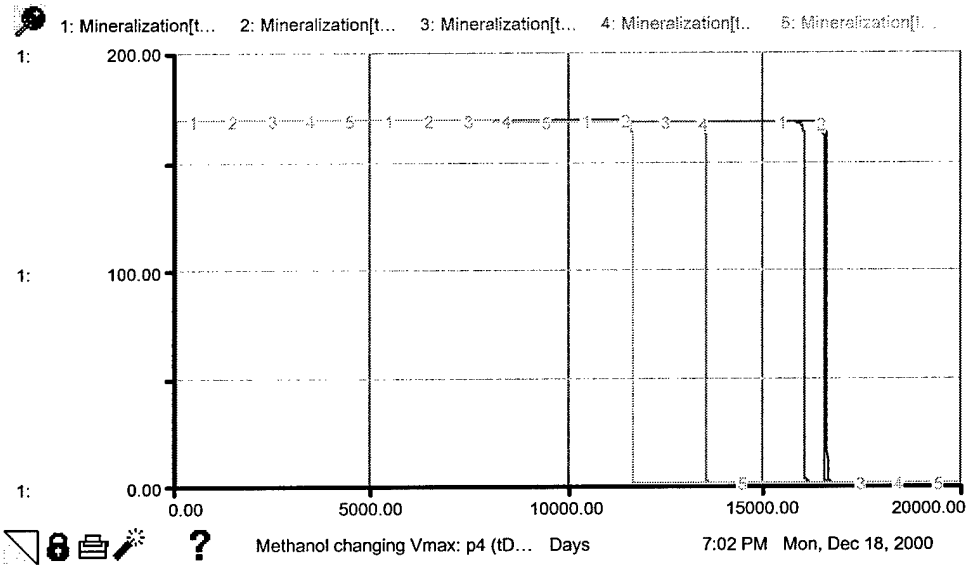

***trans*-DCE Behavior – Simulation Set 1, Changing Methanol Vmax**

Setup #9	Mon, Dec 18, 2000 6:58 PM
Input Variables	
Run #	Meth Vmax
1	10.0
2	1000
3	10000
4	100000
5	500000

Vmax Values used for Changing Methanol Simulations (Runs)

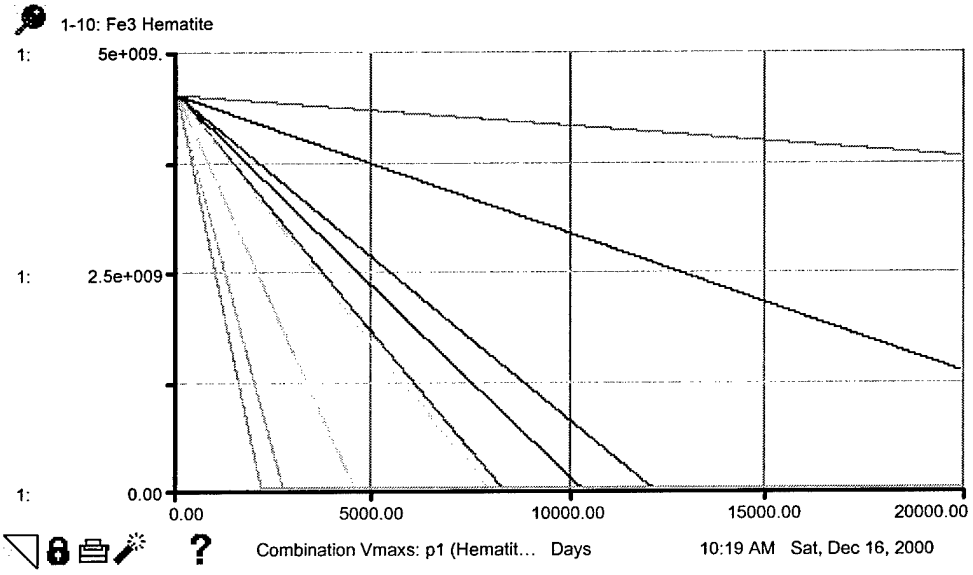

Hematite Behavior – Simulation Set 1, Combination Simulations

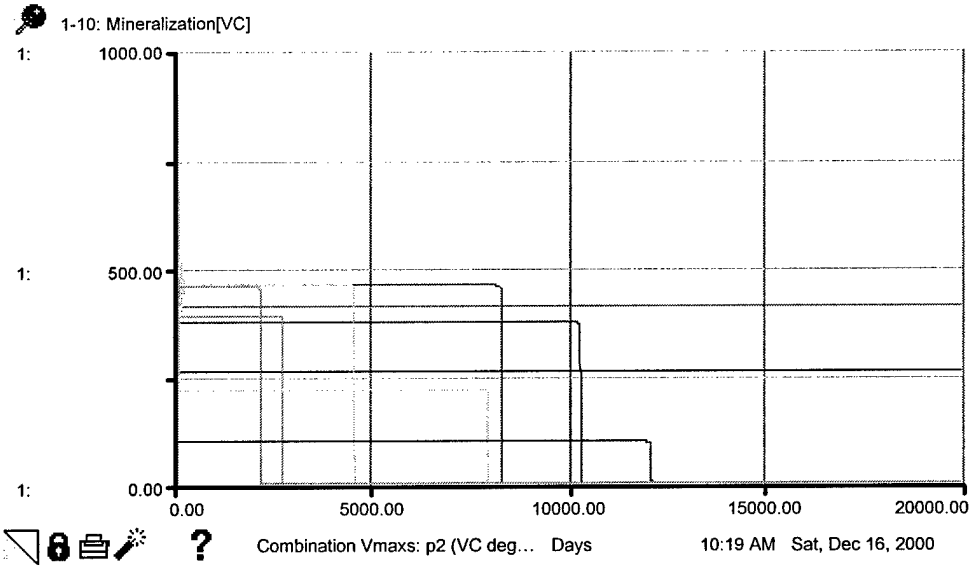

VC Behavior – Simulation Set 1, Combination Simulations

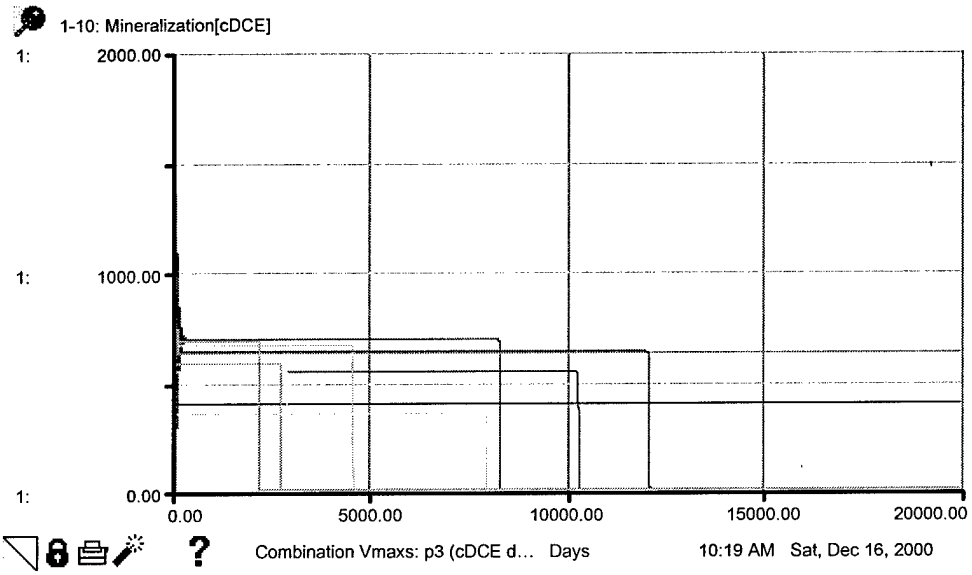

***cis*-DCE Behavior – Simulation Set 1, Combination Simulations**

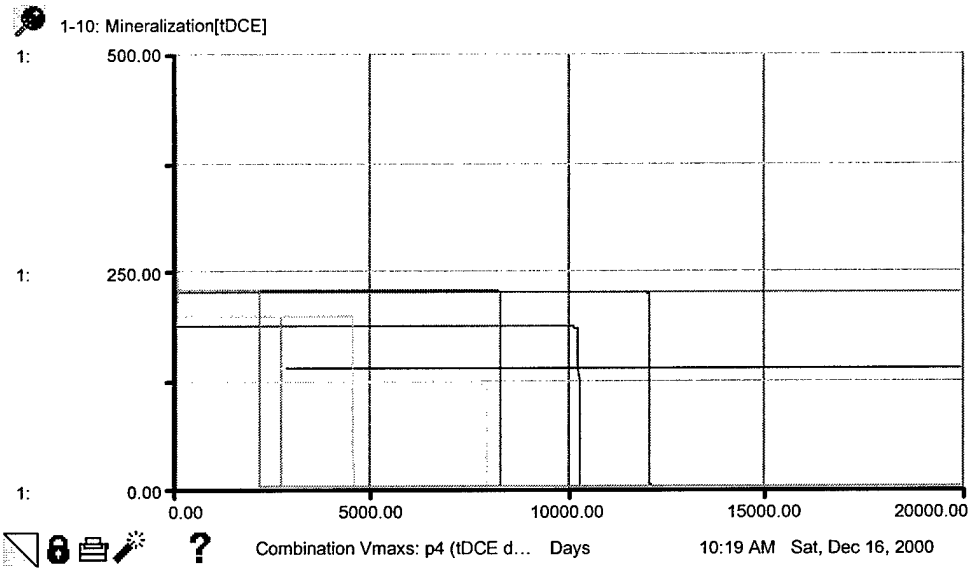

***trans*-DCE Behavior – Simulation Set 1, Combination Simulations**

Input Variables			
Run #	Cont Vmax[VC]	Cont Vmax[cDCE]	Cont Vmax[tDCE]
1	4000	5000	5000
2	9000	10000	10000
3	19000	23000	21000
4	12000	15000	20000
5	10000	12000	12000
6	3000	10000	5000
7	19000	19000	12000
8	3000	4000	4000
9	1000	16000	20000
10	18000	22000	21000

Run #	H2 Vmax	Ace Vmax	Form Vmax
1	10000	25000	25000
2	15000	70000	65000
3	50000	100000	80000
4	7000	5000	5000
5	150000	700000	90000
6	1000	400000	300000
7	200000	180000	150000
8	20000	250000	10000
9	800000	50000	40000
10	400000	500000	400000

Run #	Prop Vmax	But Vmax	Lact Vmax
1	15000	12500	11000
2	30000	50000	25000
3	80000	35000	50000
4	3000	4000	3000
5	150000	300000	50000
6	200000	80000	90000
7	100000	80000	50000
8	10000	20000	1000
9	50000	70000	30000
10	300000	80000	250000

Run #	Eth Vmax	Meth Vmax
1	10000	10000
2	50000	40000
3	30000	30000
4	2000	2000
5	100000	20000
6	75000	75000
7	100000	100000
8	5000	5000
9	20000	20000
10	500000	500000

Vmax Values used in 10 Combination Simulations (Runs)

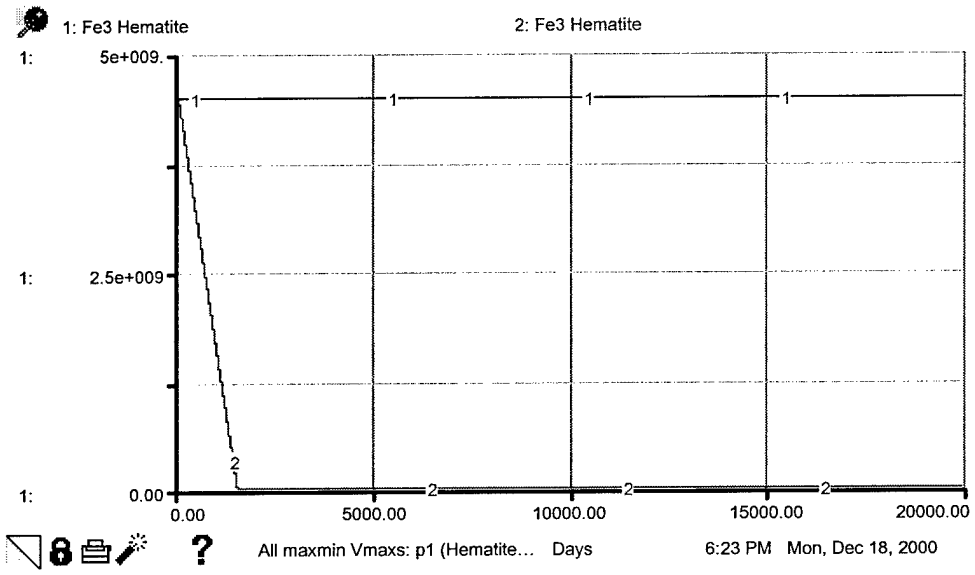

Hematite Behavior – Simulation Set 1, Max/Min Vmax Values

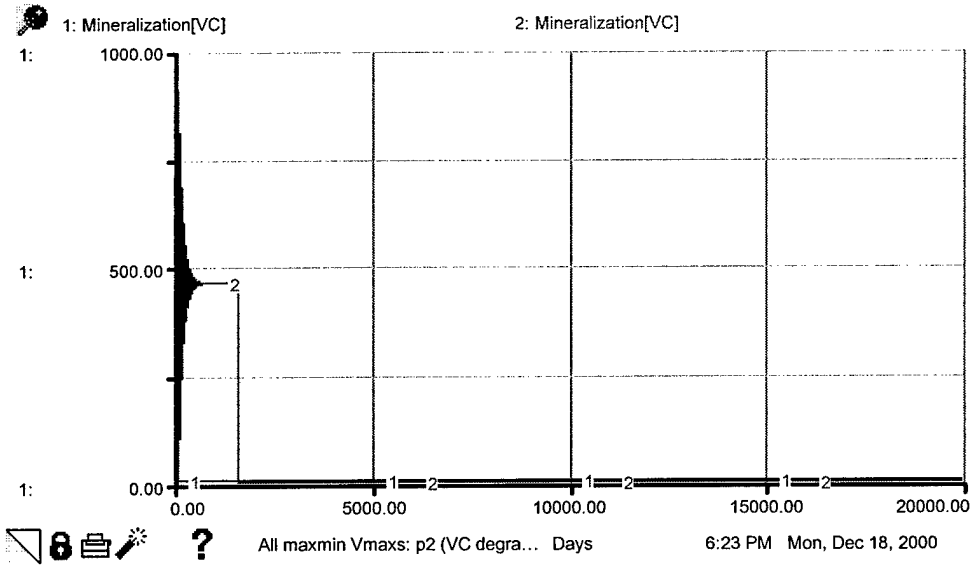

VC Behavior – Simulation Set 1, Max/Min Vmax Values

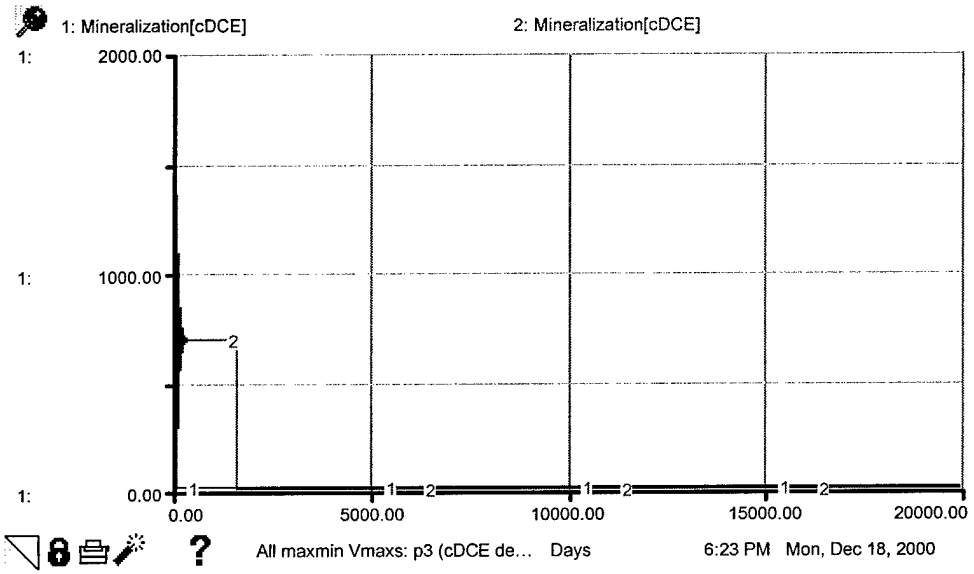

***cis*-DCE Behavior – Simulation Set 1, Max/Min Vmax Values**

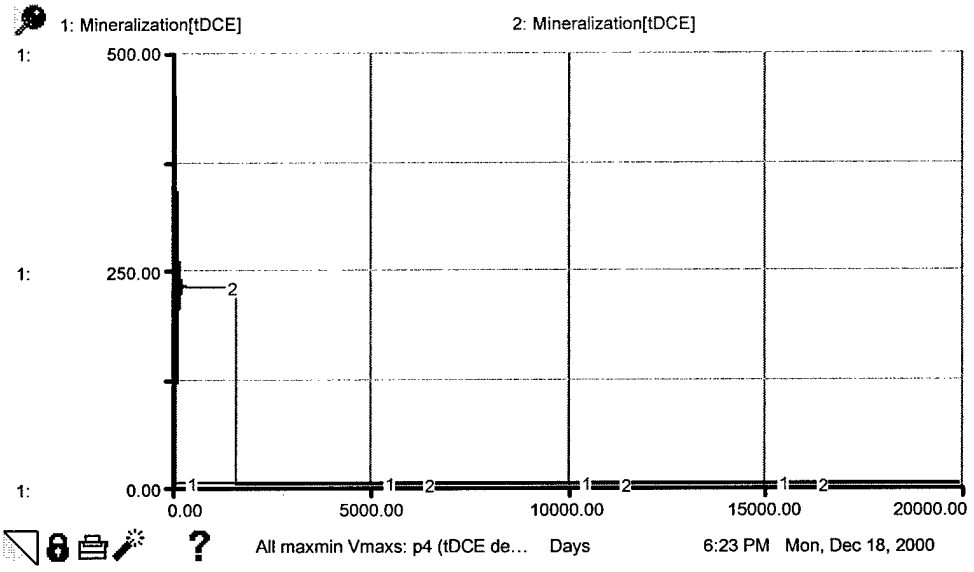

***trans*-DCE Behavior – Simulation Set 1, Max/Min Vmax Values**

Setup #2			Mon, Dec 18, 2000 6:19 PM
	Input Variables		
Run #	Cont Vmax[VC]	Cont Vmax[cDCE]	Cont Vmax[tDCE]
1	10.0	10.0	10.0
2	19200	23000	22000
Run #	H2 Vmax	Ace Vmax	Form Vmax
1	10.0	10.0	10.0
2	900000	1.2e+006	870000
Run #	Prop Vmax	But Vmax	Lact Vmax
1	10.0	10.0	10.0
2	550000	520000	520000
Run #	Eth Vmax	Meth Vmax	
1	10.0	10.0	
2	540000	500000	

Vmax Values used for Max/Min Simulations (Runs)

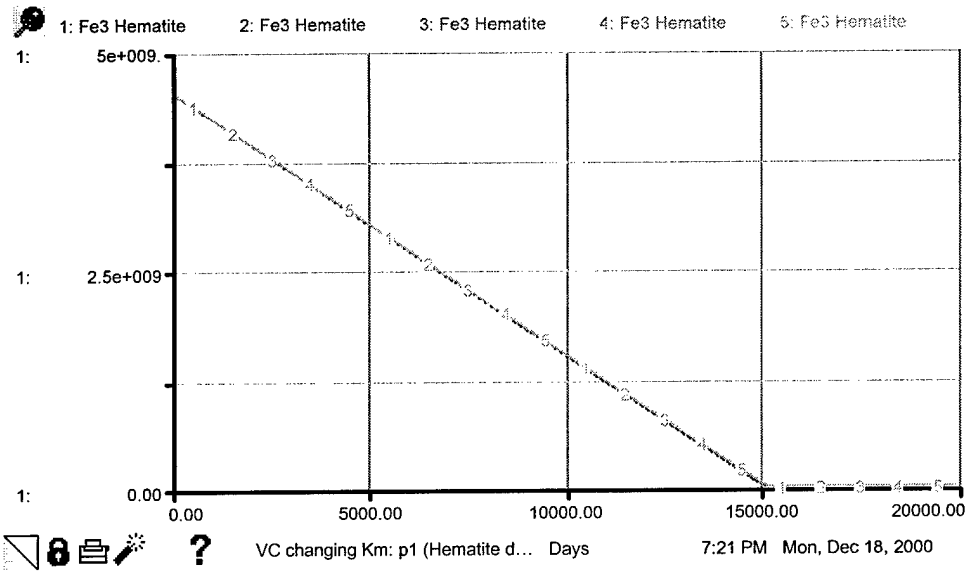

Hematite Behavior – Simulation Set 2, Changing VC Km

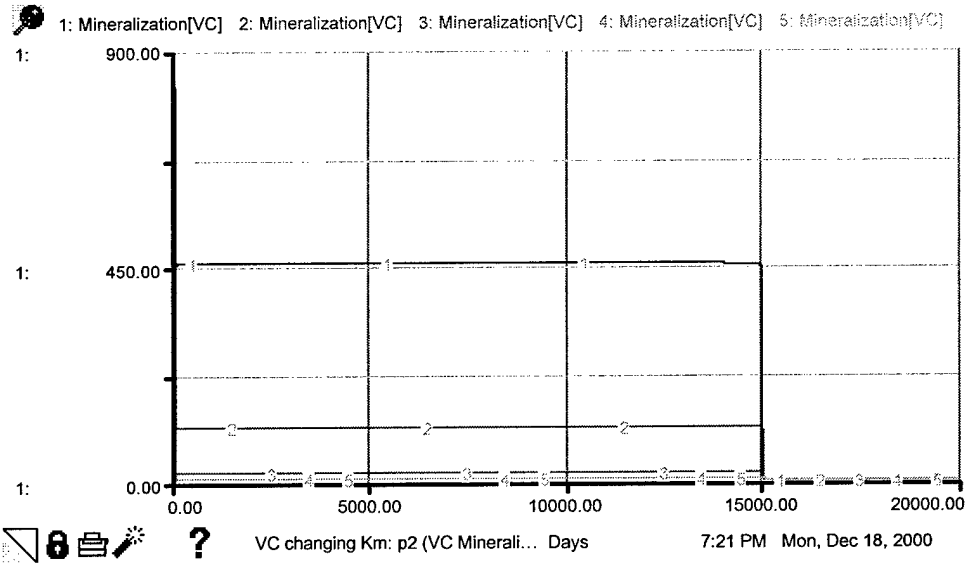

VC Behavior – Simulation Set 2, Changing VC Km

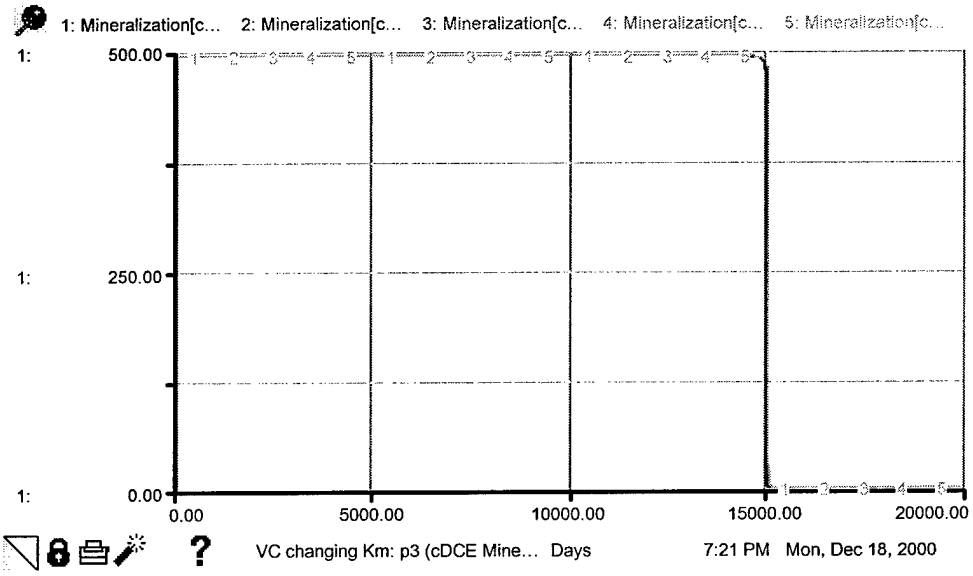

***cis*-DCE Behavior – Simulation Set 2, Changing VC Km**

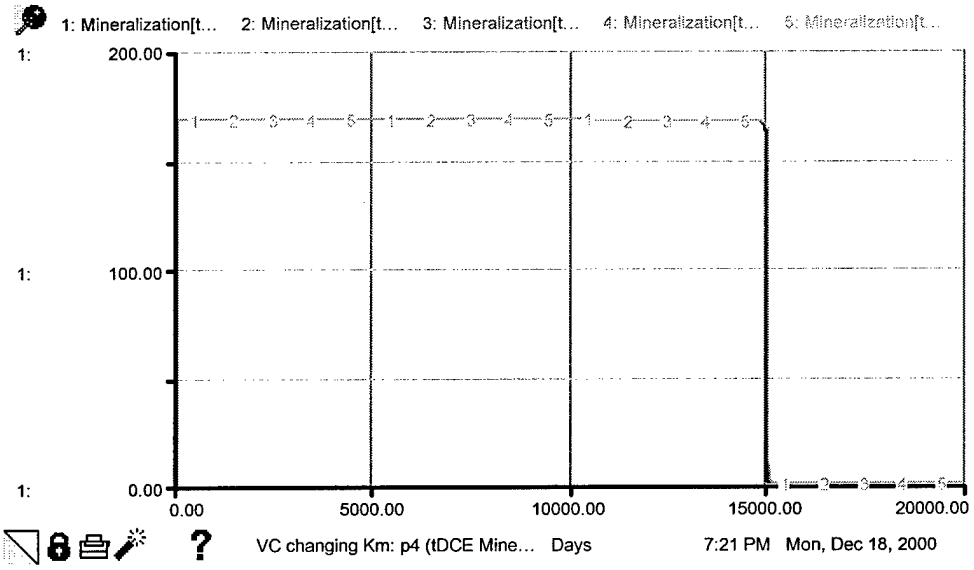

***trans*-DCE Behavior – Simulation Set 2, Changing VC Km**

Setup #1		Mon, Dec 18, 2000 7:18 PM
	Input Variables	
Run #	Cont Km[VC]	
1	0.03	
2	0.5	
3	5.00	
4	1000	
5	10000	

Km Values used for Changing VC Simulations (Runs)

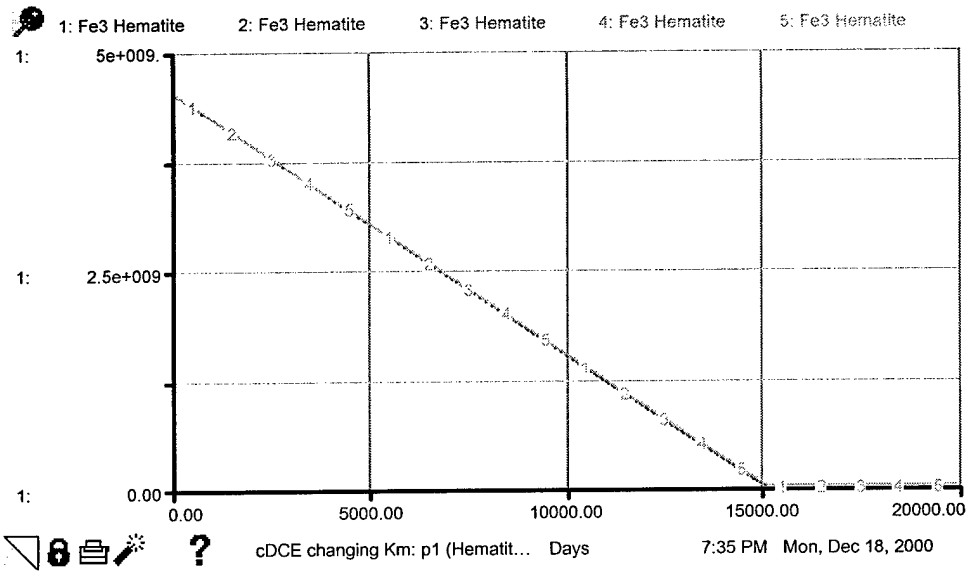

Hematite Behavior – Simulation Set 2, Changing *cis*-DCE Km

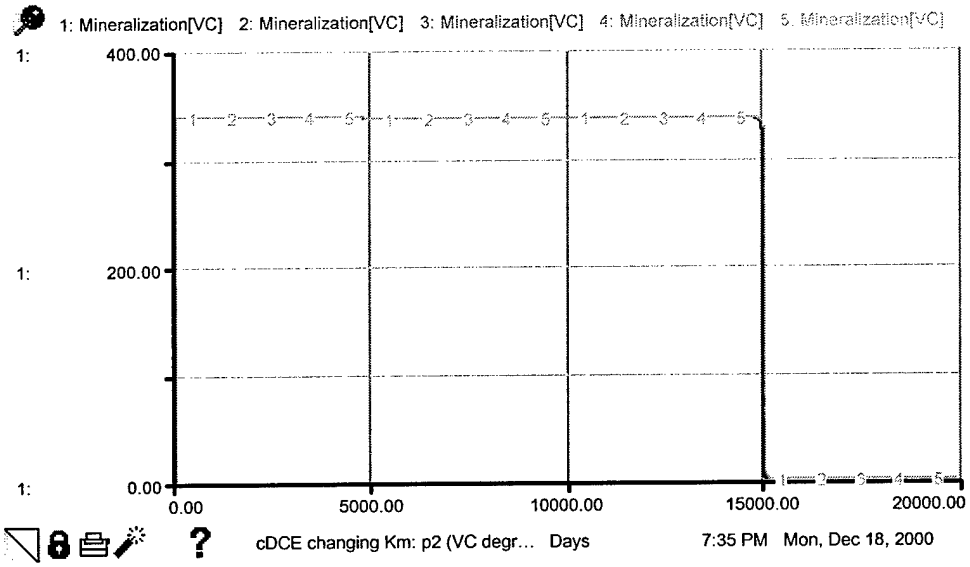

VC Behavior – Simulation Set 2, Changing *cis*-DCE Km

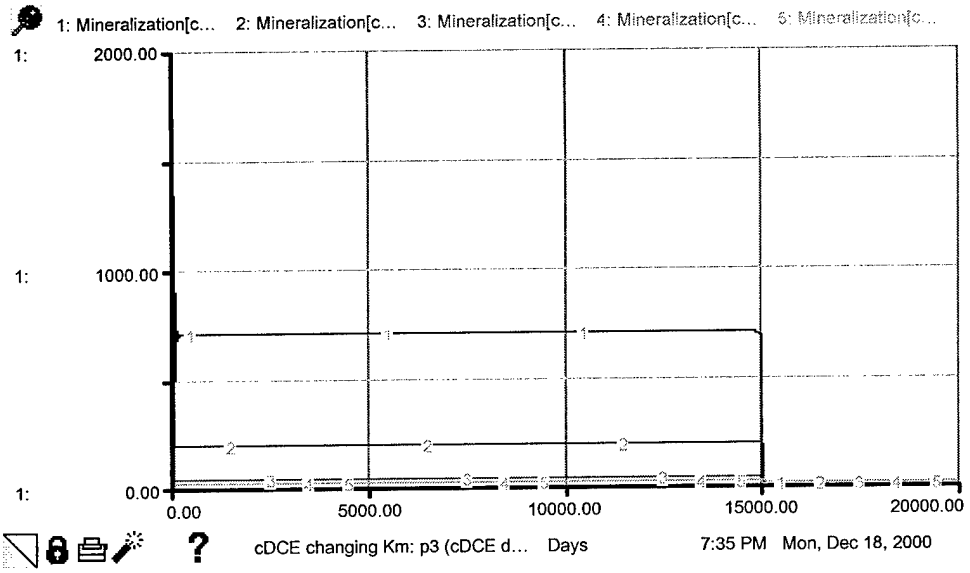

***cis*-DCE Behavior – Simulation Set 2, Changing *cis*-DCE Km**

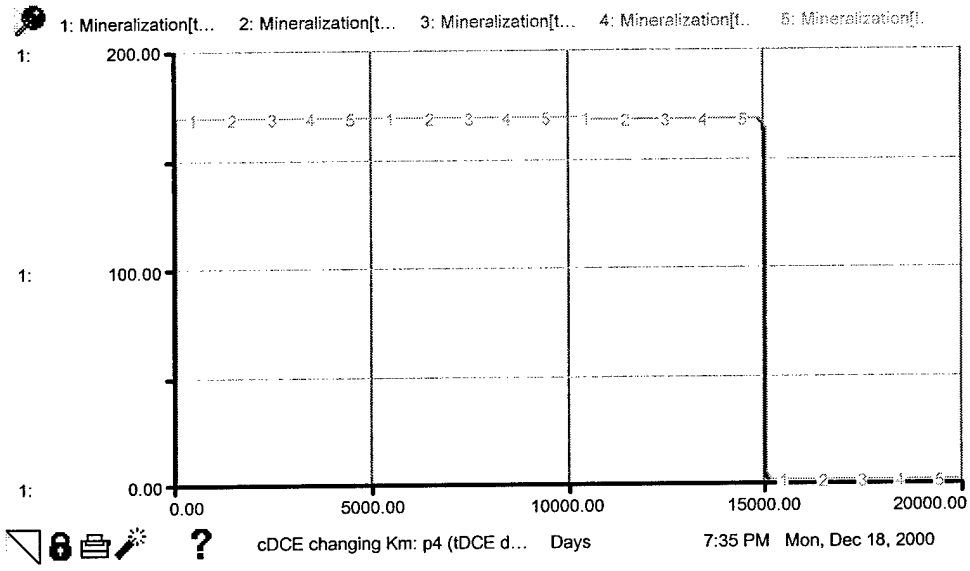

***trans*-DCE Behavior – Simulation Set 2, Changing *cis*-DCE Km**

Setup #2	Mon, Dec 18, 2000 7:31 PM
Input Variables	
Run #	Cont Km[cDCE]
1	0.03
2	0.5
3	5.00
4	1000
5	10000

Km Values used for Changing *cis*-DCE Simulations (Runs)

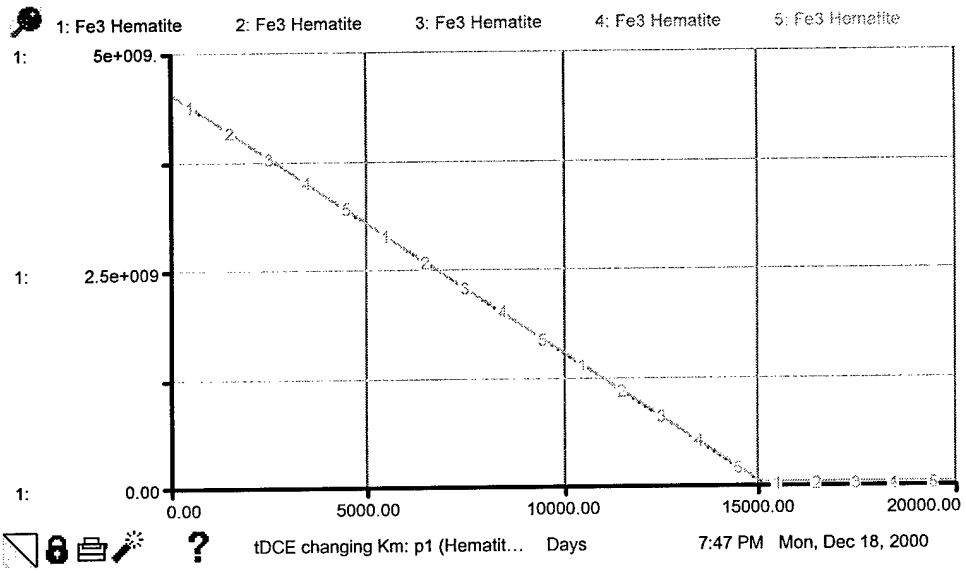

Hematite Behavior – Simulation Set 2, Changing *trans*-DCE Km

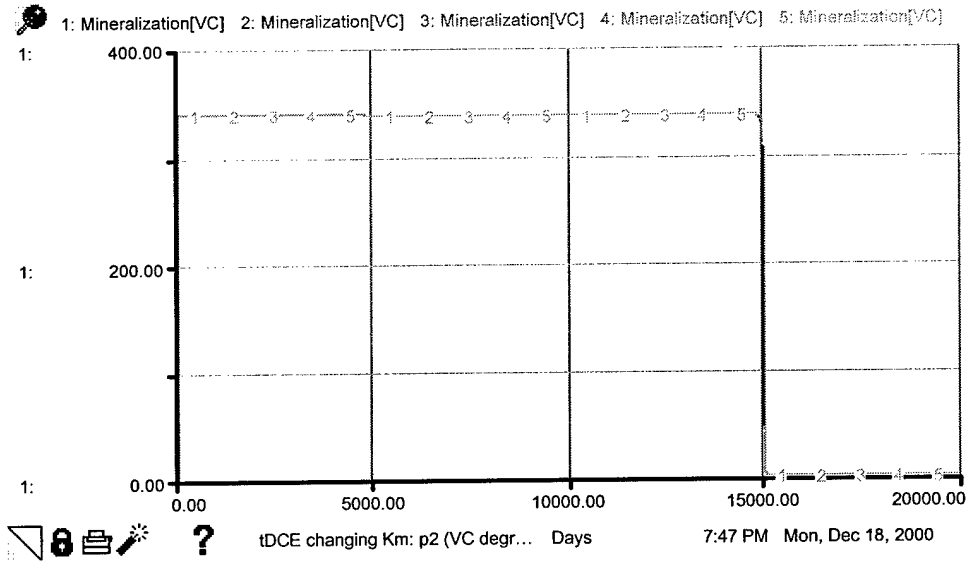

VC Behavior – Simulation Set 2, Changing *trans*-DCE Km

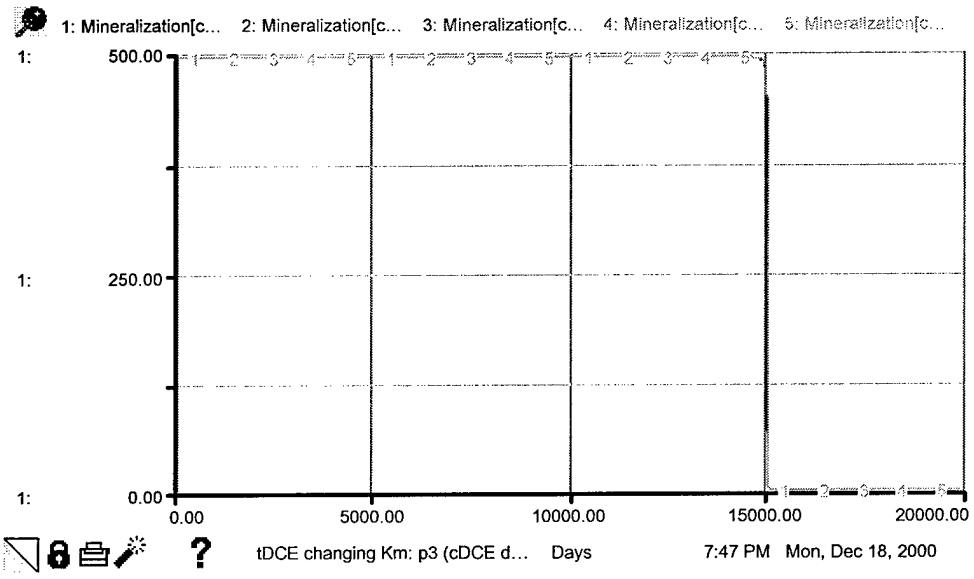

***cis*-DCE Behavior – Simulation Set 2, Changing *trans*-DCE Km**

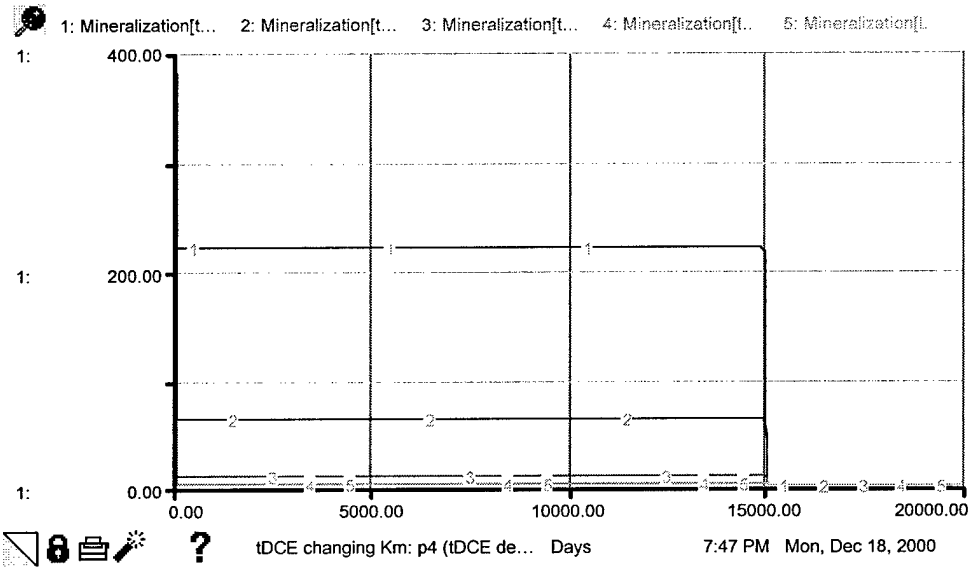

***trans*-DCE Behavior – Simulation Set 2, Changing *trans*-DCE Km**

Setup #3	Mon, Dec 18, 2000 7:43 PM
Input Variables	
Run #	Cont Km[tDCE]
1	0.04
2	0.5
3	5.00
4	1000
5	10000

Km Values used for Changing *trans*-DCE Simulations (Runs)

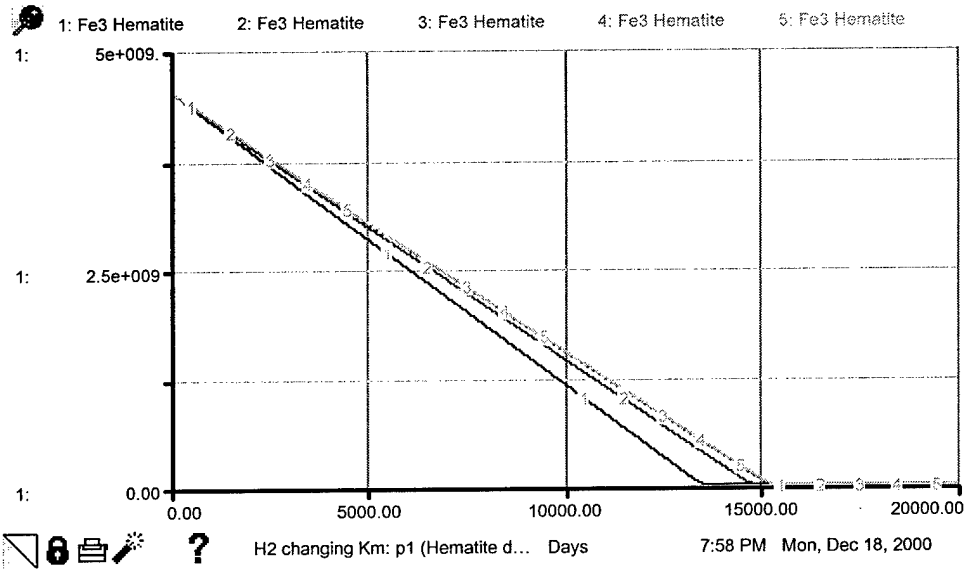

Hematite Behavior – Simulation Set 2, Changing H_2 Km

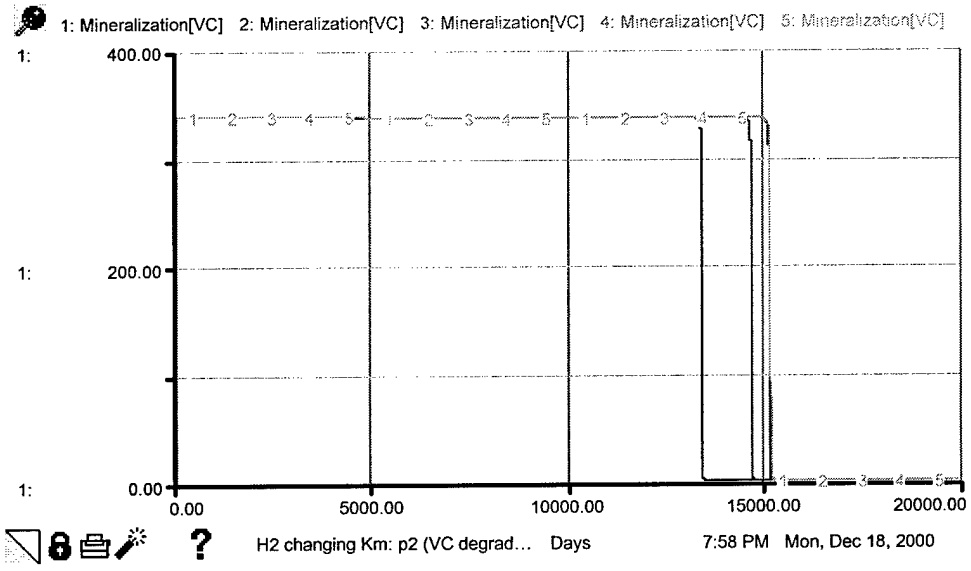

VC Behavior – Simulation Set 2, Changing H_2 Km

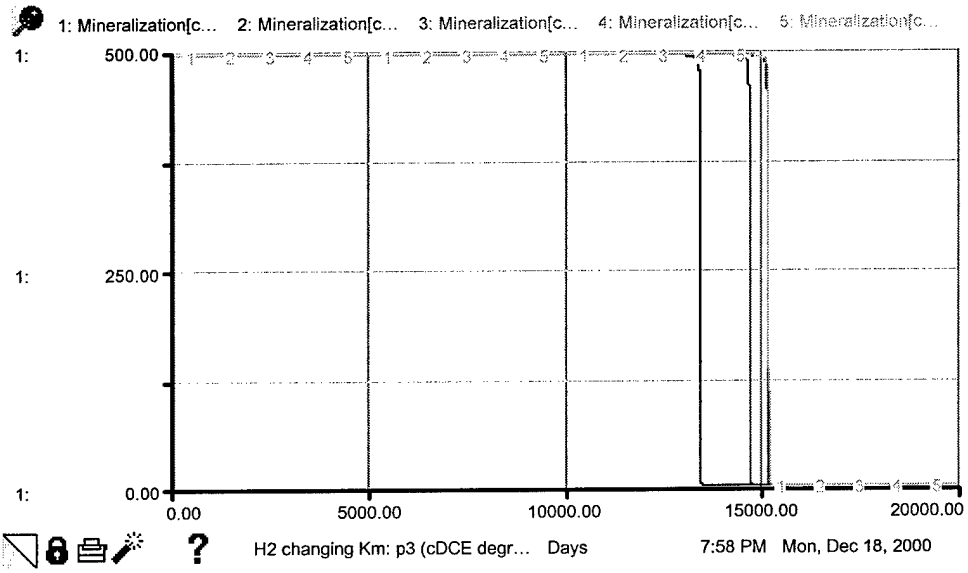

***cis*-DCE Behavior – Simulation Set 2, Changing H_2 Km**

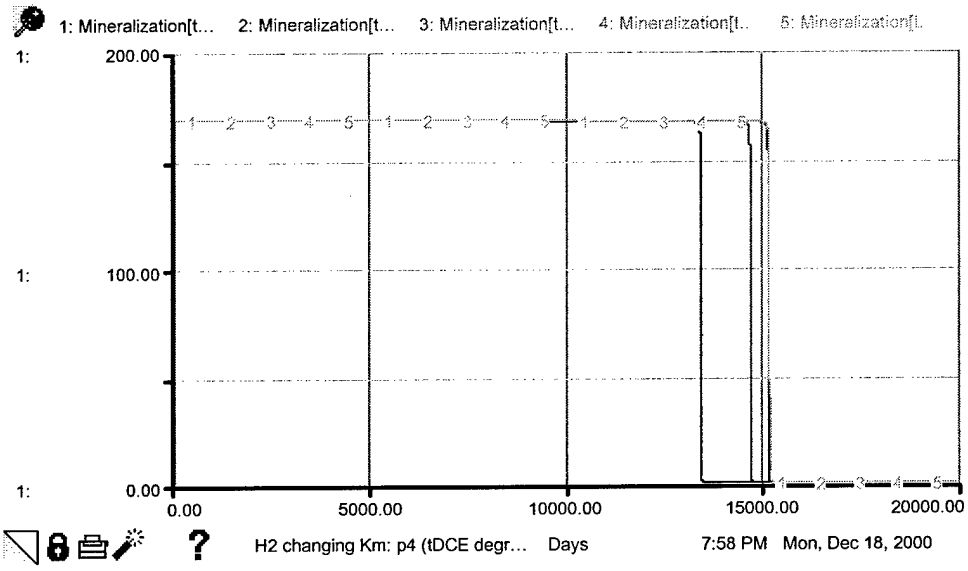

***trans*-DCE Behavior – Simulation Set 2, Changing H_2 Km**

Setup #4	Mon, Dec 18, 2000 7:53 PM
Input Variables	
Run #	H2 Km
1	0.03
2	0.5
3	10.0
4	10000
5	100000

Km Values used for Changing H_2 Simulations (Runs)

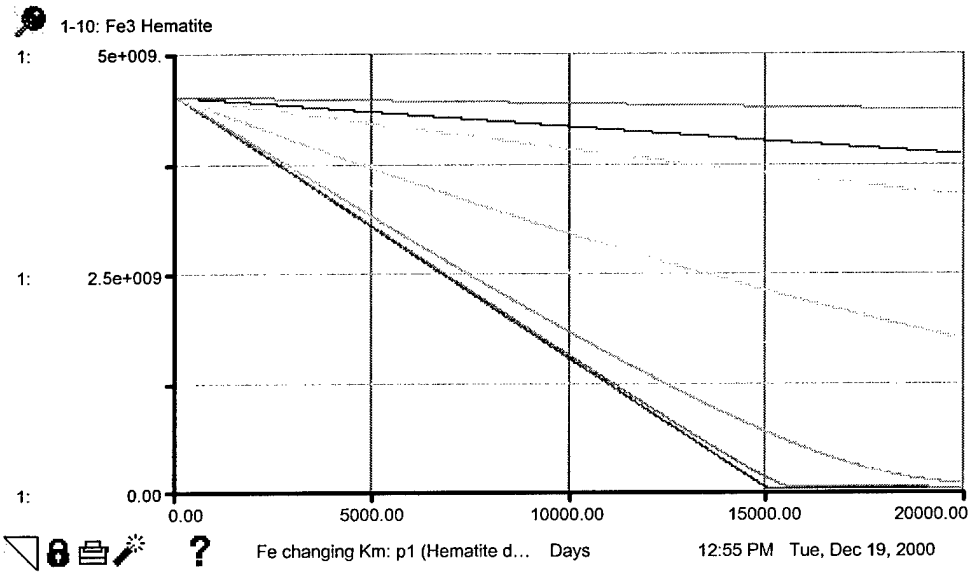

Hematite Behavior – Simulation Set 2, Changing Hematite Km

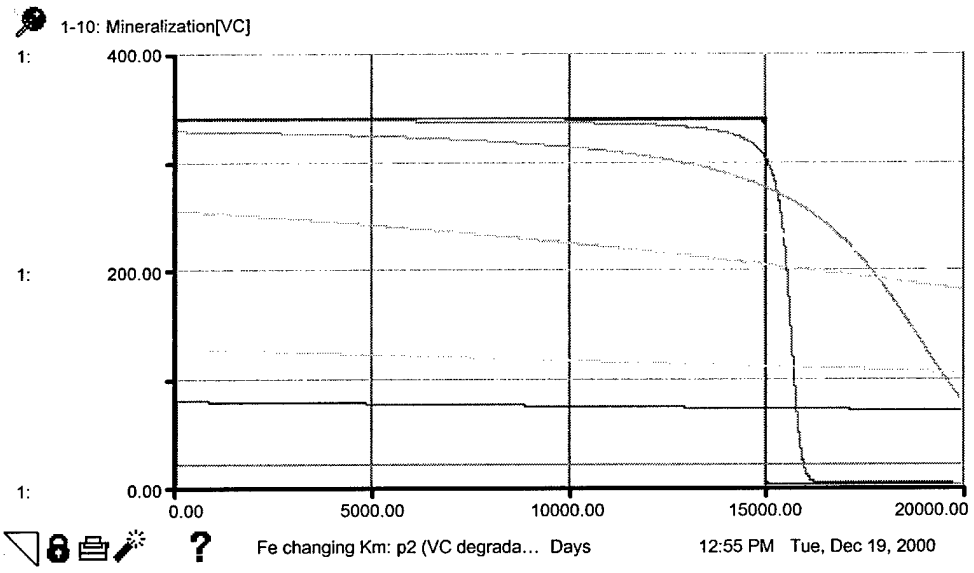

VC Behavior – Simulation Set 2, Changing Hematite Km

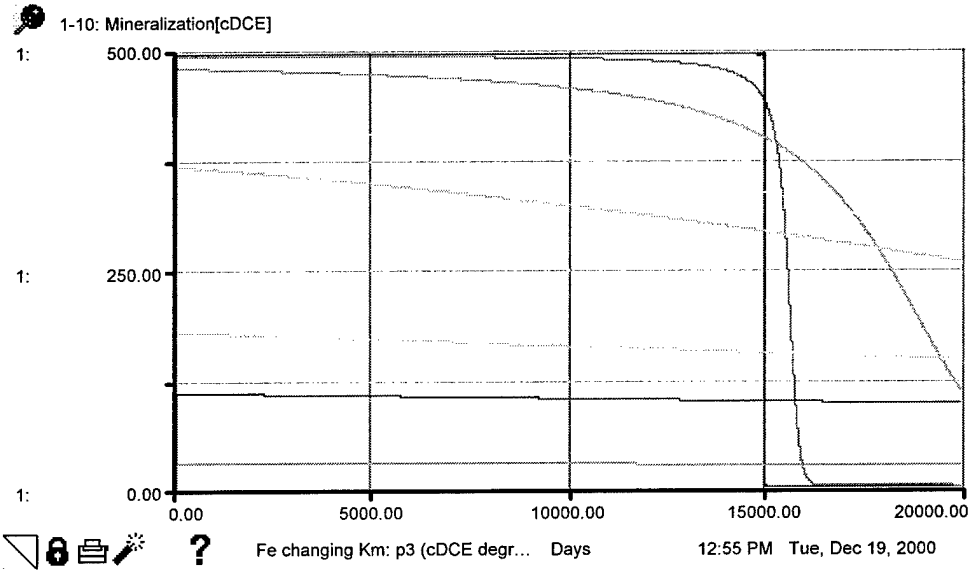

***cis*-DCE Behavior – Simulation Set 2, Changing Hematite Km**

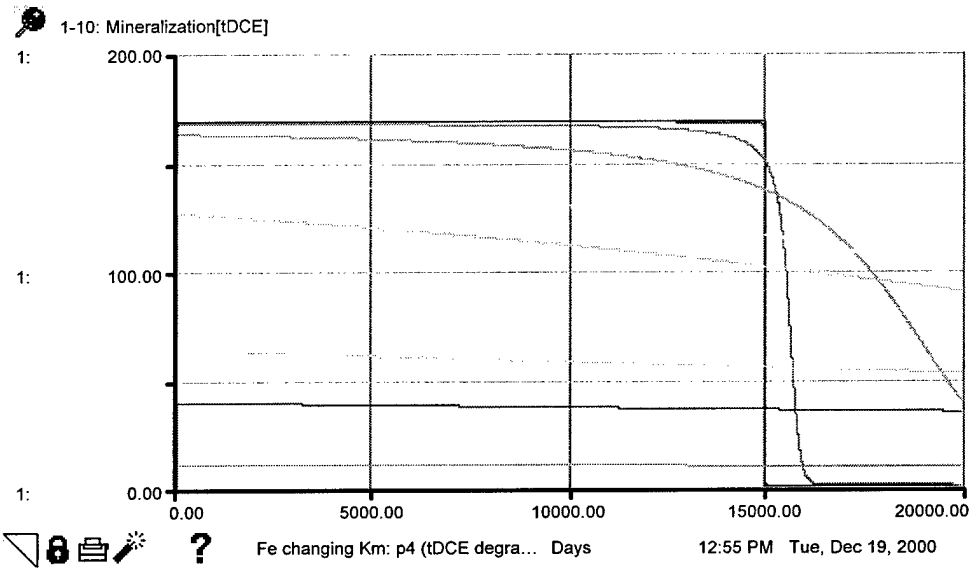

***trans*-DCE Behavior – Simulation Set 2, Changing Hematite Km**

Setup #12 — Tue, Dec 19, 2000 12:46 PM

Input Variables

Run #	Fe Km
1	0.0001
2	0.01
3	1.00
4	100
5	1000
6	5000
7	10000
8	50000
9	100000
10	500000

Km Values used for Changing Hematite Simulations (Runs)

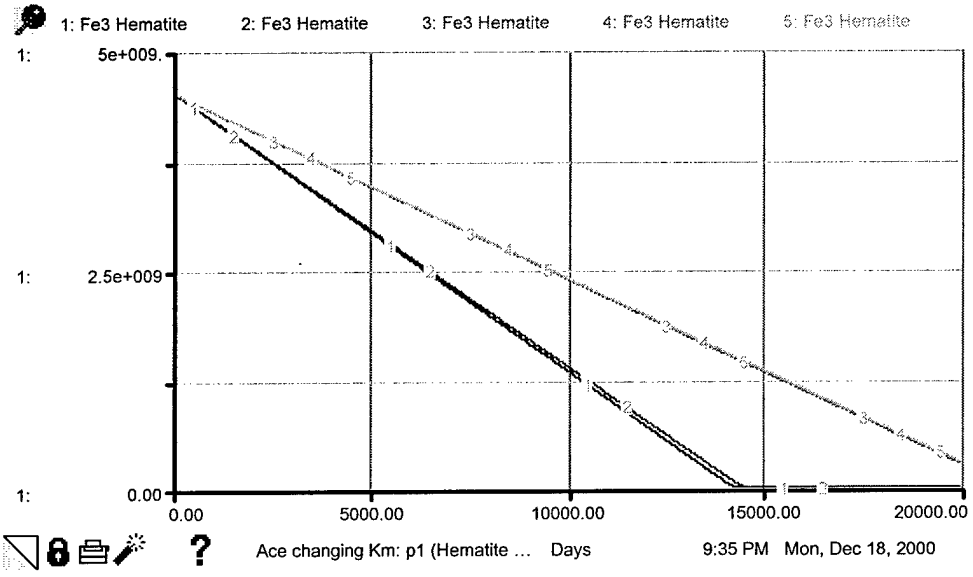

Hematite Behavior – Simulation Set 2, Changing Acetic Acid Km

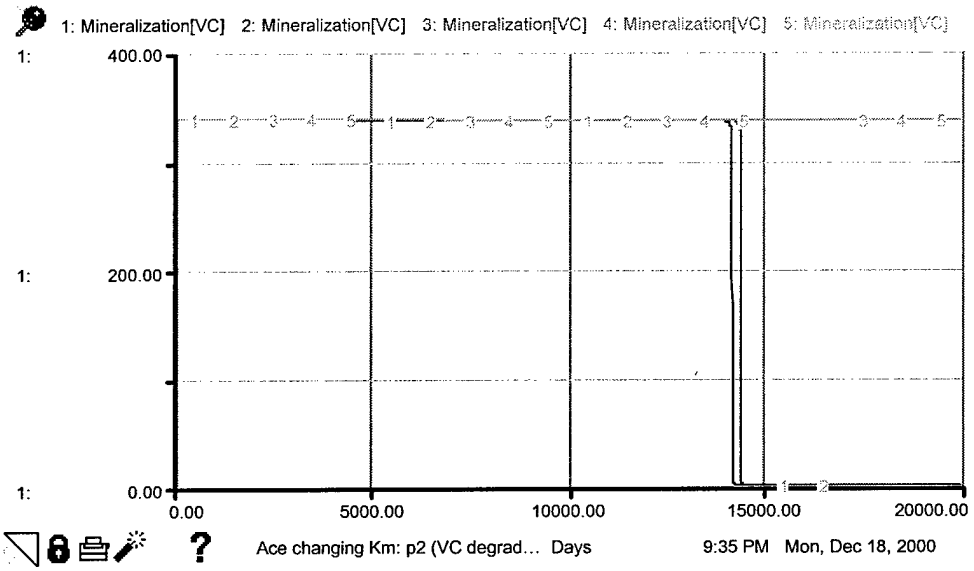

VC Behavior – Simulation Set 2, Changing Acetic Acid Km

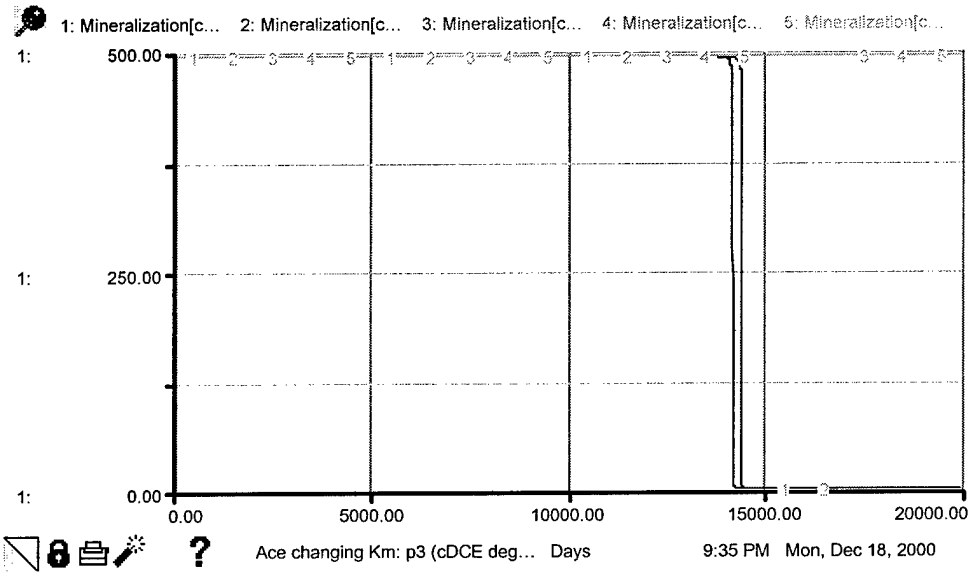

***cis*-DCE Behavior – Simulation Set 2, Changing Acetic Acid Km**

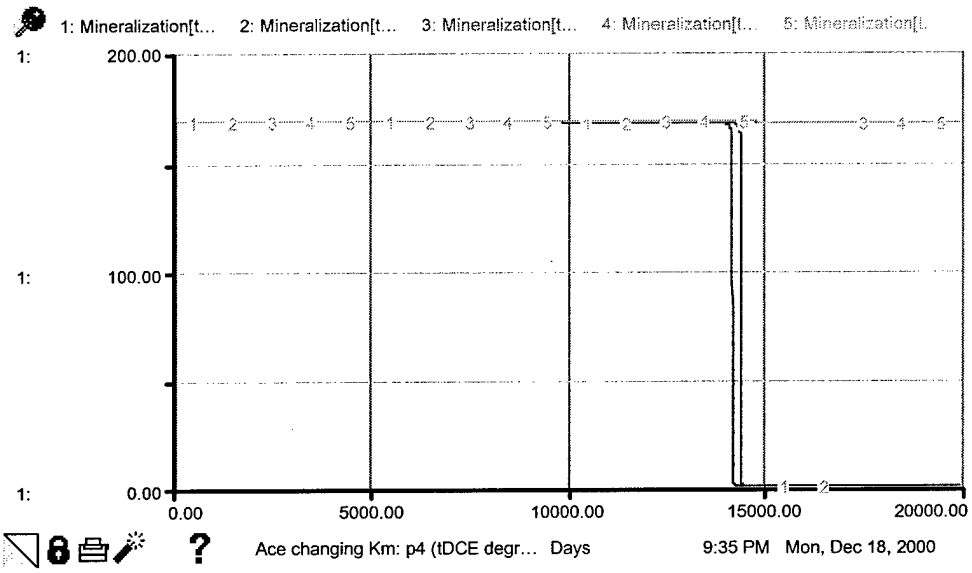

***trans*-DCE Behavior – Simulation Set 2, Changing Acetic Acid Km**

Setup #11	Mon, Dec 18, 2000 9:31 PM
Input Variables	
Run #	Ace Km
1	0.0001
2	0.5
3	1000
4	100000
5	500000

Km Values used for Changing Acetic Acid Simulations (Runs)

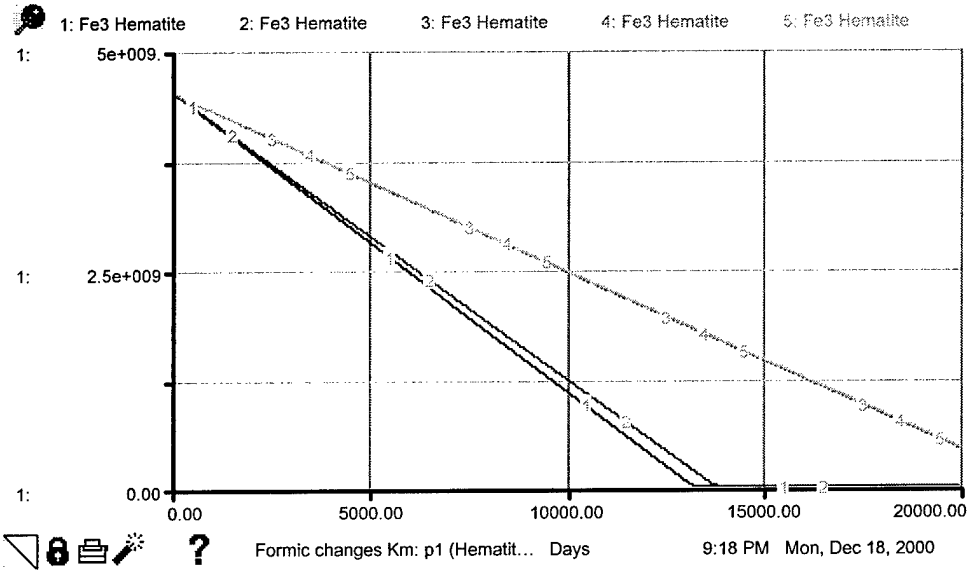

Hematite Behavior – Simulation Set 2, Changing Formic Acid Km

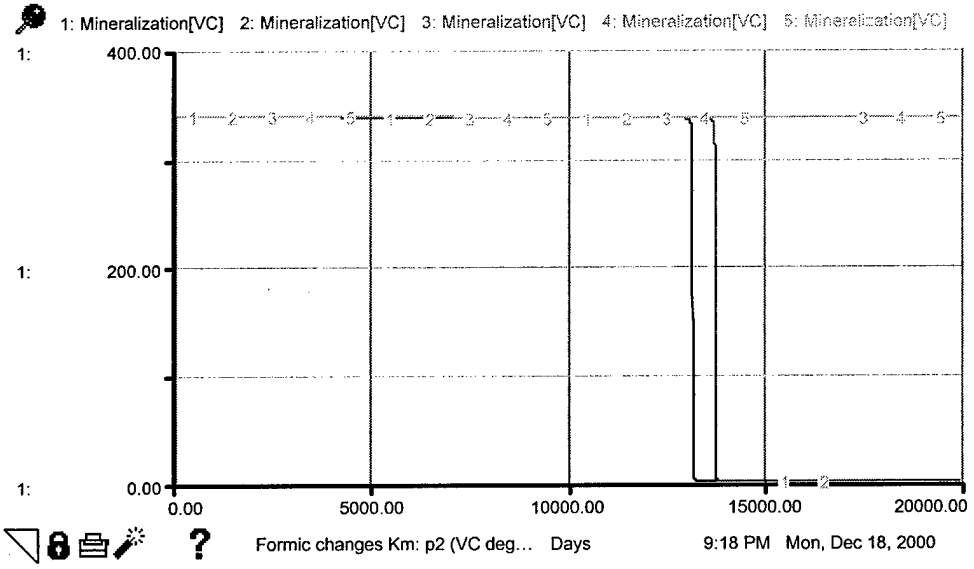

VC Behavior – Simulation Set 2, Changing Formic Acid Km

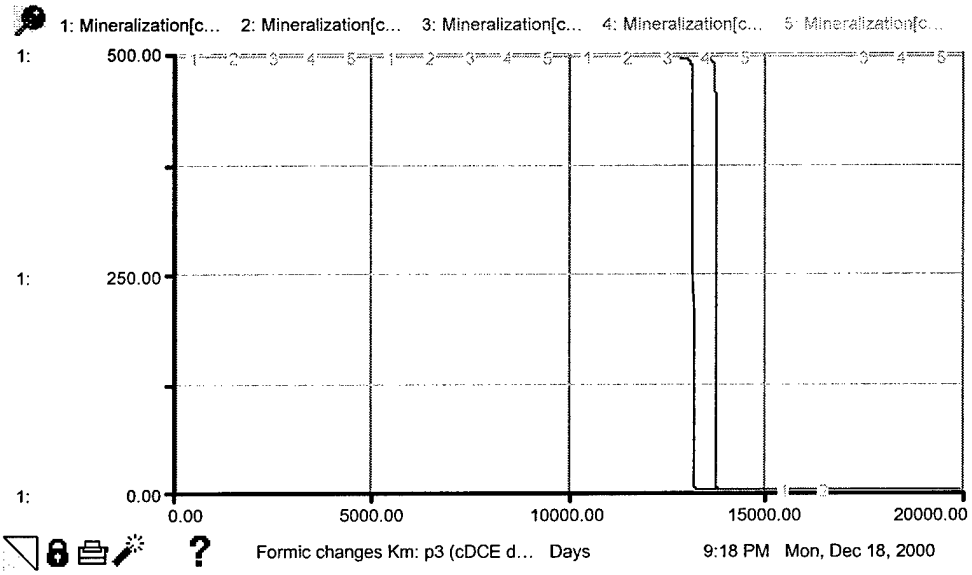

***cis*-DCE Behavior – Simulation Set 2, Changing Formic Acid Km**

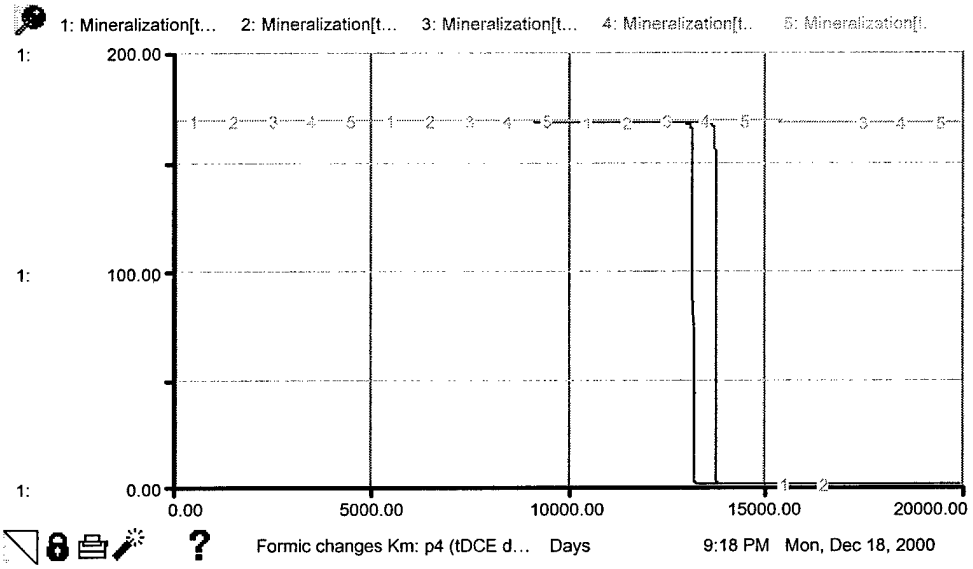

***trans*-DCE Behavior – Simulation Set 2, Changing Formic Acid Km**

Setup #10	Mon, Dec 18, 2000 9:14 PM
Input Variables	
Run #	Form Km
1	0.0001
2	0.5
3	1000
4	100000
5	500000

Km Values used for Formic Acid Simulations (Runs)

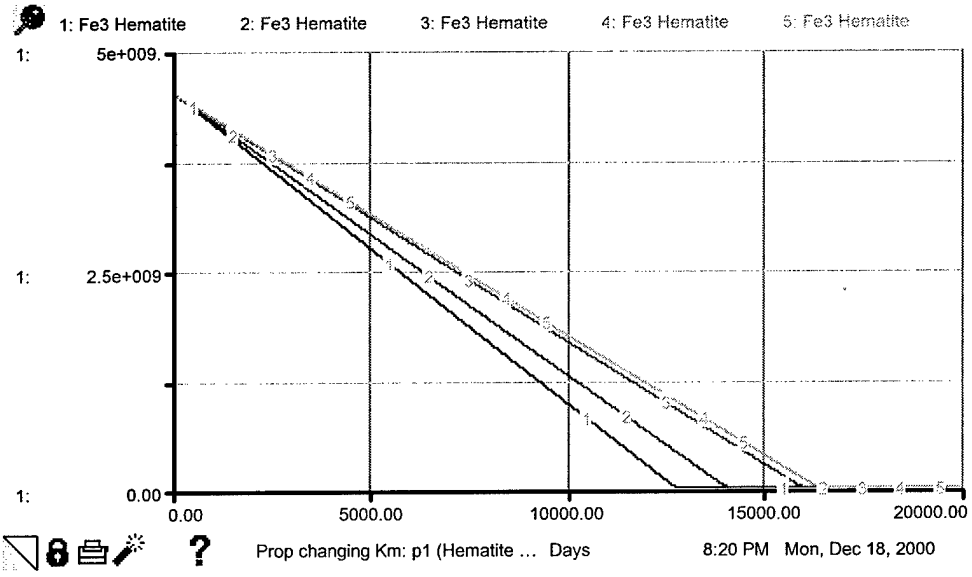

Hematite Behavior – Simulation Set 2, Changing Propionic Acid Km

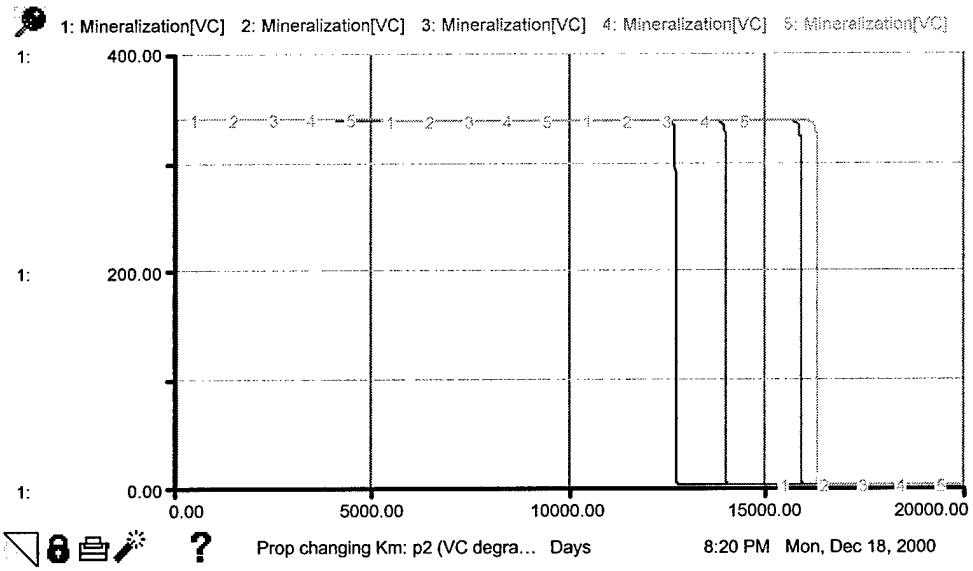

VC Behavior – Simulation Set 2, Changing Propionic Acid Km

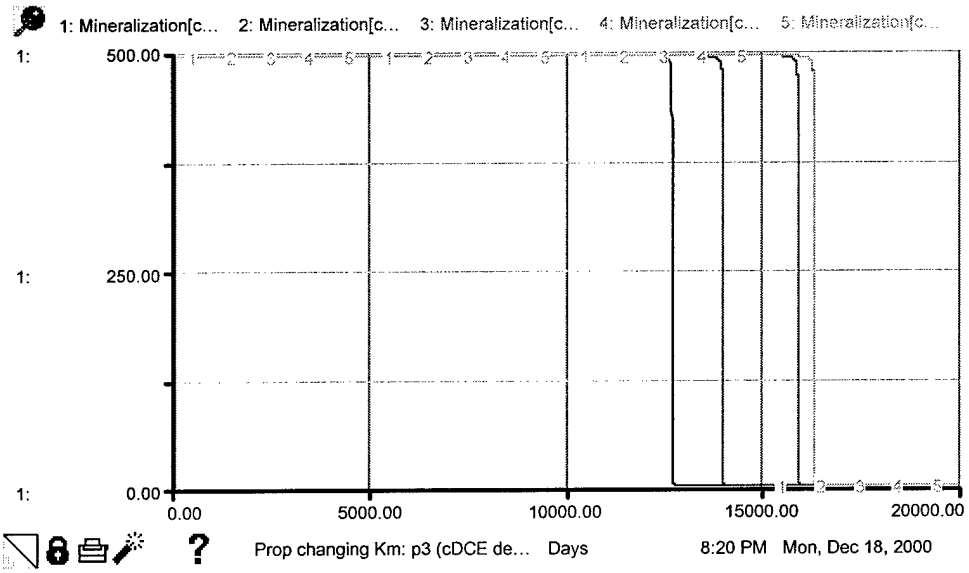

***cis*-DCE Behavior – Simulation Set 2, Changing Propionic Acid Km**

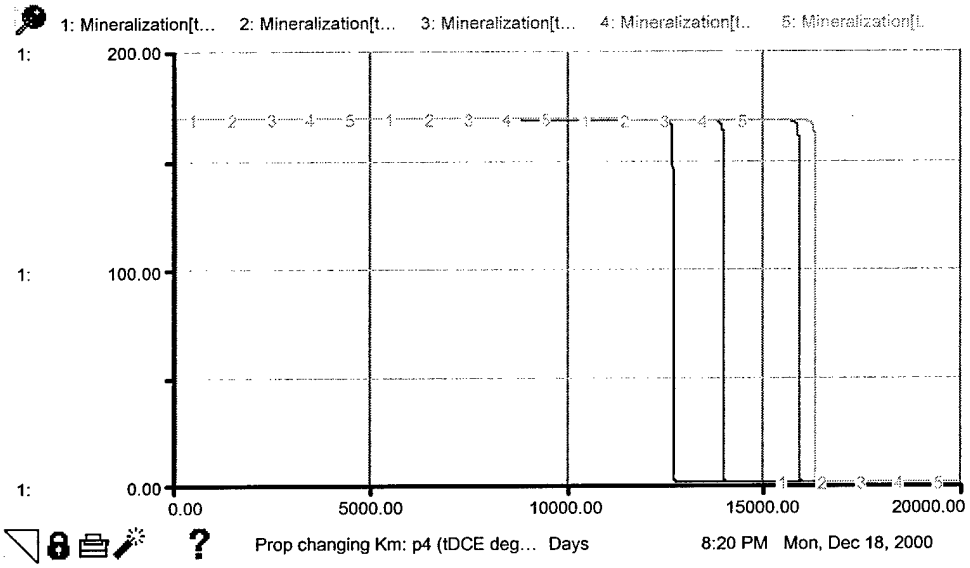

***trans*-DCE Behavior – Simulation Set 2, Changing Propionic Acid Km**

Setup #6	Mon, Dec 18, 2000 8:16 PM
Input Variables	
Run #	Prop Km
1	0.0001
2	0.5
3	10.0
4	10000
5	100000

Km Values used for Propionic Acid Simulations (Runs)

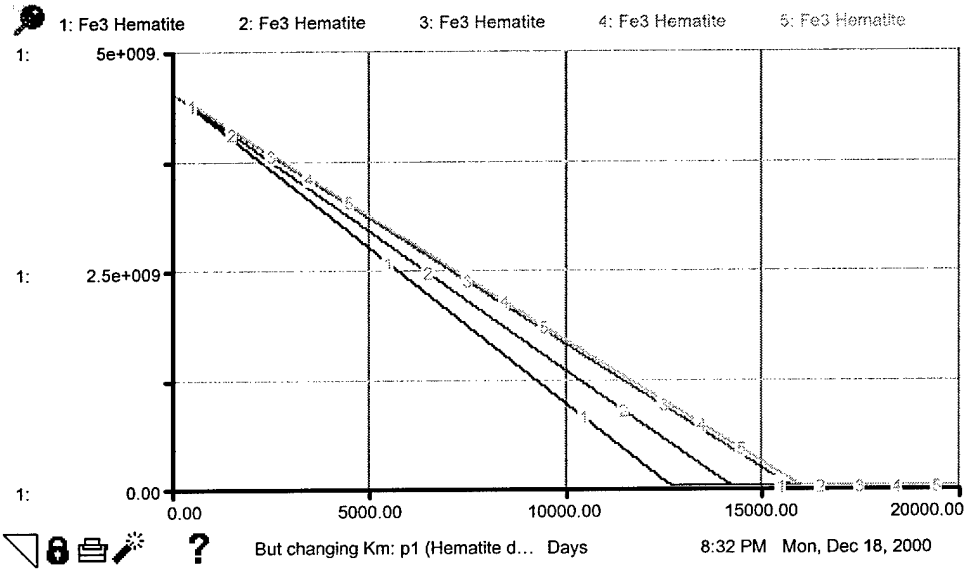

Hematite Behavior – Simulation Set 2, Changing Butryic Acid Km

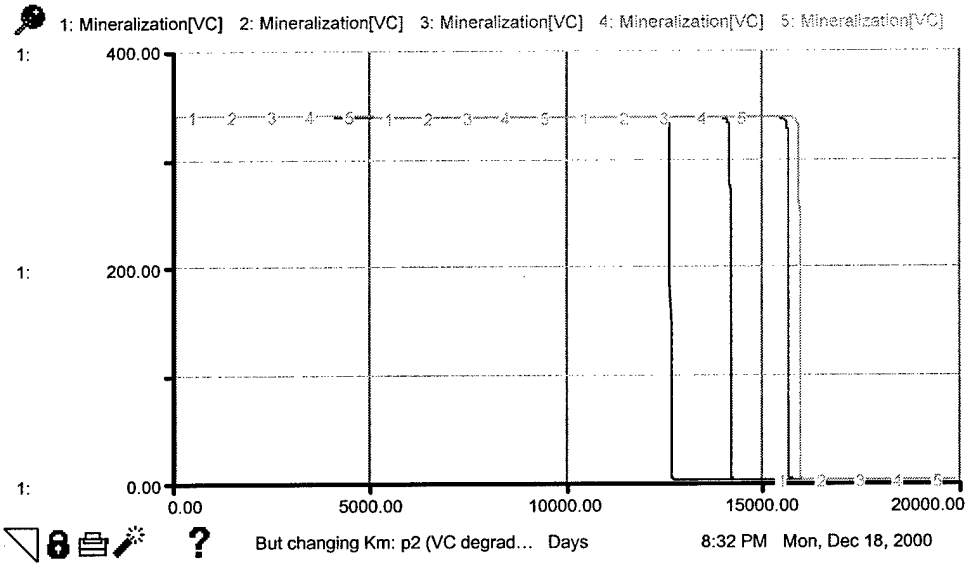

VC Behavior – Simulation Set 2, Changing Butryic Acid Km

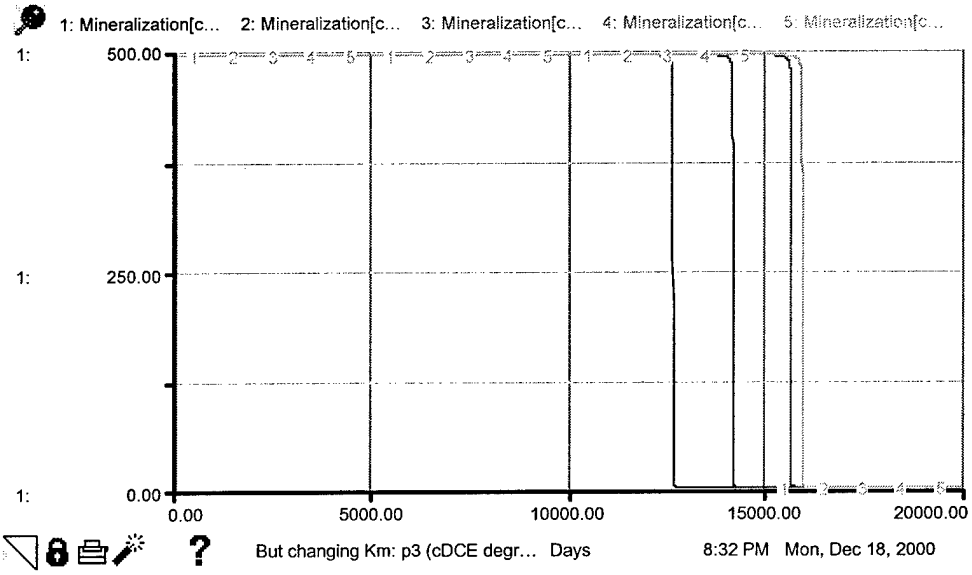

***cis*-DCE Behavior – Simulation Set 2, Changing Butyric Acid Km**

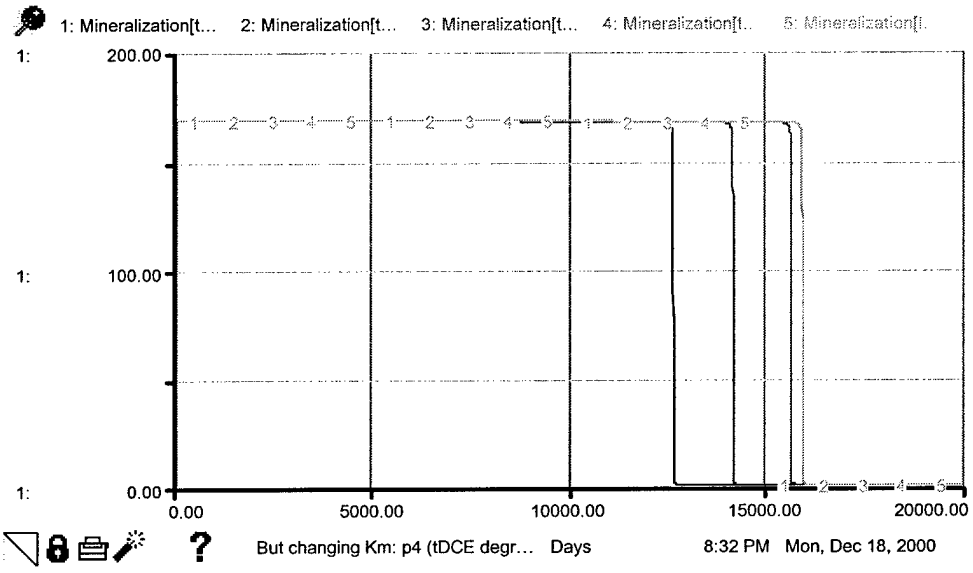

***trans*-DCE Behavior – Simulation Set 2, Changing Butyric Acid Km**

Setup #7	Mon, Dec 18, 2000 8:27 PM
Input Variables	
Run #	But Km
1	0.0001
2	0.5
3	10.0
4	10000
5	100000

Km Values used for Butyric Acid Simulations (Runs)

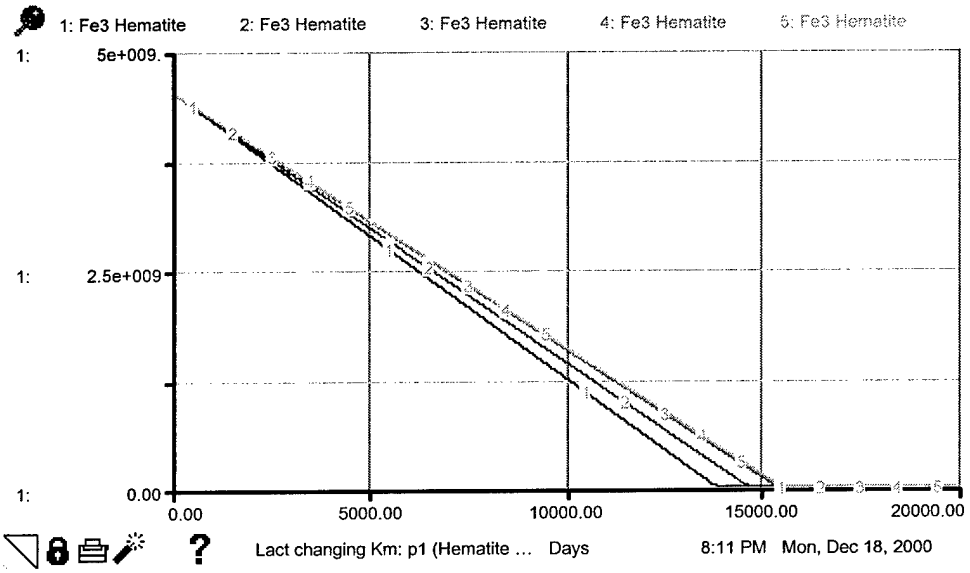

Hematite Behavior – Simulation Set 2, Changing Lactic Acid Km

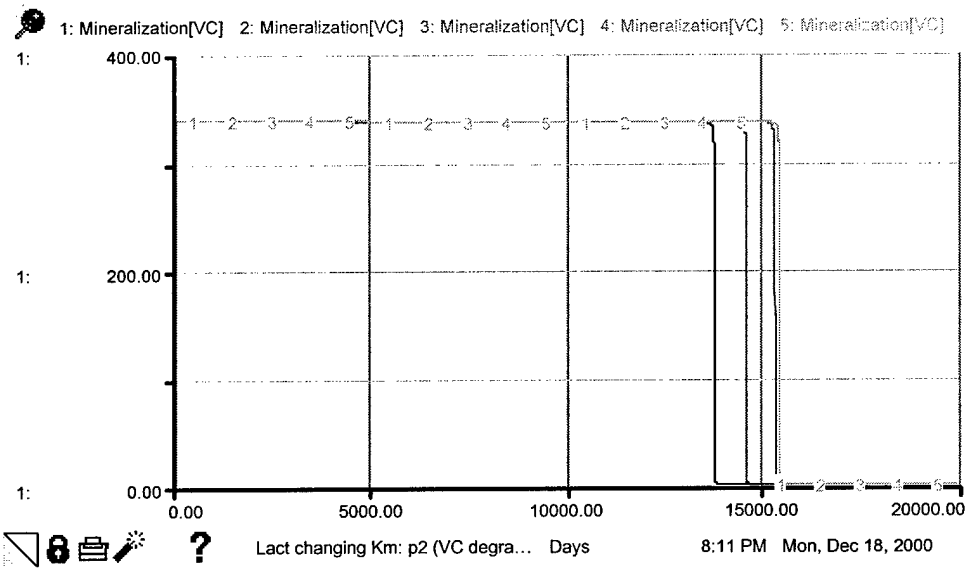

VC Behavior – Simulation Set 2, Changing Lactic Acid Km

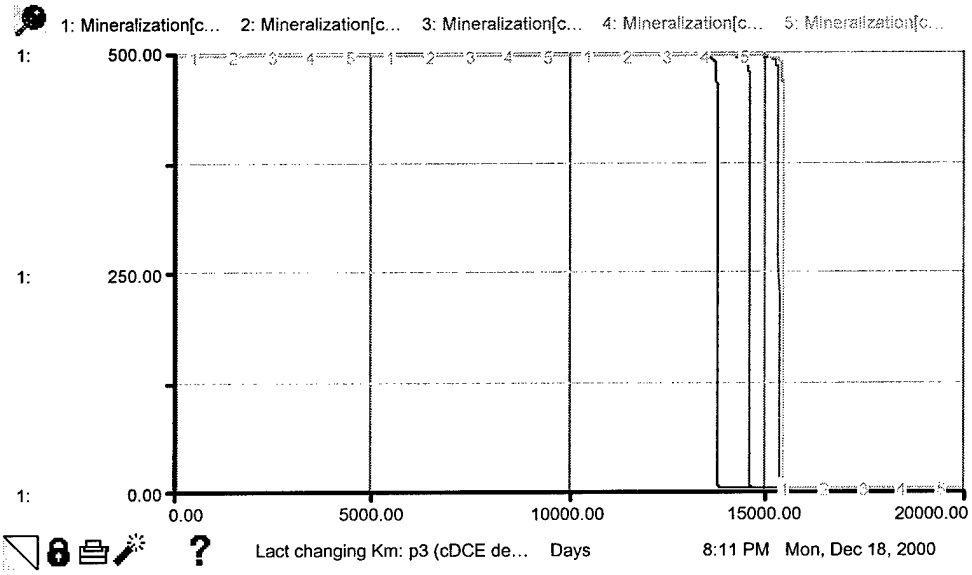

***cis*-DCE Behavior – Simulation Set 2, Changing Lactic Acid Km**

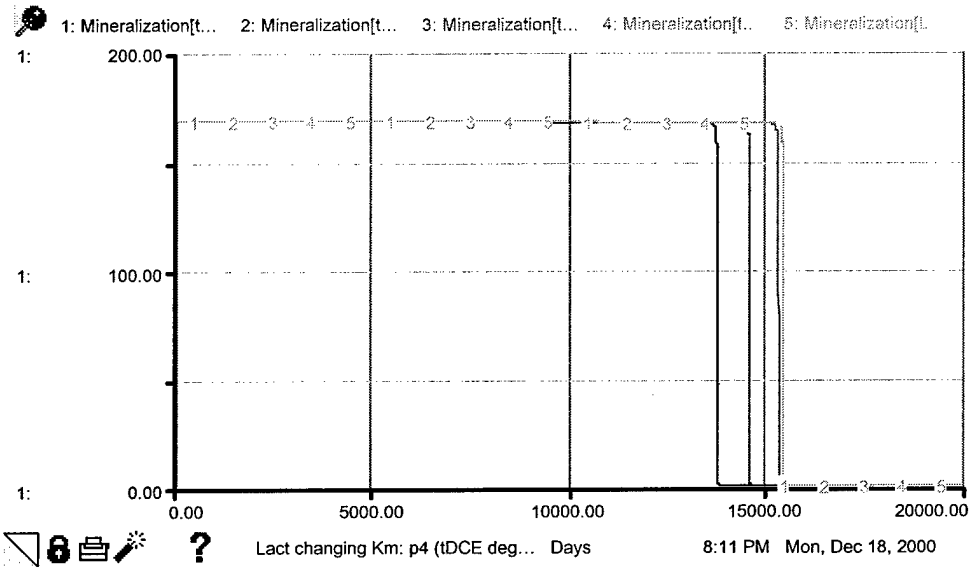

***trans*-DCE Behavior – Simulation Set 2, Changing Lactic Acid Km**

Setup #5	Mon, Dec 18, 2000 8:07 PM
Input Variables	
Run #	Lact Km
1	0.0001
2	0.5
3	10.0
4	1000
5	100000

Km Values used for Lactic Acid Simulations (Runs)

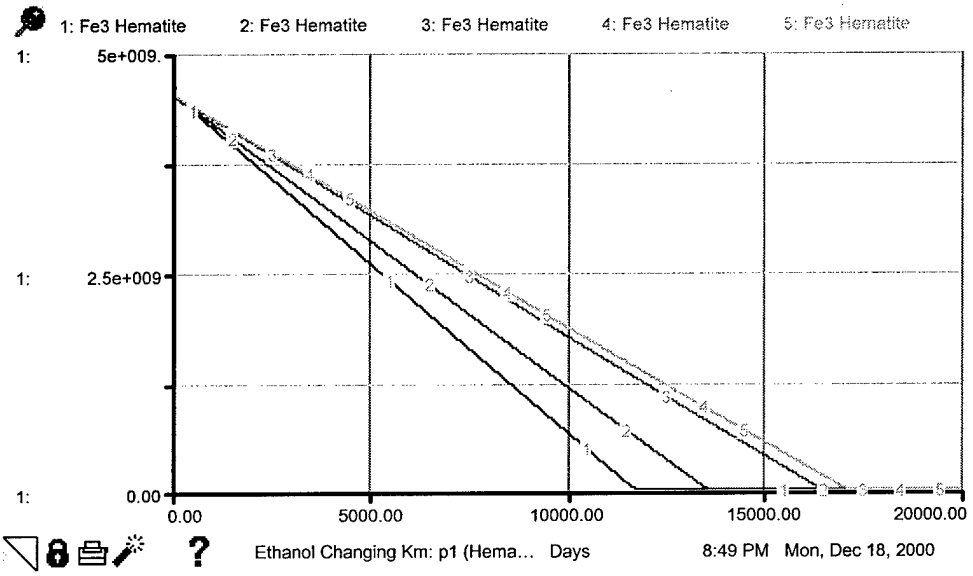

Hematite Behavior – Simulation Set 2, Changing Ethanol Km

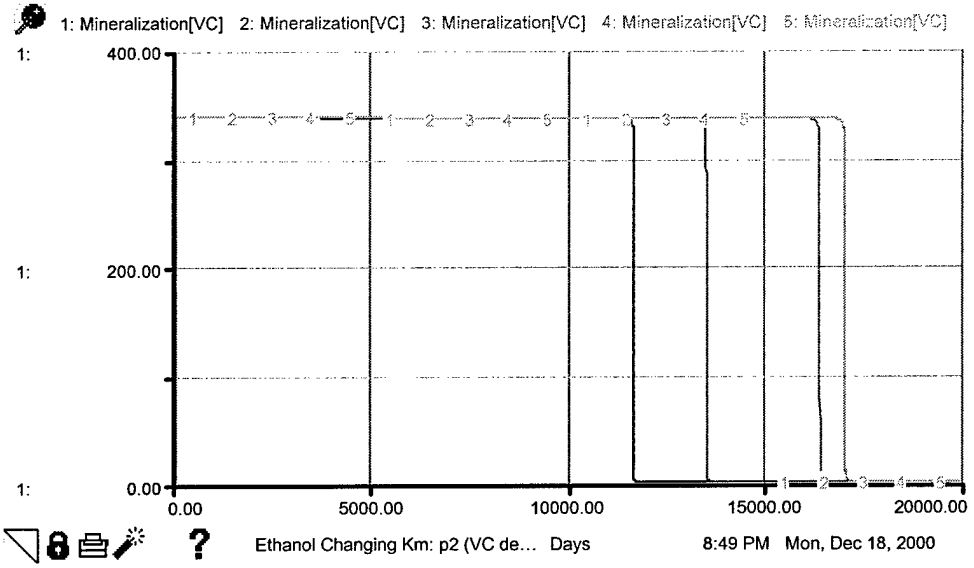

VC Behavior – Simulation Set 2, Changing Ethanol Km

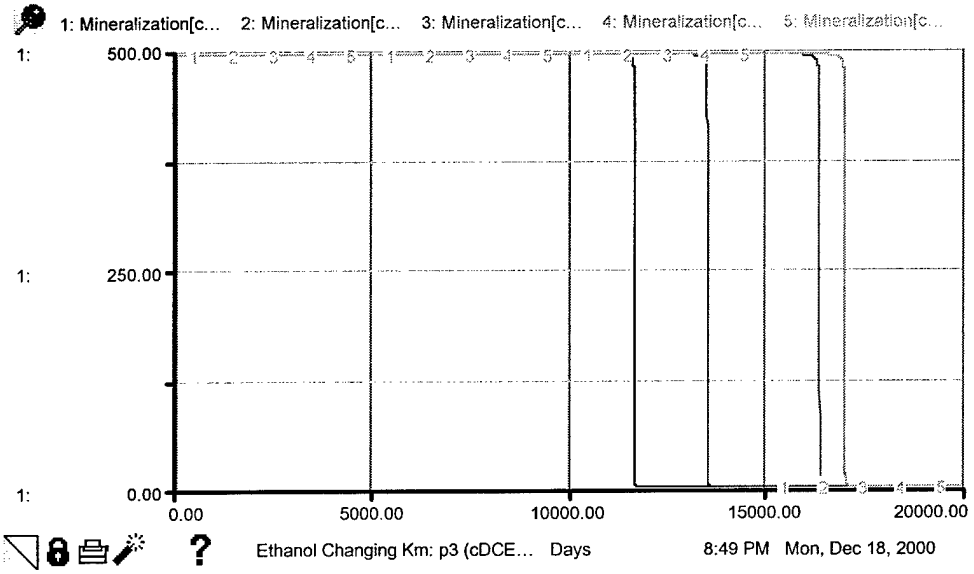

***cis*-DCE Behavior – Simulation Set 2, Changing Ethanol Km**

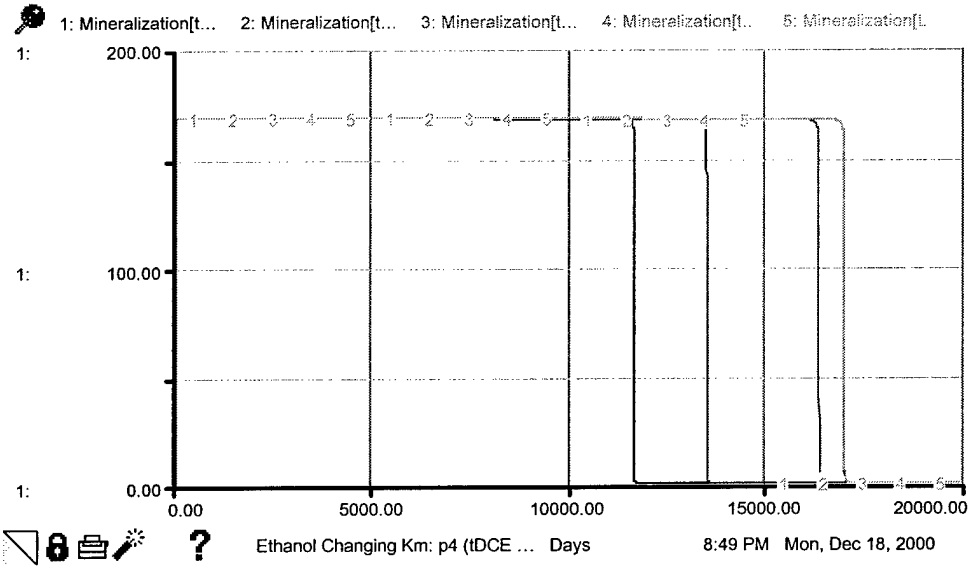

***trans*-DCE Behavior – Simulation Set 2, Changing Ethanol Km**

Setup #8	Mon, Dec 18, 2000 8:46 PM
Input Variables	
Run #	Eth Km
1	0.0001
2	0.5
3	10.0
4	10000
5	100000

Km Values used for Ethanol Simulations (Runs)

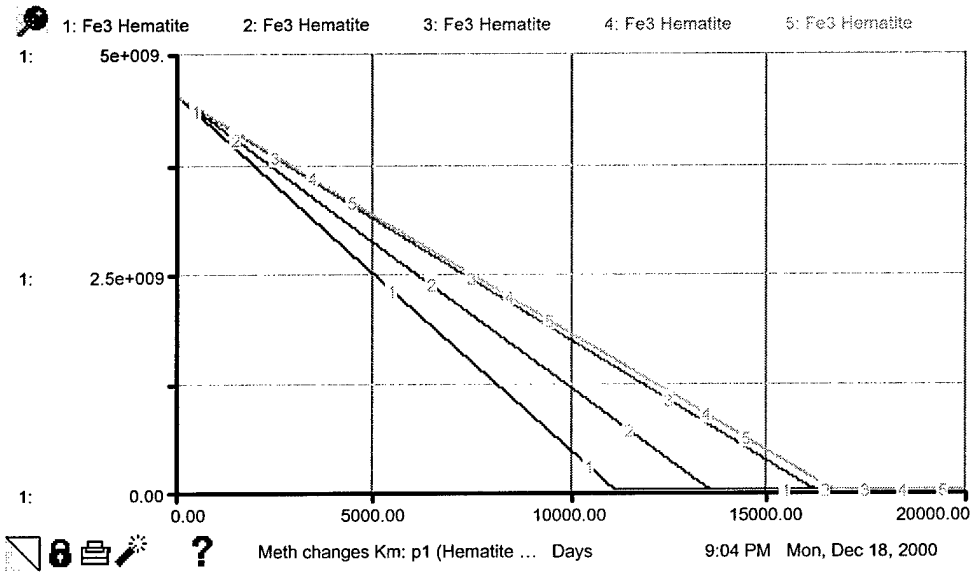

Hematite Behavior – Simulation Set 2, Changing Methanol Km

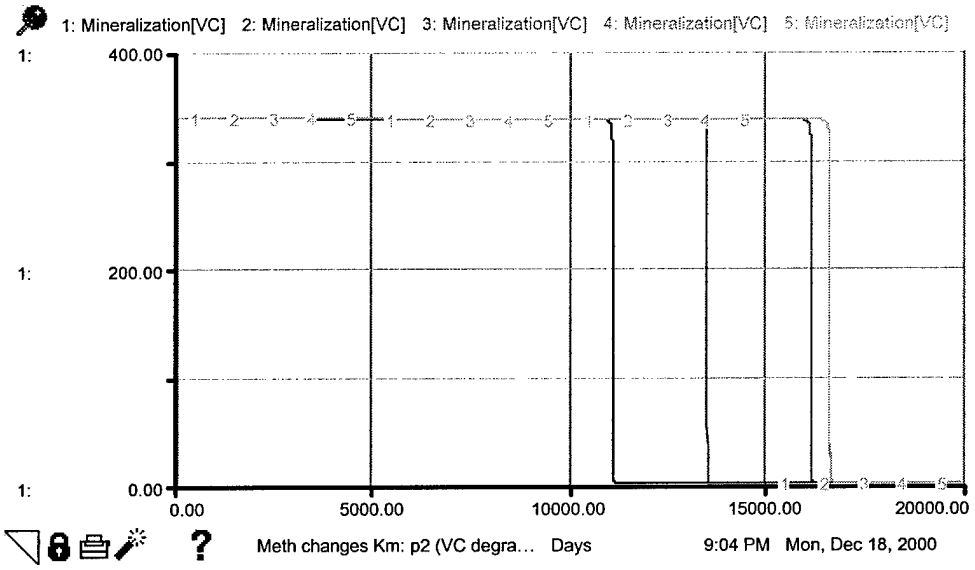

VC Behavior – Simulation Set 2, Changing Methanol Km

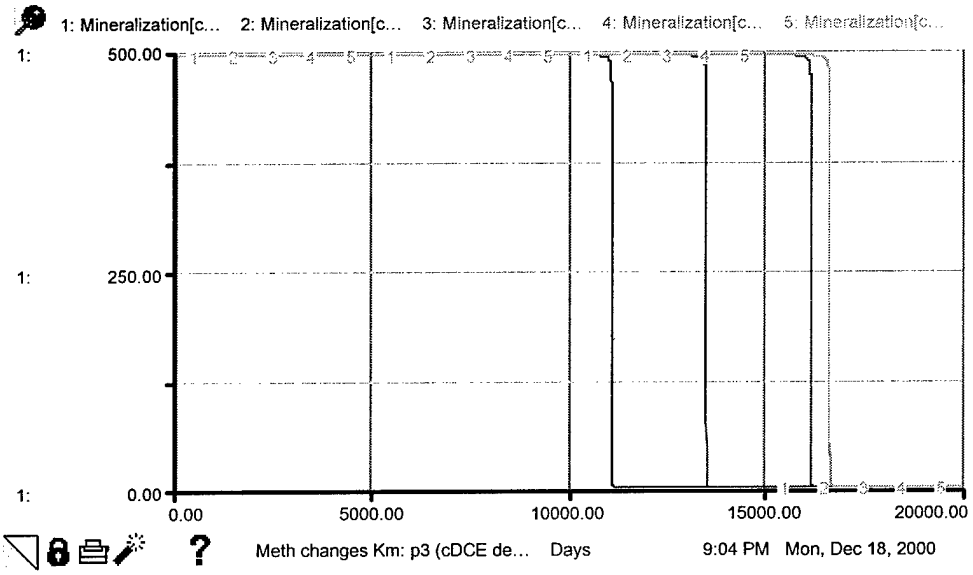

***cis*-DCE Behavior – Simulation Set 2, Changing Methanol Km**

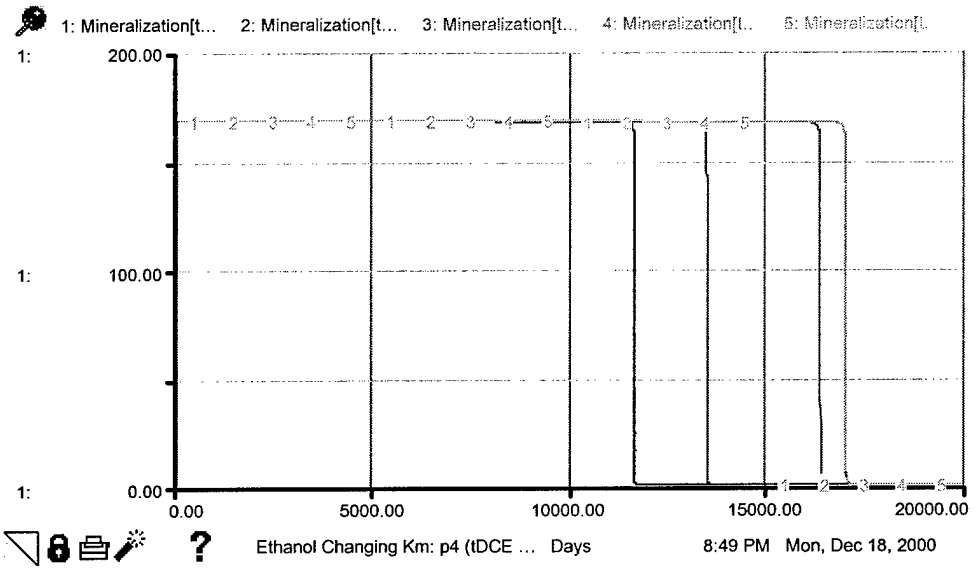

***trans*-DCE Behavior – Simulation Set 2, Changing Methanol Km**

Setup #9	Mon, Dec 18, 2000 9:00 PM
Input Variables	
Run #	Meth Km
1	0.008
2	0.5
3	10.0
4	10000
5	100000

Km Values used for Methanol Simulations (Runs)

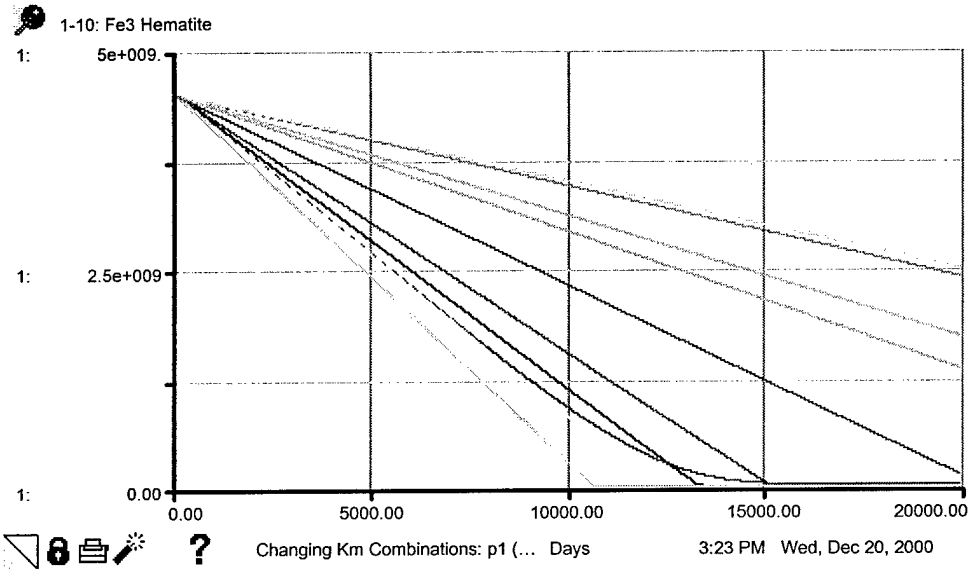

Hematite Behavior – Simulation Set 2, Combination Simulations

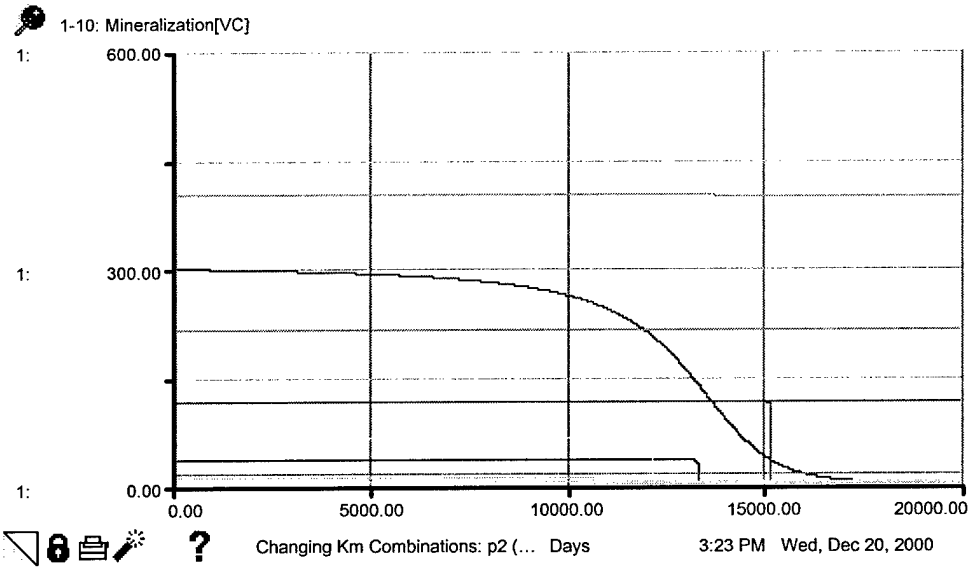

VC Behavior – Simulation Set 2, Combination Simulations

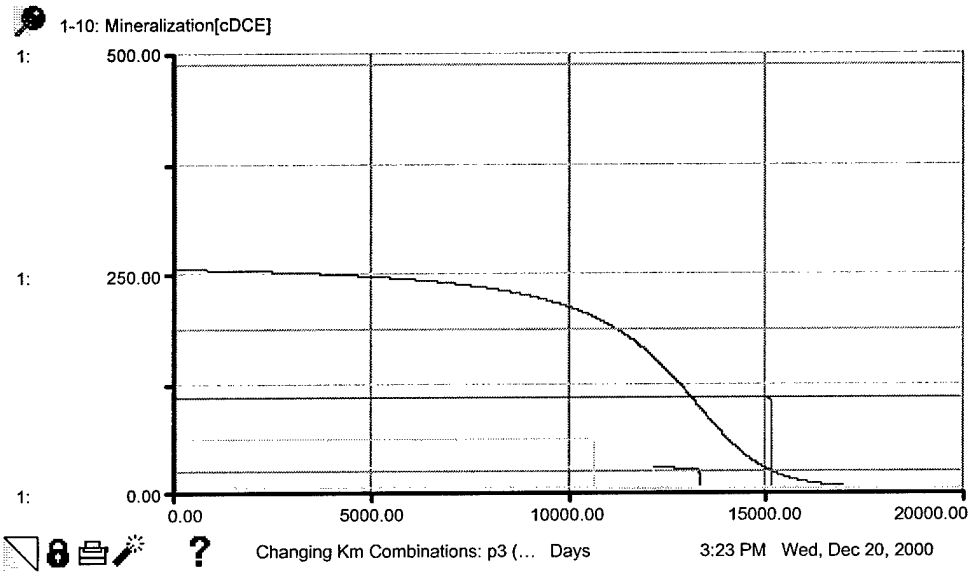

***cis*-DCE Behavior – Simulation Set 2, Combination Simulations**

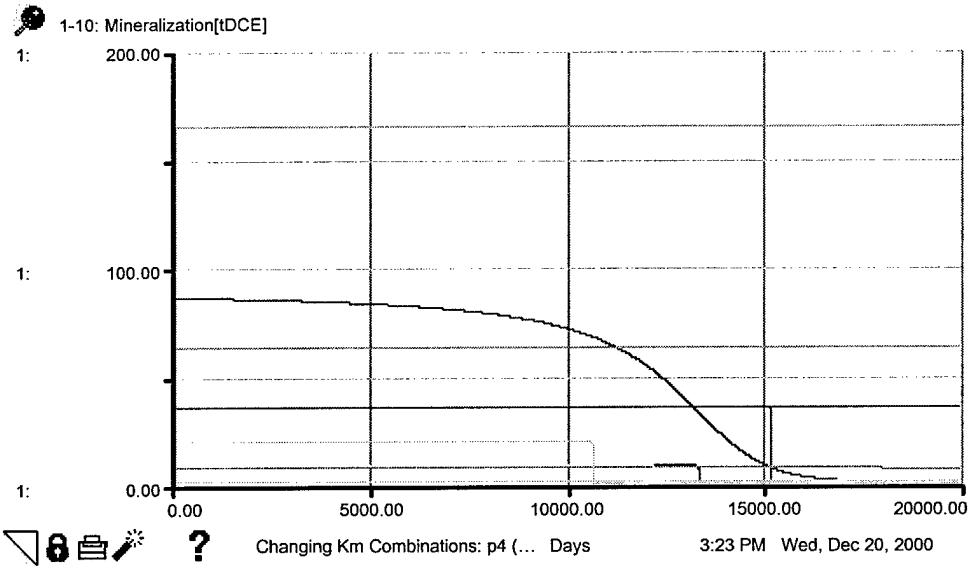

***trans*-DCE Behavior – Simulation Set 2, Combination Simulations**

Input Variables

Run #	Cont Km[VC]	Cont Km[cDCE]	Cont Km[tDCE]
1	2.00	5.00	5.00
2	0.1	0.3	0.3
3	0.5	1.00	1.00
4	5.00	6.00	6.00
5	0.05	0.1	0.1
6	1.00	5.00	5.00
7	10.0	2.00	2.00
8	1000	1200	1200
9	0.5	1.00	1.00
10	0.2	0.5	0.5

Run #	H2 Km	Ace Km	Form Km
1	10.0	5.00	5.00
2	1.50	20.0	15.0
3	0.01	0.5	0.25
4	5.00	100	500
5	100	2000	100
6	25.0	0.01	0.001
7	2.00	1.00	20.0
8	0.5	25.0	100
9	0.001	10000	7500
10	1.00	75.0	20.0

Run #	Prop Km	But Km	Lact Km
1	1.00	1.00	1.00
2	5.00	0.1	200
3	10.0	5.00	10.0
4	50.0	0.05	0.01
5	0.5	20.0	5.00
6	0.1	0.25	0.5
7	2.00	3.00	1.00
8	0.75	1000	50.0
9	100	0.01	0.75
10	1000	20.0	3.00

Run #	Eth Km	Meth Km	Fe Km
1	0.5	0.5	5.00
2	0.01	0.001	1000
3	10.0	5.00	0.1
4	50.0	20.0	50.0
5	2.00	1.00	7.50
6	100	20.0	0.25
7	0.02	0.01	0.5
8	5.00	25.0	20.0
9	10000	2000	0.01
10	3.00	0.25	10.0

Km Values used in 10 Combination Simulations (Runs)

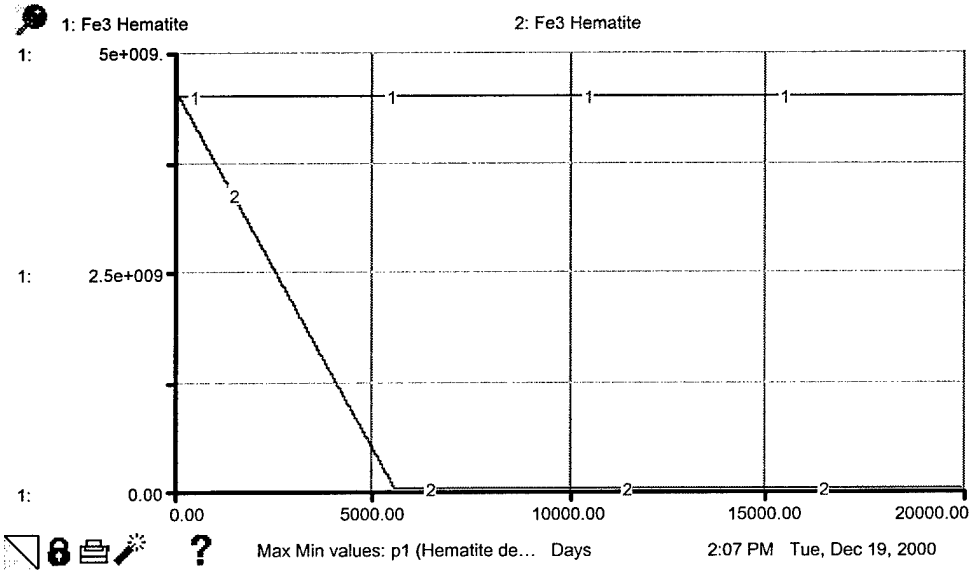

Hematite Behavior – Simulation Set 2, Max/Min Km Values

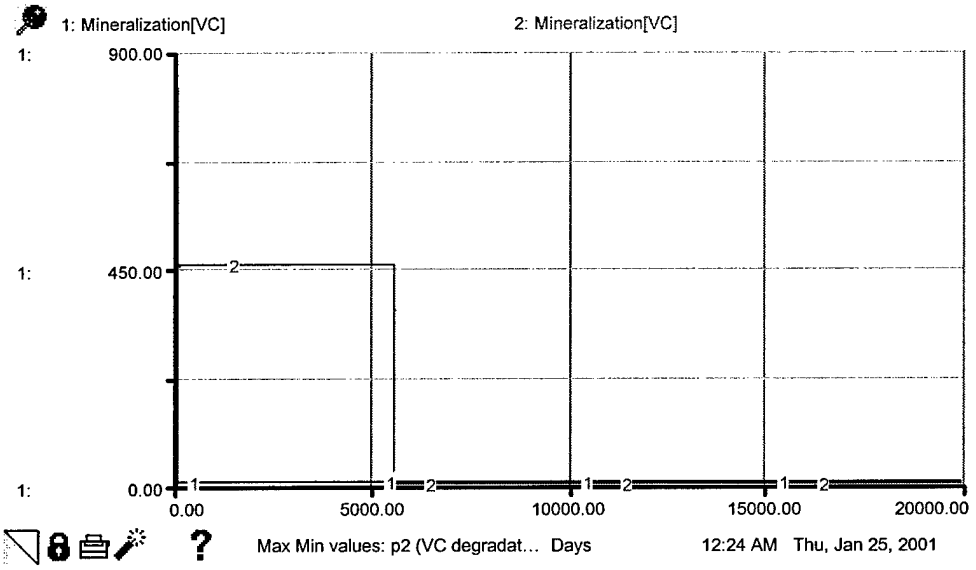

VC Behavior – Simulation Set 2, Max/Min Km Values

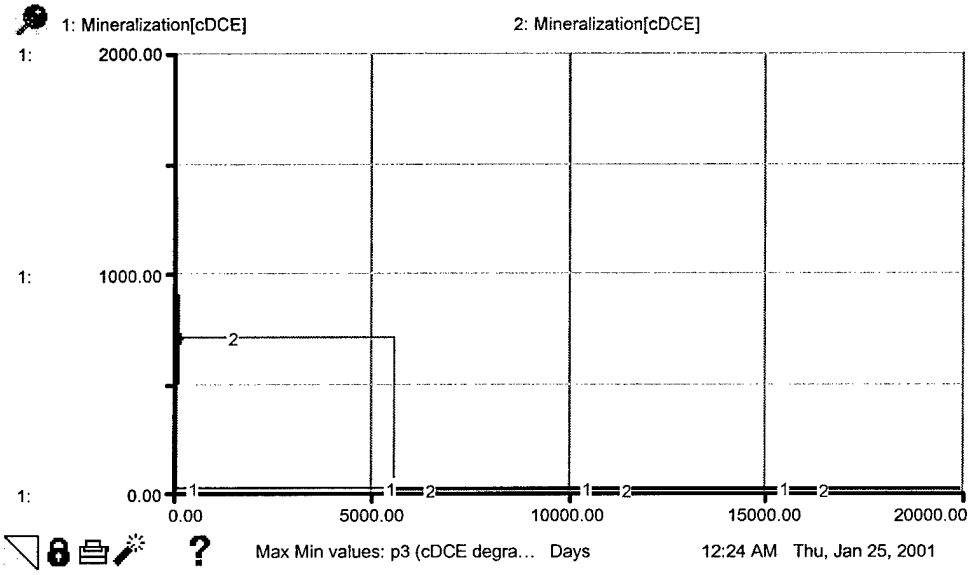

***cis*-DCE Behavior – Simulation Set 2, Max/Min Km Values**

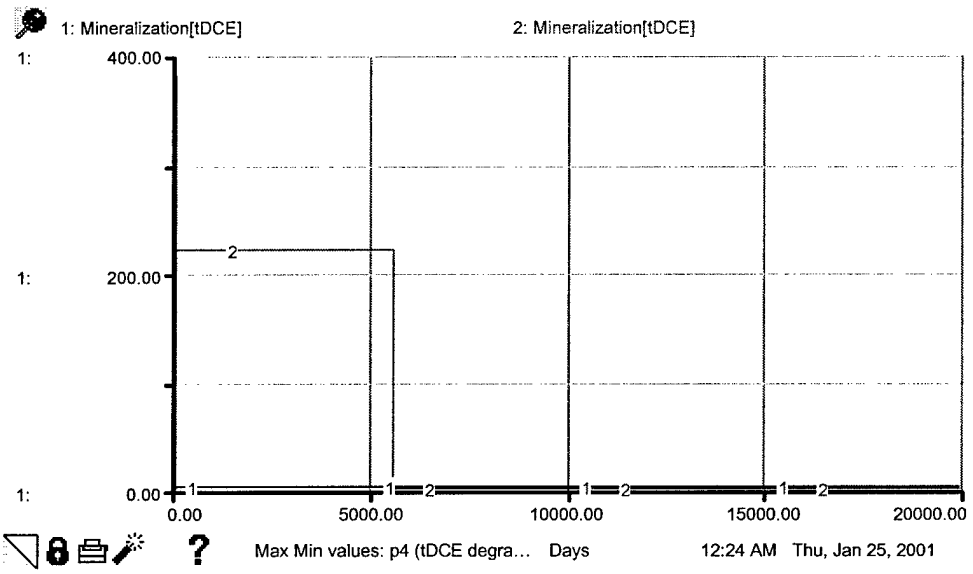

***trans*-DCE Behavior – Simulation Set 2, Max/Min Km Values**

Setup #3			Thu, Jan 25, 2001 12:22 AM
	Input Variables		
Run #	Cont Km[VC]	Cont Km[tDCE]	H2 Km
1	10000	10000	100000
2	0.03	0.04	0.03
Run #	Ace Km	Form Km	Prop Km
1	500000	500000	100000
2	0.0001	0.0001	0.0001
Run #	But Km	Lact Km	Eth Km
1	100000	100000	100000
2	0.0001	0.0001	0.0001
Run #	Meth Km	Fe Km	Cont Km[cDCE]
1	100000	500000	10000
2	0.008	0.0001	0.03

Km Values used for Max/Min Simulations (Runs)

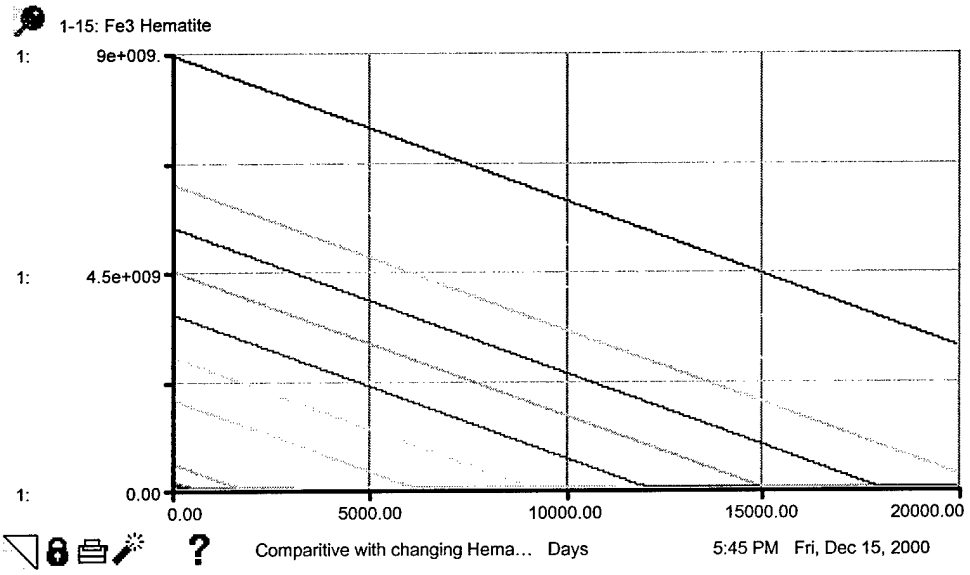

Hematite Behavior – Simulation Set 3, Hematite Changing

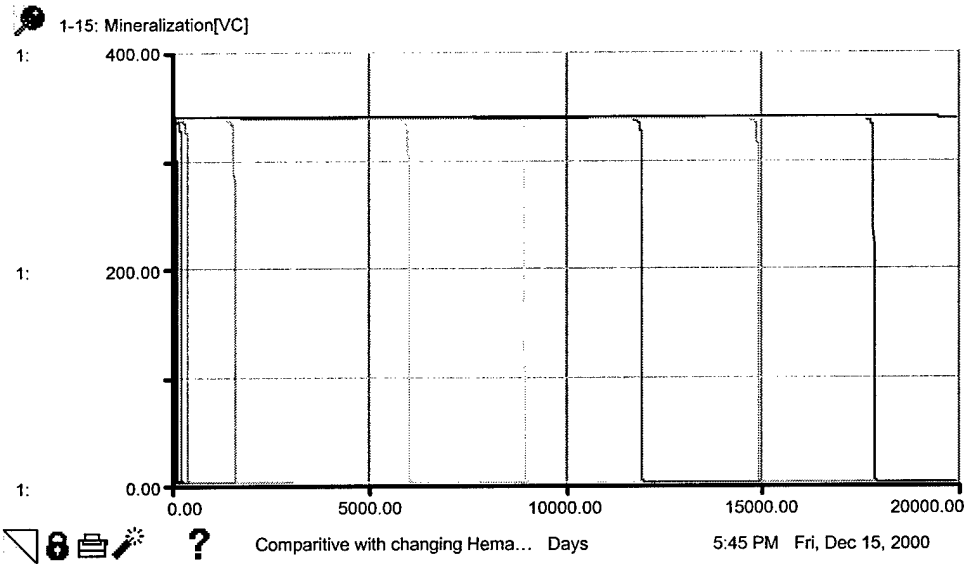

VC Behavior – Simulation Set 3, Hematite Changing

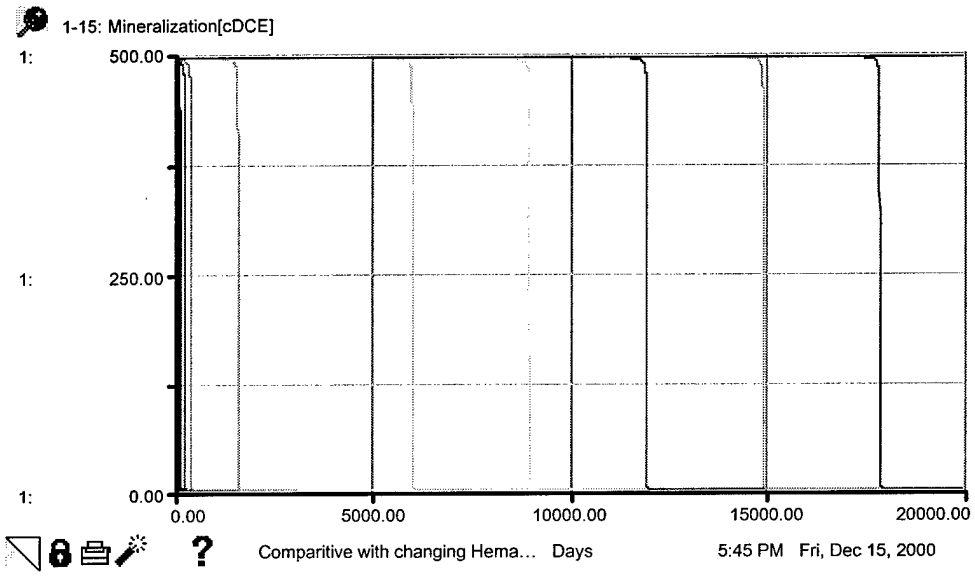

***cis*-DCE Behavior – Simulation Set 3, Hematite Changing**

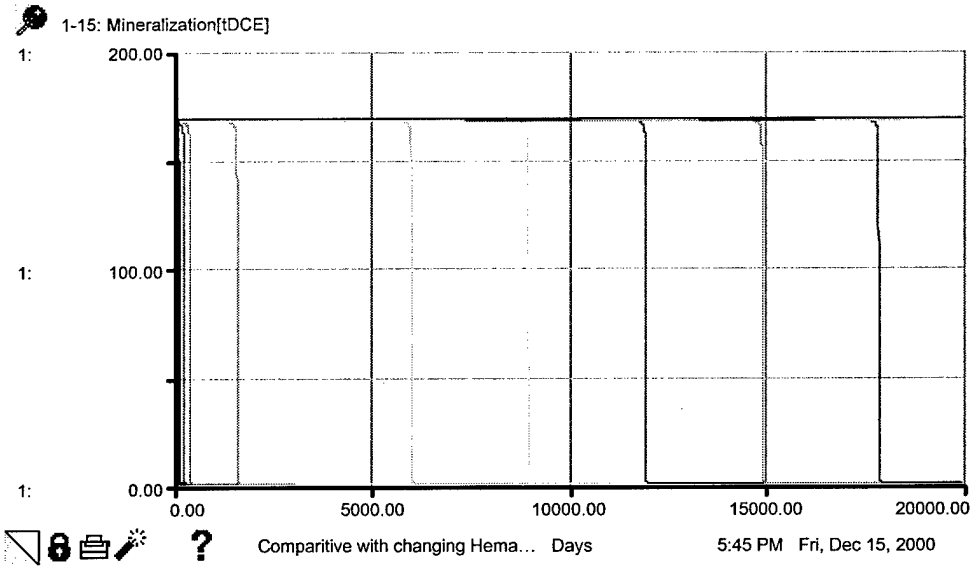

***trans*-DCE Behavior – Simulation Set 3, Hematite Changing**

Setup #1	Fri, Dec 15, 2000 5:32 PM

Input Variables

Run #	Fe3 Hematite
1	891975
2	8.9e+006
3	4.5e+007
4	8.9e+007
5	4.5e+008
6	8.9e+008
7	1.8e+009
8	2.7e+009
9	3.6e+009
10	4.5e+009
11	5.4e+009
12	6.2e+009
13	7.1e+009
14	8e+009
15	8.9e+009

Hematite Values used for Simulations (Runs)

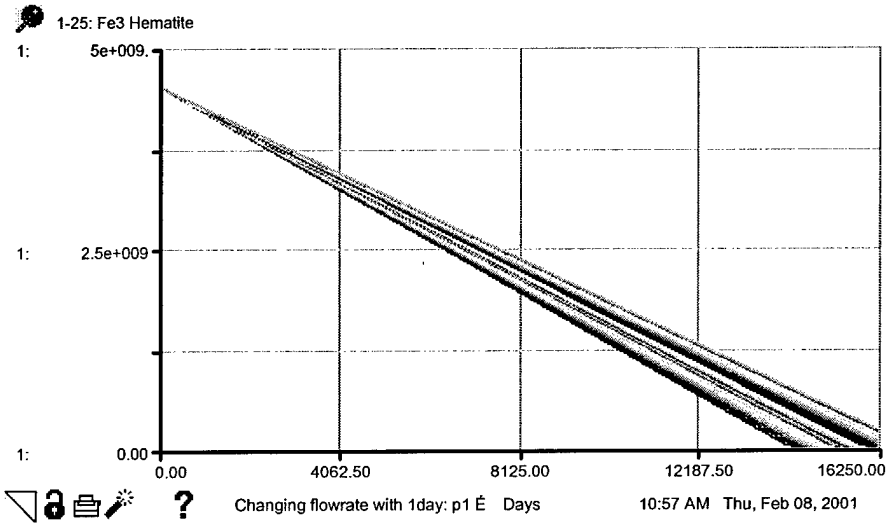

Hematite Behavior – Simulation Set 4, Flow Rate Changing

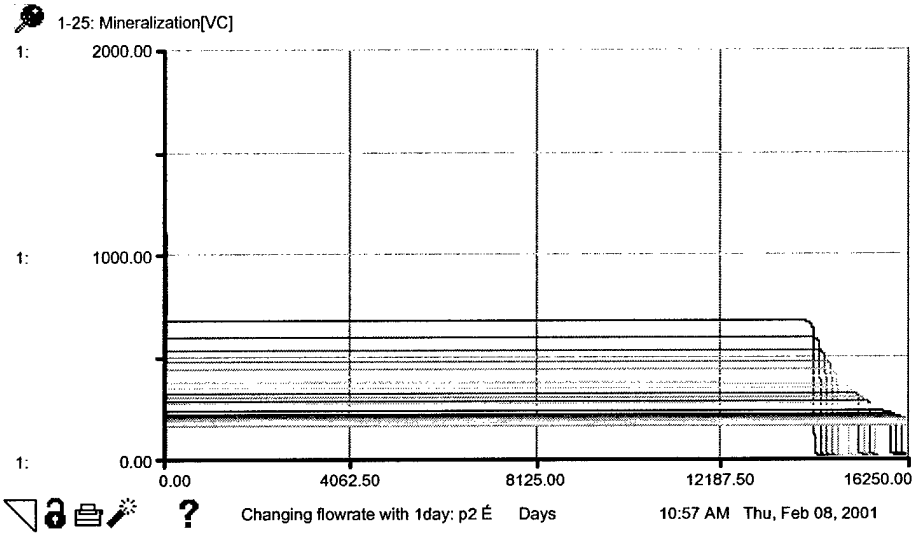

VC Behavior – Simulation Set 4, Flow Rate Changing

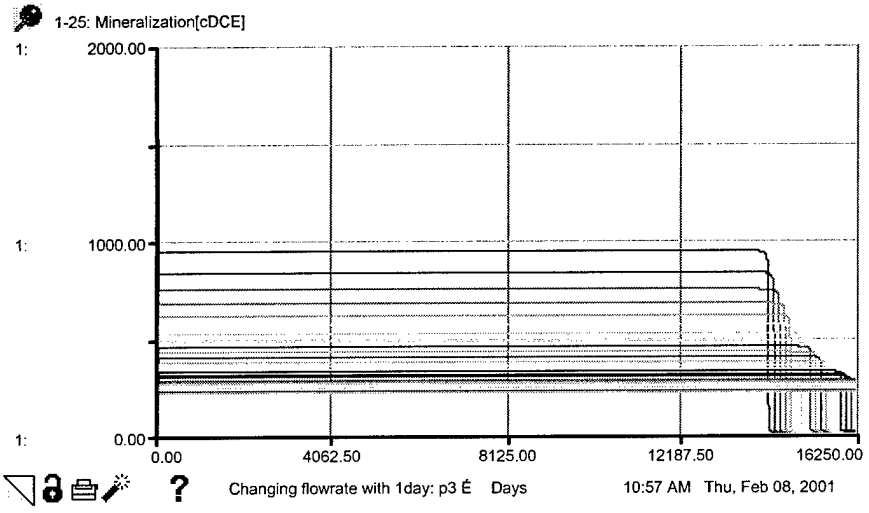

***cis*-DCE Behavior – Simulation Set 4, Flow Rate Changing**

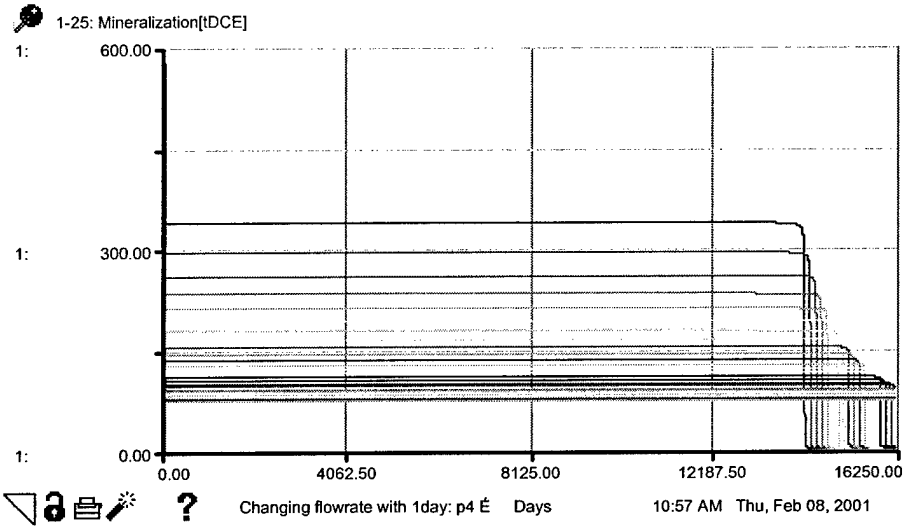

***trans*-DCE Behavior – Simulation Set 4, Flow Rate Changing**

Setup #3	Wed, Feb 07, 2001 9:42 PM

Input Variables

Run #	Flowrate
1	78.5
2	39.3
3	26.2
4	19.6
5	15.7
6	13.1
7	13.1
8	9.82
9	8.73
10	7.85
11	7.14
12	6.55
13	6.04
14	5.61
15	5.24
16	4.91
17	4.62
18	4.36
19	4.13
20	3.93
21	3.74
22	3.57
23	3.42
24	3.27
25	3.14

Flow Values used for Simulations (Runs)

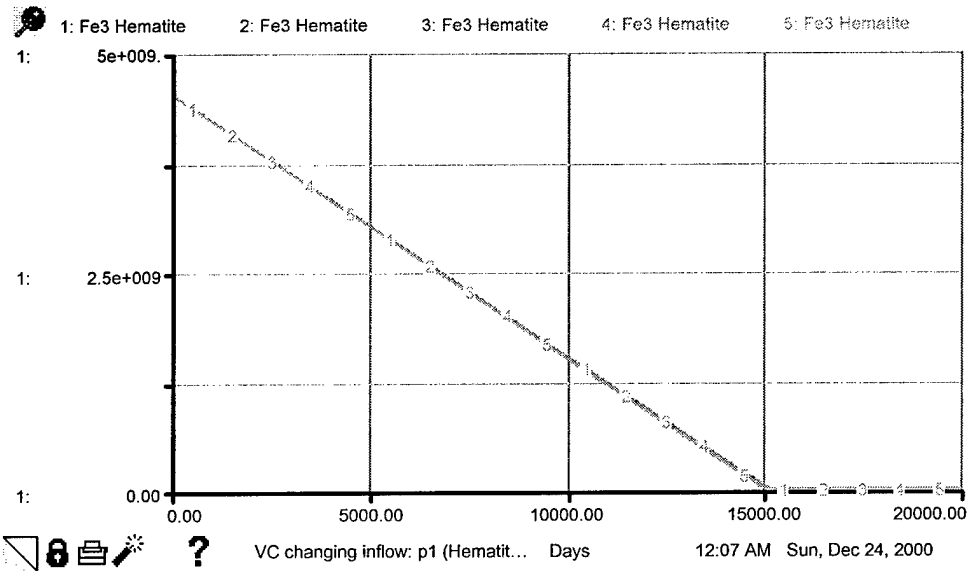

Hematite Behavior – Simulation Set 5, Changing VC Inflow Concentration

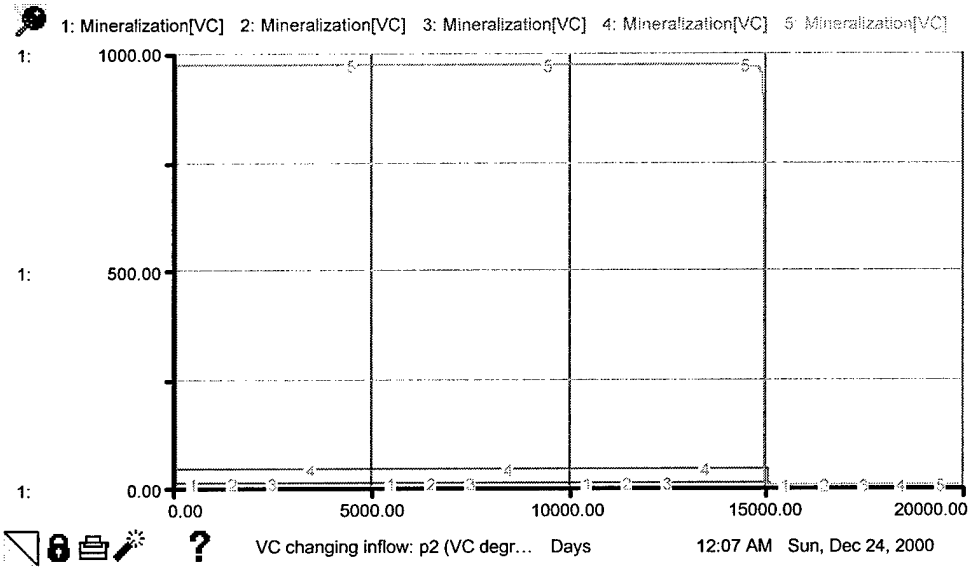

VC Behavior – Simulation Set 5, Changing VC Inflow Concentration

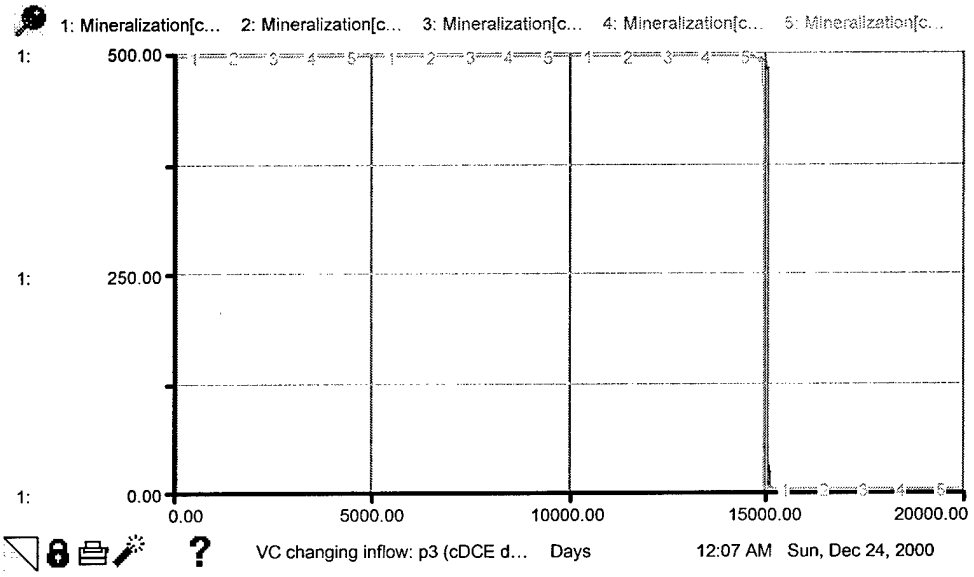

cis-DCE Behavior – Simulation Set 5, Changing VC Inflow Concentration

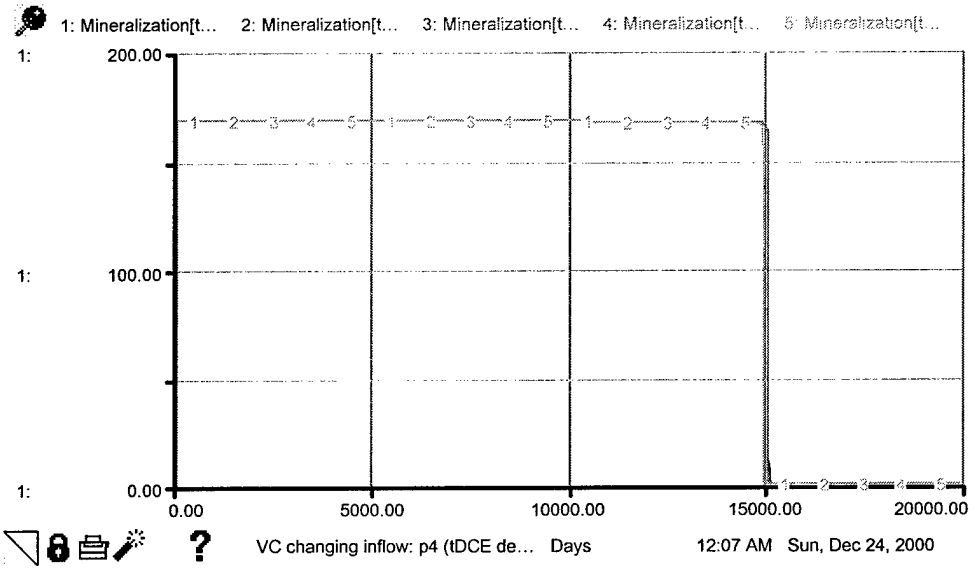

trans-DCE Behavior – Simulation Set 5, Changing VC Inflow Concentration

Setup #1	Sun, Dec 24, 2000 12:03 AM
Input Variables	
Run #	Inflow conc[VC]
1	1e-006
2	1e-005
3	0.0001
4	0.001
5	0.03

Inflow Concentration Values for Changing VC Simulations (Runs)

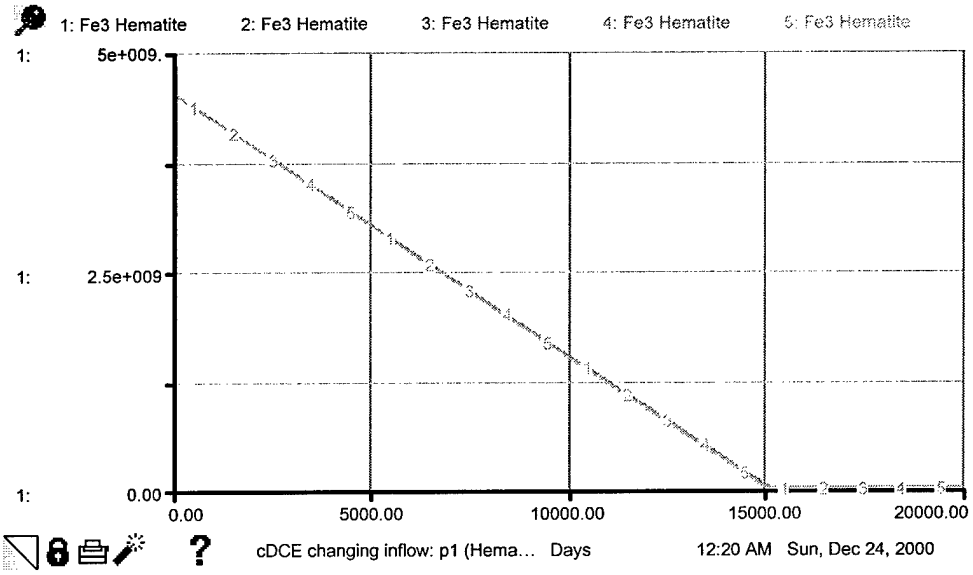

Hematite Behavior – Simulation Set 5, Changing *cis*-DCE Inflow Concentration

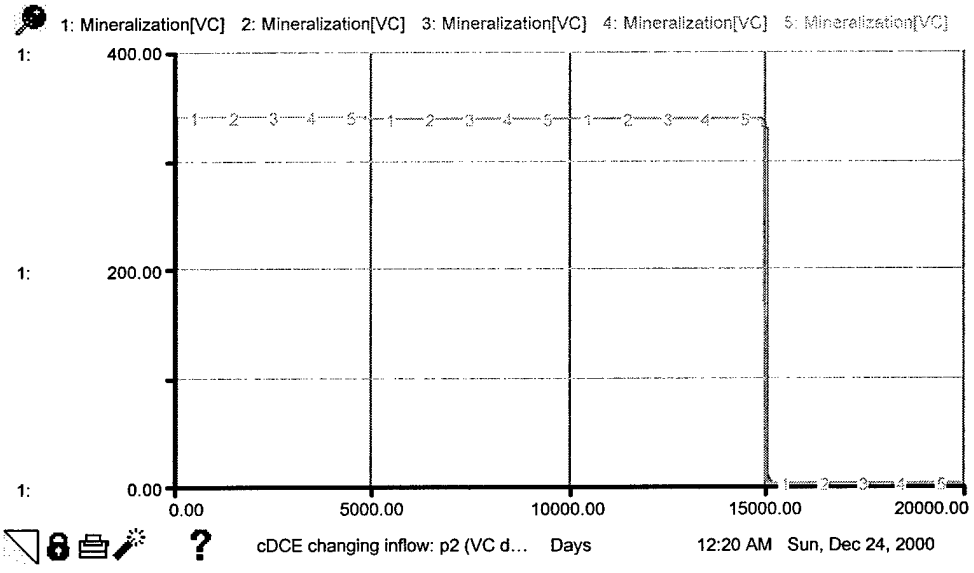

VC Behavior – Simulation Set 5, Changing *cis*-DCE Inflow Concentration

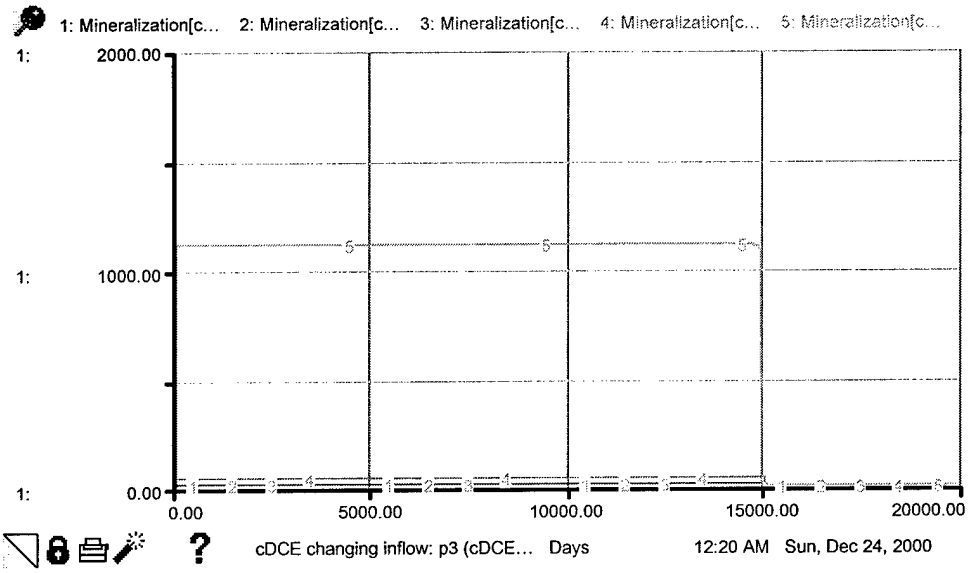

***cis*-DCE Behavior – Simulation Set 5, Changing *cis*-DCE Inflow Concentration**

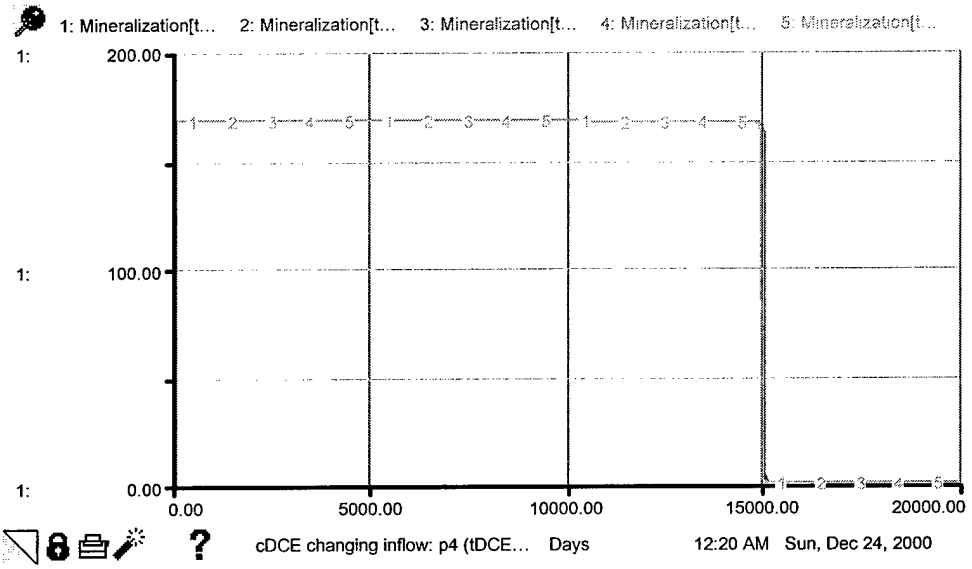

***trans*-DCE Behavior – Simulation Set 5, Changing *cis*-DCE Inflow Concentration**

Setup #2	Sun, Dec 24, 2000 12:16 AM
Input Variables	
Run #	Inflow conc[cDCE]
1	1e-006
2	1e-005
3	0.0001
4	0.001
5	0.035

Inflow Concentration Values for Changing *cis*-DCE Simulations (Runs)

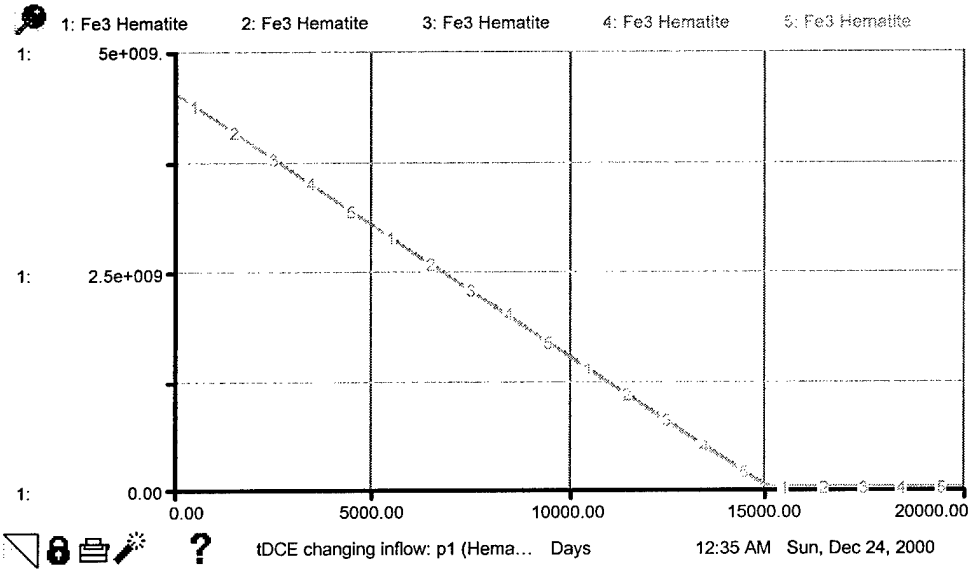

Hematite Behavior – Simulation Set 5, Changing *trans*-DCE Inflow Concentration

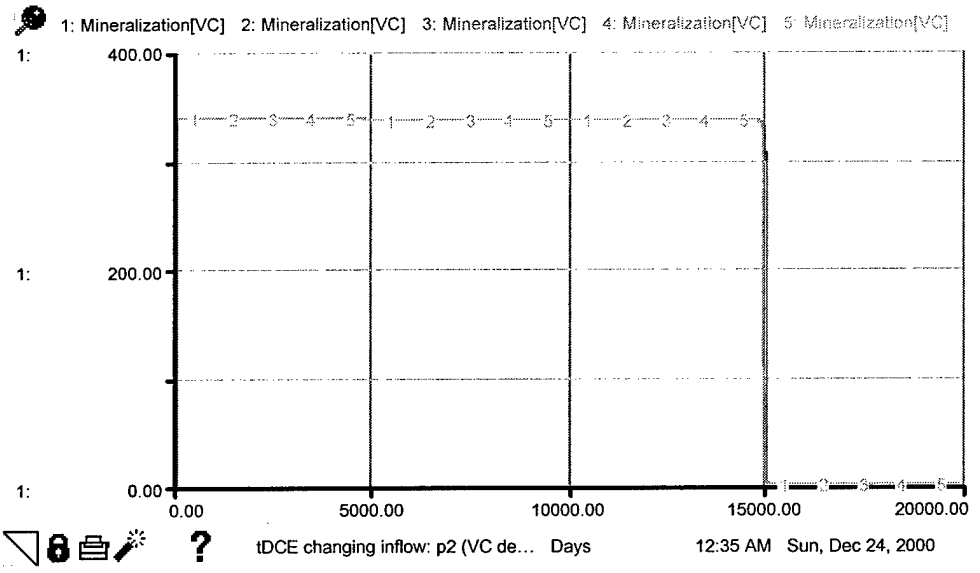

VC Behavior – Simulation Set 5, Changing *trans*-DCE Inflow Concentration

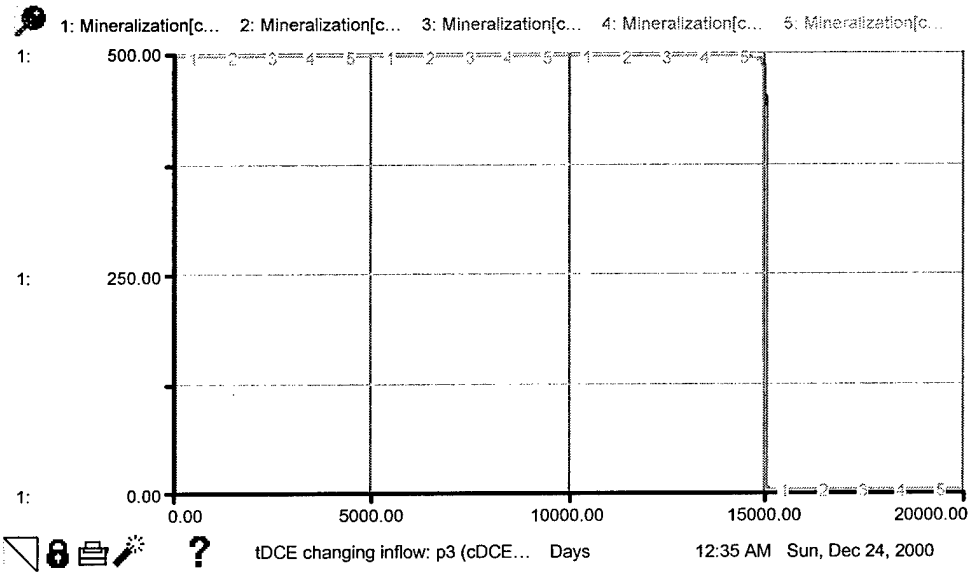

***cis*-DCE Behavior – Simulation Set 5, Changing *trans*-DCE Inflow Concentration**

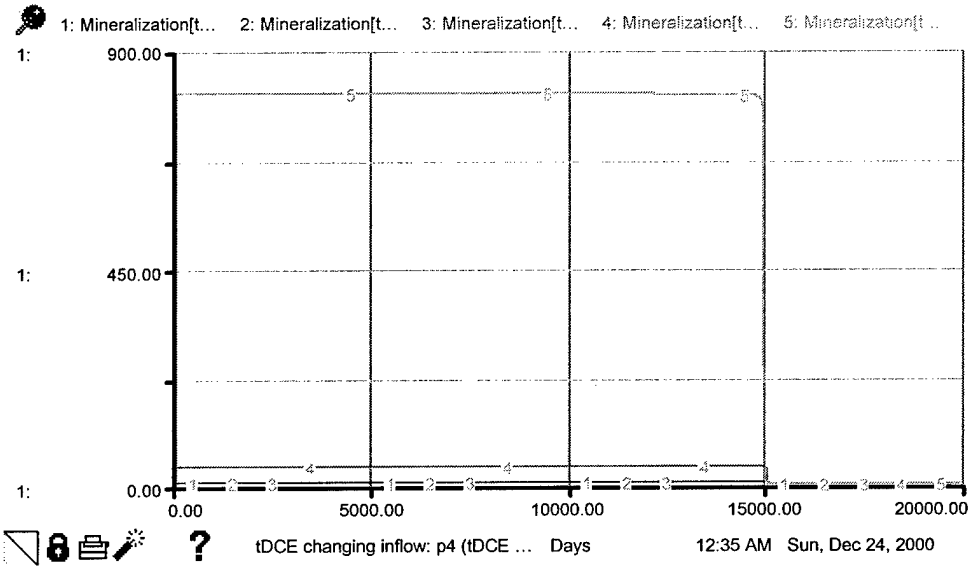

***trans*-DCE Behavior – Simulation Set 5, Changing *trans*-DCE Inflow Concentration**

Setup #3	Sun, Dec 24, 2000 12:32 AM
Input Variables	
Run #	Inflow conc[tDCE]
1	1e-006
2	1e-005
3	0.0001
4	0.001
5	0.025

Inflow Concentration Values for Changing *trans*-DCE Simulations (Runs)

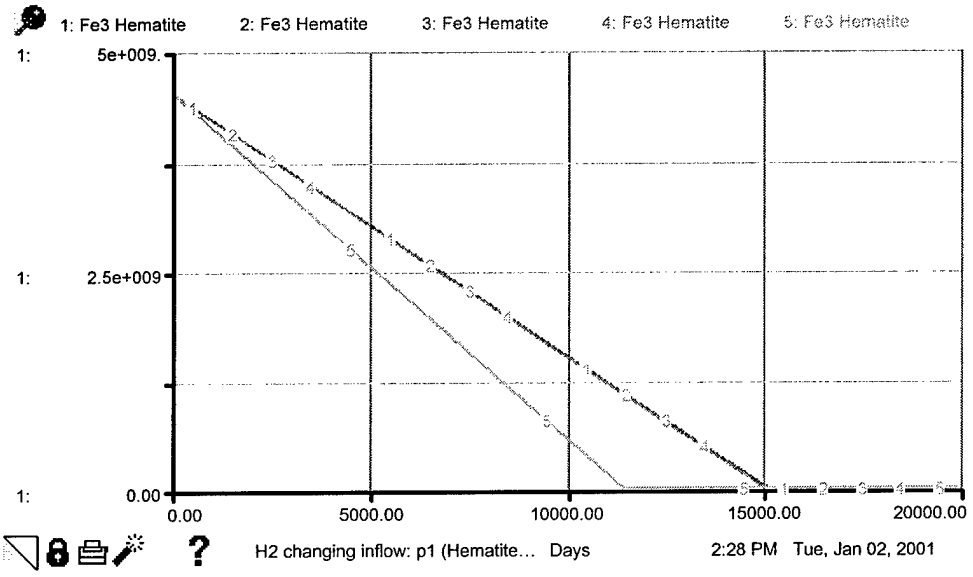

Hematite Behavior – Simulation Set 5, Changing H_2 Inflow Concentration

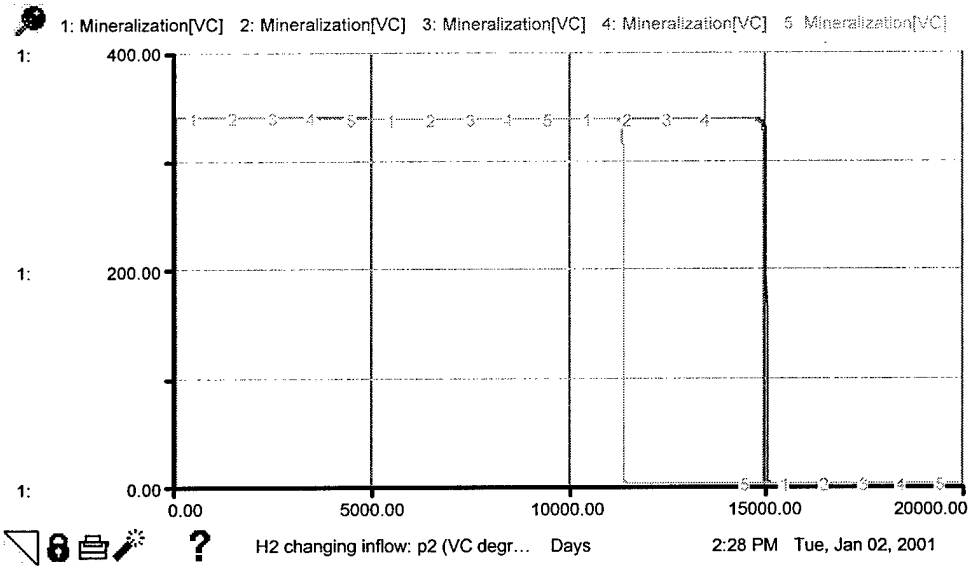

VC Behavior – Simulation Set 5, Changing H_2 Inflow Concentration

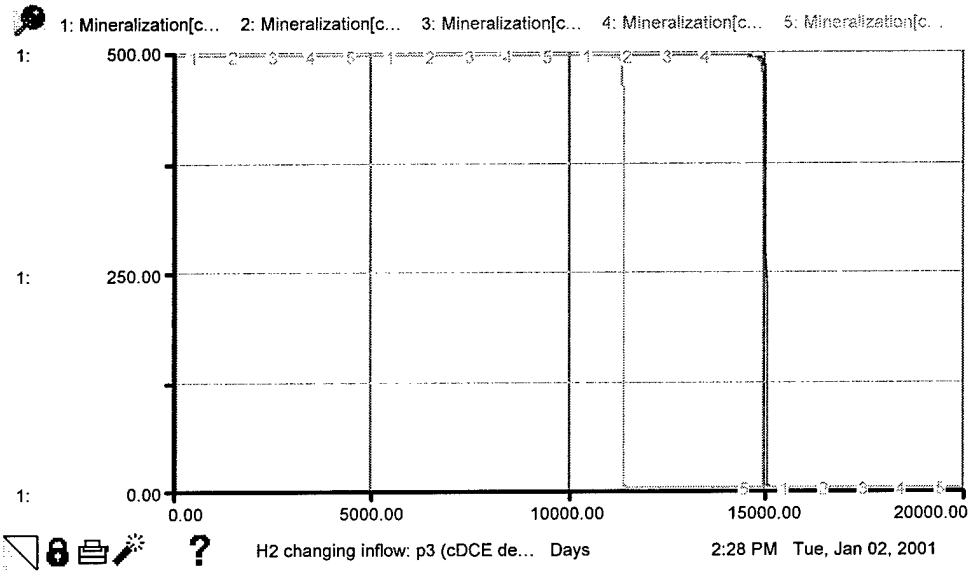

***cis*-DCE Behavior – Simulation Set 5, Changing H_2 Inflow Concentration**

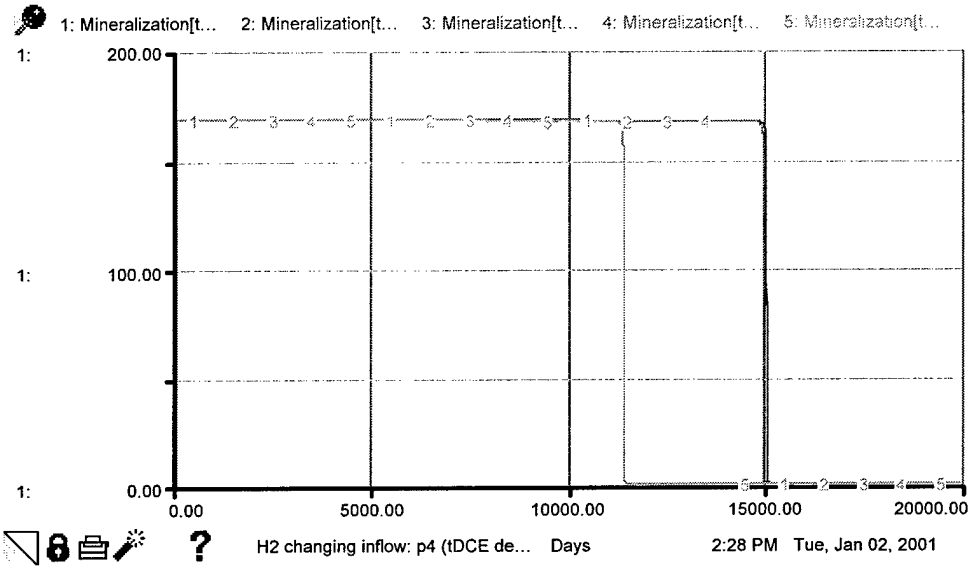

***trans*-DCE Behavior – Simulation Set 5, Changing H_2 Inflow Concentration**

Setup #6	Tue, Jan 02, 2001 2:25 PM
Input Variables	
Run #	Inflow conc H2
1	1e-011
2	1e-009
3	1e-005
4	0.01
5	1.00

Inflow Concentration Values for Changing H_2 Simulations (Runs)

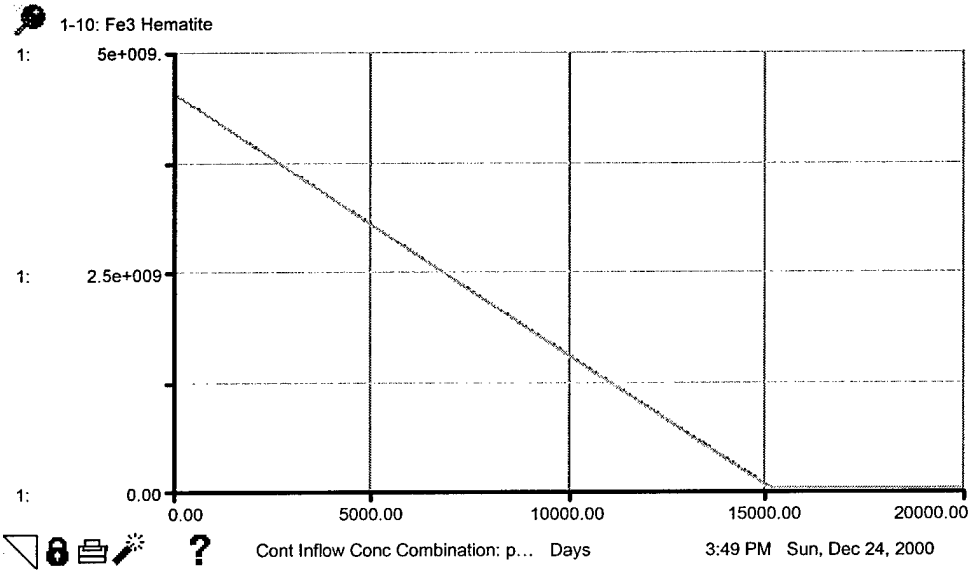

Hematite Behavior – Simulation Set 5, Combination Values Contaminants

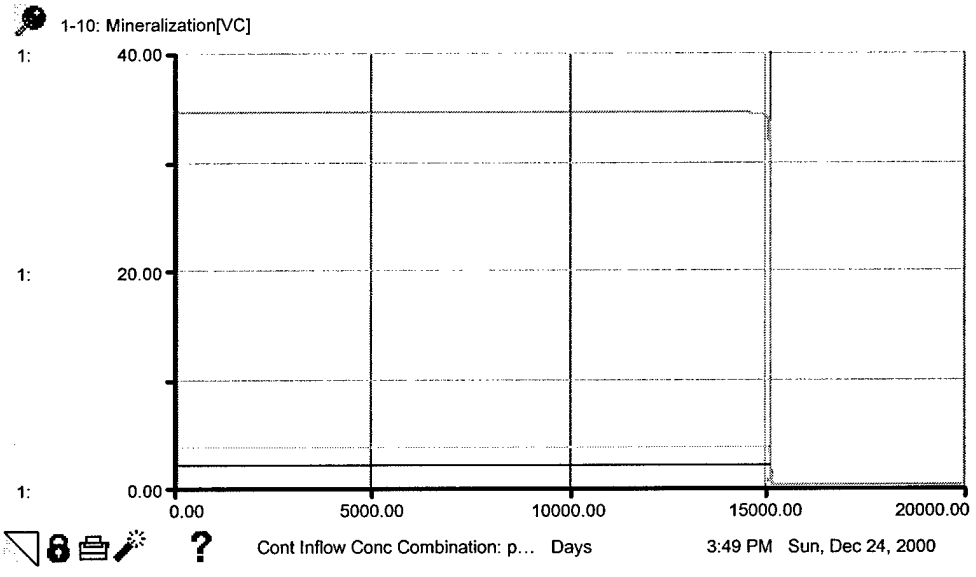

VC Behavior – Simulation Set 5, Combination Values Contaminants

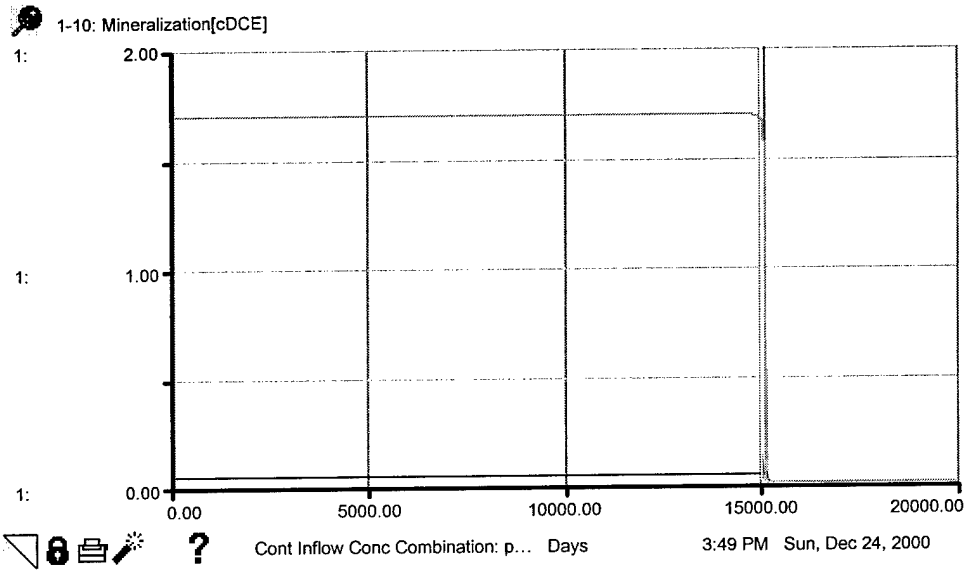

***cis*-DCE Behavior – Simulation Set 5, Combination Values Contaminants**

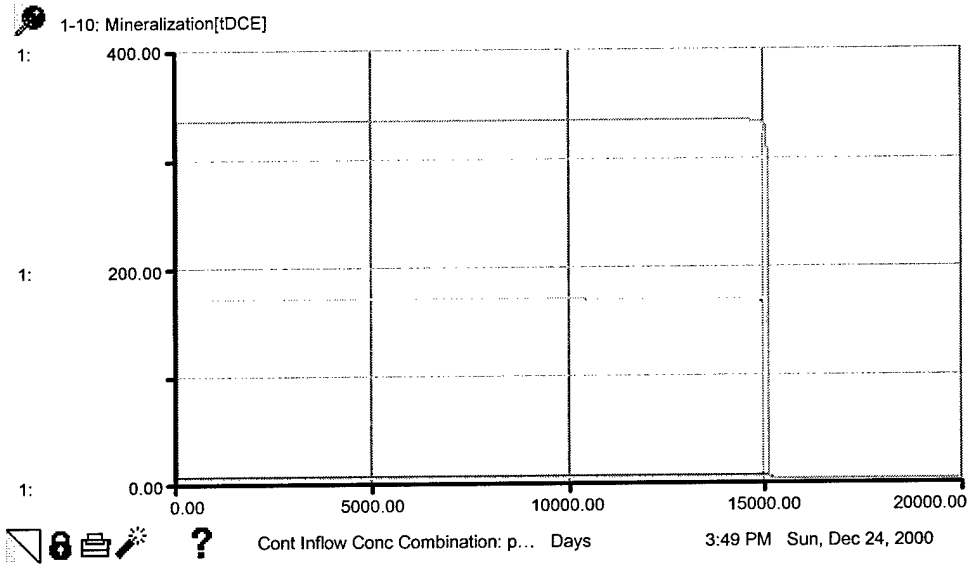

***trans*-DCE Behavior – Simulation Set 5, Combination Values Contaminants**

Setup #5			Sun, Dec 24, 2000 3:32 PM
	Input Variables		
Run #	Inflow conc[VC]	Inflow conc[cDCE]	Inflow conc[tDCE]
1	0.0001	1e-006	1e-005
2	0.01	0.0001	1e-005
3	0.005	0.01	5e-005
4	0.02	0.005	0.005
5	0.001	0.0005	5e-005
6	0.02	0.001	0.01
7	5e-005	0.005	5e-005
8	0.0001	0.01	0.005
9	5e-005	0.005	0.0001
10	0.001	5e-005	0.01

Inflow Concentration Values for 10 Combination Simulations (Runs)

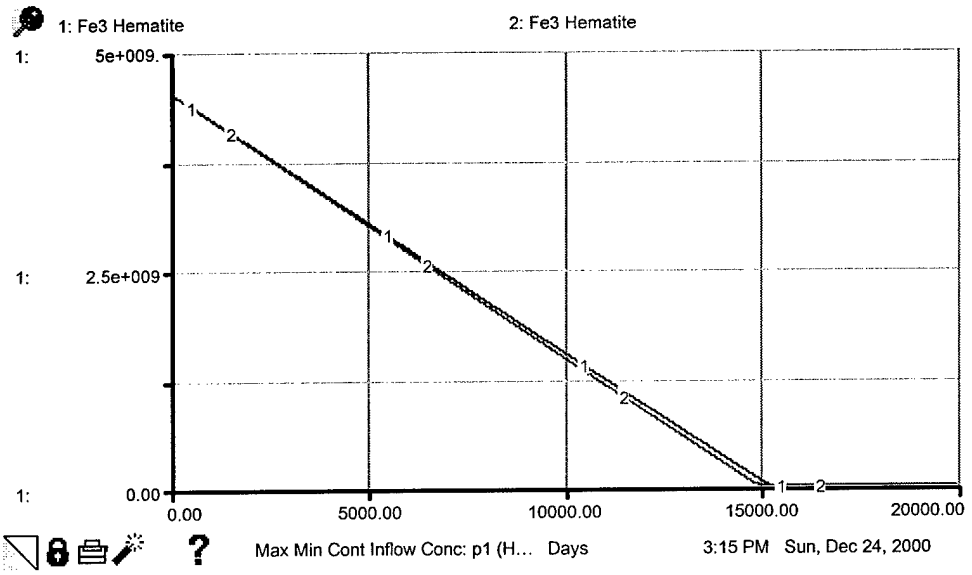

Hematite Behavior – Simulation Set 5, Max/Min Inflow Concentrations for Contaminants

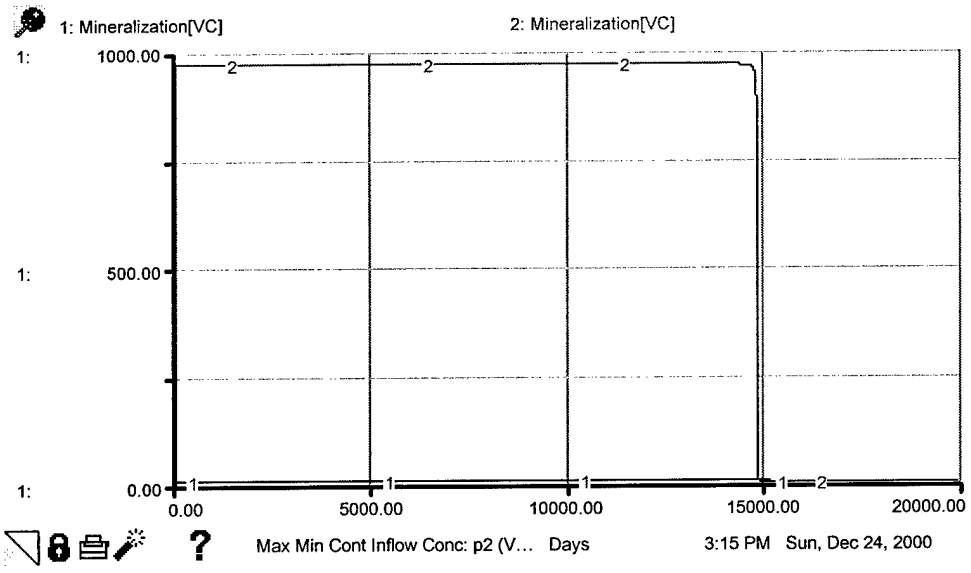

VC Behavior – Simulation Set 5, Max/Min Inflow Concentrations for Contaminants

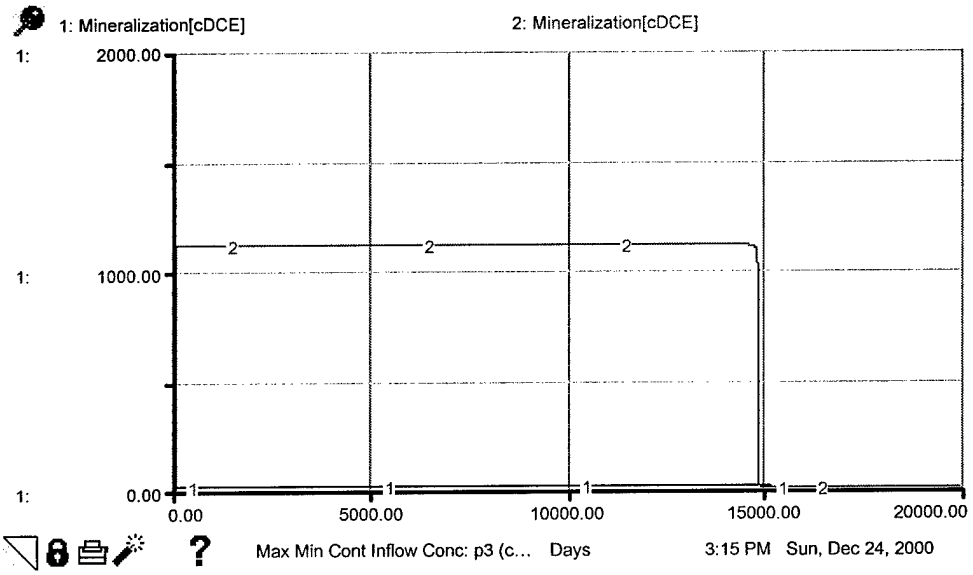

***cis*-DCE Behavior – Simulation Set 5, Max/Min Inflow Concentrations for Contaminants**

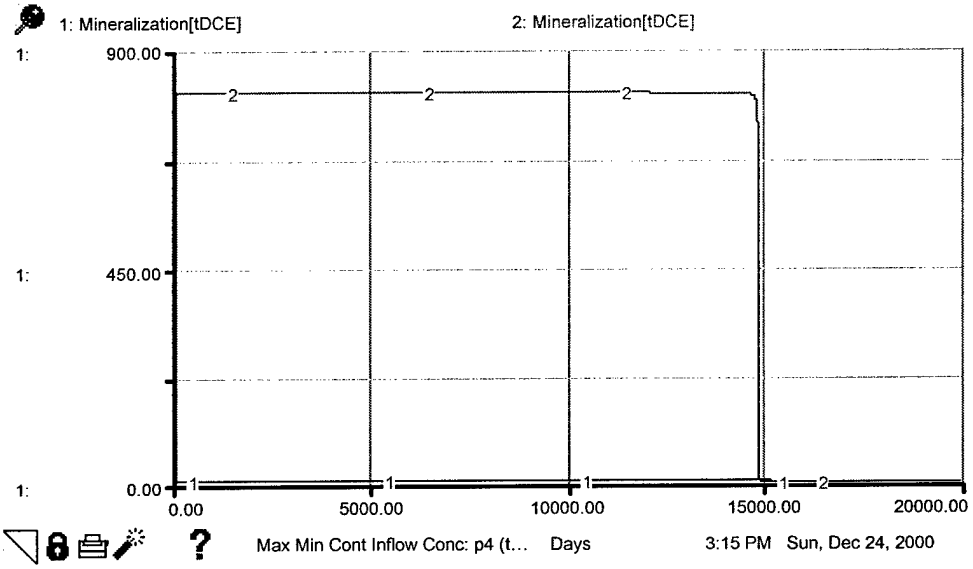

***trans*-DCE Behavior – Simulation Set 5, Max/Min Inflow Concentrations for Contaminants**

Setup #4			Sun, Dec 24, 2000 3:14 PM
	Input Variables		
Run #	Inflow conc[VC]	Inflow conc[cDCE]	Inflow conc[tDCE]
1	1e-006	1e-006	1e-006
2	0.03	0.035	0.025

Inflow Contaminant Concentration Values for Max/Min Simulations (Runs)

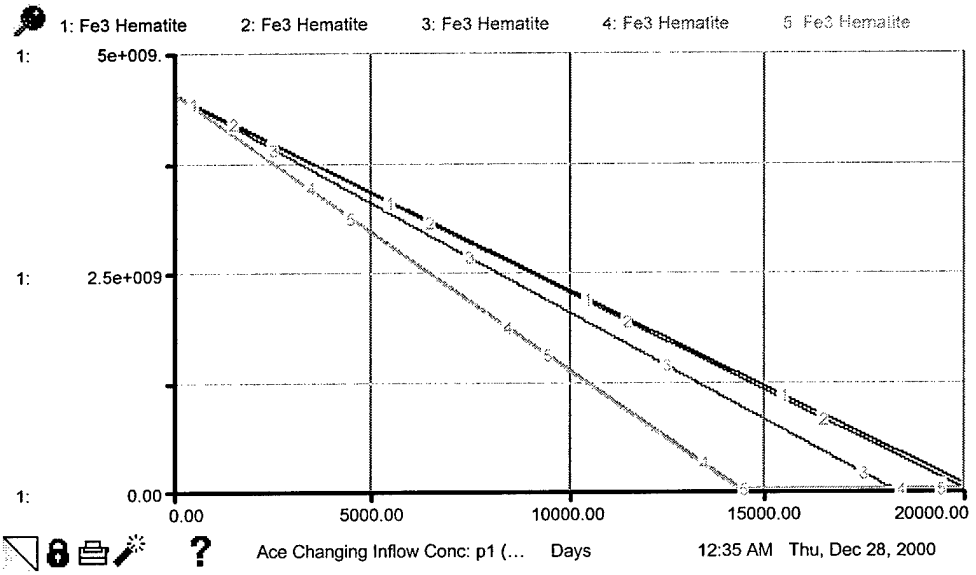

Hematite Behavior – Simulation Set 6, Acetic Acid Inflow Concentration Changing

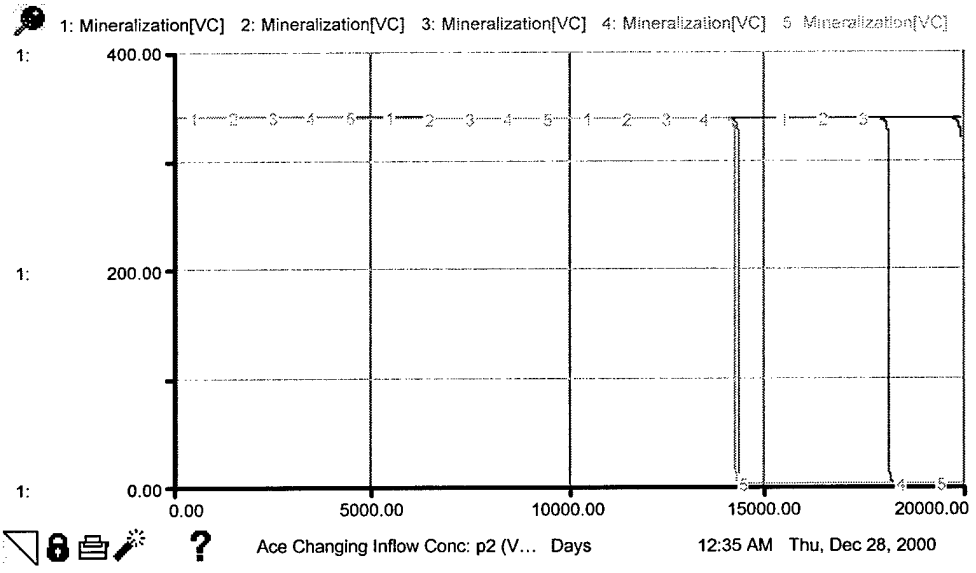

VC Behavior – Simulation Set 6, Acetic Acid Inflow Concentration Changing

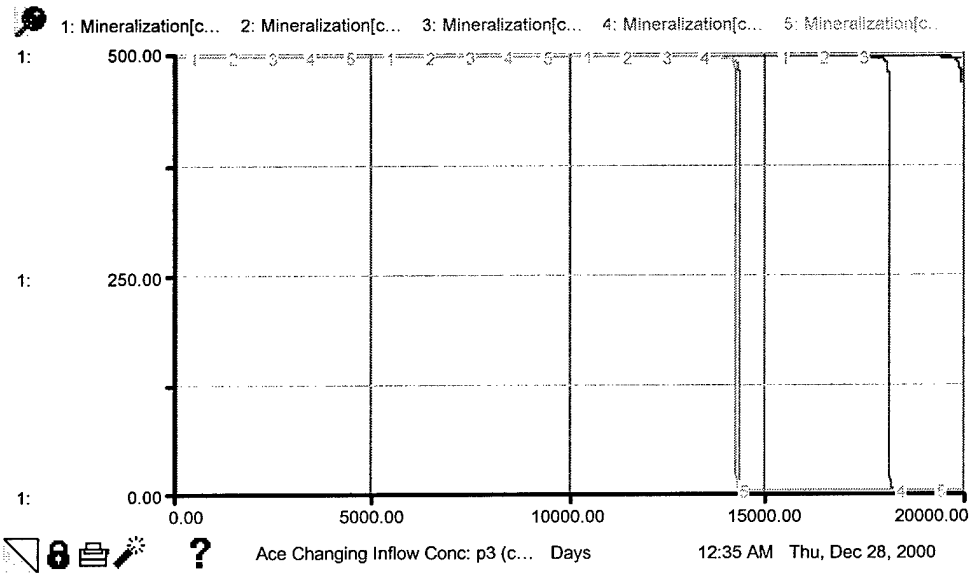

***cis*-DCE Behavior – Simulation Set 6, Acetic Acid Inflow Concentration Changing**

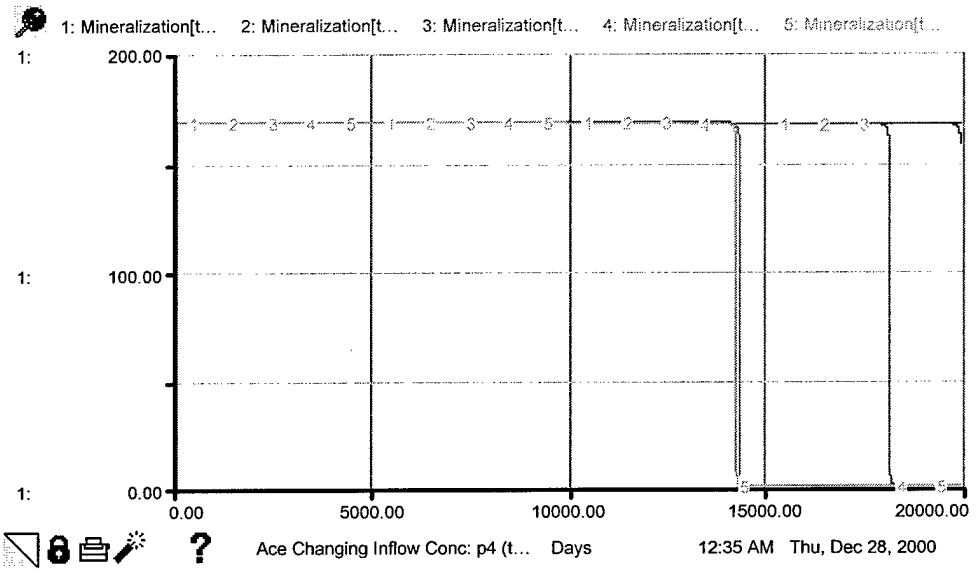

***trans*-DCE Behavior – Simulation Set 6, Acetic Acid Inflow Concentration Changing**

Setup #1	Thu, Dec 28, 2000 12:33 AM
Input Variables	
Run #	Inflow con 5
1	0.01
2	0.1
3	1.00
4	50.0
5	100

Inflow Concentration Values for Changing Acetic Acid Simulations (Runs)

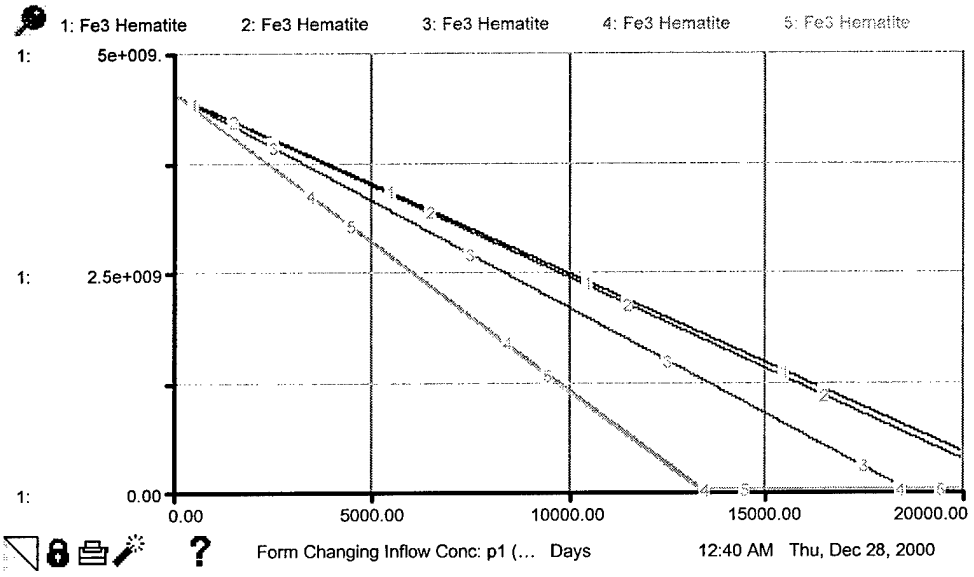

Hematite Behavior – Simulation Set 6, Formic Acid Inflow Concentration Changing

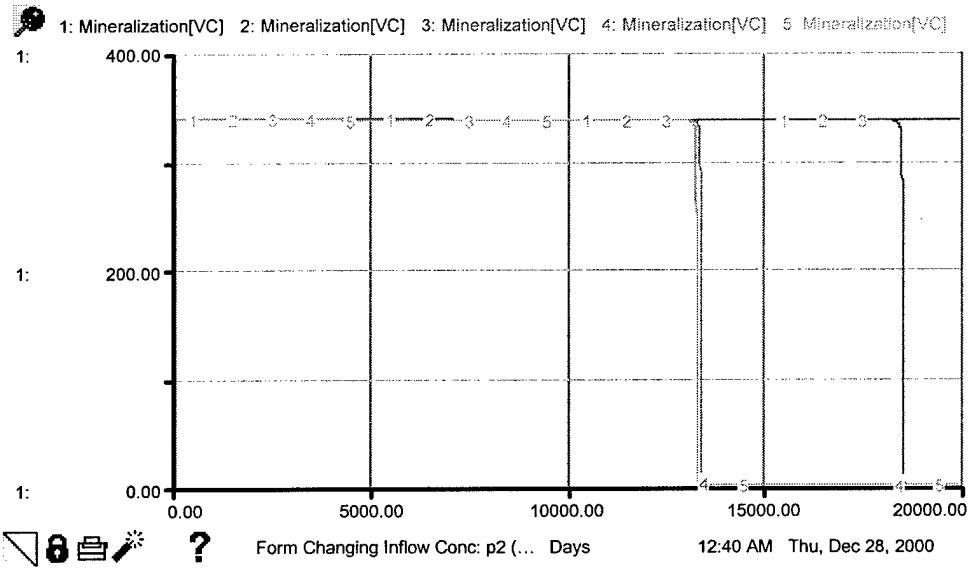

VC Behavior – Simulation Set 6, Formic Acid Inflow Concentration Changing

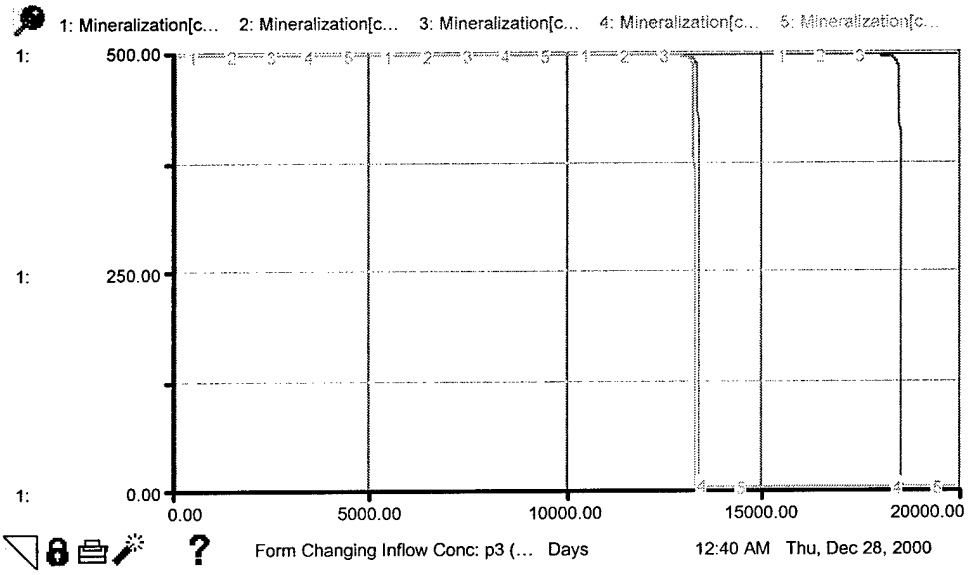

***cis*-DCE Behavior – Simulation Set 6, Formic Acid Inflow Concentration Changing**

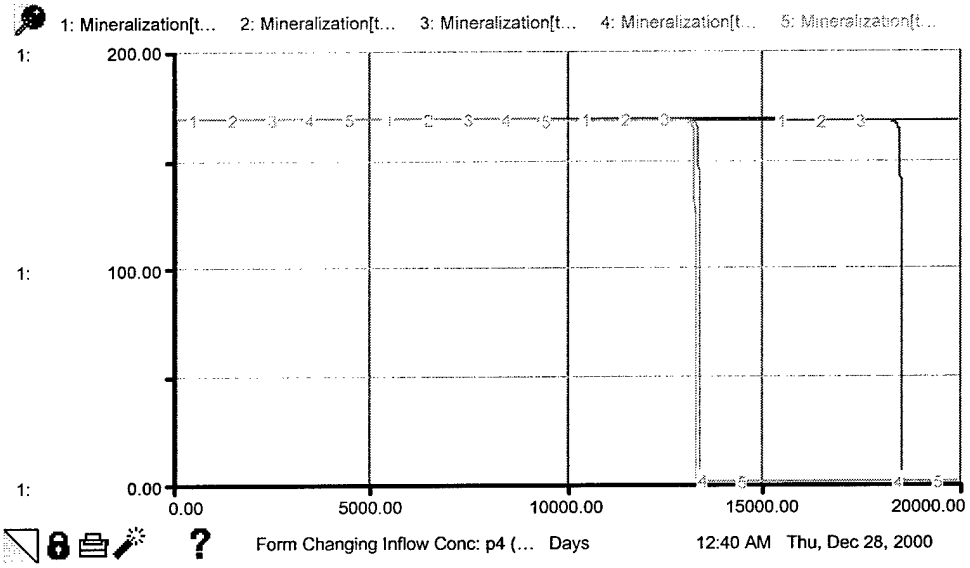

***trans*-DCE Behavior – Simulation Set 6, Formic Acid Inflow Concentration Changing**

Setup #2	Thu, Dec 28, 2000 12:38 AM
Input Variables	
Run #	Inflow con 3
1	0.01
2	0.1
3	1.00
4	50.0
5	100

Inflow Concentration Values for Changing Formic Acid Simulations (Runs)

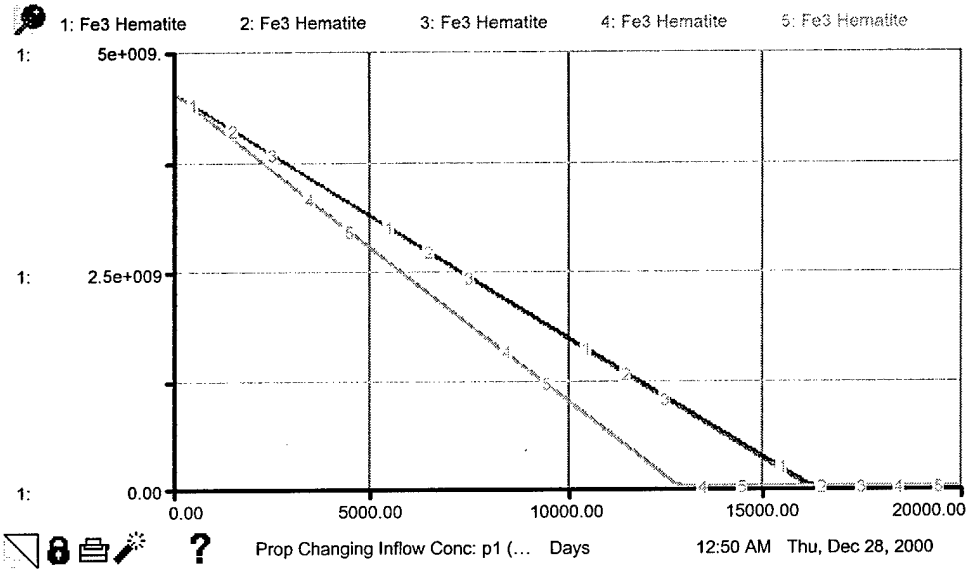

Hematite Behavior – Simulation Set 6, Propionic Acid Inflow Concentration Changing

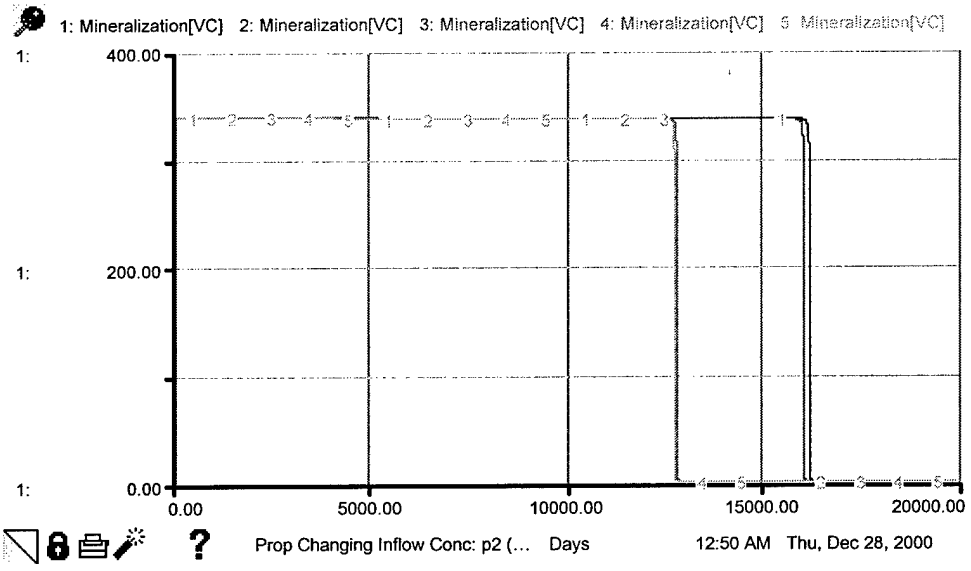

VC Behavior – Simulation Set 6, Propionic Acid Inflow Concentration Changing

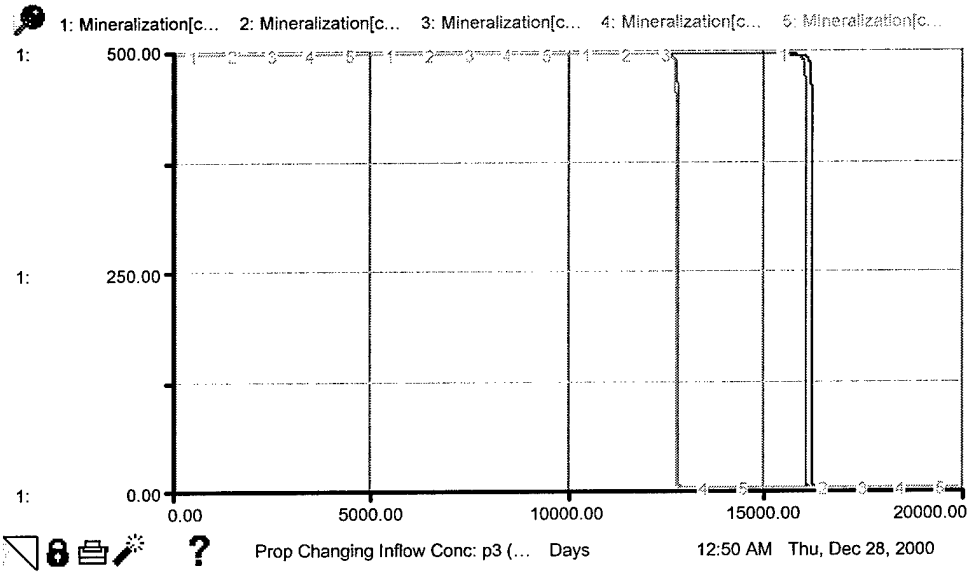

***cis*-DCE Behavior – Simulation Set 6, Propionic Acid Inflow Concentration Changing**

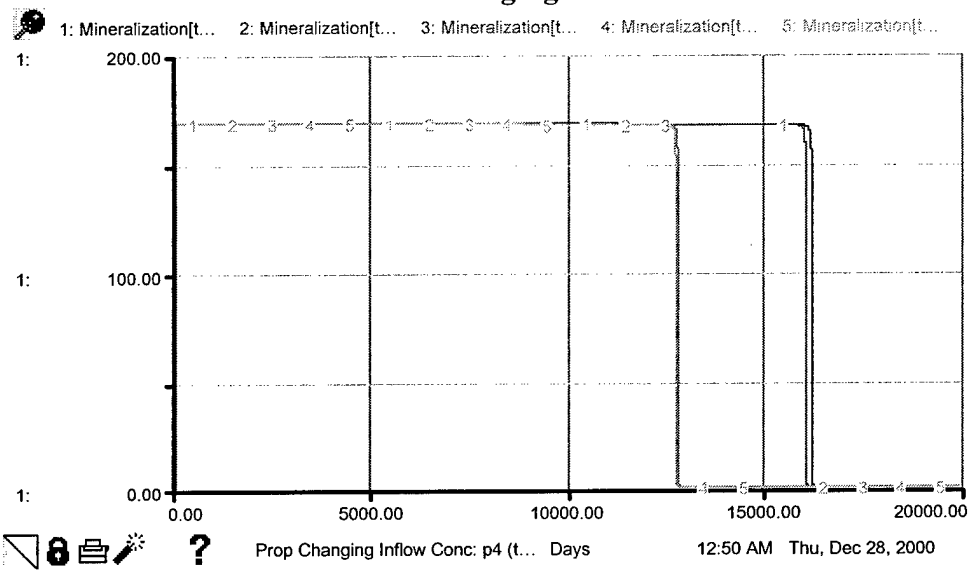

***trans*-DCE Behavior – Simulation Set 6, Propionic Acid Inflow Concentration Changing**

Setup #4		Thu, Dec 28, 2000 12:47 AM
	Input Variables	
Run #	Inflow con 2	
1	0.01	
2	0.1	
3	0.1	
4	50.0	
5	100	

Inflow Concentration Values for Changing Propionic Acid Simulations (Runs)

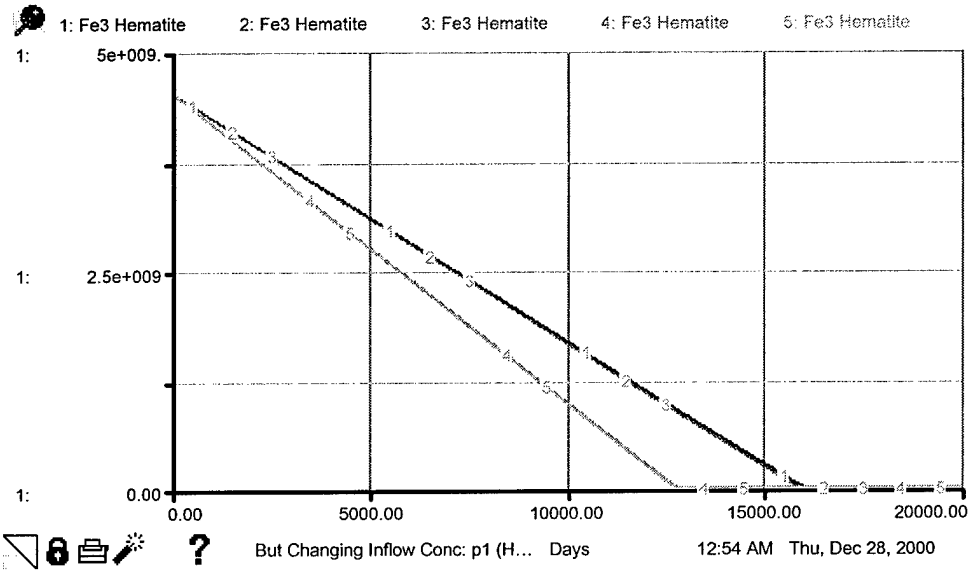

Hematite Behavior – Simulation Set 6, Butyric Acid Inflow Concentration Changing

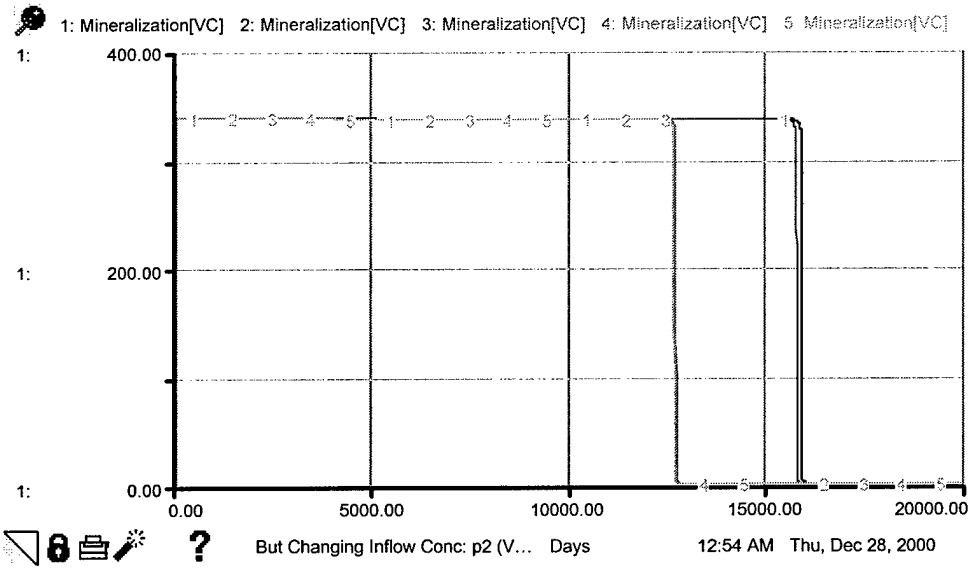

VC Behavior – Simulation Set 6, Butyric Acid Inflow Concentration Changing

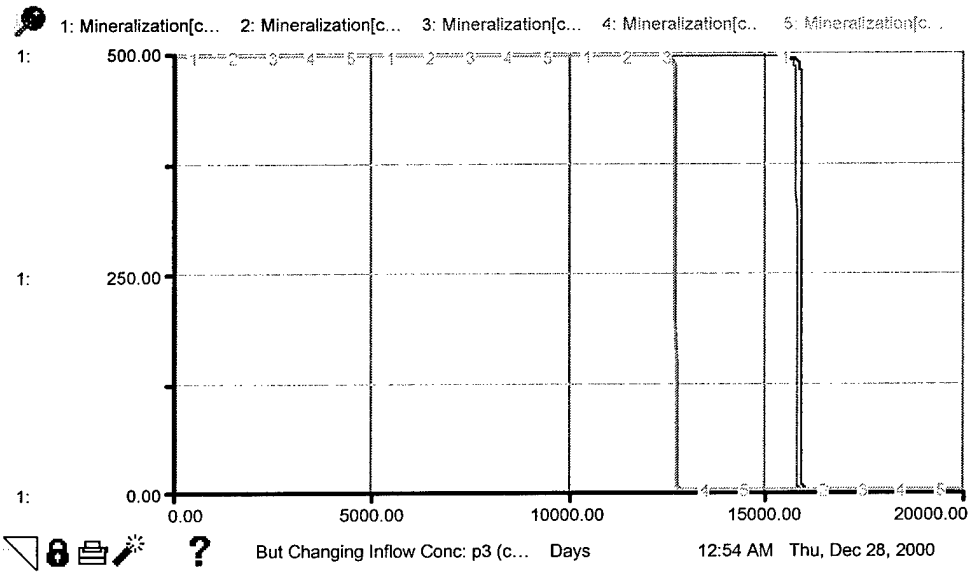

***cis*-DCE Behavior – Simulation Set 6, Butyric Acid Inflow Concentration Changing**

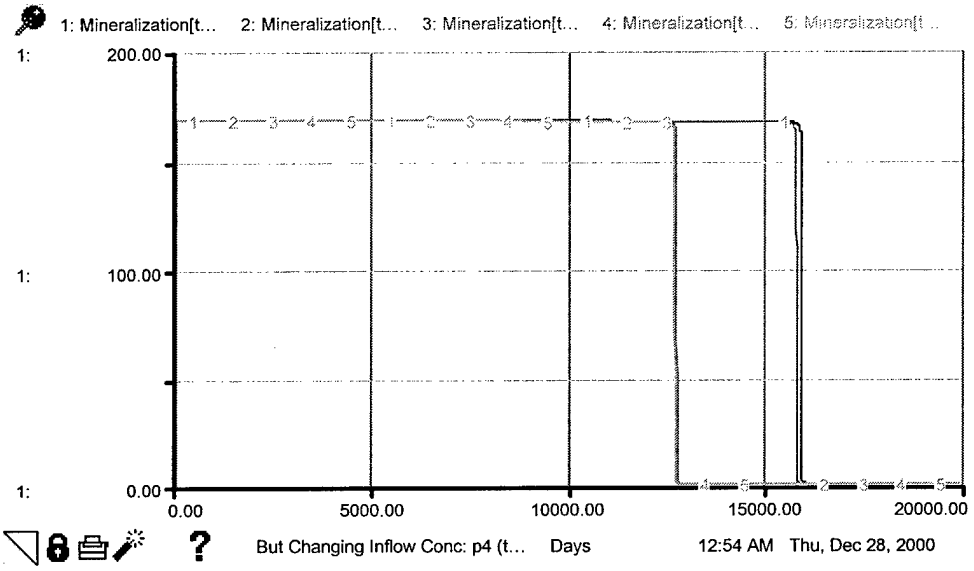

***trans*-DCE Behavior – Simulation Set 6, Butyric Acid Inflow Concentration Changing**

Setup #5	Thu, Dec 28, 2000 12:52 AM
Input Variables	
Run #	Inflow con 4
1	0.01
2	0.1
3	0.1
4	50.0
5	100

Inflow Concentration Values for Changing Butyric Acid Simulations (Runs)

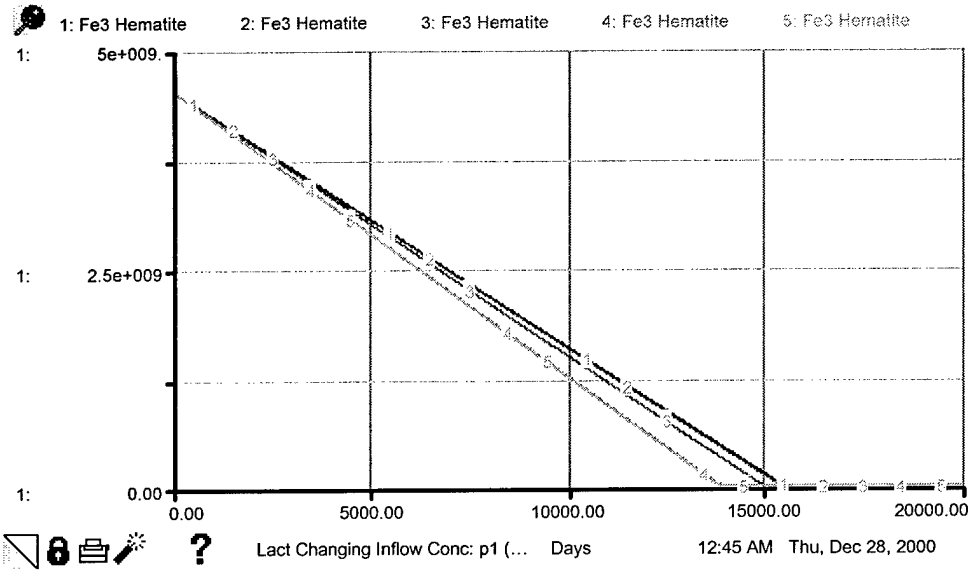

Hematite Behavior – Simulation Set 6, Lactic Acid Inflow Concentration Changing

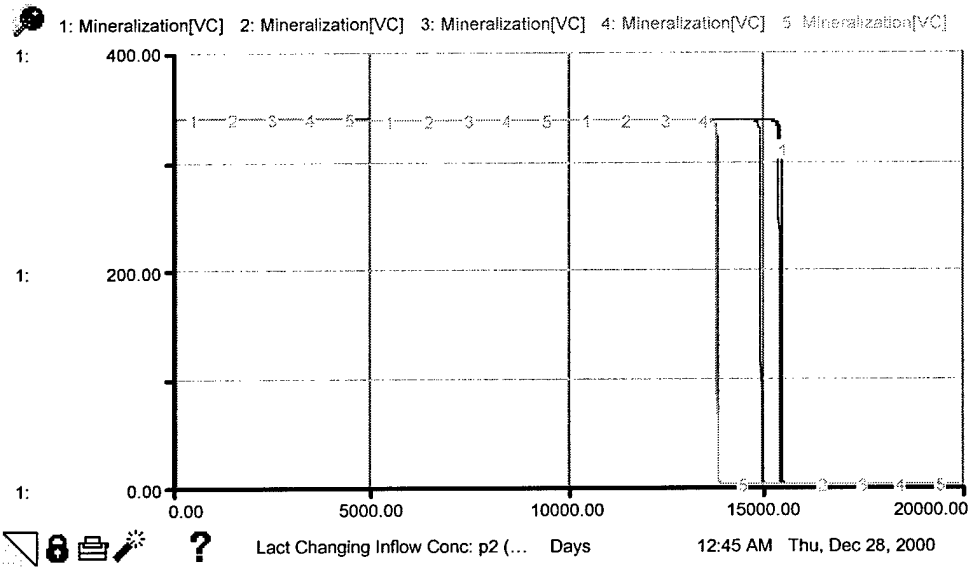

VC Behavior – Simulation Set 6, Lactic Acid Inflow Concentration Changing

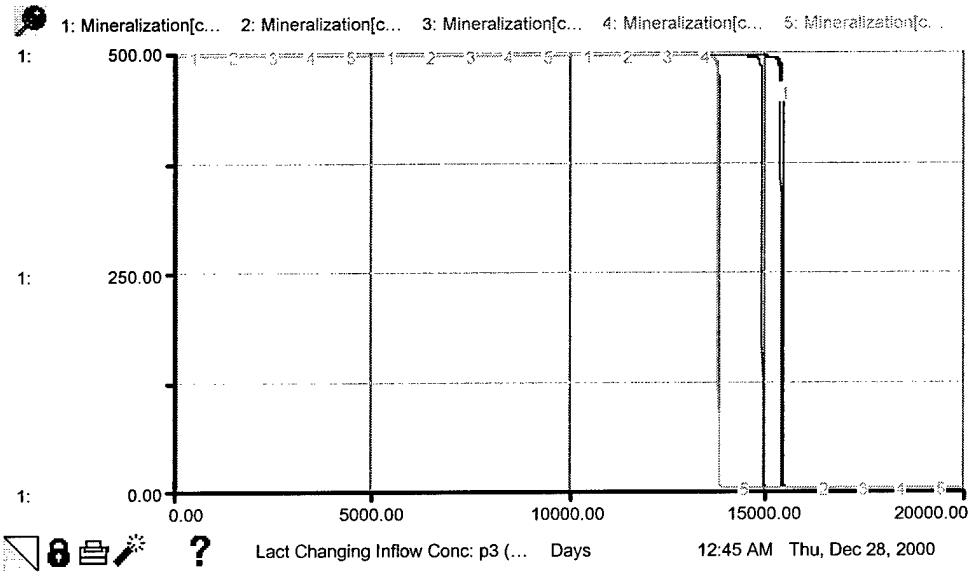

cis-DCE Behavior – Simulation Set 6, Lactic Acid Inflow Concentration Changing

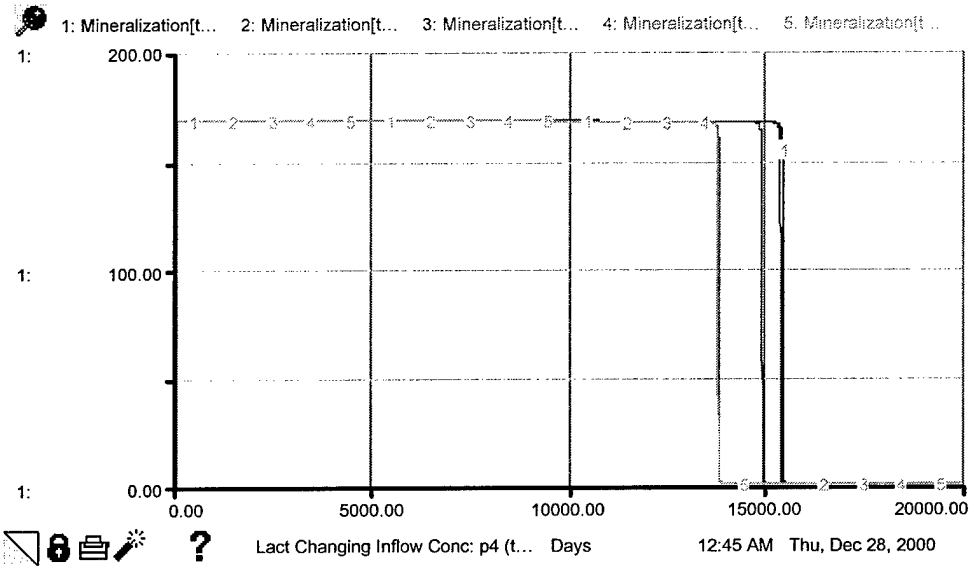

trans-DCE Behavior – Simulation Set 6, Lactic Acid Inflow Concentration Changing

Setup #3	Thu, Dec 28, 2000 12:42 AM
Input Variables	
Run #	Inflow con 1
1	0.01
2	0.1
3	1.00
4	50.0
5	100

Inflow Concentration Values for Changing Lactic Acid Simulations (Runs)

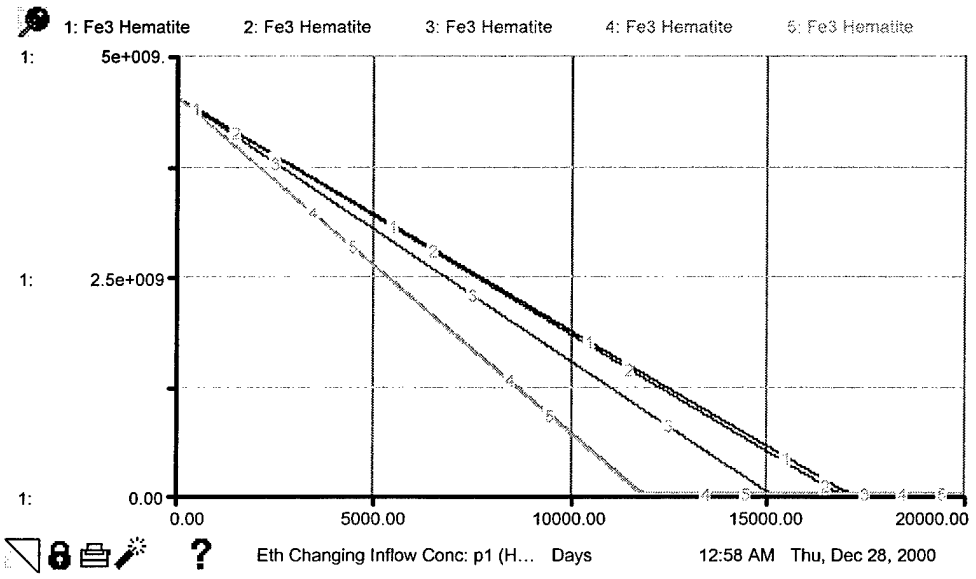

Hematite Behavior – Simulation Set 6, Ethanol Inflow Concentration Changing

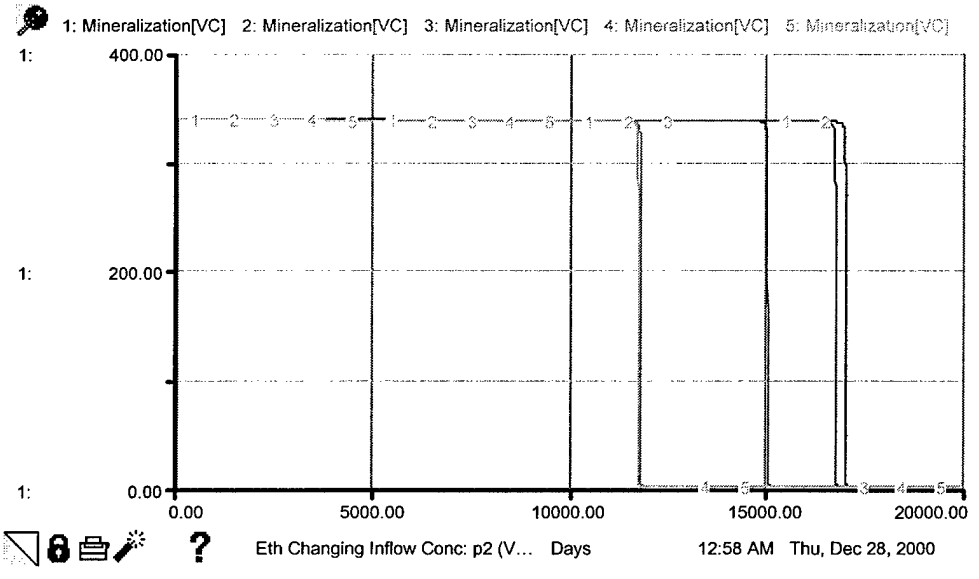

VC Behavior – Simulation Set 6, Ethanol Inflow Concentration Changing

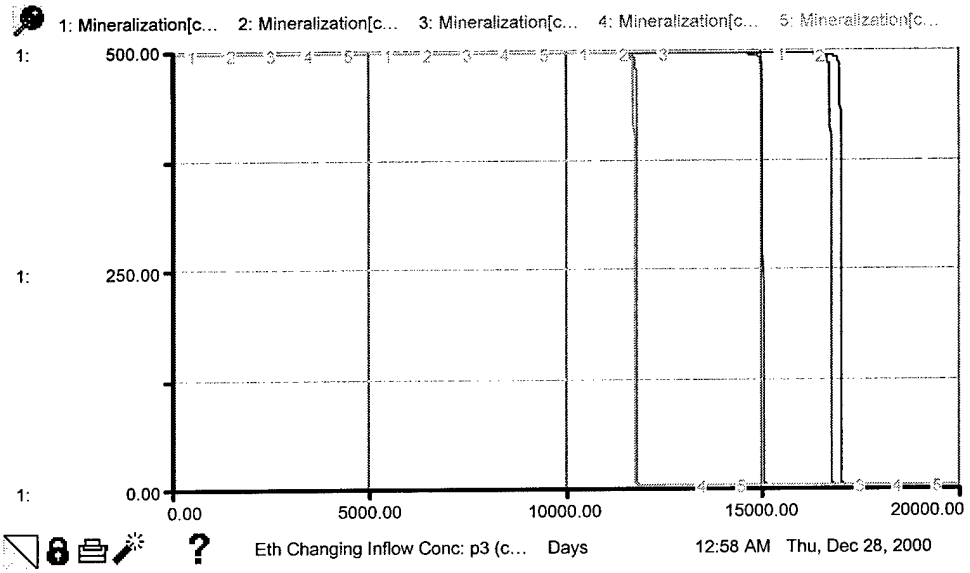

***cis*-DCE Behavior – Simulation Set 6, Ethanol Inflow Concentration Changing**

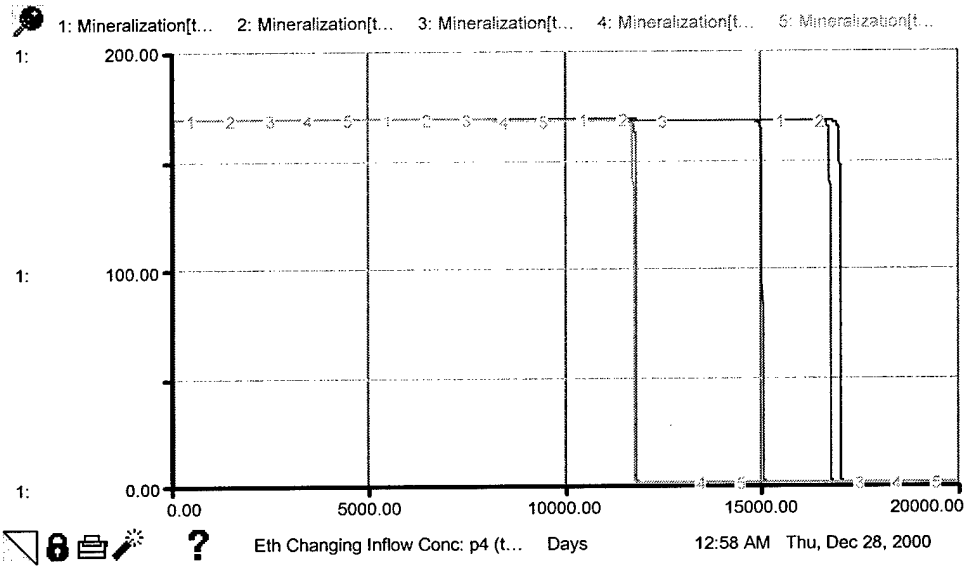

***trans*-DCE Behavior – Simulation Set 6, Ethanol Inflow Concentration Changing**

Setup #6	Thu, Dec 28, 2000 12:57 AM
Input Variables	
Run #	Inflow conc 6
1	0.01
2	0.1
3	1.00
4	50.0
5	100

Inflow Concentration Values for Changing Ethanol Simulations (Runs)

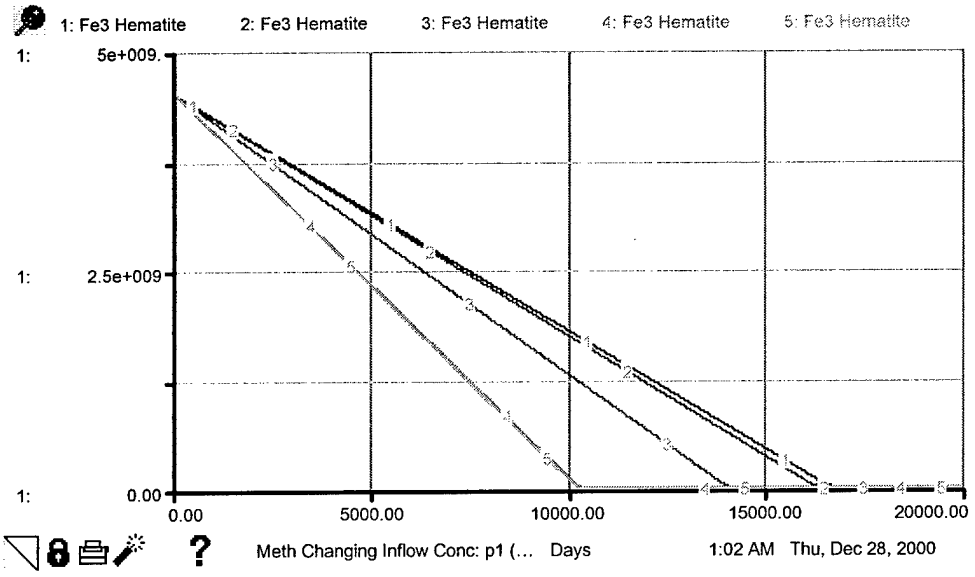

Hematite Behavior – Simulation Set 6, Methanol Inflow Concentration Changing

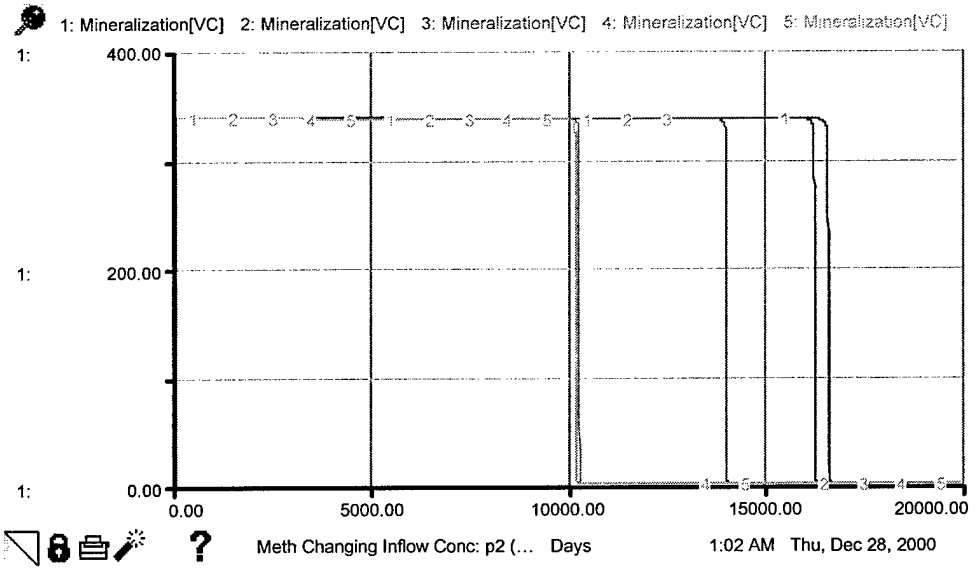

VC Behavior – Simulation Set 6, Methanol Inflow Concentration Changing

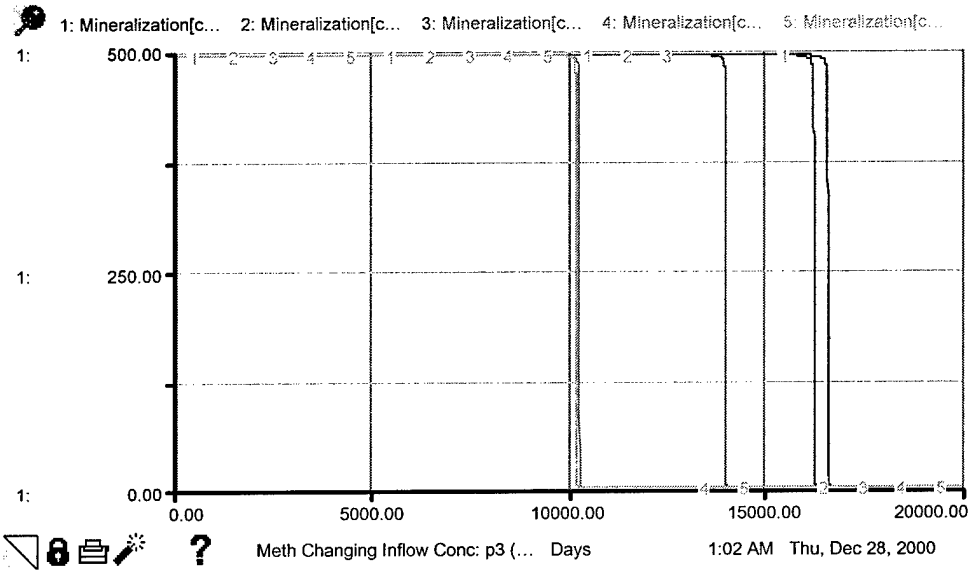

***cis*-DCE Behavior – Simulation Set 6, Methanol Inflow Concentration Changing**

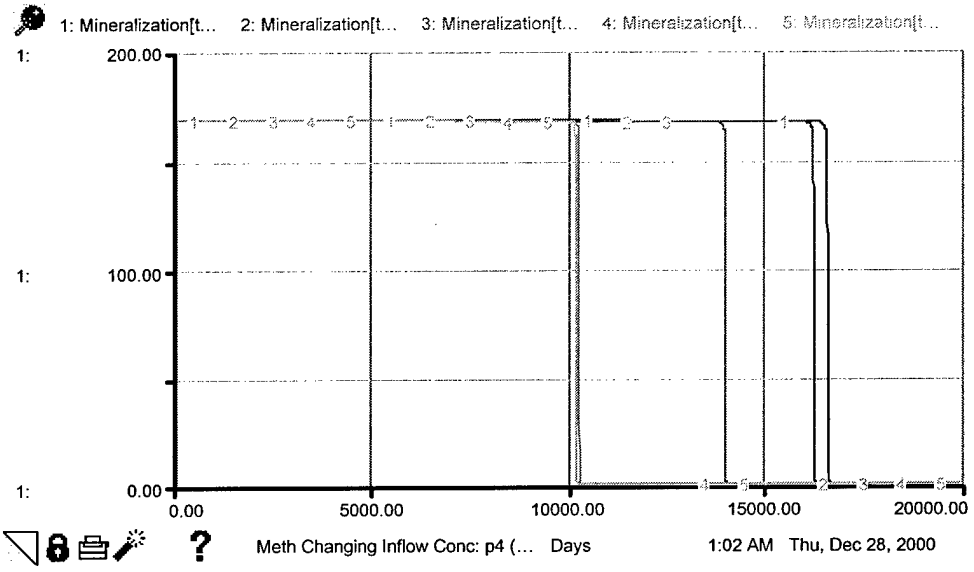

***trans*-DCE Behavior – Simulation Set 6, Methanol Inflow Concentration Changing**

Setup #7	Thu, Dec 28, 2000 1:00 AM
Input Variables	
Run #	Inflow conc 7
1	0.01
2	0.1
3	1.00
4	50.0
5	100

Inflow Concentration Values for Changing Methanol Simulations (Runs)

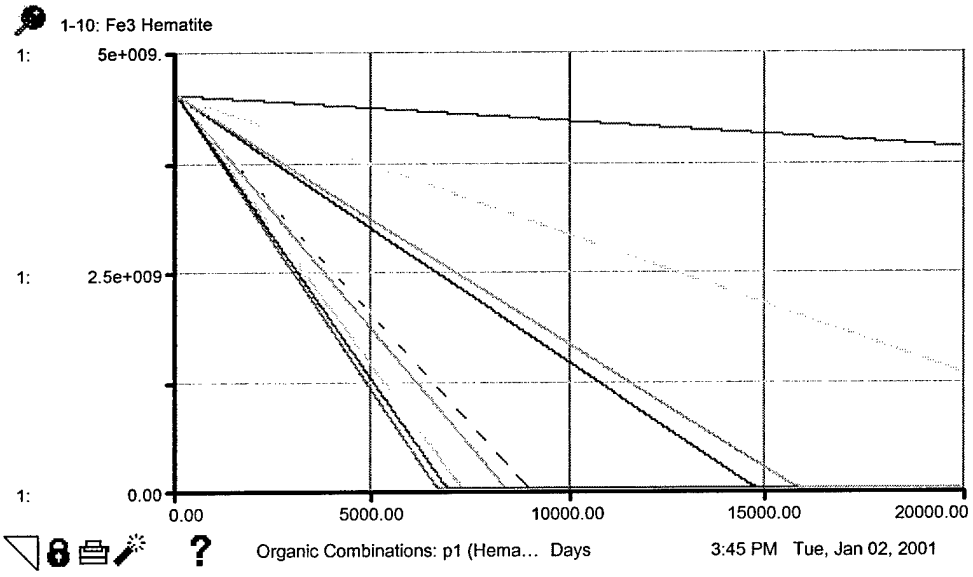

Hematite Behavior – Simulation Set 6, Organic Inflow Concentration Combinations

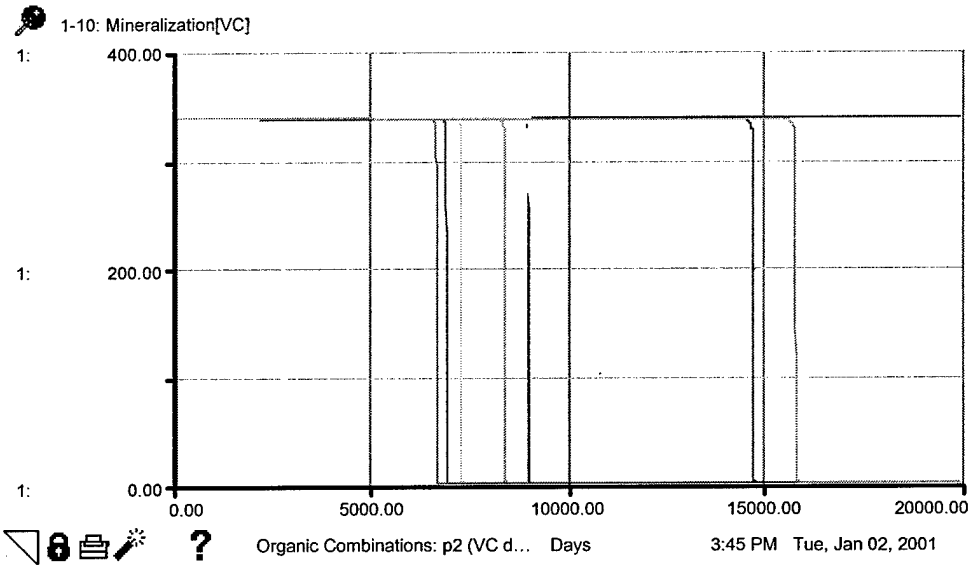

VC Behavior – Simulation Set 6, Organic Inflow Concentration Combinations

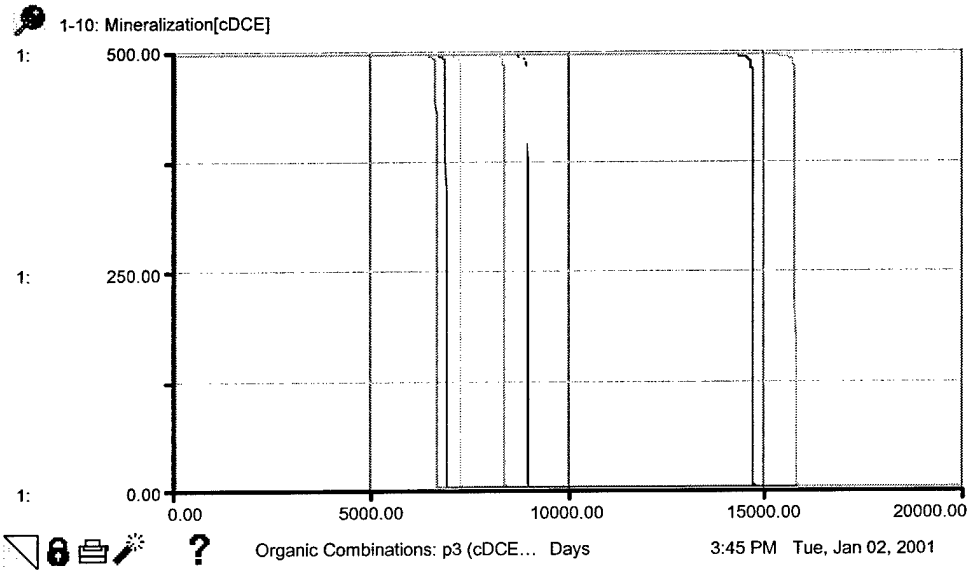

***cis*-DCE Behavior – Simulation Set 6, Organic Inflow Concentration Combinations**

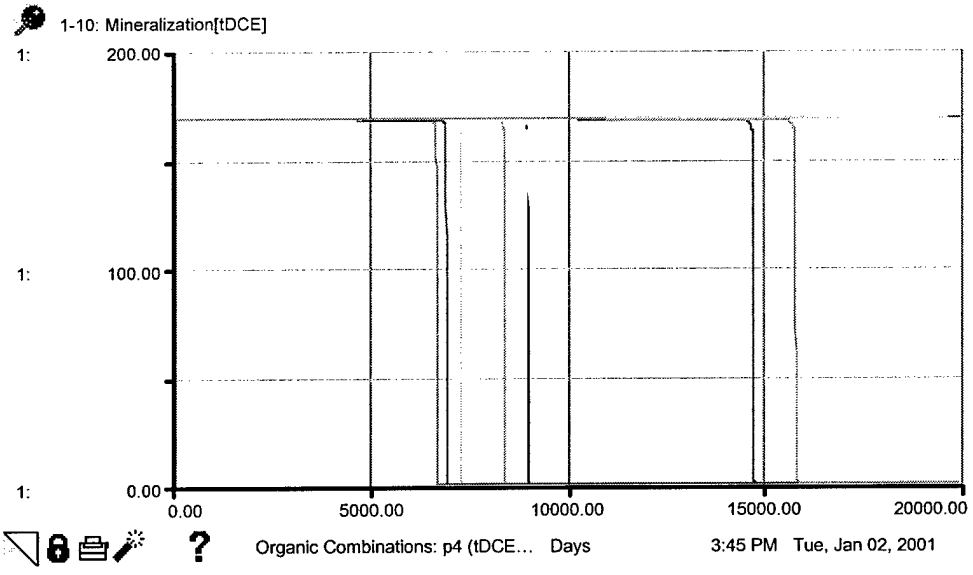

***trans*-DCE Behavior – Simulation Set 6, Organic Inflow Concentration Combinations**

Setup #2			Tue, Jan 02, 2001 3:23 PM
		Input Variables	
Run #	Inflow con 1	Inflow con 2	Inflow con 3
1	5.00	5.00	40.0
2	0.1	0.5	15.0
3	0.05	0.05	0.1
4	40.0	80.0	80.0
5	20.0	5.00	20.0
6	15.0	20.0	1.00
7	5.00	5.00	50.0
8	0.5	0.5	1.00
9	50.0	25.0	50.0
10	0.01	0.5	25.0
Run #	Inflow con 4	Inflow con 5	Inflow conc 6
1	5.00	50.0	2.00
2	1.00	20.0	0.5
3	0.05	0.5	0.01
4	70.0	75.0	50.0
5	1.00	25.0	5.00
6	20.0	1.00	10.0
7	10.0	50.0	10.0
8	0.5	5.00	0.1
9	20.0	10.0	50.0
10	1.00	30.0	0.1
Run #	Inflow conc 7		
1	2.00		
2	0.5		
3	0.01		
4	10.0		
5	5.00		
6	10.0		
7	10.0		
8	0.1		
9	10.0		
10	0.25		

Inflow Concentration Values for Organic Combination Simulations (Runs)

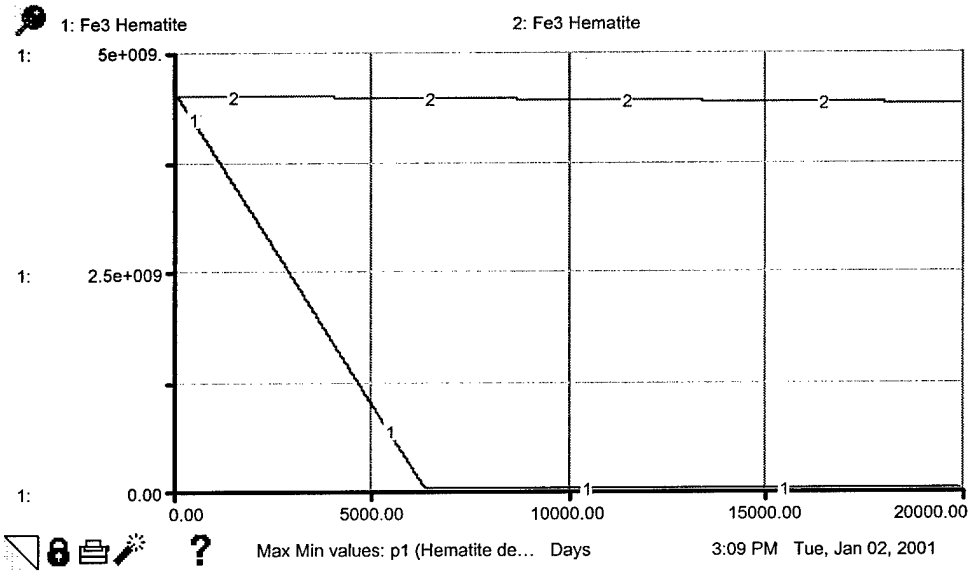

Hematite Behavior – Simulation Set 6, Max/Min Inflow Concentrations for Organics

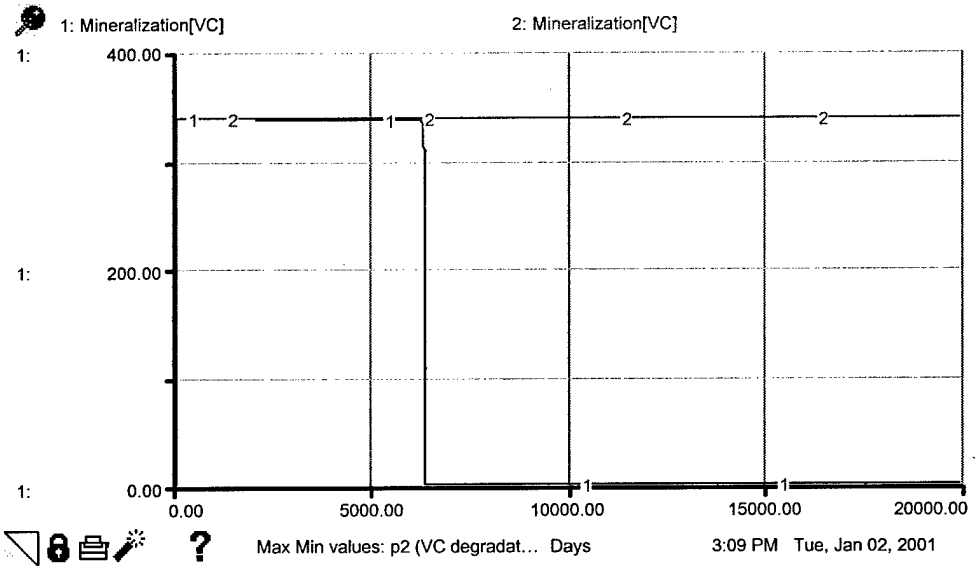

VC Behavior – Simulation Set 6, Max/Min Inflow Concentrations for Organics

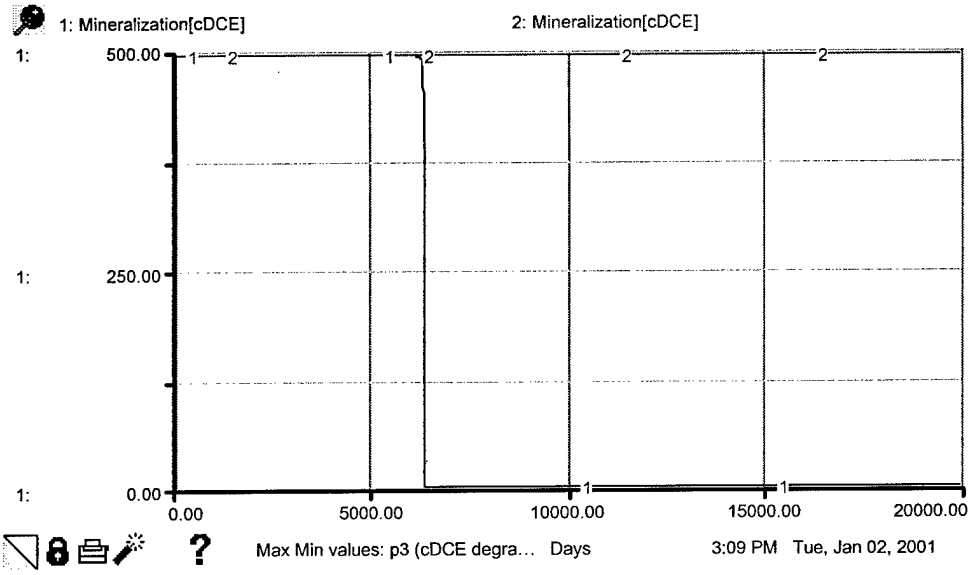

***cis*-DCE Behavior – Simulation Set 6, Max/Min Inflow Concentrations for Organics**

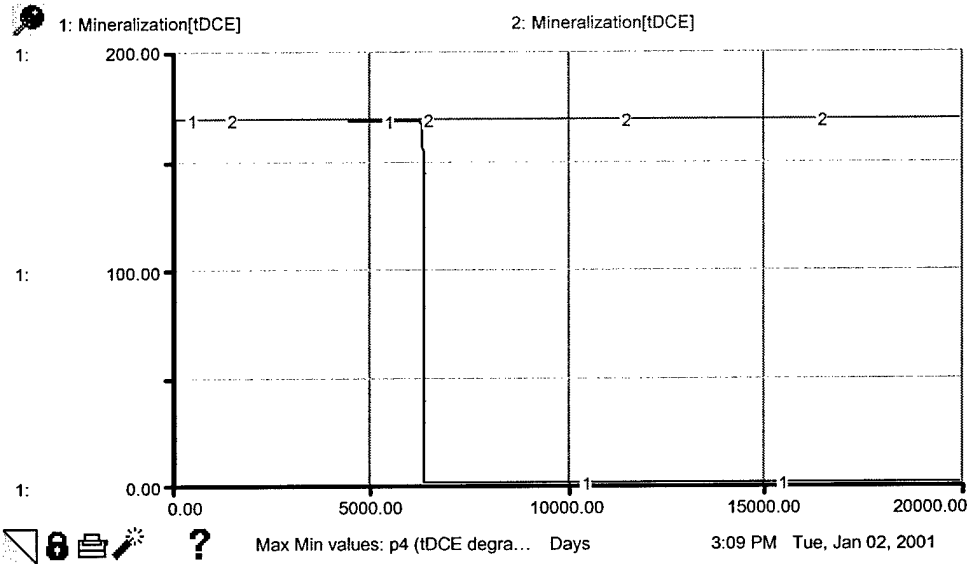

***trans*-DCE Behavior – Simulation Set 6, Max/Min Inflow Concentrations for Organics**

Setup #1 — Tue, Jan 02, 2001 3:08 PM

Input Variables

Run #	Inflow con 1	Inflow con 2	Inflow con 3
1	100	100	100
2	0.01	0.01	0.01

Run #	Inflow con 4	Inflow con 5	Inflow conc 6
1	100	100	100
2	0.01	0.01	0.01

Run #	Inflow conc 7
1	100
2	0.01

Inflow Contaminant Concentration Values for Max/Min Simulations (Runs)

Bibliography

Balashova, V. V. and G. A. Zavarzin. "Anaerobic Reduction of Ferric Iron By Hydrogen Bacteria," Microbiology, 48: 635-639 (1980).

Bradley, Paul M. "Microbial Degradation of Chloroethenes in Groundwater Systems," Hydrogeology Journal, 8: 104-111 (2000).

Bradley, Paul M. and Francis H. Chapelle. "Anaerobic Mineralization of Vinyl Chloride in Fe(III)-Reducing Aquifer Sediments," Environmental Science and Technology, 30(6): 2084-2086 (1996).

-----. "Kinetics of DCE and VC Mineralization Under Methanogenic and Fe(III)-Reducing Conditions," Environmental Science and Technology, 31(9): 2692-2696 (1997).

Bradley, P. M., F. H. Chapelle, and J. T. Wilson. "Field and Laboratory Evidence for Intrinsic Biodegradation of Vinyl Chloride Contamination in a Fe(III)-Reducing Aquifer," Journal of Contaminant Hydrology, 31: 111-127 (1998).

Caccavo, Frank, Jr., Richard P. Blakemore, and Derek R. Lovley. "A Hydrogen-Oxidizing, Re(III)-Reducing Microorganism from the Great Bay Estuary, New Hampshire," Applied and Environmental Microbiology, 58(10): 3211-3216 (October 1992).

Chapelle, Francis H. Ground-water Microbiology and Geochemistry. New York: John Wiley & Sons, Inc., 1993.

Chapelle, Francis H., Peter B. McMahon, Neil M. Dubruvsky, Roger F. Fujii, Edward T. Oaksford, and Don A. Vroblesky. "Deducing the Distribution of Terminal Electron-accepting Processes in Hydrologically Diverse Groundwater Systems," Water Resources Research, 31(2): 359-371 (February 1995).

Clark, Mark M. Transport Modeling for Environmental Engineers and Scientists. New York: John Wiley & Sons, Inc., 1996.

Fennell, Donna E. and James M. Gossett. "Modeling the Production of and Competition for Hydrogen in a Dechlorinating Culture," Environmental Science and Technology, 32(16): 2450-2460 (1998).

Fredrickson, James K., Fohn M. Zachara, David W. Kennedy, Hailang Dong, Tullis C. Onstott, Nancy W. Hinman, and Shu-mei Li. "Biogenic Iron Mineralization Accompanying the Dissimilatory Reduction of Hydrous Ferric Oxide By a Groundwater Bacterium," Giochimica et Cosmochimica Acta, 62(19/20): 3239-3257 (1998).

Hoefar, Colby D. Modeling Chlorinated Ethene Removal in Constructed Wetlands: A System Dynamics Approach. MS thesis, AFIT/GEE/ENV/00M-09. School of Engineering, Air Force Institute of Technology (AU), Wright-Patterson AFB OH, 2000.

Jones, J. Gwynfryn, Steven Gardener, and Bernard M. Simon. "Bacterial Reduction of Ferric Iron in a Stratified Eutrophic Lake," Journal of General Microbiology, 129: 131-139 (1983).

Kadlec, Robert H. and Robert L. Knight. Treatment Wetlands. New York: CRC Press, Inc., 1996.

Lee, M. D., J. M. Odom, and R. J. Buchanan, Jr. "New Perspectives on Microbial Dehalogenation of Chlorinated Solvents: Insights from the Field," Annual Reviews Microbiology, 52: 423-452 (1998).

Lonergan, Debra J., Harry L. Jenter, John D. Coates, Elizabeth J. P. Phillips, Thomas M. Schmidt, and Derek R. Lovley. "Phylogenetic Analysis of Dissimilatory Fe(III)-Reducing Bacteria," Journal of Bacteriology, 178(8): 2402-2408 (April 1996).

Lovley, Derek R. "Dissimilatory Fe(III) and Mn(IV) Reduction," Microbiology Review (55): 260-287 (1991).

Lovley, Derek R. "Microbial Fe(III) Reduction in Subsurface Environments," FEMS Microbiology Reviews, 20: 305-313 (1997).

Lovley, Derek R. and Elizabeth J. P. Phillips. "Competitive Mechanisms for Inhibition of Sulfate Reduction and Methane Production in the Zone of Ferric Iron Reduction in Sediments," Applied and Environmental Microbiology, 53: 2636-2641 (November 1987).

-----. "Manganese Inhibition of Microbial Iron Reduction in Anaerobic Sediments," Geomicrobiology Journal, 6: 145-155 (1988).

-----. "Novel Mode of Microbial Energy Metabolism: Organic Carbon Oxidation Coupled to Dissimilatory Reduction of Iron or Manganese," Applied and Environmental Microbiology, 54: 1472-1480 (June 1988).

-----. "Organic Matter Mineralization with Reduction of Ferric Iron in Anaerobic Sediments," Applied and Environmental Microbiology, 51(4): 683-689 (April 1986).

Lovley, Derek R., John F. Stolz, Gordon L. Nord, Jr., and Elizabeth J. P. Phillips. "Anaerobic Production of Magnetite By a Dissimilatory Iron-reducing Microorganism," Nature, 330(19): 252-254 (19 November 1987).

Lovley, Derek R., Elizabeth J. P. Phillips, Debra J. Lonergan, and Peggy K. Widman. "Fe(III) and S^0 Reduction by *Pelobacter carbinolicus*," Applied and Environmental Microbiology, 61(6): 2132-2138 (June 1995).

Lovley, Derek R., Elizabeth J. P. Phillips, and Debra J. Lonergan. "Hydrogen and Formate Oxidation Coupled to Dissimilatory Reduction of Iron or Mangenese By *Alteromonas putrefaciens*," Applied and Environmental Microbiology, 55(3): 700-706 (March 1989).

Lovley, Derek R., Francis H. Chapelle, and Joan C. Woodward. "Use of Dissolved H_2 Concentrations to Determine Distribution of Microbially Catalyzed Redox Reactions in Anoxic Groundwater," Environmental Science Technology, 28(7): 1205-1210 (1994).

Masters, Gilbert M. Introduction to Environmental Engineering and Science. (Second Edition). New Jersey: Prentice-Hall, Inc., 1998.

Mitsch, William J. and James G. Gosselink. Wetlands. (Second Edition). New York: John Wiley & Sons, Inc., 1993.

Mitsch, William J., Milan Straskraba, and Sven E. Jorgensen. Wetland Modeling. Amsterdam, Elsevier Science Publishers B.V., 1988.

Moorhead, Daryl L., Robert L. Sinsabaugh, A. E. Linkins, and James F. Reynolds. "Decomposition processes: Modelling Approaches and Applications," The Science of the Total Environment, 183: 137-149 (1996).

Mudgett, Leslie A. A System Dynamics Approach to Modelling the Degradation of Biochemical Oxygen Demand in a Constructed Wetland Receiving Stormwater Runoff. MS thesis, AFIT/GEE/ENV/95D-12. School of Engineering, Air Force Institute of Technology (AU), Wright-Patterson AFB OH, 1995.

National Research Council. Alternatives for Ground Water Cleanup. Washington DC: National Academy Press, 1994.

-----. Innovations in Ground Water and Soil Cleanup: From Concept to Commercialization. Washington DC: National Academy Press, 1997.

-----. In Situ Bioremediation: When Does It Work? Washington DC: National Academy Press, 1993.

-----. Natural Attenuation for Groundwater Remediation. Washington DC: National Academy Press, 2000.

Quinton, Gary E., Ronald J. Buchanan, Jr., David E. Ellis, and Stephen H. Shoemaker. "A Method to Compare Groundwater Cleanup Technologies," Remediation, 7(4): 7-16 (Autumn 1997).

Sarazin, Gerard, Jean-Fran cois Gaillard, Laurence Philippe, and Christophe Rabouille. "Organic Matter Mineralization in the Pore Water of a Eutrophic Lake (Aydat Lake, Puy de Dome, France)," Hydrobiologia, 315(2): 95-118 (1995).

Shelley, Michael L. Course Syllabus & Materials, ENVR 642, System Dynamics Modeling. Graduate School of Engineering and Management, Air Force Institute of Technology, Wright-Patterson AFB OH, Spring 2000.

Shelley, Michael L. and Leslie A Mudgett. "A Mechanistic Simulation Model of a Constructed Wetland Designed to Remove Organic Matter from a Stormwater Runoff," Journal of Environmental Systems, 27(1): 33-54 (1999).

Yang, Yanru and Perry L. McCarty. "Competition for Hydrogen Within a Chlorinated Solvent Dehalogenating Anaerobic Mixed Culture," Environmental Science & Technology, 32(22): 3591-3597 (1998).

Vita

1Lt Max E. Johnson was born in Freeport, Texas. He graduated from Lamar Consolidated High School in Rosenberg, Texas in June 1992. He entered undergraduate studies at Texas A&M University in College Station, Texas where he graduated with a Bachelor of Science degree in Civil Engineering in August 1997. He was commissioned through the Detachment 805 AFROTC at Texas A&M University and received a Reserve Commission.

His first assignment was at Maxwell AFB as a base-level engineer in October 1997. While stationed at Maxwell, he deployed overseas in February 1999 to spend four months at Eskan Village (Riyadh), Kingdom of Saudi Arabia as a design engineer for the 320th Expeditionary Civil Engineer Squadron. In August 1999, he entered the Graduate School of Engineering and Management program, School of Engineering, Air Force Institute of Technology. Upon graduation, he will be assigned to the Air Force Center for Environmental Excellence at Brooks AFB in San Antonio, Texas.

REPORT DOCUMENTATION PAGE

Form Approved
OMB No. 074-0188

1. REPORT DATE *(DD-MM-YYYY)*	2. REPORT TYPE	3. DATES COVERED *(From – To)*
20-03-2001	Master's Thesis	Aug 1999 – Mar 2001

4. TITLE AND SUBTITLE

MODELING BIODEGRADATION OF CHLORINATED GROUNDWATER CONTAMINANTS UNDER IRON-REDUCING CONDITIONS OF A CONSTRUCTED WETLAND: A SYSTEM DYNAMICS APPROACH

5a. CONTRACT NUMBER

5b. GRANT NUMBER

5c. PROGRAM ELEMENT NUMBER

6. AUTHOR(S)

Johnson, Max E., 1Lt, USAF

5d. PROJECT NUMBER

5e. TASK NUMBER

5f. WORK UNIT NUMBER

7. PERFORMING ORGANIZATION NAMES(S) AND ADDRESS(S)

Air Force Institute of Technology
Graduate School of Engineering and Management (AFIT/EN)
2950 P Street, Building 640
WPAFB OH 45433-7765

8. PERFORMING ORGANIZATION REPORT NUMBER

AFIT/GEE/ENV/01M-04

9. SPONSORING/MONITORING AGENCY NAME(S) AND ADDRESS(ES)

Dr. David Burris
Air Force Research Laboratory
Materials Directorate
Environmental Quality Division
Tyndall AFB, FL

10. SPONSOR/MONITOR'S ACRONYM(S)

AFRL/MLQ

11. SPONSOR/MONITOR'S REPORT NUMBER(S)

12. DISTRIBUTION/AVAILABILITY STATEMENT

APPROVED FOR PUBLIC RELEASE; DISTRIBUTION UNLIMITED.

13. SUPPLEMENTARY NOTES

14. ABSTRACT

The purpose of this study is to determine and explore the fundamental processes associated with biodegradation of chlorinated ethenes in iron-reducing conditions of a constructed wetland and to evaluate the impacts of changing conditions (both natural and engineer-controlled) on the system. The modeler uses a system dynamics approach to construct a model that represents behavior in the iron-reducing environment. The model incorporates hematite, a form of oxidized iron (Fe^{3+}), as the electron acceptor.

Vinyl chloride, *cis*-dichloroethene, and *trans*-dichloroethene are known to anaerobically degrade to carbon dioxide in the presence of oxidized iron. Other biodegrading processes, including those associated with hydrogen and natural organic materials, compete with the contaminant degrading processes for the oxidized iron. These processes are all incorporated into the model.

Model simulations show that the organic material parameters have a greater influence on hematite depletion compared with parameters of the modeled contaminants. By increasing the amount of hematite in the soil, the time period that biodegrading processes exist in the constructed wetlands increases proportionally. Also, by increasing flow rate through the constructed wetland, a higher amount of contaminant is degraded. With the increased flow rate, however, a greater amount of contaminants flow through the iron-reducing environment unreacted.

15. SUBJECT TERMS

Iron-reduction, Chlorinated Groundwater Contaminants, Vinyl Chloride, Dichloroethene, Constructed Wetlands, Biodegradation, System Dynamics, Hematite, Anaerobic Degradation, Oxidized Iron

16. SECURITY CLASSIFICATION OF:			17. LIMITATION OF ABSTRACT	18. NUMBER OF PAGES	19a. NAME OF RESPONSIBLE PERSON
a. REPORT	b. ABSTRACT	c. THIS PAGE			Dr. Michael L. Shelley, ENV
U	U	U	UU	229	19b. TELEPHONE NUMBER *(Include area code)* (937) 255-2998

Standard Form 298 (Rev. 8-98)
Prescribed by ANSI Std. Z39-18

Form Approved
OMB No. 074-0188